



**INSTITUTE OF BIOORGANIC CHEMISTRY**  
Polish Academy of Sciences

**Identification and functional characteristics of  
circular RNAs in glioblastoma**

**mgr Żaneta Zarębska**

This research project was carried out at the Department of Molecular  
Neurooncology Institute of Bioorganic Chemistry  
Polish Academy of Sciences

Dissertation supervisor: Dr. Hab. Katarzyna Rolle, Prof. IBCH PAS

**Poznań, 2023**



Pragnę złożyć serdeczne podziękowania:

Pani dr hab. Katarzynie Rolle, prof. ICHB PAN  
dziękuję za przekazaną wiedzę, nieocenione wsparcie w prowadzonych badaniach oraz  
okazaną życzliwość.

Panu prof. dr hab. Janowi Barciszewskiemu  
dziękuję za pokazanie mi piękna nauki.

dr Małgorzacie Grabowskiej oraz dr Konradowi Kuczyńskiemu  
dziękuję za otoczenie mnie opieką i wsparciem podczas wykonywania pracy magisterskiej, co  
przyniosło się do stworzenia niniejszej dysertacji.

mgr Adrianie Grabowskiej,  
mgr Julii Latowskiej-Łysiak,  
dr inż. Pawłowi Głodowiczowi,  
dr Dariuszowi Wawrzyniakowi,  
dr Julii Misiorek

dziękuję za porady praktyczne, ciekawe rozmowy oraz wspaniałą atmosferę w pracy.

dr Agnieszce Rybak-Wolf

dziękuję za poświęcony czas i miłą atmosferę podczas stażu oraz ciekawe dyskusje.

dr Marcinowi Sajkowi,  
dr Łukaszowi Przybyłowi,  
pani Małgorzacie Dąbkiewicz,  
pani Iwonie Gawrońskiej,  
pani Ewie Joachimiak,  
Agacie Pietrzak

dziękuję za przyczynienie się do mojego rozwoju w trakcie trwania doktoratu, pomocne  
wskazówki i okazaną życzliwość.

Rodzicom, Oli, Bartkowi oraz Babci dziękuję za okazane wsparcie i zrozumienie, a także  
nieustającą wiarę we mnie oraz wspólną radość z sukcesów.

Pawłowi dziękuję za wsparcie w dążeniu do celu, obecność i zrozumienie w trudnych  
chwilach, motywowanie do dalszej pracy oraz naukę dyplomacji.

Dla Rodziców i dzięki nim.

## **Funding**

This work resulted from the implementation of research project number 2017/25/B/NZ3/02173, funded by the National Science Center and supported by the Federation of European Biochemical Societies, which funded the Short-Term Fellowship of the dissertation's author.

Performed research was approved by the ethical committee at Poznan University of Medical Sciences with consent number 534/18.

## List of author's publications

1. Grabowska M., Misiorek J., **Zarebska Ż.**, Rolle K., (2022) Clinical Applications of noncoding RNAs in brain cancer patients. *Clinical Applications of Non-Coding RNAs in Cancer*, Elsevier, ISBN: 9780128245507. IF<sub>2022</sub> = -; MEiN = 80
2. Latowska J\*, Grabowska A\*, **Zarębska Ż.**, Kuczyński K., Kuczyńska B., & Rolle K. (2020). Non-coding RNAs in Brain Tumors, the Contribution of lncRNAs, circRNAs, and snoRNAs to Cancer Development-Their Diagnostic and Therapeutic Potential. *International journal of molecular sciences*, 21(19), 7001. IF<sub>2020</sub> = 5.924; MEiN = 140
3. Wawrzyniak O\*, **Zarębska Ż\***, Kuczyński K., Gotz-Więckowska A., & Rolle K. (2020). Protein-Related Circular RNAs in Human Pathologies. *Cells*, 9(8), 1841. IF<sub>2020</sub> = 6.600 ; MEiN = 140
4. Wawrzyniak O., **Zarębska Ż.**, Rolle K., Gotz-Więckowska A. (2018). Circular and long non-coding RNAs and their role in ophthalmologic diseases. *Acta biochimica Polonica*, 65(4), 497–508. IF<sub>2018</sub> = 1.626 ; MEiN = 40

**The presented dissertation is a part of two original manuscripts which are currently under revision.**

1. **Zarębska Ż.,\*** Latowska-Łysiak J.,\* Sajek MP.,\* Grabowska A., Buratin A., Misiorek JO., Kuczyński K., Bortoluzzi S., Żywicki M., Kosiński J., Rybak-Wolf A., Piestrzeniewicz R., Barciszewska AM., Rajewsky N., Rolle K. Transcriptome-wide analysis of circRNA-RBP interplay and their clinical significance in glioblastoma
2. **Zarębska Ż\***, Kuczyński K\*, Latowska-Łysiak J., Grabowska A., Sajek MP., Piestrzeniewicz R., Barciszewska AM., Andrzejewska B, Rolle K. Circular RNA circCLIP2 promotes the invasive properties of glioblastoma by acting as a mediator of the EMT pathway and cancer stemness.

## List of abbreviations

<b>2D</b>	two-dimensional
<b>3D</b>	three-dimensional
<b>5-ALA</b>	5-aminolevulinic acid
<b>AAV</b>	adeno-associated virus
<b>Ago2</b>	Argonaute 2
<b>ALDH1</b>	aldehyde dehydrogenase 1
<b>ALKBH1</b>	AlkB homolog 1
<b>ASO</b>	antisense oligonucleotide
<b>ATCC</b>	American Type Culture Collection
<b>ATRX</b>	alpha-thalassemia mental retardation X-linked
<b>AURKA</b>	aurora kinase A
<b>BBB</b>	blood-brain barrier
<b>BIRC5</b>	baculoviral IAP repeat containing 5
<b>CAFs</b>	cancer-associated fibroblasts
<b>CAR</b>	chimeric antigen receptor
<b>CBTRUS</b>	Central Brain Tumor Registry of the United States
<b>CDH1</b>	Cadherin 1
<b>CDK4</b>	cyclin-dependent kinase 4
<b>CDKN2A</b>	cyclin-dependent kinase inhibitor 2A
<b>cDNA</b>	complementary DNA
<b>ceRNA</b>	competing endogenous RNA
<b>CHI3L1</b>	chitinase 3 like 1
<b>circRNA</b>	circular RNA
<b>CLIP2</b>	CAP-Gly domain containing linker protein 2
<b>CNA</b>	copy number alterations
<b>CNBP</b>	CCHC-type zinc finger nucleic acid binding protein
<b>CNS</b>	central nervous system
<b>CSCs</b>	cancer stem cells
<b>CT</b>	computed tomography
<b>DMEM/F-12</b>	Dulbecco's Modified Eagle Medium F12
<b>DNA</b>	deoxyribonucleic acid
<b>EC</b>	embryonal carcinoma

<b>ECM</b>	extracellular matrix
<b>EGFR</b>	epidermal growth factor receptor
<b>eIF4A3</b>	eukaryotic initiation factor 4A3
<b>EMEM</b>	Eagle's Minimum Essential Medium
<b>EMT</b>	epithelial-to-mesenchymal transition
<b>EV</b>	extracellular vesicle
<b>f-circRNAs</b>	fusion-circRNAs
<b>FSP1</b>	fibroblast-secreted protein-1
<b>FUS</b>	fused in sarcoma
<b>GABRA1</b>	gamma-aminobutyric acid (GABA) receptor 1
<b>GBM</b>	glioblastoma
<b>GBO</b>	GBM organoids
<b>GFAP</b>	glial fibrillary acidic protein
<b>GSC</b>	glioma stem cell
<b>HBO</b>	healthy brain organoids; cerebral organoids
<b>HGF</b>	hepatocyte growth factor
<b>HIF-1</b>	hypoxia-inducing factor 1
<b>HPRT</b>	hypoxanthine phosphoribosyltransferase
<b>IARC</b>	International Agency for Research on Cancer
<b>IDH</b>	Isocitrate Dehydrogenase
<b>IFN-<math>\gamma</math></b>	interferon-gamma
<b>IHC</b>	immunohistochemistry
<b>iPSC</b>	induced pluripotent stem cells
<b>IRES</b>	internal ribosome entry site
<b>KLF4</b>	Krüppel-like factor 4
<b>KPS</b>	Karnofsky Performance Status
<b>L1CAM</b>	L1 cell adhesion molecule
<b>LGG</b>	low-grade glioma
<b>lncRNA</b>	long noncoding RNA
<b>LRRC4</b>	leucine-rich repeat-containing 4
<b>m6A</b>	N6-methyladenosine
<b>MAPK</b>	mitogen-activated protein kinase
<b>MBNL</b>	muscleblind-like
<b>MDM2</b>	murine double minute-2

<b>MDM4</b>	murine double minute 4
<b>MGMT</b>	O6-methylguanine-DNA-methyltransferase
<b>MMP9</b>	metalloproteinase 9
<b>MRI</b>	magnetic resonance imaging
<b>mRNA</b>	messenger RNA
<b>MTIC</b>	5-(3-methyltriazin-1-yl) imidazole-4-carboxamide
<b>MTOR</b>	mechanistic target of rapamycin kinase
<b>N6-ma</b>	N6-methyladenine
<b>ncRNA</b>	non-coding RNA
<b>NEFL</b>	neurofilament light chain
<b>NF1</b>	neurofibromin 1
<b>NFAT5</b>	nuclear factor of activated T-cells 5
<b>NGS</b>	next-generation sequencing
<b>NK</b>	natural killer
<b>PAF1</b>	RNA polymerase II-associated factor 1
<b>PDGFRA</b>	platelet derived growth factor receptor alpha
<b>PET</b>	positron emission tomography
<b>PIK3CA</b>	phosphatidylinositol-4,5-bisphosphate 3-kinase catalytic subunit alpha
<b>Pol II</b>	RNA polymerase II
<b>pre-mRNA</b>	pre-messenger RNA
<b>pSTAT3</b>	phospho-tyrosine705-signal transducer and activator of transcription
<b>PTEN</b>	phosphatase and tensin homolog
<b>QKI</b>	quaking
<b>RBPs</b>	RNA-binding proteins
<b>RNA</b>	ribonucleic acid
<b>RNAi</b>	RNA interference
<b>RNA-seq</b>	RNA sequencing
<b>RNP</b>	ribonucleoprotein
<b>ROC</b>	receiver operating characteristic
<b>RT-qPCR</b>	reverse transcription-quantitative polymerase chain reaction
<b>SALL4</b>	spalt like transcription factor 4
<b>scRNA-seq</b>	single-cell RNA sequencing
<b>shRNAs</b>	short hairpin RNA
<b>SLC12A5</b>	solute carrier family 12 member 5

<b>SOX2</b>	sex determining region Y-box 2
<b>SYT1</b>	synaptotagmin 1
<b>TERT</b>	telomerase reverse transcriptase
<b>TGFβ</b>	transforming growth factor-β
<b>TME</b>	tumor microenvironment
<b>TMZ</b>	temozolomide (3,4-dihydro-3-methyl-4-oxo imidazole)
<b>TNC</b>	tenascin C
<b>TP53</b>	tumor protein p53
<b>tRNA</b>	transfer RNA
<b>TSCD</b>	Tissue-Specific CircRNA Database
<b>TTFields</b>	tumor-treating fields
<b>VEGFA</b>	vascular endothelial growth factor A
<b>WHO</b>	World Health Organization
<b>WNT1</b>	Wnt family member 1
<b>WNT2</b>	Wnt family member 2

## Table of contents

Acknowledgments .....	3
Funding .....	4
List of author's publications .....	5
List of abbreviations .....	6
Abstract.....	13
Streszczenie .....	15
1. Introduction.....	17
1.1. Circular RNA .....	17
1.2. General characteristic .....	17
1.2.1. Biogenesis .....	18
1.2.2. Cellular localization .....	20
1.2.3. Function.....	21
1.2.4. Expression pattern .....	25
1.2.5. Stability and degradation.....	27
1.3. CircRNAs in cancer.....	29
1.4. CircRNAs as a new class of biomarkers .....	33
1.5. CircRNAs as a new class of therapeutics .....	34
1.6. CircRNAs in GBM.....	36
1.7. General characteristics of tumors .....	39
1.8. Tumors of the Central Nervous System .....	40
1.9. General characteristics of glioblastoma .....	41
1.9.1. Symptoms.....	42
1.9.2. Diagnostics .....	43
1.9.3. Therapy.....	44
1.9.3.1. Surgical resection.....	45
1.9.3.2. Radiotherapy .....	46
1.9.3.3. Chemotherapy .....	47
1.9.3.4. TTFields.....	48
1.9.3.5. Immunotherapy .....	49
1.9.3.6. Gene therapy .....	49
1.10. Molecular characteristics of glioblastoma.....	50
1.10.1. Glioblastoma heterogeneity.....	52
1.10.2. Tumor microenvironment .....	53
1.10.3. Glioma stem cells .....	56
1.10.4. Epithelial to mesenchymal transition .....	57
1.10.5. Non-coding RNAs in glioblastoma .....	58
1.11. Models for advanced glioblastoma research .....	60
2. Research objective .....	65
3. Materials and Methods.....	67
3.1. Chemical reagents .....	67
3.2. Buffers .....	68
3.3. Ready-to-use reagents .....	68

3.4. Laboratory equipment .....	69
3.5. Software.....	70
3.6. Glioblastoma tissues.....	70
3.6.1. RNA sequencing .....	70
3.6.2. Estimation of the gene expression level of CLIP2 gene isoforms .....	72
3.7. Cell culture and cell culture procedures .....	72
3.7.1. <i>In vitro</i> culture .....	72
3.7.2. GBM cell lines .....	73
3.7.3. GBM spheroids .....	73
3.7.4. Organoids .....	74
3.7.5. Assembloids .....	75
3.8. Cryosectioning.....	76
3.9. Immunofluorescence .....	77
3.10. Transfection with siRNA .....	78
3.11. Hypoxia treatment.....	79
3.12. Cell proliferation evaluation.....	79
3.13. Wound healing assay.....	80
3.14. Invasion assay .....	80
3.15. EMT induction with TGF $\beta$ .....	80
3.16. Magnetic separation of glioma stem cells fraction.....	80
3.17. Extraction of total RNA and DNase treatment.....	81
3.18. Reverse transcription and quantitative RT-qPCR .....	81
3.19. Total RNA libraries preparation and RNA sequencing .....	84
3.20. CircRNAs identification by RNA-seq.....	84
3.21. CircRNAs retrieval from data repository .....	84
3.22. Glioblastoma molecular subtype analysis and circRNAs clustering .....	85
3.23. Statistical analysis of the results.....	85
4. Results.....	86
4.1. Functional characteristic of circRNA deregulated in GBM.....	86
4.1.1. Selection of circRNAs candidates for functional analysis in glioblastoma .....	86
4.1.2. Knock-down of CLIP2 gene transcripts.....	90
4.1.3. Functional assays upon CLIP2 gene transcripts knock-down.....	93
4.1.4. Induction of epithelial-to-mesenchymal transition .....	96
4.1.5. Expression level of CLIP2 gene transcripts in glioma stem cells .....	100
4.2. Global analysis of circRNAs landscape in glioblastoma .....	103
4.2.1. Identification of circRNAs in primary and recurrent glioblastoma with RNA sequencing .....	103
4.2.2. Selection of proper circRNAs for further research in primary GBM.....	105
4.2.3. Selection of proper circRNAs for further research in recurrent GBM.....	107
4.2.4. Clustering of glioblastoma tissues into molecular subtypes and the identification of subtype-specific circRNAs .....	109
4.3. Generation of assembloids as a complex model for glioblastoma invasion study .....	110
4.3.1. Generation of glioblastoma organoids .....	111
4.3.2. Generation of assembloids .....	112

4.3.3.	Characterization of assembloids by immunofluorescence .....	113
4.3.4.	Characterization of circRNAs landscape assembloids .....	116
5.	Discussion.....	118
5.1.	The role of circCLIP2 in GBM .....	118
5.1.1.	The impact of circCLIP2 on cell proliferation and motility.....	118
5.1.2.	Determination of potential circCLIP2 mode of action.....	120
5.2.	CircRNAs landscape in primary and recurrent GBM .....	121
5.2.1.	Characterization of circRNA landscape in GBM.....	122
5.2.1.1.	Primary GBM .....	122
5.2.1.2.	Recurrent GBM.....	123
5.2.2.	Molecular subtyping of GBM tissues.....	124
5.3.	Assembloids as complex GBM model for the tumor invasion study.....	125
6.	Conclusions.....	128
7.	Attachments .....	130
8.	References.....	133

## **Abstract**

One of the most prominent types of non-coding RNA – circular RNAs (circRNAs) is proposed to be a significant factor in the development and progression of several disorders, especially suggested as a key factor involved in tumorigenesis. CircRNAs role is widely linked with brain neoplasm development due to its high abundance, especially in the human brain, followed by great diversity, and tissue- as well as development-specific expression patterns. The key feature of circRNAs, which could justify their importance in tumorigenesis is also their distinctive, covalently closed structure lacking 5'-to-3' polarity, allowing it to exert its biological functions through binding to numerous types of molecules, including RNA, DNA, and protein.

Despite intensive scientific endeavors, glioblastoma (GBM) is a highly aggressive and malignant form of brain tumor, which remains a major challenge for clinicians and scientists. Notwithstanding recent discoveries regarding the GBM genetic characteristics, the conventional treatment of GBM involves only surgical tumor extraction, followed by temozolomide-based chemotherapy and further radiotherapy. Presented treatment methods emerge as ineffective in many cases due to the commonly observed treatment resistance, which ultimately leads to tumor recurrence. Several key GBM features support the failure of effective GBM therapy discovery. One of the major causes is high GBM heterogeneity, described at a cellular, molecular, histological, and clinical level, which potentially facilitates the very different responses to therapeutic agents and failure of targeted therapies. Additionally, a small population of glioma stem cells (GSCs) present within the specific tumor niche is frequently reported to be responsible for tumor growth, progression, and metastasis. Moreover, the tumor microenvironment (TME), a complex and dynamic ensemble of tumor cells that are surrounded by several types of non-tumor cells and the non-cellular components of extracellular matrix (ECM), is the key structural component, which rearrangement, supports the tumor invasion and metastasis. Furthermore, as a result of reciprocal cell-cell and cell-ECM interactions and tumor cell hijacking of non-malignant cells, stromal cells lose their functional phenotypes that support the growth and invasion of tumor cells. The acquisition of invasive phenotype in solid tumor tissue is frequently linked with the epithelial-to-mesenchymal transition (EMT) process, characterized by the loss of cell-cell adhesion and higher migratory and invasive potential of the tumor cells. As tumor development and its progression are highly complex processes, which lead to high genomic instability and multiple rearrangements, advanced molecular studies are still required to comprehensively understand underlying mechanisms.

Therefore, the objective of this research is to gain a more comprehensive understanding of the circRNAs role in the development and invasion process of GBM. The first part of the dissertation is devoted to the in-depth analysis of circCLIP2 function, as several reports highlight its significance in GBM onset and progression. A variety of functional assays was applied to indicate the circCLIP2 potential involvement in GBM cells proliferation, migration, and invasion, which are, on the other hand, linked with the epithelial-to-mesenchymal transition and glioma stem cells population appearance. The second part of the work is devoted to the identification of circRNAs exhibiting deregulated expression patterns in primary and recurrent GBM by RNA sequencing of GBM tissues, which were analyzed in parallel to the circCLIP2 functional analysis. The last part of the research was designated to the development and characterization of complex, three-dimensional GBM models. In the course of the research, two GBM models were generated – the GBM organoid, derived from the GBM patient tissue, and the assembloid, which states the GBM invasion model into healthy tumor-surrounding tissues. The assembloid model is comprised of the GBM organoid and the cerebral organoid grown in coculture into the assembloid. Despite the delivery of the novel research models, the aim was to generate a substitute for commonly used two-dimensional cell lines in the research related to the neoplastic invasion processes. Moreover, this model could potentially serve as a diagnostic screening platform for GBM invasion-hindering therapies.

## Streszczenie

Koliste RNA (circRNA), jedne z najbardziej znanych i obiecujących typów niekodujących RNA są jednym z istotnych czynników rozwoju wielu chorób, szczególnie powstawania nowotworów. CircRNA są powiązane z rozwojem nowotworów mózgu ze względu na ich obfitość, zwłaszcza w ludzkim mózgu, a następnie dużą różnorodność oraz poziom ekspresji charakteryzujący się wysoką specyficnością tkankową i rozwojową. Kluczową cechą circRNA, która mogłaby uzasadniać ich znaczenie w powstawaniu nowotworów, jest także ich charakterystyczna, kowalencyjnie zamknięta struktura pozbawiona polarności 5'-3', pozwalająca im pełnić swoje funkcje biologiczne poprzez wiązanie się z wieloma typami cząsteczek, w tym RNA, DNA i białkami.

Pomimo szeroko zakrojonych badań glijak wielopostaciowy jest wysoce złośliwą postacią guza mózgu, która pozostaje poważnym wyzwaniem dla klinicyстів i naukowców. Niezależnie od ostatnich odkryć dotyczących genetyki GBM, konwencjonalne metody leczenia glijaka obejmują głównie chirurgiczną resekcję guza, a następnie radioterapię oraz chemioterapię opartą na temozolomidzie. Przedstawione podejście terapeutyczne w wielu przypadkach okazuje się nieskuteczne ze względu na powszechnie obserwowaną oporność na leczenie, która ostatecznie prowadzi do nawrotu nowotworu. Kilka kluczowych cech GBM znacząco utrudnia odkrycie i rozwój skutecznej terapii GBM. Jedną z głównych przyczyn jest wysoka heterogenność GBM, opisana na poziomie komórkowym, molekularnym, histologicznym i klinicznym, co może prowadzić do zróżnicowanych reakcji na środki terapeutyczne i niepowodzenie terapii celowanych. Ponadto często podaje się, że niewielka populacja komórek macierzystych glijaka (GSC) jest odpowiedzialna za wzrost, progresję i przerzuty nowotworu. Co więcej, mikrośrodowisko nowotworu (TME), wysoce zróżnicowany zespół komórek nowotworowych otoczonych przez kilka typów komórek nienowotworowych i niekomórkowe składniki macierzy zewnątrzkomórkowej (ECM), jest kluczowym elementem strukturalnym, którego reorganizacja, promuje inwazję nowotworu i występowanie przerzutów. Ponadto, w wyniku wzajemnych interakcji typu komórka-komórka i komórka-ECM, komórki zrębowe tracą swoje funkcjonalne fenotypy, co wspiera wzrost i inwazję komórek nowotworowych. Nabycie inwazyjnego fenotypu w tkance guza litego jest często powiązane z procesem przejścia nabłonkowo-mezenchymalnego (EMT), charakteryzującego się utratą adhezji komórkowej oraz wzrostem potencjału migracyjnego i inwazyjnego komórek nowotworowych. Ponieważ rozwój nowotworu i jego progresja są procesami niezwykle złożonymi, prowadzącymi do dużej niestabilności genomu i licznych rearanżacji, nadal

niezbędne są zaawansowane badania molekularne, aby kompleksowo zrozumieć leżące u ich podstaw mechanizmy.

Z wymienionych względów celem przedłożonej dysertacji jest analiza roli circRNA w procesie rozwoju i inwazji GBM. Pierwsza część rozprawy poświęcona jest dogłębnej analizie funkcji circCLIP2, ponieważ w doniesieniach literaturowych podkreślone zostało znaczenie circCLIP2 w rozwoju i progresji GBM. Zastosowano testy funkcjonalne, aby wykazać potencjalny udział circCLIP2 w proliferacji, migracji i inwazji komórek GBM, które potencjalnie mogą być również powiązane z przejściem epithelialno-mezenchymalnym i obecnością populacji komórek macierzystych glejaka. Druga część pracy poświęcona została identyfikacji circRNA wykazujących odbiegające od normy wzorce ekspresji w pierwotnym i wtórnym glejaku wykorzystując metodę sekwencjonowania RNA tkanek GBM, które analizowano równolegle z analizą funkcjonalną circCLIP2. Ponadto dokonano również klasyfikacji tkanek GBM poddanych sekwencjonowaniu RNA na cztery opisane w literaturze podtypy glejaka, co umożliwiło dalszą analizę profilu ekspresji circRNA w zidentyfikowanych podtypach. Ostatnia część badań została poświęcona opracowaniu i charakterystyce złożonych modeli GBM. W trakcie przeprowadzonych badań wygenerowano dwa modele GBM – organoid GBM pochodzący z tkanki pacjenta oraz asembloid, który stanowi nowoczesny model inwazji glejaka w zdrową tkankę mózgową. Model asembloidu składa się z organoidu GBM i organoidu mózgowego hodowanych jako ko-kultury do czasu uformowania asembloidu oraz ustalenia wczesnych i późnych zjawisk związanych z inwazją komórek nowotworowych. Pomimo stworzenia nowatorskich modeli badawczych, celem było wygenerowanie substytutu powszechnie stosowanych dwuwymiarowych linii komórkowych w badaniach związanych z procesami inwazji nowotworów. Co więcej, model ten mógłby potencjalnie służyć jako platforma diagnostyczna do badań przesiewowych w zakresie terapii przeciwnowotworowych.

# **1. Introduction**

## **1.1. Circular RNAs**

Circular RNAs (circRNA) – a class of single-stranded and ubiquitously expressed RNAs have been extensively studied in the last decade as they emerged as powerful transcription and translation regulators, exhibiting strong potential in glioblastoma diagnostics and therapy (1), (2). Circular RNAs were first discovered in the 1970s as infectious and covalently closed RNAs detected in plant viroids (3). It was also reported that circRNAs were circularized independently of their mRNA counterparts (4) Later, it was discovered that these molecules are also present in eukaryotic organisms. However, they were widely considered splicing intermediates or artifacts (5–7).

Recent advances in next-generation sequencing technology allowed the identification of thousands of endogenous circular RNAs in various species, including mammals (8,9). A significant breakthrough in the study of the circRNAs occurred in 2013 when Salzman's group provided evidence that some human transcripts prefer a circular form over a linear one, which was supported by data provided by Rybak-Wolf and colleagues indicating that certain transcripts exhibit a reciprocal expression pattern of circular and linear isoforms during differentiation (10,11). Currently, extensive research is being conducted to establish the exact mechanisms of circRNAs function, especially in human diseases, as circular transcripts are widely deregulated in pathological conditions (10,12)

## **1.2. General characteristic**

One of the major characteristic features of circular transcripts is that they differ structurally from other types of RNAs. CircRNAs lack a 3' poly(A) tail, and 5' cap and their ends are covalently joined, which leads to the formation of a covalent bond between both ends of the transcript known as a back-splice junction (BSJ) site or 'head-to tail' splice junction (13–15). The covalent bond formation supports higher circRNAs stability against enzymatic degradation than their mRNA counterparts. This can further imply the circRNAs functions, especially the ones related to circRNAs' action as competing endogenous RNAs (ceRNAs) - RNAs, which have the capacity to regulate gene expression by acting as miRNAs sponges(16).

It has been demonstrated that circRNAs are generated co-transcriptionally, in competition with mRNA production (16,17). As a result, the production of circRNA might lead to a decrease in mRNA synthesis from the same gene locus, acting as an RNA trap and hindering mRNA production (18). CircRNAs biogenesis is most commonly facilitated by the impact of

cis-acting elements and trans-acting factors that lead to the formation of four types of circRNAs derived from exonic and intronic sequences of primary transcripts, namely exonic circRNAs - EcRNAs, exon-intron circRNAs - EIciRNAs, intron-derived circRNAs, and intergenic circRNAs (19–21). Due to such a wide variety of origins, circRNAs can arise from nearly any part of the genome, resulting in significant variances in molecule length and generation of multiple circRNAs isoforms (22). The circRNAs' specific structure and ability to act as global regulators yield wide networks of interactions. Therefore, circRNAs draw considerable interest in RNA research.

Currently, their importance and function in health and disease, followed by susceptibility to state biological markers and therapeutic targets, are widely investigated. Up to now, several circRNAs functions have been discovered. CircRNAs are reported to serve as global regulators and are recognized to act as a miRNA sponge, which hinders miRNAs binding to the target genes (23). This process, in turn, reduces the inhibitory effect of miRNAs post-transcriptional regulation of gene expression. CircRNAs have the ability to bind not only miRNAs but also RNA-binding proteins (RBPs), which sequestration leads to the disrupted regulation of downstream RBP-target genes (24). Interestingly, it has been demonstrated that exonic circRNAs contain more RBP binding sites than the same non-circularized exons in mRNA (25). This was evidenced to lead to the prevalence of RBPs binding to some circRNAs, than to the corresponding mRNA, which was also reported to occur in a cell-type-specific manner (25). Furthermore, some circRNAs might serve as a template for protein synthesis, encoding functional peptides, which can be translated *in vitro* and *in vivo*. CircRNA-derived peptides might be further regulated by the same host circRNA by protein sponging or compete with their cognate protein isoforms derived from corresponding mRNA for binding molecules (26–28). The process of miRNA and RBP sponging led to the emergence of novel circRNAs research area – circRNAs engineering, aiming to design and produce artificial circRNAs for functional research purposes and clinical (29–31). CircRNAs are recognized to play an important regulatory role in healthy cells as well as in various human diseases, including cancer, and currently, much research focuses on circRNAs role in pathologies, as well as in prognostics, diagnostics, and clinical treatment (32–36)

### **1.2.1. Biogenesis**

Circular RNAs (circRNAs) state a noncoding RNA type with a distinctive single-stranded, covalently closed RNA structure (37). This unique structure is formed by reverse splicing of pre-mRNAs, distinguishing it from other RNA types. Several mechanisms of

circRNAs biogenesis are suggested in the literature, which allows the researchers to distinguish four major pathways: lariat-driven circularization, intron-pairing-driven circularization, circular intronic RNA, and RNA binding proteins (RBPs)-driven circularization (38–40).

Lariat-driven circularization relies on exon skipping events, where the spliced intron lariat retains the skipped exon or exons (41,42). During the transcription, the pre-mRNA is partially folded, bringing the downstream 5' back-splice site and an upstream 3' back-splice site, leading to the formation of covalently closed circRNAs instead of joining upstream 5' splice site with a downstream 3' splice site, as in canonical splicing (43–46). This process is called back-splice, the most common pathway of circRNAs biogenesis. Back-splicing results in covalent bond formation between a 3' splice donor and a 5' splice acceptor, leading to the formation of a lariat structure and the remaining exons, which undergo splicing, and further form a corresponding linear mRNA (47). Even though the formation of circRNAs is a different process from canonical splicing, the formation of a covalent bond occurs at a site flanked by canonical splice signals. It is catalyzed by the same canonical spliceosomal machinery, which might suggest their co-occurrence and/or competition of linear and circular transcript biogenesis (48–50).

Another mechanism of circRNAs biogenesis leads to the emergence of circular intronic RNA via the intron lariat formation during splicing. Lariat-derived circRNAs usually contain GU-rich elements near the 5' splice site and C-rich elements near the branch point, facilitating its stability and allowing it to escape debranching (51,52). Moreover, circRNAs generation might be supported by cis-regulatory elements and trans-acting factors, promoting the process of bringing the transcript ends to close proximity and its subsequent circularization (53,54).

Interestingly, the bioinformatic reports evidence that the circRNAs biogenesis might be facilitated by the most abundant, transposable, and primate-specific repeat element in the human genome - Alu elements (55–58). This particular mechanism of circRNAs biogenesis is known as intron-pairing-driven circularization, which is usually mediated by the base-pairing of the complementary sequence motifs. The presence of cis-regulatory elements, such as the abovementioned Alu elements, results in the formation of an exonic circRNA or an exon-intron circRNA (59).

Moreover, the *trans*-acting factors, most commonly in the form of RBPs, are reported to facilitate the formation of circular transcripts. It is frequently observed that the presence of RBPs, which bind to the flanking sites of the transcript, shorten the distance between both ends by the dimerization of the protein, leading to the generation of a closed molecule based on complementary base pairing (60,61). So far, several RBPs have been depicted to mediate

circRNAs biogenesis through RBPs-driven circularization. Among them, Muscleblind-like (MBNL), Quaking (QKI), and Fused in Sarcoma (FUS) proteins have been reported to be the most frequent mediators (62–64). Interestingly, MBL has been found to bind to the circRNA derived from its host gene, specifically – circMbl, thus circMbl biogenesis is strongly dependent on the presence of binding sites for MBL in the introns flanking the circularized exons (65). As evidence, it has been confirmed that the overexpression of fly MBL enhances circMbl biogenesis and, on the contrary, the reduction of MBL in mammalian cell culture and fly neural tissue diminished the circMbl expression level (66). Furthermore, another circRNA biogenesis regulator – QKI, has been reported to be a major regulator of circRNA biogenesis during the EMT process (67). Interestingly, QKI has been shown to be sufficient to lead to the circularization of exons that, in normal conditions, undergo canonical splicing. At the same time, the binding sites for QKI are introduced in the flanking region of exons (67). The N-terminal domain of QKI brings the free ends of the close proximity to enable the dimerization of the QKI, facilitating RNA circularization even if the target sites are distant within the RNA sequence (68). Furthermore, FUS protein plays a significant role in splicing regulation, most commonly through interaction with multiple splicing factors, and has been shown to be one of the molecules involved in amyotrophic lateral sclerosis (ALS) and frontotemporal dementia (69). FUS mutations result in the translocation of proteins from the nucleus to the cytoplasm and the subsequent formation of inclusion bodies in the cytoplasm (70). It has been reported that FUS-dependent circRNA biogenesis relies on FUS binding the introns flanking the sequence, which is supposed to form a back-splice junction, and this type of circRNA biogenesis regulation might also be reproduced in artificial circRNAs design (69).

### **1.2.2. Cellular localization**

Two major compartments can be distinguished in eukaryotic cells - the nucleus, where RNAs are transcribed and processed, and the cytoplasm, where some RNAs are translated into proteins (71). Considering the abovementioned, some types of RNAs are exported from the nucleus to the cytoplasm to perform their function - protein synthesis or maturation into functional molecules (72). Small RNAs like tRNAs and miRNAs bind directly to exporting receptors. However, large RNAs like ribosomal RNAs and mRNAs assemble into complexes with ribonucleoprotein (RNP) to recruit their exporters (73). It is important to underline that the nuclear export of long RNAs is reportedly dependent on factors recognizing a 5' cap (74). Surprisingly, circRNAs, even though they do not possess a 5' cap are also abundant in the cytoplasm (75,76). In the past, it was thought that circRNAs emerge most commonly in the

cytoplasm, which is connected with their reported functions such as acting as miRNA and RBP sponges and regulators of transcription, translation, splicing, protein decoys, scaffolds, and recruiters, followed by serving as a template for protein synthesis (77–80). Although mature circRNAs tend to accumulate in the cytoplasm, little is still understood about their nuclear export pathways to the cytoplasm, as circRNAs lack several of the common signals, which are substantial for mRNA export (81,82).

Up to now, only one potential mechanism of circRNAs nuclear export has been proposed based on the study conducted on flies. Zhengguo and colleagues reported that the depletion of the *Drosophila* DExH/D box helicase Hel25E led to the nuclear accumulation of a circdati circRNA reaching 1120nt, but not of a circclaccase2 circRNA reaching 490nt, both of which are predominately localized to the cytoplasm (83). Their finding was confirmed by further investigation of 12 other endogenous circRNAs, which vary in length, showing that the depletion of Hel25E, *Drosophila* DExH/D box helicase, led to nuclear accumulation of long (>800nt) but not short (<702nt) circRNAs. The hypothesis of the length-dependent mechanism of nuclear export of circRNAs was also investigated in human cells showing that two human orthologues of *Drosophila* Hel25E - UAP56 and URH49 are exclusively responsible for exporting long and short circRNAs, respectively. This is further supported by identifying four amino-acid regions unique to UAP56 and URH49, which are crucial in determining their circular RNA length preferences. Moreover, they also demonstrated that the nuclear export of circRNAs is an evolutionarily conserved process that is length-dependently regulated by *Drosophila* Hel25E and its human homologs - UAP56 and URH49(83). Recent studies also indicate that circRNAs are widely distributed among other subcellular fractions than the nucleus and cytoplasm, like the ribosome fraction, cytosol, exosome, and mitochondria. However, the export to those compartments is even less characterized (84,85). It is noteworthy that studies performed on hepatocellular carcinoma cell line - HepG2 show that the population of circRNAs varies in specific fractions, depending on their classification (exonic, intronic, or exonic-intronic) and factors such as GC content, length, alternative circularization, and parental gene function (86,87).

### **1.2.3. Function**

CircRNAs have been reported to play significant roles in various cellular processes both in healthy and pathological conditions (88,89). Several studies describe circRNAs as global regulators of multiple cellular processes due to the large network of circRNAs interactions (90–93).

CircRNAs are strongly recognized to affect the function of miRNA due to the presence of several binding sites allowing the interaction to occur (94–96). This process obstructs miRNAs from binding to their target molecules, leading to the increased expression of miRNA target genes (97,98). A single circRNA can bind with one or several different miRNAs, and also one circRNA might have multiple binding sites for each of specific miRNA (99). A widely investigated example of miRNA sponging mechanism and its consequences is CDR1as, a circRNA in the form of circularized long noncoding RNA (lncRNA). CDR1as is significantly enriched in the mammalian brain and is evidenced to possess more than 70 binding sites for miR-7 (100,101). It has been reported that the Cdr1as knockout impaired the ability to filter out unnecessary information, known as sensorimotor gating, which is associated with neuropsychiatric disorders (100). The mechanism of miRNAs binding by circRNAs is widely studied and described in regard to human diseases, including cancer. As miRNAs deregulation has been comprehensively described in pathological conditions, circRNAs state another player leading to even deeper disruption of the regulatory network in disease but also could state the partial explanation of miRNAs functional disturbance, which supports its function as a promising candidate for potential therapeutic target (102–104).

Interestingly, a similar mode of circRNAs action has been observed for RBPs, as most commonly, they also possess circRNAs binding sites allowing the sponging to occur (105,106). This type of interaction is essential in light of recent reports showing that RBPs have been recognized to be involved in almost all phases of the circRNA lifecycle, being engaged in circRNAs biogenesis, translation, transcriptional regulation of target genes, and extracellular transport (107). Nowadays, a number of bioinformatic prediction tools have been developed to facilitate the identification of circRNA - RBP interactions and the determination of their biological consequences, such as iCircRBP-DHN (108), CRIP (109) or CircInteractome (110). Despite RBP's contribution to circRNAs biogenesis, which was widely investigated mainly for MBNL, FUS, and QKI proteins, RBPs also played a role in circRNAs degradation. Some circRNAs have been shown to be susceptible to being degraded by nucleases, such as RNase H, Rrp44, and RNase L, upon preceding m<sup>6</sup>A modification or poly(I:C) stimulation (111–113). Moreover, the GW182 protein is also involved in the degradation of multiple circRNAs in a number of species, including human (114). CircRNAs interacting with RBPs might also serve as protein decoys, where circRNAs cooperate with the target protein to modulate its function. One of the examples of circRNA acting in an abovementioned way is circ-Amotl1, which is able to retain c-Myc in the nucleus by its binding, leading to the upregulation of c-Myc target genes, which in turn promotes the tumorigenesis by contributing to the increased cell

proliferation and reduced apoptosis (115). The previously mentioned interaction of circRNAs with MBL1 protein is a descriptive example of a broad and complex regulatory network of circRNAs. CircRNAs can facilitate posttranscriptional regulation by sequestering RBPs - MBL1 protein in this example (116,117). As stated previously, MBL1 is engaged in the biogenesis of several circRNAs, but interestingly it might also promote the circularization of the second exon of its pre-mRNA, generating circMbl. It has been reported that circMbl generation competes with mRNA production, leading to the reduced expression level of the MBL1 protein. This, in turn, leads to more efficient Mbl mRNA splicing, reducing the circMbl production; however, as the MBL1 expression increases, it binds to Mbl pre-mRNA to induce transcript circularization. Additionally, circMbl might act as an MBL protein sponge, as it possesses MBL binding sites, which leads to MBL protein sequestration and hinders its production. Therefore, circMbl is capable of regulating its expression by the sequestration of RBPs generated from its parental gene (28,118–120).

CircRNAs have been reported to have a wide regulatory role in the transcriptional regulation of their host genes, most commonly by binding to RNA polymerase II (Pol II), recruiting proteins, or forming an R-loop to target the transcriptional regulatory regions of their host genes (121). Binding to RNA polymerase II in the promotor region allows the circRNA to influence their host gene transcription's initiation and elongation step. It has been shown that some intron and exon-intron circRNAs are frequently enriched in the nucleus and might be associated with Pol II, modulating its activity. Two exon-intron circRNAs - circEIF3J and circPAIP2, were reported to presumably interact with Pol II, U1 snRNP, and host gene promoters to increase the transcription of their host genes by forming a positive feedback loop (122). Interestingly, the interaction with other molecules affects not only downstream processes like the repression of miRNA-dependent target mRNA regulation but via the interactions of circRNAs with other molecules; they might also affect their parental gene expression (123,124). The abovementioned interaction of circRNAs with RBPs allows them to act as protein decoys, scaffolds, and recruiters to gather single or multiple proteins to the target promoter region and modulate the host gene transcription (121). CircRNAs can both inhibit or activate the transcription of their host gene. For instance, circ0005276, derived from the *XIAP* gene, can recruit the FUS to the promoter region of the host gene *XIAP* and activate the expression of XIAP, leading to the onset and development of prostate cancer (125). On the contrary, the circ-HUR expression level was found to be reduced in gastric cancer tissues and cell lines and interacted with the CCHC-type zinc finger nucleic acid binding protein (CNBP) to hinder its binding to the HuR promoter, inhibiting the transcription of HuR (126). This led to the reduction

of its host gene HuR and the repression of gastric cancer development. The regulation of parental gene expression level by circRNAs was also reported to occur via splicing regulation, mRNA traps, translational modulation, and post-translational modification (127). As protein scaffolds, circRNAs might support the interaction of two or more proteins. This process was investigated in circ-Foxo3, revealing its ability to bind to p53 and the Mdm2 - E3 ubiquitin-protein ligase to facilitate Mdm2-induced ubiquitination and degradation of p53 (128). R-loops state an RNA-DNA hybrid and a displaced single-stranded DNA, usually generated by RNA polymerase pause or RNA biogenesis malfunction. R-loops play a wide role in genome stabilization and might interfere with DNA replication, repair, and transcription (129–131). It has been shown that circRNAs forming R-loops are capable of homologous exon-defective mRNA cleavage, which affects mRNA abundance and provides an mRNA trap to suspend transcription (121). circSMARCA5 has the potential to regulate host gene expression through R-loop formation during tumor development - circSMARCA5 is recruited to its host gene SMARCA5 locus to form an R-loop, which terminates the transcription, leading to the diminished expression level of SMARCA5 and the generation of nonfunctional  $\Delta$ SMARCA5 protein (132).

Due to the lack of 5' cap and 3' poly(A) tail circRNAs have been thought to state a non-coding class of RNA with widespread regulatory functions instead of RNAs that have the potential to encode proteins. However, recent studies led to the discovery of internal ribosome entry site (IRES) elements in several circRNAs sequences, which can directly recruit ribosomes and therefore are known to alternative state sites of translation initiation (133,134). In the process of the cap-independent mechanism of translation initiation led through IRES recognition, a non-standard eIF4G protein identifies the IRES, which mediates the eIF4 complex assembly and starts the translation (135,136). Up to now, more than 17,000 endogenous and synthetic sequences were identified as presumable circRNA IRES in an artificial oligo library comprising only a subset of endogenous circRNA sequences (137). Interestingly, another potential mechanism of the cap-independent translation of circRNAs was identified in eukaryotic cells – N6-methyladenosines (m6A)-mediated cap-independent mechanism (138). This pathway requires the presence of YTH domain-containing family protein 3 (YTHDF3), which states an m6A reader protein that can further interact with eIF4G2, recognizing IRESs and initiating the assembly of eIF4 complex (139,140). Moreover, it has been reported that circRNA translation might also be initiated at the IRES-like sites identified as hexamers, which in human are highly enriched in circRNAs compared to the entire pool of linear RNAs (141). The advanced bioinformatic approach allowed to identify 97 IRES-like

elements, which account for approximately 2% of all identified hexamers. Therefore, the presence of IRES-like sites can fulfill the cap-independent translation of circRNAs along with the IRES elements. Even though the molecular mechanism of circRNA translation remains largely unknown, the important role of circRNA as global regulators might also be fulfilled by the ability of circRNAs to be translated, leading to deeper disruption of the circRNA/miRNA/mRNA axis and other poorly understood mechanisms of circRNAs action. As circRNAs have been greatly recognized for their role as regulatory molecules in human pathologies, their protein-coding potential still raises questions about the functions of their protein products. RNA circularization allows for the generation of novel, alternative variants of proteins that differ in action from their full-length forms, which greatly supports protein variability. PINT87aa - 87 amino acids long protein states an interesting example of a peptide derived from the circular form of exon 2 of the non-protein-coding RNA LINC-PINT, as it operates independently of both its circRNA and the linear form of LINC-PINT (141). PINT87aa has been shown to regulate the transcriptional elongation of multiple oncogenes by interfering with the polymerase-associated factor 1 (PAF1), responsible for RNA polymerase II recruitment. The downregulation of PINT87aa was reported to lead to the improper localization of PAF1, suggesting that PINT87aa might stabilize the PAF complex on the target promoter and hinder the Pol II-dependent mRNA elongation. Interestingly, a diminished amount of PINT87aa has been linked with high tumor invasiveness, which was observed in a variety of neoplasms, including glioblastoma displaying the lowest expression of PINT87aa in comparison to the healthy reference (142). A comprehensive study on PINT87aa shows that circRNAs, not only themselves but also their translation products – circRNA-derived proteins might state a promising carcinogenesis biomarker or therapeutic target (143–145).

#### **1.2.4. Expression pattern**

The advancements in next-generation sequencing (NGS), as well as other improvements in genome biology such as the availability of complete genome sequences, allow the researchers to find out that despite various cellular localization of circRNAs, they also exhibit complex cell-, tissue-, and developmental stage-specific expression patterns (146–148). To determine and understand the functions of circular transcripts, it is important to get an insight into the specific pattern of its expression.

In 2013, Salzman and colleagues reported discovering cell specificity of circRNAs expression (149). Subsequently, Xia and colleagues revealed over 300 thousand tissue-specific circRNAs identified in adult human tissues, human fetal tissues, and mouse tissues, among

which 11.9% of circRNAs in the human adult, 10.4% in the human fetus and 34.3% in mouse were determined as tissue-specific (150). In adult humans, they observed a high abundance of tissue-specific circRNAs in the esophagus, heart, intestine, and liver, whereas in human fetal circRNAs were enriched in the brain, skeletal muscle, and uterus. In mouse tissues, they found it abundant in the brain and testis. Moreover, they also determined that tissue-specific circRNAs emerging in the human adult amounted to 69.2%, 22.6%, and 8.2% of exonic, intronic, and intergenic circRNAs, respectively. Data provided by Xia and colleagues was used to create an integrated TS circRNA database called TSCD (Tissue-Specific CircRNA Database), which possesses information on genomic location and species conservation, and predicts the association of circRNAs with microRNA and RNA binding proteins (150).

One of the breakthrough studies of Rybak-Wolf and colleagues greatly highlights circRNAs cells-, tissue- and developmental stage-specificity followed by the abovementioned differential cellular localization of circRNAs (9). Identifying circRNAs landscape in the human frontal cortex, thyroid gland, liver, and muscle provided evidence that circRNAs are more abundant in the mammalian and mouse brain than in other types of tissues. Moreover, the authors utilized publicly available mouse circRNA expression data obtained from different areas of the brain - olfactory bulb, prefrontal cortex, hippocampus, and cerebellum, revealing an overall enrichment of circRNA expression in the cerebellum, which shows a higher density of neuronal cells compared to other brain regions. To support the developmental stage-specificity, they investigated early neuronal cell specification using established cell culture models for neuronal development: mouse P19 embryonal carcinoma (EC) and human neuroblastoma cells - SH-SY5Y. They observed deregulation of circRNA expression during neuronal differentiation revealing 238 downregulated and 1,116 upregulated circRNAs during P19 embryonal carcinoma differentiation and 797 and 1,926 during primary neuron maturation of neuroblastoma cells - SH-SY5Y, respectively (9). Three independent studies confirmed that many circRNAs are enriched specifically in the brain tissue, and their expression level increase during neuronal development and differentiation (151–153), which is even highly manifested in aging animals, accumulating large amounts of circRNAs (18,154,155).

The most recent data regarding circRNAs expression pattern greatly benefit from developing highly advanced genomic technologies like single-cell RNA sequencing (scRNA-seq), which facilitate the study's higher resolution. An interesting study was reported by Wu and colleagues, where they analyzed public full-length scRNA-seq datasets from 58 human and mouse tissues or cell types, along with several bulk RNA sequencing (RNA-seq) circRNA databases (156). The study showed that approximately 32% of circRNAs were present in both

datasets, while the remaining 68% were only detected in single-cell data. Additionally, around 90% of scRNA-seq-specific circRNAs were expressed in fewer than 10 cells in both human and mouse samples, making them almost impossible to detect using bulk RNA-seq techniques. To detect the tissue- and cell-specific circRNAs, they gathered the scRNA-seq data from 17 different human and mouse tissues and cognate cancer samples, followed by bulk normal and tumor RNA-seq datasets. In total, there were 12,625 circRNAs found in one specific cell type. Among these, 6,623 circRNAs, which is approximately 52%, were also found in the bulk RNA-seq. These circRNAs were detected in various tissues and samples, indicating their potential as biomarkers for classifying cell types. Around 50% of circRNAs were expressed in more than 50% of cells or multiple cell types, suggesting their role as "housekeeping" circRNAs in specific tissues or cell types. Interestingly, several orthologous cell-type-specific circRNAs between human and mouse cells were also detected, implying the conserved biological function of these circRNA subsets. This study is of extraordinarily high biological value, as it underlines the high sensitivity and resolution of scRNA-seq to reveal circRNAs with cell specificity, which on the other hand, could not be detected in bulk RNA-seq samples due to the relatively lower number of expressing cells (156).

As circRNAs have been reported to be highly enriched in brain tissue, endeavors were made to investigate particular populations of brain cells. A study delivered by Curry-Hyde and colleagues presented a comprehensive analysis of the circRNA landscape in human brain glial cells - astrocytes, microglia, and oligodendrocytes. They found that astrocytes and oligodendrocytes show similar pattern and characteristics of circRNAs expression, whereas microglia-specific circRNAs are functionally distinct from other types of investigated cells (157). In total, utilizing two different circRNAs detection tools, 652 circRNA were identified in astrocytes, 315 in microglia, and 830 in oligodendrocytes, while 265 were unique to astrocytes, 239 to microglia, and 442 to oligodendrocytes. Interestingly, only 45 circRNAs were commonly expressed in all analyzed cell types. Moreover, the most abundant circRNAs in investigated glial cell types were identified as exonic types and most widely display a negative correlation with their linear counterparts' expression pattern, suggesting the preference of spliceosome activity towards the back-splicing mechanism instead of a canonical splicing activity (157).

### **1.2.5. Stability and degradation**

The presence of covalent bond and the resulting absence of free ends containing structures typical for processed and mature RNA transcripts significantly impacts the circRNAs

persistence in the cell and the degradation process. Studies have shown that covalently closed transcripts are more stable than their linear counterparts, as their closed structure protects ends from de-adenylation and de-capping (158).

Harland and Misher in 1988 reported that circRNAs are highly stable *in vitro*, with half-lives lasting over 40 hours. Enuka and colleagues supported this finding in a study showing that the half-lives of 60 investigated circRNAs and their linear counterparts exhibited that the median half-life of circRNAs ranged from 18.8 to 23.7 hours. This was evidenced to be at least 2.5 times longer than the median half-life of their linear counterparts, reaching from 4.0 to 7.4 hours (159). The authors suggest that one of the potential explanations for circRNAs' longer half-life compared to their corresponding mRNA is the slow response of circRNAs to cellular processes and cell environment dynamics. Furthermore, the studies show a limited possibility of modulating the circRNAs half-life using various types of molecules. It has been demonstrated that in human fibroblast cell line - Hs68, treated with actinomycin D, an inhibitor of transcription, the four investigated exonic circRNAs (circHIPK3, circKIAA0181, circASXL1, circLPAR1) are more stable than the corresponding circular transcripts and display a half-life of exceeding 48 hours (160). However, it is important to note that the prolonged actinomycin D-driven transcription inhibition might lead to changes in cell physiology and cell death, affecting the study's accuracy. Furthermore, the abovementioned study of Enuka and colleagues shows that circRNAs early response to the EGF treatment of the human epithelial cells - MCF10A is little to no compared both to mRNAs and miRNAs landscape, but also in comparison to the corresponding mRNA, which is expressed from the same host genes (159).

Despite the numerous studies aiming to identify circRNAs biogenesis, the process of circRNAs degradation still requires extensive investigation. However, a few pathways for specific circRNA degradation have already been proposed and are presented in Table 1. One of the well-known pathways of circRNAs degradation is small RNA-mediated degradation, which Hansen and colleagues extensively describe. The study reveals that CDR1as, one of the widely studied circular RNA, might be degraded by miR-671 with the help of Argonaute 2 (Ago2) (161). Furthermore, one of the novel and extensively studied areas of circRNAs research is the ability of circRNA molecules to be sorted into extracellular vesicles (EVs), such as exosomes or microvesicles to be transferred from donor cells to recipient cells, to facilitate cell-to-cell communication or to be eliminated from the cell by excretion (162–164). It has been found that circRNAs are more abundant in EVs than their linear counterparts, which supports the idea that it might be a potential mechanism by which cells eliminate circRNAs. CircRNAs, which circulate in exosomes, have also been suggested to state a promising diagnostic biomarker or

therapeutic target in cancer treatment (165–167). The abovementioned pathways of circRNAs degradation are presented in Table 1.

Pathway	Location	Interactor	Reference
Endonuclease-mediated degradation	Nuclear/cytoplasm	RNase H1, Template DNA strand/ RNase L, PKR	(168,169)
Ago2-mediated degradation	Nuclear	miRNA, Ago2	(95,170,171)
GW182-mediated degradation	-	GW182	(114)
m6A modification-mediated degradation	Cytoplasm	YTHDF2, HRSP12, RNase-P/MRP	(172–174)
Structure-mediated degradation	Cytoplasm	G3BP1, UPF1	(175)
TMAO-mediated degradation	Cytoplasm	TMAO	(176)
Exosome-mediated degradation	Extracellular space	Exosomes and Microvesicles	(177)

**Table 1. Potential pathways of circRNA degradation.** Based on Ren, L., Jiang, Q., Mo, L. et al. (162)

### 1.3. CircRNAs in cancer

Considerable attention is still paid to comprehending the biogenesis, expression pattern, and detailed functional mechanisms associated with the physiological role of circRNAs in human diseases, especially in cancer. The significant improvement in this area of research was facilitated mainly by the development of advanced genomic technologies, followed by novel genome-wide bioinformatics approaches. Despite the extensive circRNAs research, important issues still need to be thoroughly addressed, such as what are the detailed mechanisms determining circRNA localization within the cell, what the exact biogenesis mechanism looks like in the majority of circRNAs – are they generated co-transcriptionally or post-transcriptionally, and what the actual or general molecular mechanisms on circRNA biogenesis, distribution at different development stage and degradation, which even more importantly should be addressed in the course of understanding circRNAs role in disease (178,179). The abovementioned processes are of great value for establishing the circRNAs role in disease, especially as recent studies show that circRNAs might be involved in many diseases via the deregulation of the circRNA-miRNA-mRNA axis. Studies have shown that changes in circRNA

expression pattern are not limited to cancer but are also identified in neurodegenerative disorders like Alzheimer’s disease, various cardiac diseases like heart failure, autoimmune thyroid diseases, and diabetes, as well as natural cellular processes such as embryonic development, cell cycle regulation, cell signaling, and senescence (180–182).

In cancer, circRNAs have been shown to act as oncogenes or tumor suppressors (183,184). Circular transcripts are reported to be more often downregulated in cancer patients compared to the healthy control, which is most commonly justified by the diminished circRNAs expression level caused by the increased cell proliferation or the back-splicing machinery errors and circRNAs degradation (185). They have also been found to regulate all of the key hallmarks of cancer, such as cell proliferation, migration, apoptosis, invasiveness, and drug resistance, therefore, directly or indirectly influencing tumor growth and progression (186–189). The expression pattern, role, and potential mechanism of action of circRNAs identified as significant in various types of cancer have been depicted in Table 2. The obtained data suggest that even though circRNAs are most commonly downregulated in cancer, their significant upregulation is most commonly shown to promote tumorigenesis.

Cancer type	CircRNA	CircRNA expression level	Pathway and Biological Function	Reference
Bladder carcinoma	circTCF25 circ_0002623 circKDM4C	Up	circTCF25-miR-103a-3p/miR-107-CDK6 axis promotes proliferation and migration; circ_0002623-miR-1276/SMAD2 axis promotes progression; circKDM4C-miR-200bc-3p/ZEB1 axis enhances invasion and metastasis	(190–192)
	circLAMA3	Down	circLAMA3-MYCN inhibits the proliferation, migration, and invasion	(193)
Breast cancer	circABCB10 circEPSTI1	Up	circABCB10-miR-1271 interaction promotes progression; circEPSTI1-miR-4753/6809-BCL11A axis impacts proliferation and apoptosis	(194,195)
	circ-Foxo3	Down	circ-Foxo3-p53/MDM2 modulates the ubiquitination	(128)
Cervical cancer	circNRIP1 circ0001955	Up	circNRIP1-miR-629-3p/PTP4A1/ERK1/2 axis promotes migration and invasion; circ0001955-miR-188-3p/NCAPG2 axis promotes tumorigenesis and metastasis	(196,197)

	hsa_circ_0043280	Down	hsa_circ_0043280-miR-203a-3p/PAQR3 axis inhibits tumor growth and metastasis	(198)
Colorectal cancer	circLDLR circFAT1(e2)	Up	circLDLR-miR-30a-3p/SOAT1 axis facilitates cancer progression; circFAT1(e2)- miR-30e-5p/ITGA6 axis promotes tumorigenesis	(199,200)
	circLRCH3 cir-ITCH	Down	circLRCH3/miR-223/LPP axis inhibits proliferation, migration, and invasion; cir-ITCH has an inhibitory role by regulating the Wnt/ $\beta$ -catenin pathway	(188,201)
Hepatocellular carcinoma	hsa_circRNA_104348	Up	hsa_circRNA_104348- miR-187-3p/RTKN2 axis promotes progression and activation of Wnt/ $\beta$ -catenin pathway	(202)
	hsa_circ_0098181	Down	hsa_circ_0098181 inhibits metastasis via interaction with eEF2, which activates the Hippo signaling pathway	(203)
Prostate cancer	circSCAF8 circ_0062020	Up	circSCAF8-miR-140-3p/miR-335-LIF axis promotes growth and metastasis; circ_0062020- miR-615-5p/TRIP13 axis suppresses the radiosensitivity	(204,205)
	circ_0006156	Down	circ_0006156 inhibits the metastasis by blocking the ubiquitination of S100A9	(206)
Renal cell carcinoma	circCYP24A1 circMTO1	Up	circCYP24A1-miR-421-CMTM-4 axis hinders the cancer progression; circMTO1-miR9/LMX1A axis suppresses cancer progression	(207)
	circTNPO3	Down	circTNPO3 suppresses progression via binding to IGF2BP2 protein and destabilizing SERPINH1 mRNA	(208)

**Table 2. The overview of circRNAs significant for the development and progression of cancer and their mechanisms of action.**

Several circRNAs have been described as significant for GBM development and progression. One of the breakthrough research by Song and colleagues presented the possibility of a novel approach for circRNAs data retrieval, which, utilizing the back-splice junction site-specific tool named UROBORUS, allows the identification of circRNAs from the total, rRNA depleted RNA-seq data (209). They analyzed 46 glioblastoma – World Health Organization (WHO) glioma grade IV, oligodendroglioma, and normal brain samples, detecting thousands of

circRNA, of which 476 were identified as differentially expressed (209). The study presents several downregulated circRNAs such as circCDR1, circQKI, and circFAT1, while only eight overexpressed circRNAs in GBM compared to normal brain reference with a q value < 0.05, namely circCLIP2, circVCAN, circPLOC2, circCOL1A2, circPTN, circSMO, circGLIS3, circEPHB4. CircRNAs have been identified to perform numerous functions in GBM. Their potential to act as miRNA sponges, which prevents the interaction between miRNAs and mRNAs, leading to the deregulation of downstream target genes and further protein production, has been widely presented in GBM. CircMMP9 has been recognized as upregulated in GBM. Interestingly, its biogenesis is promoted by eukaryotic initiation factor 4A3 (eIF4A3), which binds to the metalloproteinase 9 (MMP9) mRNA transcript and facilitates circMMP9 cyclization, leading to the upregulation of circMMP9 in GBM (210). Moreover, EIF4A3-induced circMMP9 has been shown to act as a miR-124 sponge and thus promote gliomagenesis by increased GBM cells proliferation, migration, and invasion. Furthermore, the authors show that cyclin-dependent kinase 4 (CDK4) and aurora kinase A (AURKA) are the final targets of the circMMP9/miR-124 axis (210). Interestingly, circRNAs have also been shown to promote GBM progression by regulating GBM neovascularization. Neovascularization has been widely associated with rapid glioma progression, as high-grade gliomas are recognized as one of the most vascular solid tumors (211). It has been reported that circPOSTN plays a critical role in GBM progression as it promotes GBM neovascularization by increasing vascular endothelial growth factor A (VEGFA) secretion on the way of circPOSTN/miR-219a-2-3p/STC1 regulation (212). An interesting example, including the regulation by RBPs, is the regulation by leucine-rich repeat-containing 4 (LRRC4), which has been shown to suppress glioblastoma development and progression (213). The authors posit a hypothesis that LRRC4 promotes the biogenesis of circCD44 via the SAM68 RBP, which impacts the enrichment of eIF4A3 in conservative binding sites of CD44 pre-mRNA, leading to the elevated formation of circCD44. Furthermore, the authors show that circCD44 potentially sponge miR-326 and miR-330-5p, the downstream target - SMAD6, is involved in the progression of (213).

An interesting area of circRNAs contribution to glioblastoma are circRNA-encoded proteins. Several circRNAs-encoded proteins might promote GBM tumorigenicity. One of the interesting examples is circEGFR, which has been reported to be highly expressed in GBM (214). The open reading frame of circEGFR does not contain a stop codon, which results in the continuous translation of a non-terminating protein with an infinite open reading frame, which consists of a repeated amino acid sequence, termed rtEGFR. A rtEGFR has been established to facilitate the GBM tumorigenicity attenuating the consumption of EGFR, which is thought to

play an oncogenic role in GBM (214,215). Another interesting example of EGFR regulation in GBM, mediated by circRNA-encoded protein, has been reported. Circ-E-Cad, which originates from Cadherin 1 (CDH1) and exhibits elevated expression level in GBM, encodes a C-E-Cad, a 254-amino-acid protein, that is able to activate EGFR in GBM (216). On the other hand, some circRNAs such as circAKT3, circFBXW7, or circLINC-PINT are shown to code proteins, which have a role in suppressing tumorigenicity in GBM. The major part of those proteins act as protein decoys or regulators of elongation of multiple oncogenes and serve as anchors for RNA Polymerase II-Associated Factor 1 Homolog (PAF1) complex on target genes promoters, respectively (216–219). Most commonly circRNAs impact the process of cancer development and progression by global deregulation of signaling and metabolic pathways, mainly caused by the disruption of the mechanism of action of direct circRNAs interactors such as miRNAs and RBPs, subsequently influencing their downstream regulatory pathways. Several circRNAs and circRNA-encoded proteins have been shown to play a role in human diseases, including cancer. However, the exact mechanisms of circRNAs action still need to be widely investigated to support the circRNAs role as a novel therapeutic target.

#### **1.4. CircRNAs as a new class of biomarkers**

The delivery of early, fast, and accurate diagnosis states the primary goal of clinical observations and clinical cancer research, as early detection is an essential enabler of curative treatment (178), (220). Extensive identification of the disease-related circRNAs, followed by their high cell- and tissue-specificity, allowed them to convey their aberrant expression pattern to the clinics. The current state of knowledge concerning the clinical application of circRNAs presents several circRNAs, which might be applied as potential diagnostic biomarkers for various human diseases, including cancer. Moreover, circRNAs have been found enriched, commonly in exosomes, saliva, blood, and potentially urine or cerebrospinal fluid, supporting its usage as a clinical biomarker (221). The discovery and implementation of novel biomarkers are in high demand to support traditional biomarkers currently used in clinics, as they show lower organ specificity and low positive detection level (222).

According to a meta-analysis conducted by Ding and colleagues in 2020, there is a significant correlation between the disrupted expression pattern of circRNAs and the clinicopathology and prognosis of glioma patients (223). To support this, circNEIL3 has been suggested to state a promising glioma diagnostic biomarker of glioma progression, as it was detected in the patient's tissue as the only disrupted circRNA with upwards expression level among increasing glioma grade – from low-grade glioma (LGG) to glioblastoma. The authors

assessed the receiver operating characteristic (ROC), which allows for determining the overall diagnostic performance of a molecule or a test, which revealed that circNEIL3 might predict poor prognosis in glioma patients (224). Moreover, a study conducted by Xia and Gu revealed that three circRNAs, namely hsa\_circ\_0055202, hsa\_circ\_0074920, and hsa\_circ\_0043722, may potentially serve as GBM biomarkers detected in exosomes extracted from the GBM patients' plasma. Presented circRNAs exhibit highly stable expression in human plasma, and the ROC curve revealed a high diagnostic ability for a single investigated circRNA and all of them combined (225). As the interest is growing, several databases were generated to gather information regarding the circRNAs biomarkers candidates, such as exoRBase collecting circRNAs detected in human blood exosomes and MiOncoCirc containing the circRNAs, which were detected as promising biomarkers for prostate cancer (182,226,227).

Nevertheless, as circRNAs manifest specific features that allow them to be classified as a novel class of diagnostic biomarkers, their implementation still requires a comprehensive exploration and deep understanding of their functions and interactions, as they might impact the key regulatory pathways within the cell. A number of deregulated circRNAs are usually identified in various human diseases, however, as it is greatly highlighted in the literature, not every circRNA exhibiting a disrupted expression pattern can be considered a good biomarker. To determine the potential of circRNAs as useful biomarkers, it is essential to evaluate their sensitivity and specificity to understand their diagnostic capabilities, which usually need to be performed in up-to-date functional circRNAs research (228).

### **1.5. CircRNAs as a new class of therapeutics**

As circRNAs are deregulated in many human disorders, which most commonly also leads to the malfunction of their interactors. Therefore significant endeavors have been made to investigate the potential of circRNAs to serve as therapeutic factors. So far, the therapeutic application of circRNAs was proposed to operate in two ways - modulation of the abundance of endogenous, disease-related circRNAs by the knockdown or by ectopic expression and the second approach - engineering of artificial circRNAs with delineated effect within the cell (229).

Two approaches for therapeutic modulation of endogenous, disease-linked circRNAs have been reported by Holdt and colleagues (229). The first approach focuses on the modulation of native circRNAs expression level either by the overexpression of native and protective circRNAs utilizing the genetic vectors or depletion of endogenous disease-promoting circRNAs or the correction of aberrantly expressed circRNA-isoforms (78,230–232). The overexpression

of native protective circRNAs can be achieved utilizing standard DNA expression vectors in cell culture and from the application of lentiviral or adenoviral vectors *in vivo* (233–235). The circRNA expression vectors usually consist of a mini-gene cassette with sequence encoding desired circRNAs, endogenous splice donor, and acceptor sites (53,236). The sequence of interest also contains flanking intronic inverted repeats that promote RNA circularization(237). On the contrary, to deplete the endogenous disease-promoting circRNAs, standard genetic tools such as RNA interference (RNAi) using short hairpin (shRNAs) and small interfering siRNAs or ASO-mediated degradation were applied (238). It is important to note that for specific circRNA knockdown, the circRNA-specific back-splice junction site must be targeted (78,239). Furthermore, the RNA-targeting CRISPR/Cas13d technology has also been reported to greatly silence circRNAs utilizing single-guide RNAs designed against circRNA back-splice junction sites, allowing for specific and highly repetitive circRNA silencing (240). Another particular therapeutic approach for circRNA knockdown depends on the depletion of fusion-circRNAs (f-circRNAs), which are formed once the chromosomal translocations bring introns from two unrelated genes in close genomic vicinity, which later on undergo back-splicing (241). This approach is interesting and presumably selective in treating certain cancers and, potentially, other translocation-originated pathologies. However, as RNAi might yield off-target effects, and as naked single-stranded RNA shows low stability and is prone to nucleolytic degradation, the administration of antisense oligonucleotides (ASOs) might allow avoiding those issues (242–245). ASO, by binding and masking the regulatory splice enhancers or silencers or inverted intronic repeats in a chosen pre-mRNA before the circularization, may deliver the desired therapeutic result. However, it still requires a thorough experimental verification (246,247). Interestingly, recent reports present the possibility of producing synthetic antisense circRNAs to respond to the limited organ delivery of regular ASOs.

Antisense circRNAs might act as an alternative method for regulating RNA splicing as they have the potential to mediate exon skipping in mini-genes and endogenous transcripts both *in vitro* and *in vivo*. In addition, the authors have demonstrated that adeno-associated virus (AAV) delivered antisense circRNAs can correct the open reading frame and restore the dystrophin expression in a mouse model of Duchenne muscular dystrophy, which might suggest a great therapeutic potential of the proposed approach (248). The second approach concerns the application of artificial, unmodified, or modified, *in vitro*-produced circRNAs into cells (229). The advantage of engineered, artificial circRNAs is their capability to display desired therapeutical properties (229). Artificial circRNAs can be designed to perform the regular function of circRNAs, interacting with specifically chosen and targeted molecules. For instance,

they can specifically sponge miRNA or RBPs of interest, recognized as the key molecules in a particular disorder (249–251). Furthermore, artificial circRNAs can be translated into proteins, regulate transcription and translation of RNAs of interest, or modulate the immune system (31,252,253). Interestingly, it has been shown that artificial circRNAs generated in a cell-free system utilizing *in vitro* transcription and further ligation, which are later purified by gel extraction, are not recognized by the innate immune system. The activation of signaling pathways, which induce chemokines, cytokines, and interferons, may be bypassed (254). Moreover, identifying circRNAs capable of coding the proteins and translating laid the groundwork for the research and development of circRNA vaccines. An interesting research area is the generation of circRNAs vaccines against various COVID-19 strains utilizing the group I intron splicing RNA circularization method and translation initiation mediated by IRES with the application of lipid nanoparticles as delivery systems (255). Currently investigated vaccines against COVID-19 include the original COVID-19 strain, Delta, and Omicron BA1 variant (255). Moreover, it has been reported that the administration of circRNAs as vaccine adjuvants or immunogens generates an acute inflammatory environment that promotes the activation of potent cellular immunity (256).

## **1.6. CircRNAs in GBM**

With the development of high-throughput sequencing, bioinformatics and adjustment of the algorithms for circRNA detection and quantification with non-poly(A) RNAs, the identification and characterization of circRNAs have significantly increased (257). This has allowed for a comprehensive examination of circRNAs in cancer, which indicated their potential role in the development and progression of the disease. In fact, Josh N. Vo has conducted a comprehensive study utilizing exome capture RNA sequencing which has revealed the intricate landscape of cancer-related circRNAs across 2000 samples derived from lung cancer, thyroid cancer, breast cancer, bladder cancer (258). Moreover, recent experimental-based reports confirmed that circRNAs play significant roles in tumor growth, metastasis, EMT transformation, and therapy resistance (259,260). Such research has paved the way for a better understanding of the pathogenesis and progression of cancer and might lead to the development of novel therapeutic strategies. Nowadays, scientists across the world deliver the RNA-seq data performed on GBM patient's resected tissue, identifying hundreds of deregulated circRNAs (209,261,262).

A number of circRNAs have been shown to play a significant role in GBM onset and progression (263,264). The literature reports several circRNAs involved in GBM progression

by modulation of GBM cells proliferation, motility, and invasiveness (265,266). The example could state circUBAP2, which is overexpressed in GBM. It has been demonstrated that *in vitro* circUBAP2 upregulates cell proliferation, migration, and invasion while decreasing apoptosis and regulating tumor development *in vivo*. The evidenced mechanism of action includes sponging of miR-1205 and miR-382, which in turn regulate the GPRC5A (267). Another example is circPARP4, which is known to enhance GBM cell proliferation, migration, invasion, and epithelial-mesenchymal transition. The study of circPARP4 revealed that it acts as a miRNA sponge interacting with miR-125a-5p, which in turn regulates FUT4 to act as a GBM oncogene. Interestingly, a low expression level of miR-125a-3p was observed in CD133+ stem-like GBM cells compared with the CD133+ cells. It has been suggested that miR-125a-3p plays a role in regulating glioma stem cells by inducing the differentiation of stem-like GBM cells, therefore, miR-125a-3p is considered a tumor suppressor regulated by the oncogenic circ-PARP4 (268). The study of GBM tissues by microarrays revealed circ-ENTPD7, whose expression level is upregulated. The elevated expression level of circ-ENTPD7 in GBM patients is linked with low overall survival, as circ-ENTPD7 has been shown to modulate glioblastoma cell motility and growth by sponging miR-101-3p, in turn, regulating ROS1 expression level (269). Many other circRNAs are known to regulate GBM cells motility and invasiveness, such as circ-FLNA regulating miR-1993p (270), circ-LGMN sponging miR-127-3p (271), circFOXO sponging miR-138-5p and miR-432-5p (272), circ-0074027 modulating miR-518a-5p/IL17RD signaling (273), circSKA3 inhibiting miR-1 (274) and circ-NF1 inhibiting miR-340 maturation in GBM cells (275). Some circRNAs are described to modulate the GBM angiogenesis, such as cZNF292, which suppressed glioma tube formation via the Wnt/ $\beta$ -catenin pathway (276). RBPs also might interact with circRNAs to regulate tumor angiogenesis. For instance, FUS binds to circ\_002136 and inhibition of FUS or circ\_002136 greatly suppressed tube formation of U87 glioma-exposed endothelial cells (277). Other circRNAs might regulate transcription and splicing, such as ci-ankrd52 and ci-SIRT7, which were shown to interact with elongating pol II complex and positively regulate the transcription of their parental genes (278). CircSEP3, nuclear-retained circRNA also was shown to modulate the splicing of its linear counterpart through RNA:DNA hybrid or R-loop (279).

Hsa\_circ\_0002755, known as circCLIP2, has been revealed as upregulated in GBM samples by Song et al. in 2016. CircCLIP2 has been suggested to state good potential GBM biomarker and potential GBM oncogene, as its linear counterpart does not exhibit disrupted expression level in GBM (209). CircCLIP2 is located at chr7:73770739-73771807 and represents an exonic type of circRNA consisting of exons 5 and 6 of the *CLIP2* gene (Fig. 1).

Based on the information available in the circBase database (280) and CircInteractome (110), its genomic length is 1068 nucleotides, and after splicing, circCLIP2 reaches 412 nucleotides. CircCLIP2 corresponding mRNA indicated by both sources is Homo sapiens CAP-Gly domain containing linker protein 2 (CLIP2), transcript variant 1, mRNA - NM\_003388. Little is known about circCLIP2 biogenesis. However, the CircInteractome indicates several proteins matching circCLIP2, which might serve as potential circCLIP2 interactors or might be involved in its biogenesis. The tool differentiates the RNA-binding protein sites matching circCLIP2 junction sequence reporting EIF4A3 only and RNA-binding protein sites matching flanking regions of circCLIP2 revealing AGO1, AGO2, EIF4A3, and FUS proteins. The CircInteractome based on the TargerScan database predicted 11 miRNAs, which might interact with circCLIP2. One of them, hsa-miR-767-3p, was predicted to contain two binding sites of the 7mer-m8 site type potentially. The remaining 10 miRNAs, namely hsa-miR-1248, hsa-miR-515-3p, hsa-miR-515-5p, hsa-miR-519e, hsa-miR-576-3p, hsa-miR-585, hsa-miR-646, hsa-miR-647, hsa-miR-663b, and hsa-miR-671-5p are predicted to contain only one potential binding site of 7mer-m8 or 7mer-1a site type. None of the predicted miRNA binding sites targets the specific head-to-tail junction site of circCLIP2.

CircCLIP2 is suggested to act as an oncogene in GBM and was also reported to promote GBM progression through the miR-195-5p/HMGB3 axis however, its detailed mechanism of action remains unknown (209,281). Interestingly, potential GBM therapy targeting circCLIP2 was suggested utilizing Sevoflurane, an inhaled anesthetic, which has been discovered to hinder the metastasis of glioma cells by inhibiting cell viability, migration, invasion, and promoting cell apoptosis (282). For a long time, the mechanism of sevoflurane action remained unknown. However, recent reports show that sevoflurane might affect the miR-628-5p/MAGT1 axis through circCLIP2 (282). Even though the reports on circCLIP2 deliver information about circCLIP2 potential interactors, the detailed mechanisms underlying its impact on GBM cells still need to be discovered and presented work aimed at solving the mystery of how circCLIP2 could impact the key processes involved in tumorigenesis and tumor progression.

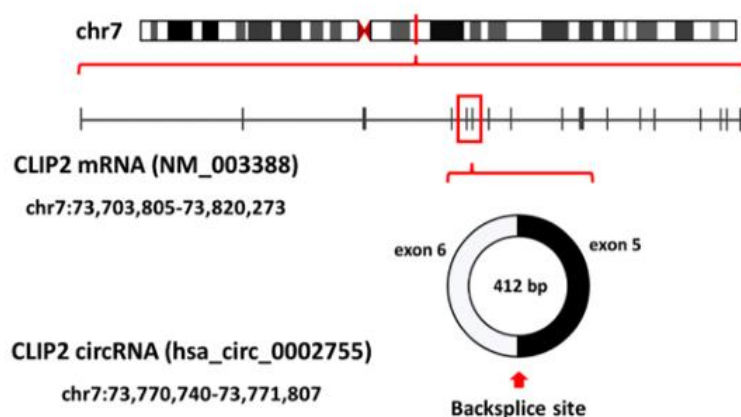


**Figure 1. The chromosomal location of the *CLIP2* gene and circCLIP2 (*hsa\_circ\_0002755*).** CircCLIP2 comprises of exons 6 and 5 of the *CLIP2* gene encoding the CAP-GLY domain-containing linker protein 2. Based on circBase database (280).

### 1.7. General characteristics of tumors

According to the WHO, cancer, despite the comprehensive endeavors of the scientists and medical communities, was still one of the leading causes of premature death, accounting for nearly one in six deaths in 2020 (WHO). The scientists from the International Agency for Research on Cancer (IARC) reported that cancer and cardiovascular disease were the major causes of premature death at ages 30–70 years in 127 countries worldwide, where cancer was the leading death cause in 57 countries (283). Based on the observed trends, scientists predict that cancer might surpass cardiovascular disease as the leading cause of premature death in most countries over the course of this century. The cancer statistics estimated in 2023 by Siegel and colleagues show that in the United States for women, breast cancer, lung cancer, and colorectal cancer account for more than half of all newly diagnosed cases, with breast cancer alone accounting for 31% of female cancers (284). On the other hand, prostate, lung, bronchus, and colorectal cancers also reached almost half of all of the diagnoses in men, with a strong prevalence of prostate cancer accounting for 29% of cases (284). The presented report indicates that the cancer prognoses are positive for the patients, as even despite the COVID-19 pandemic significantly limiting the proper diagnostics and treatment, the cancer death rate continued to decline from 2019, contributing to a 33% overall reduction since 1991. However, this trend might be hindered by the increasing prevalence of breast, prostate, and uterine corpus cancers, which exhibit the greatest differences in mortality rates among different racial groups (284). Presented data indicates that despite the significant development of knowledge about cancer

onset and progression and metastasis, followed by the discovery of multiple potential therapies, effective measures still need to be taken to reduce cancer mortality.

### **1.8. Tumors of the Central Nervous System**

Primary tumors of the central nervous system (CNS) are known as tumors developing predominantly in the brain and spinal cord but also affecting the meninges and eyes (285). Primary brain tumors are recognized as developing in the brain, and they can be categorized by the specific type of tissue from which they originate (286). Up to now, more than 100 histologically different types of tumors have been recognized within a class of CNS tumors (287). They state a heterogeneous group of malignancies comprising both benign and malignant tumors (287). Although half of CNS tumors are benign, those, if not susceptible to treatment, can pose a serious threat to the patient's life (285). This is due to significant growth and tumor mass enlargement within the confined space of the skull, leading to increased intracranial pressure destroying adjacent nerve tissue, causing the mass to spread and impact a constant volume (288). The growth and spread of the cancer tissue lead to the demonstration of symptoms, such as headache, seizures, and altered mental status (289). Even though CNS tumors are not as common as other tumors, as primary malignancies account for about 2% of all cancers, they are recognized as one of the leading causes of death in children and adults, being the second leading cause of death in children and the third leading cause of death in adults (289,290). The etiology of brain neoplasms which are usually highly incurable is still poorly understood and no strong underlying carcinogenic factors have been verified so far (291). However, some potential risk factors have been identified, which presumably might impact the development of CNS tumors, such as ionizing radiation, some serum compounds such as N nitrous compounds, air pollution, and the radio spectrum of electromagnetic waves (287). Interestingly, the National Cancer Institute reports that suffering from certain genetic syndromes such as neurofibromatosis type 1 or 2, von Hippel-Lindau disease, tuberous sclerosis, Li-Fraumeni syndrome, Turcot syndrome type 1 or 2, and nevoid basal cell carcinoma syndrome may increase the risk of brain tumors development (National Cancer Institute, (292)). Moreover, several factors impact tumor aggressiveness and affect a patient's survival chances. These include tumor size and location, age at diagnosis, histologic and genetic markers and burden, and general functional status, which usually has a significant negative correlation with age (293).

According to the Central Brain Tumor Registry of the United States (CBTRUS) Statistical Report assessing the Primary and other CNS tumors diagnosed in the United States

in 2015–2019, the most frequently emerging malignant tumor was glioblastoma stating 14.2% of all tumors and 50.1% of all malignant tumors, and the most frequently emerging non-malignant tumor was meningioma stating 39.7% of all tumors and 55.4% of all non-malignant tumors in adults (294). The updated, fifth edition of the WHO Classification of Tumors of the Central Nervous System - CNS5, published in 2021, introduces significant changes that include and underline the role of molecular changes that have clinical and pathologic significance, enhancing their impact on the precise classification of CNS tumors. WHO CNS5 introduced a novel approach to divide the Gliomas, Glioneuronal Tumors, and Neuronal Tumors, classifying them into 6 different groups of cancer: (1) Adult-type diffuse gliomas, (2) Pediatric-type diffuse low-grade gliomas, (3) Pediatric-type diffuse high-grade gliomas, (4) Circumscribed astrocytic, (5) Glioneuronal and neuronal tumors and, (6) Ependymomas. Choroid Plexus Tumors, showing epithelial tumor features, are now separated from the category of Gliomas, Glioneuronal Tumors, and Neuronal Tumors (295). Fourteen newly recognized types have been added to the classification of Gliomas, Glioneuronal Tumors, and Neuronal Tumors such as Diffuse low-grade glioma, mitogen-activated protein kinase (MAPK) pathway-altered, for which the additional histological and molecular interpretation is crucial to support the proper diagnosis.

### **1.9. General characteristics of glioblastoma**

Glioblastoma (GBM) is one of the most common primary brain neoplasms in adults stating 14.2% of all tumors and 50.1% of all malignant tumors (294). GBM cells possess the ability to infiltrate the adjacent healthy brain tissue and blood vessels to quickly invade the neighboring areas leading to tumor expansion, which prevents the tumor tissue from complete surgical removal (294). The extraordinary case states the butterfly glioblastoma, which invades both hemispheres by crossing the corpus callosum. That leads to significant consequences, such as poor patient prognosis and limited surgical treatment, as tumor resection is technically difficult due to the unfavorable location and shows a poor risk-to-benefit ratio (296). However, glioblastomas emerging in the subventricular zone are reported to be associated with decreased survival and a higher risk of multifocal or distant progression (297). Most GBM patients survive approximately 15 months after the diagnosis, and only 5.5 % of patients survive an estimates five years post-diagnosis. The majority of the cases state primary GBMs, accounting for 80% of the patients, and typically affect patients of an average age of 62 years. On the other hand, secondary GBMs arise from lower-grade astrocytoma or oligodendroglioma and tend to occur in younger patients with an average of 45 years (298). The GBM incidence reports show an

average of 3.19 to 4.17 cases per 100,000 person-years in adults, whereas the incidence in the pediatric population is 0.85 per 100,000, which makes GBM the second-most-common type of cancer in children and the most common solid tumors in children (299,300). Primary GBMs are more frequent in men, with a male-to-female ratio of 1:0.33, whereas secondary GBMs emerge more often in women, with a male-to-female ratio of (0.65:1) (301).

The fifth edition of the WHO Classification of Tumors of the Central Nervous System, published in 2021, classifies glioblastoma as glioblastoma Isocitrate Dehydrogenase-wildtype (IDH) CNS WHO grade 4, as it exhibits necrosis and/or microvascular proliferation. As it was observed that IDH-wildtype astrocytomas regarded as grades 2 or 3 were shown to clinically behave much as glioblastomas, molecular predictors of aggressive behavior, such as EGFR amplification, were assessed and recommended as a conventional diagnostics support (302). Therefore, an IDH-wildtype diffuse astrocytoma, which exhibits at least one of the aggressive behavior molecular features, might be classified as glioblastoma IDH-wildtype CNS WHO grade 4. Moreover, gliosarcoma, epithelioid cell glioblastoma, and giant cell glioblastoma still state as a subtype of glioblastomas (302).

### **1.9.1. Symptoms**

Patients diagnosed with primary brain tumors may encounter neurological, cognitive, and psychiatric symptoms that significantly impact their day-to-day life (303). The most common symptoms attributed to glioblastoma are seizures, cognitive dysfunction, drowsiness, dysphagia, headache, confusion, aphasia, motor deficits, fatigue, and dyspnea (304,305). Moreover, attention also should be paid to psychological disorders such as depression, mood issues, hallucinations, pseudobulbar affect-like states, manic-like states, and anxiety (303,306). Psychotic symptoms were mainly observed in individuals with tumors located in the temporal lobes and less frequently in the frontal lobes and corpus callosum (306). Neurobehavioral symptoms are common in brain tumor patients, and the major difficulty is that they often occur concurrently, significantly impeding the estimation of proper diagnosis (303). Another important point is that in some cases, especially when the tumor is of great size, increased internal pressure on the brain occurs, which can be detected by neuroimaging. Therefore, one of the recommended medical examinations for neurological and psychiatric patients is the imaging of the brain to exclude ongoing tumorigenesis as one of the causes (307).

### **1.9.2. Diagnostics**

Glioblastoma has several characteristic features that make it challenging to diagnose accurately. These hallmarks include the infiltration of adjacent tissues due to unclearly defined margins, local invasion, and the formation of secondary lesions (308,309). Additionally, the substantial tumor heterogeneity facilitates the complexity of establishing a proper diagnostic framework (310,311). Therefore, for CNS tumors, the standard diagnostics procedure involves the application of imaging methods. The most commonly used techniques for this purpose are computed tomography (CT) and magnetic resonance imaging (MRI) (312,313). The use of CT allows fast image acquisition, most commonly is wide availability, and most importantly, allows for the initial differential diagnosis between cancer and brain hemorrhage (314). On the other hand, MRI greatly facilitates the evaluation of brain tumors based on, in comparison to CT, better anatomic detail of normal brain structures and the easier detection of tumor-infiltrated areas (312). The most conventional MRI sequences commonly used for the evaluation of CNS tumors are T1-weighted or T2-weighted MRI and fluid-attenuated inversion recovery MRI (315,316). These MRI types provide high anatomic resolution and state versatile techniques, as, for example, the use of a gadolinium-based contrast agent indicates the areas of the compromised blood-brain barrier (BBB) (317). Even though MRI is of great value compared to CT, it comprises substantial limitations, such as the difficulty in recognizing various glioma grades and their histological differences or the difficulty in distinguishing gliomas from other brain lesions such as metastasis, abscess and tumefactive multiple sclerosis (312). Therefore, positron emission tomography (PET) imaging states another valuable tool that delivers complementary information to anatomical MRI data, as it non-invasively supports MRI imaging with biochemical information about tumor metabolism (312). PET as a tool relying on biomarker-guided diagnosis includes the tracers for multiple markers of proliferation, hypoxia sensing, and ligands for inflammation, followed by newer imaging targets stating a promising tool for glioblastoma detection, such as programmed death ligand 1, poly-ADP-ribose polymerase, and isocitrate dehydrogenase (318).

Following CNS imaging, the biopsy and histological assessment of the sample are performed. Examining GBM samples, it is worth noting that extraordinary GBM heterogeneity significantly increases the risk of obtaining non-representative tumor samples for histological assessments (319). Therefore, GBM diagnostics requires the study of multiple groups of factors, such as genetic and epigenetic abnormalities, the identification of molecular markers, and the rate of cell growth and death of tumor cells (309). The histological picture of GBM most commonly consists of hypercellularity, nuclear atypia, microvascular proliferation necrosis, and

harboring of CSCs (309,320). Moreover, some immunohistochemical (IHC) biomarkers might be identified to support the GBM diagnosis, such as epidermal growth factor receptor (EGFR) overexpression, phosphatase and tensin homolog (PTEN) mutations, cyclin-dependent kinase inhibitor 2A (CDKN2A) (p16) deletions, loss of heterozygosity of 10q, murine double minute-2 (MDM2) amplification, whereas tumor protein p53 (TP53) mutations, IDH 1-R132H mutation and alpha-thalassemia mental retardation X-linked (ATRX) mutation (321,322). The study of 102 GBM patients revealed that overexpression of molecular markers was detected in 52% of patients for EGFR, 26% for p53, 72% for IDH1, and 83% for MDM2, and the EGFR overexpression was highly associated with increased age and worse survival of the patients (323). According to a study delivered by Marton and colleagues, young individuals with methylation of the MGMTp, a lack of TERTp gene mutations, and mutated IDH1 or IDH2 genes exhibit longer survival (324).

### **1.9.3. Therapy**

GBM treatment is challenging mainly due to the high intra- and intertumoral heterogeneity (325,326). Therefore, some tumor cells might positively respond to the treatment, while others might present treatment resistance, leading to subsequent tumor recurrence (327). Moreover, unlike other tumors, GBM shows no clear tumor margin and exhibits high infiltration of the adjacent healthy tissue (328,329). High tumor invasion, as well as difficult anatomical location, significantly impede tumor surgical removal, increasing the risk of the development of recurrent tumors, post-surgical brain function impairment or overall patient survival (330–333). Additionally, several drugs cannot efficiently pass the BBB to reach the brain, including chemotherapeutics (334,335). GBM treatment also poses a significant burden for patients' organisms and patients' initial condition right after the diagnosis also has a large impact on the subsequent stages of the treatment (336).

Despite the great advancements in surgery, radiotherapy, and pharmacotherapy, patients' outcomes are still typically fatal, with a median overall survival of 14.6 to 20.5 months. This prognosis is even worse for elderly patients, with an average survival rate of less than 8.5 months after diagnosis. Due to the limited success of current treatments for GBM, new therapeutic approaches are urgently needed. A broad initiative conducted by the Brain Tumor Research and Treatment Organization and the National Research Institute, The Canadian Clinical Research Group of Cancer set a new standard of treatment for glioma worldwide. Currently, the standard approach to GBM treatment assumes the implementation of the Stupp protocol published in 2005, which highlights the importance of the administration of

temozolomide to radiotherapy for newly diagnosed glioblastoma applied after surgical resection of the tumor (337). The study showed that implementation of the Stupp protocol in the form of radiotherapy (fractionated focal irradiation in daily fractions of 2 Gy given 5 days per week for 6 weeks, for a total of 60 Gy) facilitated with continuous daily temozolomide administration (75 mg per square meter of body-surface area per day, 7 days per week from the first to the last day of radiotherapy), followed by six cycles of adjuvant temozolomide (150 to 200 mg per square meter for 5 days during each 28-day cycle) increased the two-year survival rate in patients to 26.5%, compared to only 10.4% with radiotherapy alone (337). The retrospective study conducted by Lakomy and colleagues confirmed a clear trend in extending overall survival over the last decade with the application of a full Stupp regimen (338). Interestingly, the implementation of silibinin, an inhibitor of pSTAT3, into the Stupp protocol has been proposed to state a novel therapeutic approach for unresectable glioblastoma expressing , phospho-tyrosine 705-signal transducer and activator of transcription (pSTAT3), a modulator of glioblastoma microenvironment. Concomitant application of silibinin and Stupp protocol was shown to reduce the tumor infiltration, thus allowing for tumor resection in case of initially inoperative glioblastoma cases (339). Despite the establishment and implementation of the Stupp protocol in the clinics, serving as the gold standard in the treatment of glioblastoma patients, the establishment of modern treatment methods, allowing to improve the overall survival and patients' quality of life, are in high demand.

### **1.9.3.1 Surgical resection**

Despite the progress made in GBM treatment, surgical resection continues to be a highly effective option for treating intra-axial gliomas. The extent of resection is most commonly directly related to patient survival, which might provide long-term remission or at least disease control when combined with adjunctive treatments (340). Most commonly, supramaximal resection, gross total resection, near-total resection, and subtotal resection can be distinguished, followed by tumor biopsy, which does not provide therapeutic benefits, however, is applied in older patients or patients with low Karnofsky Performance Status (KPS) who would show low toleration for surgery and patients with inoperable GBM (341). Although surgical resection may be effective, it also carries potential risks and complications (342,343). These complications fall into three categories: neurologic, regional, and systemic, including direct injuries to the brain and surrounding structures, difficult surgical wound healing or infections, and post-surgery complications (340). The other important factor affecting the likelihood of experiencing postsurgical complications is the patient's condition before the surgery, estimated by the

Karnofsky performance score (344). One of the elements allowing to navigate neurosurgeons is based on the use of functional MRI (fMRI), functional monitoring, and fluorescence-based visualization of tumor tissue with 5-aminolevulinic acid (5-ALA) or fluorescein (345). In cases where the tumor affects important areas of the brain, functional tools like brain mapping in awake patients or electromyography have shown to be useful and effective in achieving favorable neurological functional outcomes (346,347). Furthermore, a new advancement that has the potential to greatly enhance the degree of tumor removal during surgery is intraoperative mass spectrometry. Its specific type, namely desorption electrospray ionization mass spectrometry (DESI-MS) serves as a valuable tool for detecting the cancer cells in examined tissue, allowing the surgeons to distinguish tumor from healthy tissue during the surgery (348,349). In principle, a fully automated DESI-MS instrument allows the fast acquisition of a set of images, allowing to conduct the lipidomic studies in cancer (350,351). Therefore, the glioblastoma lipid signature allows to differentiate between healthy and tumor tissue, as well as between different grades of gliomas (352). DESI-MS has been also reported as a powerful tool for the detection of other types of cancer cells, such as skin, ovarian, and breast (350,353,354).

### **1.9.3.2 Radiotherapy**

In recent decades, several advancements in radiotherapy treatment and image guidance technology were developed and reported, which greatly enhanced the capability of optimizing both definite and salvage treatment (355). An optimal radiotherapy treatment aims to administer a significant amount of radiation to the tumor while minimizing exposure to the healthy surrounding tissue. Commonly applied radiotherapy relies on bony landmarks to determine the treatment area, using multiple beams that overlap to create a central region with a high-dose distribution (356). This leads to unnecessary irradiation of the surrounding area, increased toxicity, and acute reactions, which have been fully addressed with the development of novel approaches in radiotherapy (357–359). A significant advancement in oncology is photon-based Intensity-Modulated Radiotherapy (IMRT). It allows for the precise delivery of the radiation dose, reducing the maximum dose to the organs at risk, diminishing long-term morbidity, and improving local control (356,360,361). IMRT is also a commonly used treatment method for other types of cancer, such as breast, lung, and prostate cancer (362). Currently, the clinical trial aiming to assess whether proton beam instead of photon beam radiotherapy will support the clinical reduction of toxicity is being conducted under the NCT04752280 identifier (363). The estimated clinical trial completion date is set in 2027, however, other collective studies already

showed that the application of proton beam therapy in recurrent GBM patients is well tolerated, and its efficacy rate is similar to photon-reirradiation (364). Taking the above into consideration, radiotherapy is considered a part of the standard GBM treatment approach. However, the application of radiation still raises significant issues regarding radiation regimens for the elderly and patients previously treated with radiation, the potential synergy of immunotherapy and radiation, and the stem cell-directed radiation approaches aimed at limiting the recurrence rate (355,365,366).

### **1.9.3.3 Chemotherapy**

Temozolomide (TMZ, 3,4-dihydro-3-methyl-4-oxo imidazole), an oral alkylating agent, was initially developed in the early 80s at Aston University in Great Britain (367,368). It states the first-choice chemotherapeutic agent in GBM treatment, applied as a concomitant drug for radiotherapy, as a follow-up treatment after the tumor extraction (369).

TMZ's key therapeutic features are rapid oral absorption, lipophilic properties, and small size, which allow it to easily pass through the BBB (370). Initially, TMZ was developed to treat patients with malignant melanoma metastases in the brain. However, it was later discovered to have positive effects on relapsed GBM patients (371). TMZ remains stable when the pH is less than 5, however, it undergoes rapid hydrolysis to 5-(3-methyltriazene-1-yl)imidazole-4-carboxamide (MTIC) when the pH is greater than 7 (372). MTIC methylates a number of nucleobases, most importantly, performs the O6-methylation of the guanine (367). O6-methylguanine is mutagenic, and its formation results in the formation of nicks in the DNA and triggers the subsequent apoptosis because cellular repair mechanisms are unable to adjust to the methylated base (367). The effect of TMZ is highly pH-dependent; it has been shown that slightly more basic intracellular pH values in cancer cells favor the damage induced by TMZ in tumor cells (370). The mechanisms that play a crucial role in the TMZ mechanism of action are the DNA repair systems such as O6-methylguanine-DNA-methyltransferase (MGMT), DNA mismatch repair (MMR), and base excision repair (BER) (373). This knowledge is particularly important, as the DNA repair ability of MGMTs poses a significant obstacle in GBM patients' treatment as it leads to resistance to TMZ (369). MGMT is a protein in a size of 22 kDa, present in the cytoplasm and cell nucleus (374). Its main function is to demethylate DNA by removing the methyl groups from the O6 position of the guanine and transferring them to the cysteine residue (373,375). This results in an auto-inactivating reaction, which repairs DNA and inactivates MGMT through a process known as suicide inhibition. The availability of MGMT molecules limits the efficiency of DNA repair (373). Patients with low

levels of MGMT expression are more responsive to TMZ treatment and tend to have better outcomes, as the cell damage remains unrepaired, which activates the apoptotic pathways and subsequent cell death (376).

Nevertheless, there is a high demand for novel chemotherapeutic discovery as approximately 50% of newly diagnosed GBM patients are TMZ-resistant and express high levels of MGMT (376). Interestingly, it has been reported that S-nitroso-N-acetylpenicillamine (SNAP) has anti-cancer properties in both TMZ-sensitive and TMZ-resistant glioma cells (377). The exposure to SNAP led to apoptosis, mitochondrial dysfunction, and increased expression of hypoxia-inducible factor 1 (HIF-1), as well as a reduction in MGMT expression, thereby increasing the sensitivity of GBM cells to TMZ. Moreover, the combination of SNAP and TMZ resulted in improved inhibition of tumor growth, both *in vitro* and *in vivo* (377). Furthermore, it was also shown that disrupting the mitochondrial dynamics might lead to the reduction of the GBM cells' sensitivity to TMZ, which was also confirmed *in vitro* and *in vivo* (378). Another interesting example of a potential GBM chemotherapeutic is QBS10072S, a novel treatment agent capable of overcoming TMZ resistance (379). It has been shown to pass the BBB and, unlike TMZ, be cytotoxic to GBM cells with high and low levels of MGMT expression. Furthermore, it also exhibits the potential to be useful in recurrent GBM treatment, both as a monotherapy or in combination with radiotherapy (379).

In 1997, Gliadel wafers were approved by the FDA for the treatment of recurrent GBM (380,381). These wafers contain Carmustine, a type of alkylating agent that inhibits DNA synthesis, RNA production, and translation by creating cross-links in DNA and RNA. Gliadel wafers are implanted into a surgical cavity after the removal of a tumor to release the Carmustine. In 2003, Gliadel wafers were also approved for the treatment of primary WHO grade III and IV gliomas (381). As a result, Gliadel wafers are now approved for use in recurrent GBM patients and newly diagnosed patients with high-grade glioma as an adjuvant to surgery with or without radiotherapy (382). Additionally, GBM patients treated with a combination of Carmustine and TMZ therapy also showed longer overall survival rates than those who received only TMZ (381). Carmustine is currently used to treat brain tumors, including glioma, as well as multiple myeloma, Hodgkin's and non-Hodgkin's lymphomas, and melanoma, lung, and colon cancer (383).

#### **1.9.3.4 TTFields**

A promising treatment for GBM is the use of tumor-treating fields (TTFields), which rely on alternating electric fields to disrupt cancer cell division (384). This non-invasive therapy

involves the use of low-intensity (1-3V/cm), intermediate-frequency (100-300kHz) fields that are delivered through transducer arrays placed on the skin near the tumor (385,386). While originally developed to target mitotic apparatus and inhibit cancer cell proliferation, TFields are now recognized to have a broad mechanism of action that elicits therapeutic effects. TFields work regionally to inhibit tumor growth and have been shown to disrupt a variety of biological processes, including DNA repair, cell permeability, and immunological responses (384,387). TFields therapy has been approved by the FDA for the treatment of GBM and mesothelioma. TFields therapy, in combination with the application of temozolomide, has been introduced in clinics (388). Moreover, ongoing clinical trials are exploring its safety and efficacy in treating non-small cell lung cancer, lung adenocarcinoma, and pleural mesothelioma with the application of TFields (ClinicalTrials.gov Identifier: NCT02973789, NCT05764954, NCT05538806).

#### **1.9.3.5. Immunotherapy**

In recent years, the FDA has approved various immunotherapies as the standard treatment for many types of cancers, as they show high efficacy in reducing or eliminating tumors, including highly metastasizing types of cancer (389,390). However, none have been able to improve the survival rate for patients with GBM. The goal of immunotherapy is to activate the immune system to target and destroy cancer cells in a tumor-specific manner (391,392). In the case of GBM, various immunotherapy methods have been explored, such as checkpoint inhibitors, chimeric antigen receptor CAR T-cell therapy, vaccines, viral vector therapies, and cytokine-based treatments (393,394). Although there have been no major breakthroughs yet, many studies are currently being conducted. The future directions of GBM therapy is advancing towards an approach that involves the commonly applied methods such as maximal tumor resection followed by radio- and chemotherapy and the combination of immunotherapy with the purpose of eradicating cancerous cells and stimulating an immune response (395). This innovative approach seeks to enhance the effectiveness of treatment through the activation of the immune system.

#### **1.9.3.6. Gene therapy**

Gene therapy is a quickly developing branch of novel treatment approaches, which focuses on the delivery of therapeutic molecules to the pathologically altered area to repair or augment a cell's genetic program, leading to a change of its behavior in a therapeutically useful manner (396). Interestingly, it might also enhance the immune response to combat tumor

growth, reprogram the tumor microenvironment (TME) and normalize the formation of blood vessels (397). The manner of therapeutic molecule delivery might also have contributed to the therapeutic process, as nano-particle-mediated gene therapy aiming to overcome BBB is currently being developed (397,398). The BBB states one of the biggest challenges in terms of brain-targeted therapeutics, which requires bypassing the BBB to efficiently perform its function (399,400). Magnetic nanoparticles, despite their transporting role, might be used for tumor diagnostic purposes as they deliver more intense contrast enhancement and can accumulate in neoplasms for longer periods compared to gadolinium-based contrast agents (401–403). For example, magnetic Fe<sub>3</sub>O<sub>4</sub> nanoparticles (NPs) are frequently utilized in clinics as contrast agents for MRI scans, as they enhance T2-weighted MR imaging by improving BBB uptake, targeting tumors, and reducing transverse relaxation time (401,404). Moreover, oncolytic viruses are currently being explored as a potential means to improve the effectiveness of GBM treatment, as they have the ability to trigger anti-tumor immunity, although there are still concerns regarding the specificity and transduction efficiency of potential therapy (405,406).

Despite the establishment of the Stupp protocol as the gold standard for GBM treatment, scientists and clinicians still strive to establish modern therapeutic approaches. Besides the commonly applied methods, which are tumor resection, frequently followed by the use of chemotherapy and radiotherapy, great scientific endeavors are put into immunotherapy and targeted gene therapy combined with functionalized nanocarriers. These ultimately aim to enhance patient survival rate and quality of life, minimizing the risk of tumor recurrence.

### **1.10. Molecular characteristics of glioblastoma**

Taking into consideration the large endeavors of scientists and clinicians and the resulting little success in the development of effective GBM treatment approaches, it is crucial to identify and understand the pathophysiological mechanisms of GBM. Comprehending the mechanism of GBM development and progression supports the discovery of GBM subtype- and patient-tailored therapies according to specific tumor features like grade, histological differences, molecular subtypes, aggressiveness, and response to treatment (407). Better patient stratification significantly facilitates the patient's survival rate, quality of life, and subsequent recurrence prognosis and decreases adverse effects of the applied therapy. The collaboration between the National Cancer Institute and the National Human Genome Research Institute resulted in the establishment of The Cancer Genome Atlas Research Network (TCGA), which presents the classification of the key genomic alterations in the most common types of cancer

(408). The analysis of the provided data, Verhaak and colleagues established a novel molecular classification of GBM, dividing it into proneural, neural, classical, and mesenchymal subtypes based on the investigation of multidimensional genomic data of gene expression patterns, genetic mutations, and DNA copy number (409). Moreover, they investigated the response to aggressive therapy, which differs among the established subtypes, exhibiting the greatest benefit in the classical subtype and no benefit in the proneural subtype (409). The project indicates that the proneural subtype is associated with younger age, IDH1 and tumor protein P53 (TP53) mutations, and platelet derived growth factor receptor alpha (PDGFRA) abnormalities, which previously were a common signature of secondary GBM. Neural subtype was typified based on the expression of neuron markers namely neurofilament light chain (NEFL), gamma-aminobutyric acid (GABA) receptor 1 (GABRA1), synaptotagmin 1 (SYT1), and solute carrier family 12 member 5 (SLC12A5). Their expression pattern appears to be very similar to normal brain tissue samples, indicating a differentiated cells phenotype. Classical GBM subtype exhibits the set of the most common genomic aberrations revealed in GBM, such as chromosome 7 amplifications and chromosome 10 deletions, EGFR amplification, and homozygous deletion of the Ink4a/ARF locus, followed by lack of abnormalities in TP53, neurofibromin 1 (NF1), PDGFRA, or IDH1. Furthermore, the mesenchymal GBM subtype exhibits a high expression level of chitinase 3 like 1 (CHI3L1) and MET, a high frequency of NF1 mutation/deletion, and low levels of NF1 mRNA expression. The mesenchymal subtype of GBM also shows the expression of Schwann cell markers, specifically the S100A family, along with microglial markers (409). Although many efforts have been made to understand GBM genetics and implement this knowledge in the clinics, different molecular subtypes of GBM are still being treated with similar approaches based on the Stupp regimen, which in some countries, is also facilitated by the tumor-treating fields approach (410). The GBM molecular classification states powerful advancement in terms of subtype-tailored therapy, however, it also leads to the necessity of rethinking and redesigning future GBM clinical trials and provides the framework for the discovery and testing of novel targeted therapies for particular glioma subtypes.

The new version of hallmarks of cancer, which underlines the vast complexity of cancer phenotypes and genotypes, greatly covers the key characteristics of GBM (411). These include selective advantages of growth and proliferation, altered stress response, sustained vascularization, tissue invasion and metastasis, metabolic alteration, immune modulation, and, as a result of the abovementioned, tumor microenvironment promotion (407). One of the most important features of cancer, including GBM, is the activation of tumor cell invasion and

metastases. These competencies give the ability to spread cancer both within the tissue occupied by the tumor, causing the adjacent tumor invasion, and also outside it, leading to metastasis (412,413). Cancer progression and metastasis are important mechanisms that can significantly affect the course of treatment and the survival prognosis of affected patients (414).

### **1.10.1. Glioblastoma heterogeneity**

High GBM heterogeneity, followed by its invasive potential and poor response to chemo- and radiotherapy, state the predominant causes of challenging GBM treatment (415). A breakthrough discovery of recent decades is the identification of various GBM molecular subtypes, which greatly underlines the diverse nature of the tumor, showing high intertumoral heterogeneity (409). Intertumoral heterogeneity describes the differences found between tumors among different patients (416). The approach is facilitated by the presence of intratumoral heterogeneity, referring to distinct tumor cell populations, showing different molecular and phenotypical profiles, present within the same tumor (417). The studies show that intratumoral heterogeneity could be more relevant for an efficient treatment and patient outcome than intertumoral heterogeneity (418).

The inter- and intratumoral heterogeneity might be identified at various structural levels, including molecular, cellular, histological and clinical, and biological (419). However, a more functional GBM heterogeneity classification has been proposed, spanning the molecular, genetic, expression, and epigenetic heterogeneity (420). Molecular heterogeneity of the GBM is usually described as histological variations observed even within the same tumor, most commonly in the form of different estimations of necrosis, nuclear size, astrocytic differentiation, cell size, number of mitotic cells, distribution of cell density and vascularization (420,421). The genetic heterogeneity allows to assess the commonly observed genetic alterations of GBM also observed within the same tumor (422). The alterations include disruption of EGFR, telomerase reverse transcriptase (TERT), PDGFRA, CDK4, MDM2, Murine double minute 4 (MDM4), phosphatidylinositol-4,5-bisphosphate 3-kinase catalytic subunit alpha (PIK3CA), phosphatase and tensin homolog (PTEN), ATRX, IDH1, and TP53 (409,420,423). Furthermore, the study of bulk GBM tissue showed that the driver aberrations and copy number alterations (CNA) could differ even in the same tumor tissue (424). The authors also found that loss of cyclin-dependent kinase inhibitor 2A (CDKN2A/B) and amplification of EGFR, CDK6 and MET state the features of early tumor development, while alterations in PDGFRA, PTEN and TP53 are characteristic for later malignant events (424)

The epigenetic pathways that might be contributing to therapeutic resistance and tumor recurrence are currently widely investigated. The methylation of the MGMT promoter is one of the widely studied epigenetic changes, as the MGMT methylation status states important epigenetic indicators of GBM patients' survival (425,426). The MGMT gene encodes a DNA repair protein that eliminates alkyl groups from the O6 position of guanine, which states a key DNA alkylation site (427). GBM patients with a hypomethylated MGMT promoter exhibit high levels of the MGMT protein and, therefore, higher to alkylating agents like TMZ, the GBM first-choice chemotherapeutics (420). A significant increase of another epigenetic modification known as N6-methyladenine (N6-ma), has been identified in GBM (428). The level of N6-ma is regulated by AlkB homolog 1 (ALKBH1), which reduction resulted in the transcriptional silencing of several oncogenic pathways due to reduced chromatin accessibility. Moreover, an increase in N6-methyladenosine (m6A) mRNA modifications has been detected also in cancer stem cells (428).

GBM has already been recognized to have wide genetic and phenotypic alterations, leading to disruption of downstream biological interactions both spatially and temporally, affecting the response to treatment (429). The field of GBM heterogeneity recently benefited from the application of advanced genomic technologies at single-cell resolution to map the transcriptome landscape of GBM to potentially explore the mechanism of drug resistance of GBMs at a single-cell level (430). The study of primary and recurrent GBM samples in which recurrence and drug resistance developed after treatment with the standard Stupp regime revealed the overexpression of stemness- and cell-cycle-related genes in recurrent GBM. The comparison of primary and recurrent GBM tissues revealed a reduced proportion of microglia in recurrent GBM tissues. Additionally, recurrent GBM exhibited high expression of VEGFA and BBB permeability and activation of the O6-methylguanine DNA methyltransferase-related signaling pathway (430).

### **1.10.2. Tumor microenvironment**

The tumor microenvironment is a complex and dynamic ensemble of tumor cells that are surrounded by several types of non-tumor cells like fibroblasts and immune cells, but also the non-cellular components of the extracellular matrix such as collagen, fibronectin, and many others, is the key structural component that supports the tumor growth. (431,432). Moreover, TME plays a crucial role in tumor invasion, progression, and response to therapies. The TME is a heterogeneous and interconnected network of various cell types, ECM components, and signaling molecules. Cancer cells are the primary cells that constitute the tumor and drive its

growth and invasive behavior. They often exhibit abnormal proliferation and survival mechanisms, leading to uncontrolled growth (411). Cancer cells are facilitated by the stromal cells, non-cancerous cells that support tumor growth. This category includes fibroblasts, most commonly referred as cancer-associated fibroblasts (CAFs) that support tumor growth, and invasion, promote ECM remodeling and secrete factors that promote tumor cell survival and angiogenesis, such as growth factors, for example, hepatocyte growth factor (HGF) and cytokines into adjacent cancer cells (433,434). Another factor produced by CAFs is fibroblast-secreted protein-1 (FSP1), which is reported to facilitate cancer cell growth (433). It has been demonstrated that metastatic cancer cells transplanted into FSP1 knockout mice are less likely to form tumors, which was restored by the co-injection of fibroblasts that overexpress FSP1 with the same tumor cells (435). Moreover, among all the stromal components, fibroblasts play a vital role in synthesizing the ECM, as they produce fibronectin and various types of collagen (436).

Another key player of TME, immune cells have a crucial role in the tumor microenvironment, as they can either suppress tumor growth or promote it. Some immune cells, like cytotoxic T-cells and natural killer (NK) cells, are capable of recognizing and eliminating cancer cells (437,438). Cytotoxic T-cells are able to detect abnormal tumor antigens present on cancer cells and initiate their destruction. Cytotoxic T-cells have been also reported to suppress tumor angiogenesis by producing interferon-gamma (IFN- $\gamma$ ), therefore the detection of cytotoxic T-cells in the TME is often associated with positive outcomes in cancer patients (439). T-cells expressing CD4<sup>+</sup> antigen commonly differentiate into multiple subtypes which allow them to coordinate a wide scope of immune responses, for example, T helper 1 cells act as proinflammatory factors that support immune cells expressing CD8<sup>+</sup> through the secretion of IFN- $\gamma$  and interleukin-2 (440,441). Furthermore, NK cells monitor the bloodstream and identify tumor cells or cells infected with viruses. NK cells are highly effective in destroying cancer cells present in the bloodstream and can also prevent developing metastasis (442–444). However, they may not be as effective in killing cancer cells within the tumor microenvironment. NK cells are highly efficient at killing tumor cells within the circulation and can participate in blocking metastasis but are less efficient at killing within the tumor microenvironment (445). Moreover, one of the hallmarks of cancer clearly illustrates the key obstacle of tumor immune defense, as tumors can evade immune surveillance and recruit immunosuppressive cells, which dampen the anti-tumor immune response (411,446,447).

The ability of immune cells to infiltrate tumor mass strongly relies on the presence of blood vessels. Tumors require a blood supply in order to receive nutrients and oxygen to grow

(448). The process of angiogenesis, which is commonly initiated by the release of pro-angiogenic factors by cancer cells, supports the formation of new blood vessels in the tumor (449). As the tumor grows, it promotes the formation of local hypoxic spots that lead to the development of leaky and unorganized vessels, which state the obstacle in the delivery of therapeutic agents to the tumor cells (450). The abnormal tumor vessels reduce tissue perfusion and the ability of the immune system to target the tumor, which in turn promotes the growth of aggressive tumor cells within the tumor microenvironment (451). Under oxygen deficiency conditions, factors that promote the growth of blood vessels bind to receptors on the surface of endothelial cells, leading to their dilatation and activation(452) . Moreover, the low oxygen level leads to the increased expression level of proteases responsible for the degradation of the basement membrane and the pericytes detaches (453,454). This allows the highly mobile endothelial cells to migrate toward the areas where the blood vessels are needed. As the endothelial cells proliferate, new blood vessels start to form leading to the development of the tumor's vascular system (455).

In GBM, at least three vasculature-related niches have been identified, including the perivascular tumor niche, vascular-invasive tumor niche, and hypoxic-necrotic tumor niche (456,457). Brain hypoxia, a key characteristic of the tumor microenvironment, is linked to tumor progression, and facilitation of tumor angiogenesis, and radioresistance (458–460). Moreover, it triggers mechanisms such as HIF signaling and EMT, which play a significant role in glioma stem cell regulation. The critical role of the microenvironment regarding GBM aggressiveness and invasiveness is supported by the observation that GSCs reside in the abovementioned niches and play an indispensable role in homeostasis, regeneration, maintenance, and repair (461–463). Therefore, understanding the crosstalk between GSCs and their niches is crucial in supporting GSC self-renewal, tumor invasion, metastasis, and escape from therapy.

The ECM, another key player of tumor microenvironment, is a complex network of proteins and carbohydrates that provide structural support to cells (464,465). Brain ECM has a distinct composition from ECM in other tissues, which is characterized by low stiffness and loose cells distribution. In GBM ECM consists of over 300 different proteins, including proteoglycans and glycoproteins, forming dense ECM characterized by increased levels of total fibrillar collagen, fibronectin, proteoglycans, and tenascin C (TNC) (466–468). The changed protein profile within ECM increases the stiffness of cancerous tissue, which may lead to enhanced cell–ECM adhesion through the involvement of local adhesion proteins (469). Therefore, the capability to synthesize specific and cancer-related ECM components has been

shown to be relevant for the high invasiveness of tumor cells. Malignant GBM invasion is linked to certain anatomic pathways that follow blood vessels and myelinated fiber tracts (470). In addition to anatomical and physical aspects, it has been described that specific ECM components such as hyaluronan, vitronectin, and TNC are upregulated at the border of the spreading GBM (470). As molecular guidance cues during cell invasion and metastasis are often dependent on the tumor ECM, the underlying mechanism of GBM invasion and the supporting role of ECM states a promising target for treating GBM (470). Among the most extensively developed GBM therapies targeting the ECM molecules are the collagen-, TGF- $\beta$  receptor-, angiotensin II type 1 receptor- and fibronectin-targeting therapies (465).

Taking together, the TME states a highly dynamic ensemble and can change over time in response to various stimuli, including therapeutic interventions. Understanding the complexity of the TME is essential for developing effective cancer treatments that target not only cancer cells but also the supportive elements that sustain tumor growth. Research in this field continues to uncover new insights that may lead to novel therapeutic strategies for cancer patients.

### **1.10.3. Glioma stem cells**

Numerous studies have identified the presence of stem cell-like cells in solid tumors, namely cancer stem cells (CSCs) (471–473). Studies have shown that these cells possess a high level of plasticity and are capable of proliferation, self-renewal, and giving rise to other types of cells that comprise the tumor (474,475). Studies of the isolated fraction of CSCs revealed that they might be responsible for tumor development, treatment resistance, tumor metastasis, and recurrence (476). There are several factors contributing to the resistance of chemo- and radiotherapy. These include their CSCs quiescence, their DNA repair abilities, high mitochondrial reserve, and their location in hypoxic niches (477). To effectively combat the therapeutic resistance of CSCs, it is crucial to comprehend the mechanisms of resistance and the implication of the tumor microenvironment, as those two factors highly depend on each other (478). In recent years, it has been established that glioblastoma stem cells are crucial for the development, maintenance, and recurrence of GBM, which indicates the significance of targeting GSCs in the treatment of GBM (477,479,480). Singh and colleagues were the first to present evidence of GSCs presence in GBM, as they discovered a population of cells that could initiate tumor growth *in vivo* (481). The first accepted GSC surface marker was CD133, a glycosylated transmembrane protein, encoded by Prominin-1 (482,483). CD133 expression level enables the characterization of cell self-renewal capacity, as there is a decrease in the

expression of this surface marker during cell differentiation (483). Additional markers that collectively define a characteristic of GSCs have also been presented, such as the presence of dual CD133+/Ki-67+ cells, indicating poor GBM patients' prognosis (479,484). Moreover, CXCR4 chemokine receptor and enhanced expression of HIF-1 markers are overexpressed in GSCs (485–487). Other characteristics identified in GSCs includes the cell-surface glycoprotein CD44, the cell-surface gangliosides A2B5, CD90, and sex determining region Y-box 2 (SOX2), as well as NANOG, aldehyde dehydrogenase 1 (ALDH1), L1 cell adhesion molecule (L1CAM), Krüppel-like factor 4 (KLF4), spalt like transcription factor 4 (SALL4), and glial fibrillary acidic protein (GFAP) (488). As GSCs are described to hold self-renewal properties and they are capable of differentiating into other specific GBM subpopulations, they have been presented to be responsible for GBM relapse after primary standard therapy and are linked with the poor prognosis of recurrent GBM patients. The failure of currently used therapies aiming to eliminate the GSC subpopulation has been considered a major obstacle attributed to the inevitable recurrence in GBM patients following treatment (489).

#### **1.10.4. Epithelial-mesenchymal transition**

Epithelial to mesenchymal transition is a complex biological process that occurs in various contexts, including embryonic development, wound healing, and cancer progression (490,491). It involves the transformation of epithelial cells, which are typically organized in horizontally and have cell-cell adhesion, into mesenchymal cells that exhibit highly motile, mesenchymal phenotype and facilitate tumor invasion and spread (492,493). In the context of glioblastoma, EMT plays a role in enhancing the invasive and metastatic properties of tumor cells. The first step is the loss of epithelial characteristics of the GBM cells. In glioblastoma, tumor cells that undergo EMT lose their epithelial characteristics (494,495). Epithelial cells are characterized by tight cell-cell junctions, expression of epithelial markers and a polarized cell structure (496). During EMT, cells downregulate epithelial markers like E-cadherin,  $\beta$ -catenin and occludin which are cell adhesion molecules responsible for maintaining epithelial integrity (497,498). Loss of adhesion molecules negatively impact cell-cell adhesion, allowing tumor cells to detach from the primary tumor mass. As tumor cells undergo EMT, they acquire mesenchymal characteristics. Mesenchymal cells are more migratory and invasive, with increased motility and resistance to apoptosis (499). These cells often display increased expression of mesenchymal markers such as N-cadherin, Zeb1, Zeb2, vimentin, and fibronectin (500). Tumor cells exhibiting mesenchymal phenotype become more mobile and capable of infiltrating surrounding tissues (501). This is a critical step in glioblastoma progression, as

invasion into adjacent brain tissue is one of the hallmarks of the disease's aggressiveness (502). Interestingly, it has been shown on breast cancer that mesenchymal cells can exhibit increased resistance to conventional therapies like chemotherapy (503). This resistance is thought to be associated with their altered gene expression profile and enhanced ability to evade treatment-induced cell death. Moreover, mesenchymal cells in glioblastoma often display properties associated with cancer stem cells, such as self-renewal and multi-lineage differentiation potential (504). This contributes to tumor heterogeneity and the ability of the tumor to regenerate after treatment. Those cells might also contribute to angiogenesis, which is crucial for tumor growth and progression (505). Taken together, EMT in glioblastoma contributes to tumor aggressiveness, invasion, and therapeutic resistance, stating an important focus of research in understanding and targeting glioblastoma progression, as well as other abovementioned processes, which have been summarized in the Figure 2.

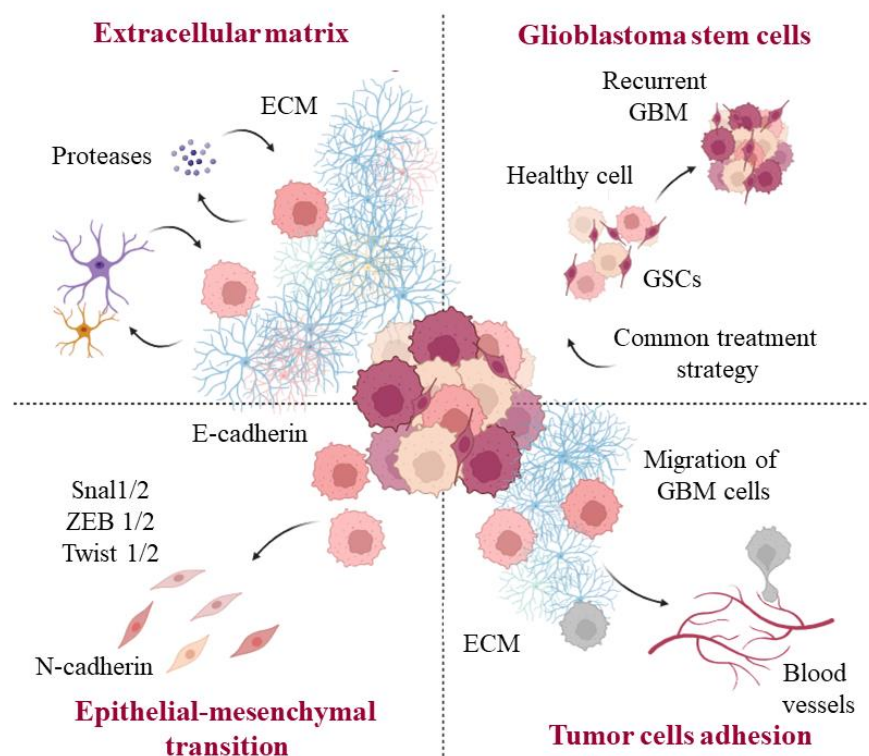


**Figure 2. Overview of key events involved in GBM invasion process with the strong impact on tumor microenvironment rearrangements.** Adapted from Velásquez et al. 2019. (506)

### 1.10.5. Non-coding RNAs in glioblastoma

Non-coding RNAs (ncRNAs) play a crucial role in various cellular processes, and their importance in cancerous and non-cancerous diseases becomes increasingly evident (507–509).

Glioblastoma is one of the most aggressive and challenging-to-treat brain cancers, and understanding the role of ncRNAs in its development and progression is of great significance. ncRNAs are widely presented as key factors regulating gene expression at the transcriptional and post-transcriptional levels (510–512). Widely described transcription regulators are microRNAs (miRNAs), a type of small ncRNA, known to act by binding to mRNAs and leading to their degradation or translation inhibition (510,511). In glioblastoma, dysregulation of miRNAs might lead to abnormal expression of genes involved in tumor growth, invasion, and resistance to treatment (513,514). To date, a number of miRNA profiling studies of GBM patients' tissues utilizing NGS technology and microarrays have been published (515–517). Some miRNAs have been indicated as potential glioma biomarkers such as miR-202, miR-1290, miR-1207, miR-20a-3p, miR-500-3p, miR-494, miR-483, as there are associated with regulation of key cancer-related genes such as TP53, PTEN, mechanistic target of rapamycin kinase (MTOR), Wnt family member 2 (WNT2), and Wnt family member 1 (WNT1) or baculoviral IAP repeat containing 5 (BIRC5) (517). The miRNAs expression profile together with the mRNA expression pattern was also described as a factor allowing to distinguish various GBM subclasses among the patients and evaluate the patients' prognosis(518,519).

Another key ncRNAs role in glioblastoma is tumor suppression and oncogenesis. Some non-coding RNAs may act as tumor suppressors by inhibiting cell proliferation, promoting apoptosis, and suppressing tumor growth (520). An interesting example are tumor suppressors - long non-coding RNA MEG3 and microRNA-377, which play an important role in glioma cell invasion and migration (521). MEG3 is known to sequester oncogenic miRNAs, which results in the regulation of cancer cells proliferation and apoptosis rate. However, it has been shown that the overexpression of both lncRNA MEG3 and miR-377 inhibited the invasion and migration of glioma cells, suggesting the tumor-suppressive effect of MEG3 and miR-377 in glioma cells (521). Furthermore, certain ncRNAs can function as oncogenes by promoting cell proliferation, invasion, and angiogenesis. Dysregulation of these ncRNAs can lead to uncontrolled cell growth and contribute to glioblastoma development. In glioblastoma, miR-10b, an oncogenic miRNA, is recognized to be overexpressed in GBM tissue and is required for tumor growth (522). Oncogenic miRNAs are characterized by the phenomenon of oncogene addiction, as the tumor cells require continuous expression of the oncogenic miRNAs for survival, which might state an interesting therapeutic target (507).

Several ncRNAs are evidenced to be involved in epigenetic regulation, which impacts gene expression with no change in the DNA sequence (523,524). Epigenetic modifications are frequently altered in glioblastoma and can affect the tumor's behavior (525,526). Glioblastoma

is widely known for its resistance to conventional therapies such as radiation and chemotherapy. Some ncRNAs have been linked to drug resistance by regulating gene expression in drug metabolism, DNA repair, and cell survival pathways. Interestingly, lncRNAs have been shown to play a role in GBM chemotherapy resistance through the epigenetic mechanism of action. Long noncoding RNA (lncRNA) SNHG12, which is shown to be activated by abnormal DNA demethylation, has been shown to induce TMZ resistance in GBM cells (527). The mechanism of SNHG12 action includes the promotion of cell proliferation and inhibition of cell apoptosis by acting as a sponge of miR-129-5p. This results in the elevated expression level of MAPK1 and E2F7 and activates the MAPK-ERK pathway (527).

The understanding of the role of ncRNAs in therapy resistance might also lead to the development of novel therapeutic approaches utilizing ncRNAs as therapeutic targets. The dysregulated expression of non-coding RNAs in glioblastoma presents opportunities for targeted therapies. Researchers are exploring the use of RNA-based therapies, such as miRNA mimics or inhibitors, siRNAs, shRNAs, ASO anti-microRNAs (antimiRs), miRNA sponges and therapeutic circular RNAs to restore normal cellular processes and inhibit tumor growth (528). Moreover, a recently emerging field is the application of ncRNAs as diagnostic and prognostic biomarkers (529,530). Their altered expression patterns in tumor tissues and bodily fluids can provide valuable information about disease progression, response to treatment, and overall patient outcomes (531,532).

Taking together, ncRNAs emerged as key players in the molecular mechanisms underlying glioblastoma development and progression. Their roles in gene regulation, epigenetics, drug resistance, and diagnostic and prognostic applications make them important subjects of research for improving the understanding of glioblastoma biology and developing innovative therapeutic strategies.

### **1.11. Models for advanced glioblastoma research**

Brain tumor cells create an appropriate microenvironment for migration and invasion by modifying and degrading the ECM and enhancing the ability of GBM cells to invade surrounding tissues, which leads to a desperate need for new and innovative GBM invasion models (432,533). Currently available models are mostly based on the application of two-dimensional (2D) cell lines alone or as a co-culture with three-dimensional (3D) models such as tumor spheroids or spheres (534–536). Moreover, to better recapitulate the tumor microenvironment and heterogeneity, co-culture of either GSC alone or as patient-derived neurospheres fused with human cerebral organoids has been described (534,537). Despite the

lack of advanced structural and functional characteristics, generated systems encounter substantial limitations, which are distinctive of *in vitro* cancer model formation, such as an inability to simulate the interactions between tumor cells and the healthy microenvironment, followed by the absence of blood vessels and immune cells (538).

GBM research involves the use of various 2D and 3D models to better understand the disease, test potential treatments, and develop new therapeutic strategies. Most commonly used 2D models in GBM research are 1) GBM cell lines, commonly applied to study the biology of the disease and test potential drugs, as they allow for easy experimental manipulation (539); 2) primary cell cultures, which derive from patient samples and provide a more accurate representation of the tumor's characteristics and heterogeneity, also applied for *in vitro* experimentation (540); 3) co-culture models, involving GBM cells along with other cell types like neurons, endothelial cells, or immune cells, which allows to mimic the tumor microenvironment and interactions between different cell types (541,542). 2D models might be useful in early-stage research to generate hypotheses and gather preliminary data before investigating complex 3D or animal models. These models show high simplicity of use and accessibility, they are cost-effective and easy to maintain in the culture (543). 2D models are also useful in high-throughput screening of therapeutic drugs and compounds, as a large number of potential therapies in a short time might be investigated (544). Adherent cell lines allow researchers to study specific molecular and cellular mechanisms underlying glioblastoma development and progression. They provide a controlled environment for investigating signaling pathways, gene expression, and other cellular processes, as the gene editing and manipulation techniques protocols are widely tested and adjusted for the application of 2D models (545). Those techniques might be applied more easily in 2D models, allowing researchers to investigate the effects of specific genetic alterations on glioblastoma behavior before applying complex models. Cell lines are also a more ethically and financially feasible model compared to 3D models (546). Even though 2D cell culture models are valuable tools in glioblastoma research, they also exhibit substantial limitations that need to be considered, such as the limited influence of tumor microenvironment, as 2D cultures do not accurately represent the complex 3D architecture and cellular interactions found within glioblastoma tumors (547). Tumors *in vivo* exist in a dynamic microenvironment with surrounding stromal cells, blood vessels, and extracellular matrix components, which play crucial roles in tumor behavior (548). 2D cultures may not fully capture this heterogeneity, potentially leading to a simplified representation of the patient's condition. The hallmarks of cancer, such as mechanisms of tumor invasion and metastasis and disrupted biological signaling are underrepresented in 2D tumor

models, as 2D cultures do not effectively replicate the invasive characteristics of glioblastoma cells and their interactions with surrounding tissues (549,550). These models also experience altered signaling pathways due to the absence of critical interactions with neighboring cells and the extracellular matrix, leading to discrepancies in signal transduction pathways compared to the *in vivo* models (551). Moreover, cells grown in 2D cultures might exhibit different behavior compared to their *in vivo* counterparts. This includes altered growth rates, gene expression patterns, and drug sensitivities, which can limit the translatability of findings to the clinics (552). While 2D models are useful for initial drug screening, they might not accurately predict the responses of drugs targeting specific pathways in the complex context of a 3D tumor. This phenomenon might be linked with limited and underrepresented responses to drugs observed in 2D cultures, as they do not accurately present how the same drugs will perform in a 3D tumor environment. The lack of proper tumor architecture and microenvironmental cues can affect drug penetration and efficacy (553). Mechanical cues, highly linked with altered tumor microenvironment, such as ECM stiffness, are important regulators of cell behavior (554). These cues are highly limited in 2D cultures, which can impact cell morphology, migration, and differentiation. Presented limitations turned the scientific community towards more complex 3D models, which better recapitulate the tumor microenvironment and improve the relevance and translatability of their findings to clinical practice.

The most commonly used 3D GBM models are 1) spheroids and tumoroids formed by either cell line- or patient-derived aggregating cells; 2) GBM organoids, complex 3D structures derived or containing patient-derived components, that greatly resemble the architecture of the original tumor; 3) animal models, such as patient-derived xenografts or genetically engineered animal models, allow researchers to study tumor growth, invasiveness, preserve the characteristics and heterogeneity of the original tumor and can be used to test personalized treatment approaches and response to therapies *in vivo* and models provide insights into the genetic factors driving glioblastoma development (555,556). 3D models play a critical role in glioblastoma research by providing a more physiologically relevant environment to study the complex nature of the disease (557). These models better capture the interactions between different cell types, the tumor microenvironment, and the spatial architecture of glioblastoma tumors (558). 3D models allow for the recreation of the tumor microenvironment more accurately. GBM cells interact with various cell types, extracellular matrix components, and signaling molecules, and 3D models better mimic these interactions compared to traditional 2D models (559). GBMs are highly heterogeneous tumors, with distinct subpopulations of cells contributing to tumor growth, invasion, and resistance. 3D models can capture this

heterogeneity, helping researchers understand the roles of different cell types within the tumor (560). GBM cells exhibit high cell-cell and cell-matrix interactions and 3D models allow for the study of these intricate interactions, which play a crucial role in tumor progression and treatment response (561). Therefore, 3D models also enable to observe and investigate the mechanisms of cell invasion and migration more realistically compared to 2D models (562). Tumor invasion depends on the oxygen gradient that exists in tumors and this phenomenon is greatly recapitulated by 3D GBM models (562). The tight cellular aggregation allows studying drug distribution and penetration within the tumor, which is important for understanding drug efficacy and optimizing treatment regimens (563,564). Therefore researchers might explore the underlying mechanisms of drug resistance by simulating the tumor microenvironment and studying how resistant cells interact with their surroundings (565). Patient-derived 3D models might be used to test individual patient responses to treatments, facilitating the development of personalized treatment strategies. The abovementioned advantages might link molecular research and clinical applications, leading to relevant insights into potential therapeutic strategies. While 3D models offer multiple advantages over 2D models in capturing certain aspects of glioblastoma biology, they also present some limitations (565). One of the leading 3D model's limitations is confined access to patient samples, which might not always be readily available or the quality of the extracted material might show poor experimental utility (566). Moreover, even though these models commonly derive from patients' material, they might still not fully represent the complexity and diversity of glioblastoma tumors observed in patients. Proper vascularization and the presence of immune cells are also key features of the tumor microenvironment, difficult to sustain over long culture periods (567). Glioblastoma tumors also evolve over time, and this dynamic process might not be accurately captured in static 3D models, especially those that are not long-term or continuously cultured (568). Generating and maintaining 3D models might be also technically challenging, leading to some level of variability due to the dynamic nature of the tumor microenvironment, leading to challenges in reproducing results across experiments. The interpretation of results obtained from 3D models can be complex due to the intricate interplay between cells, extracellular matrix, and microenvironment. Despite the molecular and technical limitations, it is important to highlight that 3D models require significant resources in terms of time, materials, and equipment, increasing the overall cost of research (569). The use of animal models, such as xenografts also raises ethical and regulatory concerns. Despite these limitations, 3D models remain valuable tools for glioblastoma research, as they provide a more relevant context for understanding tumor behavior and therapeutic responses (547,570)). Researchers often use a combination of 2D and

3D models to address different research questions and overcome the respective limitations of each approach (571).

The newly emerged field of advanced disease models states the highly innovative platforms for the development of complex settings utilizing patient-derived material. 3D bioprinting technology can be used to create complex 3D structures that mimic glioblastoma tumors (572,573). This allows for precise control over the architecture and composition of the model. Another example states microfluidic platforms, which create controlled microenvironments to study glioblastoma behavior, enable the observation of cell migration, invasion, and responses to drugs in a more physiologically relevant context (574–576). Multi-omics approaches, which integrate genomics, transcriptomics, proteomics, and metabolomics data from various models might provide a comprehensive understanding of glioblastoma biology and identify potential therapeutic targets (577,578). These models collectively contribute to advancing our understanding of glioblastoma and developing innovative treatment strategies, as no single model perfectly replicates the complexity of the tumor, and a combination of approaches is often required for comprehensive research.

## 2. Research objective

The presented dissertation focuses on a comprehensive understanding of the GBM development and progression, with special attention to the invasion process, considering the potential function of circRNAs, acting as competing endogenous RNAs (ceRNAs), which through a broad network of interactions might modulate the function of their interactors and/or targets. To support the tumor complexity, novel and highly advanced GBM models were generated and applied in the study. For the purpose of the broad characteristics of circRNAs function in GBM tumorigenesis and its progression, the research objective assumed the achievement of the following goals:

**1. Establishment of the potential functions of circCLIP2. circCLIP2 was reported in the literature as the highly overexpressed in GBM. Thus, I intended to explore its function in GBM onset and progression.** The loss-of-function approach utilizing siRNAs was adopted to determine the potential role of circCLIP2 in GBM. The downregulation of the circCLIP2 expression level allowed to investigate its function in key processes related to tumorigenesis and tumor progression. Simultaneously, the mRNA counterpart of circCLIP2 was studied to examine whether both CLIP2 gene transcripts are involved in the analyzed function and investigate the potential interplay between both isoforms.

**2. The global-scale identification of the circRNAs exhibiting disrupted expression patterns in GBM and the selection of the most prominent candidates for further research with the therapeutic, diagnostic and/or prognostic potential.** To achieve this aim, primary and secondary GBM tissues were subjected to RNA sequencing, and the expression level of identified circRNA was compared to their expression level in healthy brain reference. This approach gave insight into the landscape of deregulated circRNAs in both types of GBM.

**3. Establishing complex and innovative 3D GBM models allowing to determine the key drivers of GBM invasion utilizing advanced global characteristic techniques with the special interest on the circRNAs function.** To get a more comprehensive insight into the GBM biology and structure, GBM neurospheres and organoids were generated and deployed into research. As the common GBM invasion models are still limited and poorly recapitulate the tumor structure and microenvironment composition, a novel invasion model was generated, consisting of glioblastoma organoids cocultured with cerebral organoids, so-called assembloid. This part of the research was conducted

as a part of the FEBS Short-Term Fellowship, of which the author of this dissertation was awarded. The generation of assembloids was conducted in collaboration with the Organoid Platform at Max Delbrück Center for Molecular Medicine (MDC) in Berlin.

### 3. Materials and Methods

#### 3.1. Chemical reagents

**Table 3. Chemical reagents used in the study.**

Reagent's Name	Manufacturer and Catalog Number
TRI Reagent® Solution	Invitrogen, AM9738
Chloroform	POCH, 234430427
2-Propanol (Isopropanol)	Sigma-Aldrich, 563935
EtOH	POL-AURA Odczynniki Chemiczne, 113964200#10L
SYBR™ Safe DNA Gel Stain	ThermoFisher Scientific, S33102
Agarose	Sigma-Aldrich, A9539-500G
DNA Gel Loading Dye (6X)	ThermoFisher Scientific, R0611
Tris	BioShop, TRS001
Boric acid	POCH, 531360738
DAPI	Sigma-Aldrich, D9542
Matrigel	Corning, 356234
Geltrex	ThermoFisher Scientific, A1569601
StemPro Accutase	ThermoFisher Scientific, A1110501
Trypsin	Sigma-Aldrich, T4049-100ML
TGFβ	ThermoFisher Scientific, PHG9214
PBS tablets	Millipore, 524650-1EA
Bovine Serum Albumin (BSA)	Biowest, A0296
Ethylenediaminetetraacetic acid (EDTA)	POCH, 593280117
rRNA DNA Oligos for Ribodepletion	Designed by our collaborators from MDC, Berlin
Hybridase Thermostable RNase H	Epicentre, H39500
Agencourt AMPure XP beads	Beckman Coulter™, A63880
Freezing Medium Cryo-SFM	Sigma-Aldrich, C-29912
MACS® Tissue Storage Solution	Miltenyi Biotec, 130-100-008
Tissue-Tek® O.C.T. Compound	Sakura Finetek USA, 4583
Paraformaldehyde (PFA)	Sigma-Aldrich, 158127
Sucrose	Sigma-Aldrich, 721891
Gelatin	Sigma-Aldrich, 1.04078
Normal Goat Serum (10%)	ThermoFisher Scientific, 50197Z
Triton™ X-100	Sigma-Aldrich, 1.08643
ProLong™ Gold Antifade Mountant	ThermoFisher Scientific, P36930

### 3.2. Buffers

**Table 4. Ten times concentrated TBE for agarose gel electrophoresis**

<b>TEB 10x pH 8,3</b>	
<b>Reagent</b>	<b>Final concentration</b>
Tris-HCl	500 mM
Boric acid	500 mM
EDTA	10 mM
ddH <sub>2</sub> O	Up to 1 L

**Table 5. Buffer for magnetic separation of glioma stem cells, pH 7.2**

<b>Reagent</b>	<b>Final concentration</b>
Bovine Serum Albumin (BSA)	0.5%
Ethylenediaminetetraacetic acid (EDTA)	2 mM
Phosphate-buffered Saline (PBS)	Up to 200 mL

**Table 6. 5x Hybridization buffer, pH 7.5**

<b>Reagent</b>	<b>Final concentration</b>
NaCl	1 M
Tris-HCl	0.5 M

**Table 7. 5x RNase H buffer, pH 7.5**

<b>Reagent</b>	<b>Final concentration</b>
NaCl	1 M
Tris-HCl	0.5 M
MgCl <sub>2</sub>	250 mM

### 3.3. Ready-to-use reagents

**Table 8. Ready-to-use reagents used in the study**

<b>Ready-to-use reagent name</b>	<b>Manufacturer and Catalog Number</b>
DNA-free™ DNA Removal Kit	ThermoFisher Scientific, AM1906
TURBO DNA-free™ Kit	ThermoFisher Scientific, AM1907
Transcriptor High-Fidelity cDNA Synthesis Kit	Roche, 04379012001
LightCycler® 480 SYBR Green I Master Mix	Roche, 04707516001
CD133 MicroBead Kit	Miltenyi Biotec, 130-100-857

RiboCop rRNA Depletion Kit	Lexogen, 144.96
TruSeq® Stranded mRNA Library Prep	Illumina, 20020594
TruSeq RNA Single Indexes Set A	Illumina, 20020492
TruSeq RNA Single Indexes Set B	Illumina, 20020493
NEXTFLEX Small RNA-Seq Kit v3 with Unique Dual Index Barcodes	PerkinElmer, NOVA-5132-23
Spatial Transcriptomics Reagents	Technology delivered by our collaborators from MDC, Berlin.

### 3.4. Laboratory equipment

**Table 9. Laboratory equipment used in the study**

Name	Model	Manufacturer
Centrifuge	MiniSpin® plus, 5810R	Eppendorf
Centrifuge	Centrifuge 5430/ 5430 R	Eppendorf
Electrophoresis Chamber	Mini-Sub® Cell GT Cell	BioRad
Electrophoresis Power Supply	PowerPac Basic	Bio-Rad
Gel Analysis System	GelDock-it	UVP
Cell Culture Incubator	INCO153med	Memmert
Incubator Shaker	New Brunswick S41	Eppendorf
Laboratory Incubator	SI-950	UVP
Laminar Flow Cabinet	CAB1199	Scientific Laboratory Supplies
Laboratory Fume Hood	D1000	Alpina
Shaker	MS3 basic, 130 basic	IKA
Spectrophotometer	NanoDrop 2000	ThermoFisher Scientific
Thermocycler	CFX Connect	Bio-Rad
Thermomixer	Comfort	Eppendorf
Fluorescent Microscope	BZ-X700	Keyence
Fluorescent Microscope	ZEISS Primovert	ZEISS
Vortex	0003340000	IKA
Tissue dissociator	130-093-235	Miltenyi Biotec
Cryotome	CryoStar™ NX50	Epredia™
Incucyte System	Incucyte® S3 Live-Cell Analysis Instrument	Sartorius
Magnetic Stand	MACS® MultiStand	Miltenyi Biotec
Magnetic Separator	MidiMACS Separator	Miltenyi Biotec
Magnet	DynaMag™-2 Magnet	ThermoFisher Scientific
Fluorometer	Qubit Fluorometer	ThermoFisher Scientific

Tape Station	Screen Tape Assay Agilent D1000, 4200	Agilent
Fragment Analyzer	5200 Fragment Analyzer System	Agilent
Cryotome	Epredia™ CryoStar™ NX50	Epredia

### 3.5. Software

**Table 10. Software deployed for the analysis of the obtained data and micrographs.**

Name	Purpose
GraphPad Prism 8	Statistical analysis and visualization of the data
CFX Maestro	Real-Time PCR data collection, analysis, and statistical analysis
BZ-X700 analyzer	Micrograph acquisition and initial analysis
ZEN Blue	
BioRender.com	Preparation of schematic diagrams

### 3.6. Glioblastoma tissues

The GBM tissues were obtained from the Department and Clinic of Neurosurgery and Neurotraumatology at the University of Medical Sciences in Poznań and the Department of Neurosurgery at the Multidisciplinary City Hospital in Poznań. Prior to the surgery, the approval of the Bioethics Council of the Poznan University of Medical Science Council (consent number 534/18) and the donors' consent had been obtained.

#### 3.6.1. RNA sequencing

To characterize the landscape of circRNAs in GBM tissues, 26 GBM patients' tissues (primary GBM n=23 and recurrent GBM n=3) were subjected to RNA sequencing. Table 11 summarizes the characteristics of GBM patients and analyzed tumors. Four commercial samples of pooled human brain (HB) total RNAs were used as healthy brain reference, depicted in Table 12.

**Table 11. GBM patient-derived tissues subjected to RNA sequencing.**

Patient ID	Sex	Age	Symptoms			Tumor location (hemisphere)			Extent of resection		RNA RIN value
			Headache	Aphasia	Other	Right	Left	Both	Total	Subtotal	
P01	Male	59			x		x			x	8.1
P02	Female	58			x		x		x		9
P03	Female	56	x		x	x			x		9.2
P04	Female	65	x		x	x				x	9.9
P05	Male			x	x		x			x	9.4
P06	Male				X	x			x		8.8
P07	Female	58			X	x			x		8.2
P08	Male	61			X		x		x		7.6
P09	Female	63			x	x			x		8.7
P10	Male	52	x		x	x			x		8.8
P11	Male	62			x	x			x		8.4
P12	Male	67	No data available								8.5
P13	Male	49		x			x		x		8.6
P14	Male	60	x	x		x			x		7.8
P15	Female	70	x		x			x		x	7.8
P16	Male	83	x		x	x			x		9.3
P17	Male	64		x				x	x		7.6
P18	Female	74			x	x				x	8.4
P19	Male	68			x	x				x	8.2
P20	Male	65	x	x	x		x		x		7.4
P21	Female	68			x	x			x		8.6
P22	Female		No data available								8.4
P23	Female	58	No data available								8
R1	Female	52								x	7.5
R2	Male	49		x	x		x		x		8.9
R3	Male	47			x		x		x		7.7

**Table 12. Healthy brain reference RNA subjected to RNA sequencing.**

Product name	Manufacturer	Catalog Number and Lot Number	Number of patients	RNA RIN value
First Choice Human Brain Reference RNA	Ambion	AM6050, 1204014	23	9.1

FirstChoice® Human Brain Reference Total RNA	Ambion	6051, 105P055201A	12	9
Human Brain Total RNA	Clontech	636530, 1812054	3	8.2
Human Brain Total RNA	Takara	636530, 1602002	3	8.8

### 3.6.2. Estimation of the gene expression level of CLIP2 gene isoforms

Tumor tissues (primary GBM n=12 and recurrent GBM n=7) from GBM patients were collected up to one hour after tumor excision. As a control for the CLIP2 gene expression level estimation by RT-qPCR, we used a commercially available sample of 23 pooled human brain total RNAs - First Choice Human Brain (purchased from Ambion, cat. No# AM6050, depicted in Table 12).

**Table 13. GBM patient-derived tissues subjected to RNA sequencing.**

Patient ID	Sex	Age	Symptoms			Tumor location (hemisphere)			Extent of resection		RNA RIN value
			Headache	Aphasia	Other	Right	Left	Both	Total	Subtotal	
P005	Male	68			x	x				x	8.2
P008	Female	68			x	x			x		8.6
S008	Female	63			x	x			x		8.7
S010	Male	62			x	x			x		8.4
S013	Male	49		x			x		x		8.6
S019	Male	83	x			x			x		9.3
S021	Male	64		x				x	x		7.6
P010	Male	61	No data available								7.6
P006	Male	65	x	x	x		x		x		7.4
P009	Male	74	No data available								8.8
S011	Male	67	No data available								8.5
P004	Male	65	No data available								8.5

## 3.7. Cell culture and cell culture procedures

### 3.7.1. *In vitro* culture

Cell culture experiments were conducted under sterile conditions, deploying the chamber with a laminar airflow. The adherent cell lines, spheroids, and organoids used for the study were grown in 75 cm<sup>2</sup> and 25 cm<sup>2</sup> culture flasks, 6-, and 96-well plates in incubators

providing optimal conditions for the growth of animal cells: temperature 37°C, humidity 95%, CO2 concentration 5%, unless stated differently. While the experiments were completed, cell and organoid biobanks were created by transferring them to a Freezing Medium Cryo-SFM a, gradually cooling to -80 °C, and transferring them to liquid nitrogen for a long-term deposition. Prepared stock cultures served as a source of cells for conducting further experiments after their quick recovery to a temperature allowing for culturing on 25 or 75 cm<sup>2</sup> bottles (cell lines) and 6- or 12-well plates (GBM organoids), depending on the number of previously banked cells and organoids.

### 3.7.2. GBM cell lines

GBM cell lines used in the study are U251-MG and U138-MG. Cells were cultured as follows:

**Table 14. GBM cell lines used in the study and their characteristics.**

Line	Type	Manufacturer	Culture condition	Medium	Medium replacement
U251-MG	GBM	American Type Culture Collection (ATCC)	5% CO <sub>2</sub> , in 37°C and 95% humidity	As stated in point Y	Every second day for regular culture
U138-MG					

**Table 15. Composition of the media used for GBM cell lines culture.**

Reagent	Manufacturer and Catalog Number	The amount used per 50 mL of ready-to-use media
Eagle's Minimum Essential Medium (EMEM)	Corning, 10-009-CV	44,5 mL
Fetal bovine serum (FBS)	Sigma-Aldrich, F7524-500ML	5 mL
Penicillin/Streptomycin Solution (100x)	Life Technologies, P0781	500 µl

### 3.7.3. GBM spheroids

Human GBM cell lines U-251 MG and U-138 MG were used to create 3D spheroid structures according to the protocol developed by Vinci and colleagues (579). Cells were seeded in the amount of 3x10<sup>3</sup> cells/mL onto a non-adherent 96 U-bottom plate in 200 mL of media, composed as depicted in Table 15. Cells were centrifuged at 300 rpm for 3 minutes and grown

into spheroids for four days in the incubator under standard culture conditions. The media composition used for GBM cell line-derived spheroid culture is the same as for GBM cell lines, depicted in Table 15.

### 3.7.4. Organoids

GBM organoids, further named GBO in this work, were obtained from the GBM patient's tissue according to the protocol described by Jacob and colleagues (580). The characteristics of obtained GBM organoids are presented in Table 16. The tissues were collected and processed up to one hour after the surgical tumor resection based on the permission of the Bioethics Committee at Medical University of Karol Marcinkowski in Poznań (consent number 534/18). To generate the organoids, the obtained tissues were cleaned, minced, and placed in a culture medium described in Table 17. The GBM organoids were cultivated for 90 days in a culture incubator with a shaking platform, as depicted in Table 16. Processed tissue began to form the organoids after 14 days and the culture that did not produce structures larger than 50  $\mu\text{m}$  or the shape was not consistent with the abovementioned protocol, was discarded. In the course of the research, cerebral organoids, further named HBO in this work delivered by a collaborator from Organoid Platform at Max Delbrück Center (MDC), were used, also depicted in Table 16.

**Table 16. Organoid lines used in the study and their characteristics.**

Line	Type	Manufacturer	Culture condition	Medium	Medium replacement
P061	GBM	Patient-derived material generated by the thesis author	5% CO <sub>2</sub> , in 37°C and 95% humidity, 70 RPM orbital shaking	As stated in point X	Every second day for regular culture
P064					
GBO 141222					
HBO T1°6	iPSC-derived healthy brain	iPSC-derived structures, generated by collaborators from Organoid Platform, MDC			

**Table 17. GBM organoids media composition.**

Chemical reagent	Manufacturer and Catalog Number	The amount used per 50 mL of ready-to-use media
DMEM/F-12	Gibco, 11320033	23,47 mL
Neurobasal medium	Gibco, 21103049	23,47 mL
GlutaMAX™	Gibco, 35050061	500 µl
MEM non-essential amino acids	Gibco, 11140050	500 µl
Penicillin/Streptomycin Solution	Life Technologies, P0781	500 µl
N2 supplement	Gibco, 17502048	500 µl
B27 supplement without vitamin A	Gibco, 12587010	1 mL
2-Mercaptoethanol	Gibco, 21985023	50 µl
Human insulin solution	Sigma-Aldrich, 19278	10 µl

### 3.7.5. Assembloids

Assembloids were generated by the coculture of GBM organoids (GBO) and cerebral organoids (HBO). The dimpled parafilm square was prepared to serve as a well for the assembloids formation, where each of the wells was 0,7 cm in diameter. Parafilm wells were placed into a 60-mm tissue culture dish. Subsequently, one GBO and one HBO organoid were transferred to a common parafilm well and embedded in 7 µl of Geltrex. A dish containing organoids in parafilm wells was placed in the incubator in standard conditions and without shaking for 15 minutes to allow the Geltrex to solidify. In due course, fixed organoids were washed away from the parafilm wells to the wells of the f 6-well plate with the assembloids culture media. Assembloid medium composition is detailed in Table 19. Assembloids were cultivated for 3 weeks and handled as described in Table 18; afterward were harvested for characteristic purposes.

**Table 18. Assembloid lines used in the study and their characteristics.**

Line	Age at fusion	Type	Manufacturer	Culture condition	Medium	Medium replacement
ABO T106_P061	103 days	GBO-HBO co-culture	Generated by the thesis author and collaborator from Organoid Platform, MDC	5% CO <sub>2</sub> , in 37°C and 95% humidity, 70 RPM orbital shaking	As stated in point X	Every day
ABO T106_P064	63 days					
ABO T106_GBO 141222	33 days					

**Table 19. Assembloid medium composition.**

Chemical reagent	Manufacturer and Catalog Number	The amount used per 53,5 mL of ready-to-use media
DMEM/F-12	Life Technologies, 11320074	25 mL
Neurobasal Plus	Life Technologies, A3582901	25 mL
GlutaMAX™	Life Technologies, 35050038	500 µl
N2 supplement-A	Stem Cell, 07152	250 µl
B27 supplement with vitamin A	Stem Cell, 05711	1 mL
2-Mercaptoethanol	Merck Milipore, 8057400005	1,75 µl
Human insulin solution	Sigma, I9278	12,5 µl
Ascorbic acid (0.4mM)	Sigma, A92902	200 µl
Chemically Defined Lipid Concentrate	Life Technologies, 11905031	500 µl
MEM Non-essential Amino Acid Solution	Sigma, M7145	250 µl
Penicillin-Streptomycin	Life Technologies, P0781	500 µl

### 3.8. Cryosectioning

Organoids and assembloids were harvested, washed with PBS buffer, and fixed in 4% paraformaldehyde for 30 minutes. In due course, the specimen was washed in PBS 3 times for 10 min each. Subsequently, the sample was incubated in 40% sucrose dissolved in PBS overnight. Next, the specimen was embedded in 10% gelatin and 7.5% sucrose in PBS solution and transported into disposable molds with the Tissue-Tek® O.C.T., which supports the structure maintenance during freezing. The molds were placed in a -80°C freezer for 30 minutes until completely frozen. The slide sections were prepared for staining using an Eprelia™ CryoStar™ NX50. During the cryosectioning of organoids, the temperature of the cryostat

chamber was -17°C, and the blade temperature was -18°C. The thickness of the sections was 12 µm. The sections were transferred to glass slides, immediately subjected to immunofluorescence, or stored in a -80°C freezer.

### 3.9. Immunofluorescence

GBO, HBO, and assembloids were subjected to the immunofluorescence analysis to detect and localize the antigens characteristic for both organoid types and characterize the glioblastoma cells' invasive front. Slides prepared during cryosectioning were either immediately subjected to immunofluorescence or thawed. Slides were incubated with warm PBS for 15 min to remove the embedding gelatin/sucrose envelope. Subsequently, the slides were fixed with 4% paraformaldehyde for 15 min at room temperature and washed 3 times with PBS for 10 minutes each. Consequently, specimens were blocked and permeabilized in 0.25% Triton-X and 5% normal goat serum in PBS for 1 hour. Next, the slides were incubated with primary antibodies in 0.1% Triton-X and 5% normal goat serum overnight at 4°C. The list of the primary antibodies used in the study is presented in Table 20. Upon the incubation; specimens were washed 3 times for 10 minutes, each with PBS containing 0.1% of Triton. Subsequently, the samples were incubated with secondary antibodies at room temperature for 2 hours and were stained with DAPI at a final 1µg/ml for 10 min. Slides were washed 3 times with PBS containing 0.1% of Triton, and the coverslips were mounted with the mounting medium antifade and left to dry overnight at 4°C.

**Table 20. Antibodies used in the study.**

Full Antibody Name	Abbreviation	Manufacturer and Catalog Number	Dilution used in the study
Tenascin C	TNC	ThermoFisher Scientific, MA5-16086	1:250
β III Tubulin	Tuj1	BioLegends, 801201	1:1000
Homeodomain-only Protein Homeobox	Hopx	ThermoFisher Scientific, PA5-72855	1:500
Glial Fibrillary Acidic Protein	GFAP	Sigma Aldrich, AB5804	1:1000
Secondary antibody 1	-	Abcam, ab150077	1:1000
Secondary antibody 2	-	Abcam, ab150115	1:1000

### 3.10. Transfection with siRNA

Experiments conducted with GBM cell lines and GBM spheroids involved the delivery of selected synthetic oligoribonucleotides - siRNA to the cells. The list of the siRNA is depicted in Table 21.

**Table 21. Oligoribonucleotides used in the study.**

siRNA Name	Sequence
Unspecific (scrambled) siRNA	5'-GCUGAACAUAGUCACAGAU-3' 5'-AAGGCACAGCAUGAGCAGGUA-3'
siRNA linCLIP2	5'-GUGUUUGUAACAAUAACGU-3' 5'-AGUUUAUUGUUACAAACAC-3'
siRNA circCLIP2	5'-AAGGCACAGCAUGAGCAGGUA-3' 5'-UACCUGCUCAUGCUGGCCUU-3'

To deliver the siRNA to the cells, a chemical transfection, deploying a polyamine-based siPORT™ Amine Transfection Agent was applied (ThermoFisher Scientific, AM4502). Adherent GBM cell lines were seeded onto the plate 24 hours prior to the transfection. The cell number per well is depicted in Table 22.

**Table 22. Details of the GBM cells seeding for the transfection.**

Plate type	Number of cells	The volume of cultural media
6-well	$1.8 \times 10^5$	2 mL
96-well	$3 \times 10^3$	0,1 mL

For all the experiments that required cell transfection, unspecific siRNA was used as a control and administered at the same final concentration. The transfection procedure was carried out after 24 hours if the cells reached 75-90% confluence. GBM spheroids were prepared as presented in point 3.7.3. and were only subjected to transfection on a 96-well plate. Before the application of the transfection mixture, the culture medium was removed from the cells and spheroids, and the cultures were rinsed with PBS buffer (phosphate-buffered saline). Furthermore, the wells were filled with the non-supplemented medium, reduced by the volume of the transfection mixture. Cells and spheroids were transfected with siRNA at a final concentration of 100 nM. The first step of the transfection mixture preparation is combining of siPORT™ Amine Transfection Agent and Opti-MEM™ I Reduced Serum Medium

(ThermoFisher Scientific, 11520386), (Table 23, Mixture 1), and separately siRNA and Opti-MEM™ I Reduced Serum Medium (Table 23, Mixture 2), which are incubated at room temperature for 10 minutes in the ratio depicted in Table 23. The transfection mixture was prepared as follows (amount calculated per one reaction):

**Table 23. Transfection mixtures composition.**

<b>Transfection mixture 1</b>		
<b>Reagent</b>	<b>6-well</b>	<b>96-well</b>
Opti-MEM™ I Reduced Serum Medium	95 µL	9,7 µL
siPORT™ Amine Transfection Agent	5 µL	0,3 µL
<b>Transfection mixture 2</b>		
Opti-MEM™ I Reduced Serum Medium	97,5 µL	9,75 µL
siRNA	2,5 µL	0,25 µL

Furthermore, prepared mixtures were combined and incubated for 10 minutes at room temperature, and the obtained mix was administered to the culture wells containing the previously added non-supplemented medium. The transfection was performed for 48 hours in optimal cell growth conditions.

### **3.11. Hypoxia treatment**

Spheroids were subjected to oxygen deficiency conditions for 5 days in a 1% oxygen incubator. Following that, total RNA was extracted from the cells as described in Section X. The presence of oxygen deficit was confirmed by evaluation of the expression level of hypoxia indicators using reverse transcription-quantitative polymerase chain reaction (RT-qPCR).

### **3.12. Cell proliferation evaluation**

The proliferation of transfected cells was measured using the Incucyte® S3 Live-Cell Analysis Instrument. In 150 mL of the recommended culture media, cells were seeded onto 96-well Corning Falcon plates at a  $3 \times 10^3$ /well density. Upon the transfection, Adherent-Cell-by-Cell scans were used to track proliferation changes. Images of proliferating cells were taken every 3 hours. The data was analyzed using the Incucyte® Cell-by-Cell Analysis Software Module, as recommended by the manufacturer.

### **3.13. Wound healing assay**

They were subjected to wound healing assay to estimate the migratory potential of GBM cells. U251-MG and U138-MG cells were transfected with the siRNA, and after 48 hours, we scratched the adherent monolayer of the cells with a 200  $\mu$ l pipette tip to generate the wound. The images were gathered every 24 hours until the control wound (C – C-scrambled siRNA) was closed. The data were analyzed by TScratch software.

### **3.14. Invasion assay**

U-251 MG- and U-138 MG-derived spheroids transfected with siRNA have been subjected to the assessment of their invasive potential. The invasion assay was carried out using the IncuCyte® S3 3D Spheroid Invasion Assay protocol. The media was changed upon transfection, and the Matrigel® (Corning Cat. No. 356234) was diluted for the 2.8 mg/mL of final assay protein concentration and added to the top of the culture media. Subsequently, the plate was incubated a 37° C for 30 minutes to polymerize the Matrigel®. Furthermore, the vessel was removed from the incubator, and 50  $\mu$ L/well of complete culture media was added gently on the top. The plate was returned to the incubator and monitored for invasion changes for 96 hours.

### **3.15. EMT induction with TGF $\beta$**

The adhesive layer of U-251 MG was seeded into 6-well plates in recommended culture media at a concentration of  $1.8 \times 10^5$  cells/mL, and the U251-MG-derived spheroids were formed as described above. Both culture types were treated with TGF $\beta$  to a final concentration of 5ng/mL in standard culture conditions. The cells were harvested after 24 and 48 hours and subjected to RNA extraction and RT-qPCR analysis of the expression levels of EMT markers and circRNAs.

### **3.16. Magnetic separation of glioma stem cells fraction**

U-251 MG- and U-138 MG-derived spheroids were cultured for two weeks to enrich the GSCs fraction and subjected to magnetic separation. The magnetic separation principle is based on CD133/1 antibody-labeled beads recognizing epitope 1 of the CD133 antigen exhibited by the GSCs. Magnetic separation was performed according to the CD133 MicroBead Kit manufacturer's protocol. Firstly, spheroids were gently dissociated with StemPro Accutase, magnetically labeled, and separated using pre-prepared LS columns. Obtained fractions – the

population of GSCs (CD133+ fraction) and the flowthrough (FT) were subjected to RNA extraction and RT-qPCR evaluation of GSCs markers and circRNAs expression level.

### **3.17. Extraction of total RNA and DNase treatment**

Total RNA extraction from GBM patient tissue, cell lines, spheroids, and organoids was performed with TRIzol reagent according to the manufacturer's protocol. The culture media was discarded from the culture, and the specimen was washed with PBS. Subsequently, 500 µl of TRIzol was added to each sample and was incubated for 10 minutes at room temperature. GBM tissues and organoids, due to their size, require additional dissociation steps after TRIzol application. In due time, the cell lysate was transferred to 1,5 ml tubes, and 100 µl of chloroform was added to separate the fractions. After 15 seconds of gentle upside-down shaking, the lysate was incubated for 10 minutes at room temperature. The aqueous and organic particles were separated by centrifugation for 15 minutes at 13000 rpm at 4 °C. Subsequently, the aqueous fraction was transferred to new 1,5 ml tubes, and 250 µl of isopropanol was added to precipitate the RNA. The samples were incubated for 15 minutes and centrifuged at 13000 rpm at 4 °C. The supernatant was removed and replaced with 1 ml of cold 80% ethanol. The sample was centrifuged for 8 minutes at 7000 rpm at 4°C temperature. After discarding the supernatant, the pellet was allowed to dry for 15 minutes at room temperature and dissolved in 20 µl of double-distilled, sterile water. The quality of extracted RNA was measured by NanoDrop 2000 spectrophotometer and confirmed by the agarose gel electrophoresis. Subsequently, RNA samples were subjected to DNase I treatment using a ready-to-use DNA-free™ DNA Removal Kit reagents. For RNA sequencing purposes, RNA integrity was verified utilizing Agilent Bioanalyzer 2100. RNA extracted from GBM patients' tissues with RIN at least 7 were used for library preparation and RNA-seq analysis, followed by RT-qPCR analysis for validation purposes.

### **3.18. Reverse transcription and quantitative RT-qPCR**

According to the manufacturer's recommendations, the reverse transcription reaction was carried out using a ready-to-use Transcriptor First Strand cDNA Synthesis Kit (Roche). The template for reverse transcription reaction was total RNA isolated from all of the types above of culture and GBM tissues. The composition of the reaction mixture and the subsequent reaction steps are presented in Table 24. The product of reverse transcription - complementary DNA (cDNA) was used as a template in a RT-qPCR. Calculation of the expression level of

selected genes was performed utilizing hypoxanthine phosphoribosyltransferase (HPRT) as an endogenous control.

**Table 24. The composition of the reverse transcription reaction mixture.**

Step	Reagent	Amount	Conditions
1	cDNA	500 ng	10 minutes incubation in 65°C, cooled on ice
	Random hexamer primer (600 pmol/μl)	1 μl	
	ddH <sub>2</sub> O	up to 13 μl	
2	Reaction buffer (5x)	4 μl	10 minutes incubation at 25°C, subsequently transferred to 50 °C for 60 minutes
	Protector RNase Inhibitor 40U/μl	0,5 μl	
	Deoxynucleotide Mix, 10 mM	2 μl	
	(Transcriptor Reverse Transcriptase, 20U/μl)	0,5 μl	
Denaturation	-	-	5 minutes in 85 °C
Long-term storage	-	-	-20 °C

RT-qPCR was performed to quantify the mRNA expression level in real time for selected genes, depicted in Table 25. The template used in RT-qPCR was the final product of reverse transcription reaction - cDNA. The response was carried out using the CFX96 Real-Time System thermal cycler (BioRad). The procedure was started with the preparation of the reaction mixture as follows: 5 μl of LightCycler® 480 SYBR Green I Master Mix, 1 μl of forward primer oligodeoxynucleotide (10 μM), 1 μl of reverse primer oligodeoxynucleotide (10 μM) and 2μl ddH<sub>2</sub>O. The reaction mixture was pipetted in triplicates of 9 μl per well on 96-well clear bottom plates (BioRad), then 1 μl of the appropriate cDNA template was added. Subsequently, the vessel was sealed and centrifuged for 1 min at 1000 rpm. Each sample was analyzed in triplicate. Prior to the expression level estimation, standard curves for each primer pair were obtained by amplifying a series of cDNA dilutions (x1, x2, x4, x8, x16, x32). The results were interpreted using a dedicated thermal cycler Bio-Rad CFX Maestro software version 2.0.

**Table 25. The oligodeoxynucleotides used in the study.**

<b>Primer</b>	<b>Forward primer 5' → 3' sequence</b>	<b>Reverse primer 5' → 3' sequence</b>
HPRT	TGACCTTGATTTTGCATACC	CGAGCAAGACGTTTCAGTCCT
CLIP2_L	CGAGAATTAGCGGACAACA	GACCCGAGTGCAACAG
CLIP2_C	GAGGTGGAGAAGGAGATTG	GTAGATGGGAAGCCGATAC
CADPS2_L	ATTGCCACTCCCATAACCAGC	GCAGGAGATGCCTGGTTCAT
CADPS2_C	GAAGTCAGTTGCTCCCAATCG	GTTCCCTTCTGATCTGGGCT
EPB41L5_L	CATGCTTTCTTCCGCCTTCG	GCCTGTTGGGAGCCATTACT
EPB41L5_C	GGGCCTGTAGCTGGAATACG	TCCATAGTGTGATGCCCCA
UNC13_L	GAGATGTGGCCATGACCCTG	CACTTCATGCCTTGCCTTGC
UNC13_C	AAGCAAATGGCAGAGTTGGAAG	CAAACCAGAAGCAAAGCTCCA
USP45_L	GACTTTTCTGGAAGCGTCGTG	GACTTTTCTGGAAGCGTCGTG
USP45_C	AAATATTCATCAACCTAGAGCTGCC	GGCCTTTTACTTCTTTTGGCTTTCT
ARID1A_L	AGCCGAATCTCATGCCTTCC	GCCGCTTGTAATTCTGCTGTT
ARID1A_C	CCAGTAAGGGAGGGCAAGAAG	CTGTTGCTGCGAGTATGGGT
GUSBP1_L	AAAACACTGGGGCTGGTGAAT	TGTTTCGTGCATCAGGTACGG
GUSBP1_C	CGTGTATGGAGTGGAAACGC	GCCTGGTTGTCCACGACTTT
PLOD2_L	CATGGACACAGGATAATGGCTG	AGGGGTTGGTTGCTCAATAAAAA
PLOD2_C	AGTATTGGAGGGGGCCAGAA	GGAATCCATCACTTTCTTTTGTGTC
VCAN_L	AGGTGGTCTACTTGGGGTGA	CGATGGTTGTAGCCTCTTTAGGTTT
VCAN_C	AGAAGCTGCAGAAGCTAGG	AACATCAGGCTCACCACCTG
EGFR_L	GACAGGCCACCTCGTCG	TCGTGCCTTGCAAACCTTC
EGFR_C	AAACAACACCCTGGTCTGGA	GGGTGGCACTGTATGCACTC
HLA-B_L	ATGGCGAGGACCAAACCTCAG	CACAACCTGCTAGGACAGCCA
HLA-B_C	TGGCTGTCCTGGTTGTCCTAGC	CACCCCACTTACACGCA
Intergenic circRNA	GCCTCTCACAGGACGTTTTTC	GCCCAACACCCAACACACAT
N-cadherin	GCCCAAGACAAAGAGACCCA	GCTGACTCCTTCACTGACTCC
SNAL2	GACCTGGTTGCTTCAAGGA	TGTTGCAGTGAGGGCAAGAA
Zeb1	GCACCTGAAGAGGACCAGAG	TGCATCTGGTGTTCATTTT
VIM	AGGTCAAGACGTGCCAGA	CGGGAGAAATTGCAGGAGG
SNAL1	ACCACTATGCCGCGCTCTT	GGTCGTAGGGCTGCTGGAA
OCT4	GTGGAGAGCAACTCCGATG	TGCTCCAGCTTCTCCTTCTC
SOX2	CGAGTGGAAACTTTTGTGCGGA	TGTGCAGCGCTCGCAG
Nanog	ATTCAGGACAGCCCTGATTCTTC	TTTTTGCACACTCTTCTCTGC
GLUT1	TTGCAGGCTTCTCCAACCTGGAC	CAGAACCAGGAGCACAGTGAAG
ANG1	CAACAGTGTCTTCAGAAGCAGC	CCAGCTTGATATACATCTGCACAG
PDK1	CATGTCACGCTGGGTAATGAGG	CTCAACACGAGGTCTTGGTGCA

### **3.19. Total RNA libraries preparation and RNA sequencing**

Libraries for circRNAs were prepared according to the TruSeq® Stranded mRNA Library Prep kit. Prior to the procedure, 300 ng of total RNA was subjected to ribodepletion utilizing RiboCop rRNA Depletion Kit. After synthesis of both stands of cDNA, adaptors were ligated according to the manufacturer's instructions. Subsequently, cDNA fragments were amplified with PCR for 8-15 cycles. After the purification with AMPure XP beads, the DNA concentration was measured with Qubit, and the length of the fragments was defined with the 4200 Tape Station System. RNA sequencing of GBM tissues and healthy brain references was performed using Hi-seq 4000 with 150 paired-end reads. RNA sequencing of GBM organoids, cerebral organoids, and assembloids was performed using NovaSeq 6000 SP v1.5 with 150 paired-end reads.

### **3.20. CircRNAs identification by RNA-seq**

CircRNA identification was performed by the Institute of Human Genetics collaborator, utilizing the data obtained in RNA sequencing of the GBM tissues and healthy brain reference. The process required initial quality control of raw sequencing reads, utilizing FastQC (<https://www.bioinformatics.babraham.ac.uk/projects/fastqc/>). Next, the adapters were removed using Trimmomatic (581), version 0.38, with the following parameters ILLUMINACLIP:2:30:10 SLIDINGWINDOW:10:25 MINLEN:35. Subsequently, second quality check with FastQC was performed. A genomic index was created for the GRCh37 human genome obtained from Gencode using Burrows-Wheeler aligner (582), version 0.7.17 (bwa -bwtsw). Then, reads were mapped with the following parameters: bwa-mem -T 19. CircRNAs were detected from alignment files with CIRI version 2.0.6, using default parameters. CircRNA annotation and differential expression analysis were performed using the circMeta R package (583). Subsequently, the differential expression (DE) analysis was performed by deploying the edgeR (584) method. Heatmaps were prepared using the heatmap R package (pheatmap: Pretty heatmaps [Software] R Kolde. URL <https://CRAN.R-project.org/package=pheatmap>, 2018), and data were normalized using the TMM method from edgeR R package (584). Data were visualized using the ggplot2 R package (585,586) (586)

### **3.21. CircRNAs retrieval from data repository**

To identify circRNAs significant for the GBM onset and progression, the data provided by Song et al. (2016) were utilized (209). The analysis was performed on 46 GBM and 46 non-cancer samples. To establish differentially expressed circRNAs, the edge R package in R was

utilized. The applied cutoff criteria were fold change (FC) > 2 and detecting circRNAs presence in at least 50% of the analyzed samples. Final identification of detected circRNAs was performed utilizing the circBase database (280).

### **3.22. Glioblastoma molecular subtype analysis and circRNAs clustering**

The collaborators from Adam Mickiewicz University performed Glioblastoma subtype analysis and further circRNAs clustering utilizing data obtained upon RNA sequencing of the GBM tissues and healthy brain reference. First, raw sequencing data were subjected to a quality check using the FastQC tool (<https://www.bioinformatics.babraham.ac.uk/projects/fastqc/>). The adaptors were trimmed, and the reads were filtered to eliminate the low-sequencing-quality bases using Trimmomatic (581). Furthermore, the RNA-seq reads were mapped to the human reference transcriptome (ENSEMBLE V.102) to quantify the expression level of the transcripts. The transcript-level estimates were summarized and associated with the gene IDs for gene-level analysis using tximport (587). For the samples categorization we used genes indicated in the TCGA GBM dataset ([https://jokergoo.github.io/cola\\_examples/TCGA\\_GBM/#tcga-glioblastome-dataset](https://jokergoo.github.io/cola_examples/TCGA_GBM/#tcga-glioblastome-dataset)) and other genes that are significant for GBM molecular subtyping including SLC12A5, SYT1, GABRA1, NEFL, CDKN1A, NF1, MET, PDGFRA, BOP1, ILR4 were included. CircRNAs differentially expressed within the subtypes were identified using the circMeta R package (583) with edgeR (584) method for DGE.

### **3.23. Statistical analysis of the results**

GraphPad Prism ver. 8 was used to analyze the experimental results statistically. The results are presented as mean values with standard deviation (SD). Each experiment was performed in three biological replicates having three technical replicates. The differences in mean values between the studied and control samples were evaluated using ANOVA variance extended by Bonferroni posthoc tests. Statistically significant results were denoted by the following symbols: \* for  $p < 0.05$ ; \*\* for  $p < 0.01$ ; \*\*\* for  $p < 0.001$ ; \*\*\*\* for  $p < 0.0001$  and no statistical significance for  $p > 0.05$ .

## 4. Results

### 4.1. Functional characteristic of circRNA deregulated in GBM

CircRNAs have been reported to perform numerous functions in GBM, therefore, the circRNAs investigation spanned not only their identification in primary and recurrent GBM tissues but also included the functional characterization of selected molecules.

#### 4.1.1. Selection of circRNAs candidates for functional analysis in glioblastoma

To identify circRNAs significant for the GBM onset and progression, the data provided by Song and colleagues in 2016 were utilized (209). Prior to the identification of circRNA in GBM tissues, the data derived from high-throughput RNA sequencing deposited in <https://www.ncbi.nlm.nih.gov/sra/term=SRA050270> were analyzed. The analysis was performed on 46 GBM and 46 non-cancer samples.

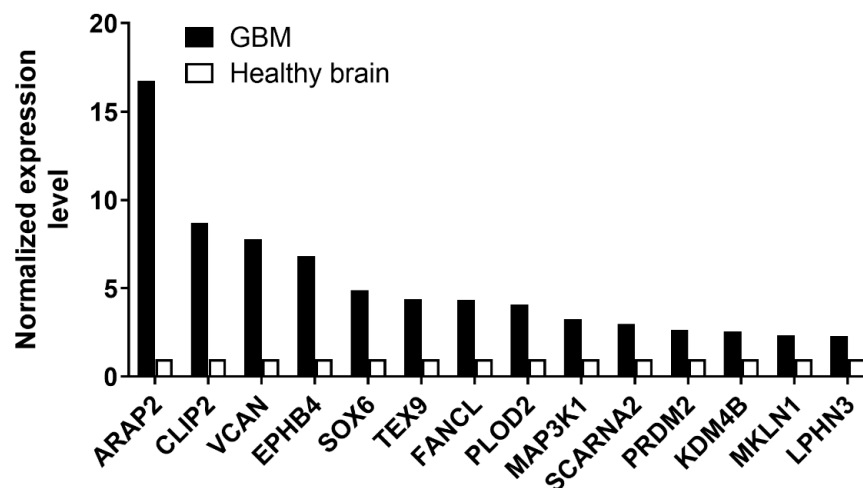


**Figure 3.** Meta-analysis of the data provided by Song et al. (2016) allowed to establish circRNAs expression in GBM samples (n=19). CircRNAs presented in the graph are overexpressed in GBM compared to healthy brain reference.

The analysis revealed significant overexpression of several circRNAs, presented in Figure 3. Three of them, exhibiting the highest upregulation in GBM samples compared to healthy brain reference, were chosen for further experimental validation – circARAP2, circCLIP2, and circVCAN. Selected circRNAs characteristics are presented in Table 26.

Gene symbol	circRNA ID	Chromosomal coordinates	Genomic length	Spliced length	Corresponding mRNA
ARAP2	hsa_circ_0069399	chr4:36230203-36231267	1064	1064	NM_015230
CLIP2	hsa_circ_0002755	chr7:73770739-73771807	1068	412	NM_003388
VCAN	hsa_circ_0073237	chr5:82832825-82838087	5262	5262	NM_004385

**Table 26. The characteristics of selected circRNAs exhibiting upregulated expression level in GBM compared to healthy brain reference.** The Table was generated based on the circBase database (280).

To evaluate the retrieved bioinformatical data provided by Song and colleagues, the expression level of the abovementioned circRNAs was examined by RT-qPCR in the following groups of specimens: healthy brain reference, primary (n=12), and recurrent (n=7) GBM. The expression level of selected circRNAs is presented in Figure 4. In the course of the experimental validation utilizing primary and recurrent GBM tissues, circARAP2 and circVCAN were shown to be overexpressed mainly in one type of the GBM (circARAP2 in recurrent GBM – 4,40-fold and circVCAN in primary GBM – 16,49-fold), exhibiting lower, and not statistically significant expression level in the other type of tumor. Moreover, the circVCAN linear counterpart is also overexpressed in primary GBM, reaching 14,98-fold, which could impact the functional analyses with the loss-of-function approach. Taking the above into consideration, over the course of the research, circARAP2 and circVCAN were excluded from further analyses due to the encountered experimental difficulties. On the other hand, circCLIP2 expression level is 9.85-fold higher in primary GBM tissue and 4,93-fold higher in recurrent GBM compared to healthy brain control. Simultaneously, the expression level of the linear transcript of the CLIP2 gene is not significantly elevated in both types of tissue (primary GBM – 1,9-fold, recurrent GBM 2,19-fold), which is pivotal for further functional research.

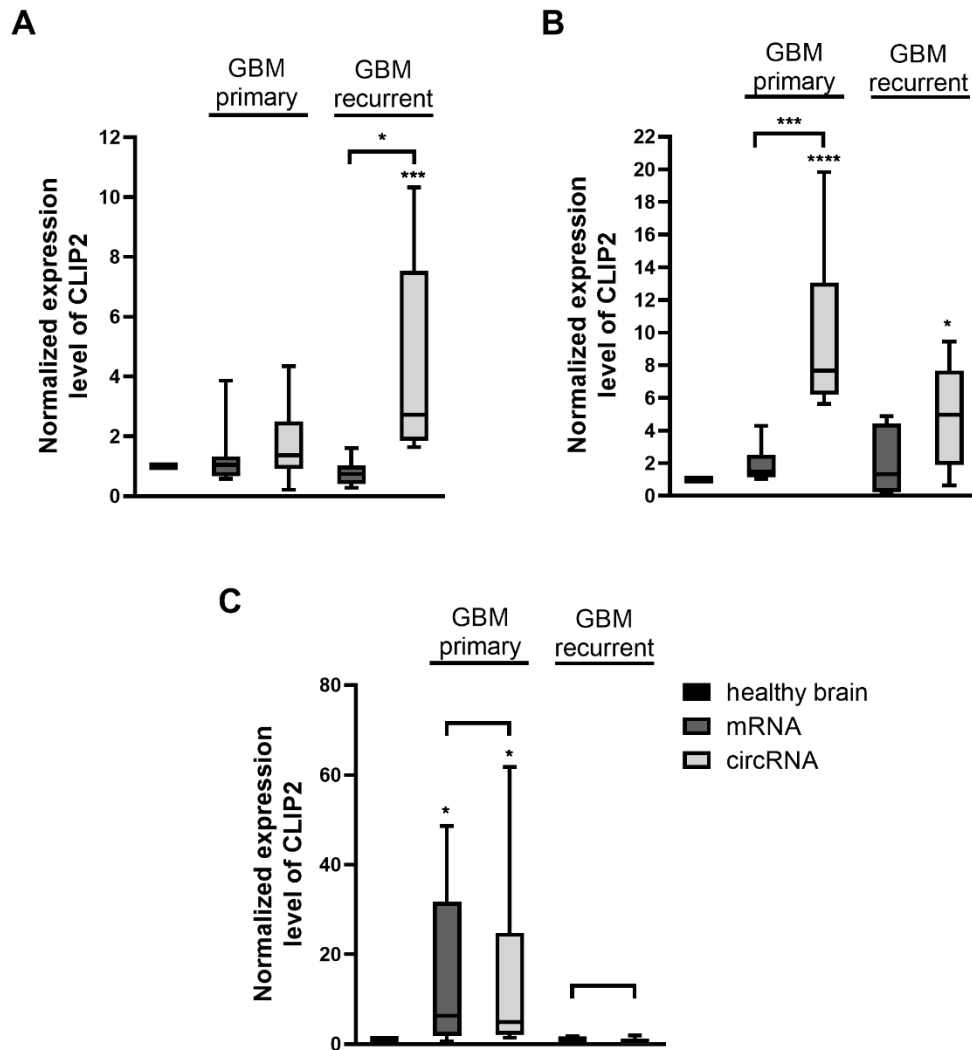


**Figure 4. Expression level of selected circRNAs and their linear counterparts established in primary and recurrent GBM.** The expression level of ARAP2 (A), CLIP2 (B), and VCAN (C) gene transcripts in primary and recurrent GBM was evaluated by RT-qPCR. The analysis was carried out utilizing primary (n=12) and recurrent (n=7) GBM patients' tissue, different than the tissues subjected to the sequencing due to the insufficient amount of extracted RNA. The expression level of both transcripts was compared to healthy brain control. Data are shown as the mean  $\pm$  SD values and results were statistically evaluated using one-way ANOVA followed by post hoc Bonferroni test. Statistically significant results were denoted by the following symbols: \* for  $p < 0.05$ ; \*\* for  $p < 0.01$ ; \*\*\* for  $p < 0.001$ ; \*\*\*\* for  $p < 0.0001$  and no statistical significance for  $p > 0.05$ .

Moreover, samples with higher circCLIP2 expression levels also express linear transcript at higher levels (Pearson correlation in primary GBM = 0.8376 (Fig. 5A) and recurrent GBM = 0.9656 (Fig. 5B)). To experimentally confirm the existence of a circular form of CLIP2 gene and avoid the technical bias, Sanger sequencing was carried out, confirming the presence of back-splice junction site joining exon 6 and exon 5 of CLIP2 gene (Fig. 5C).

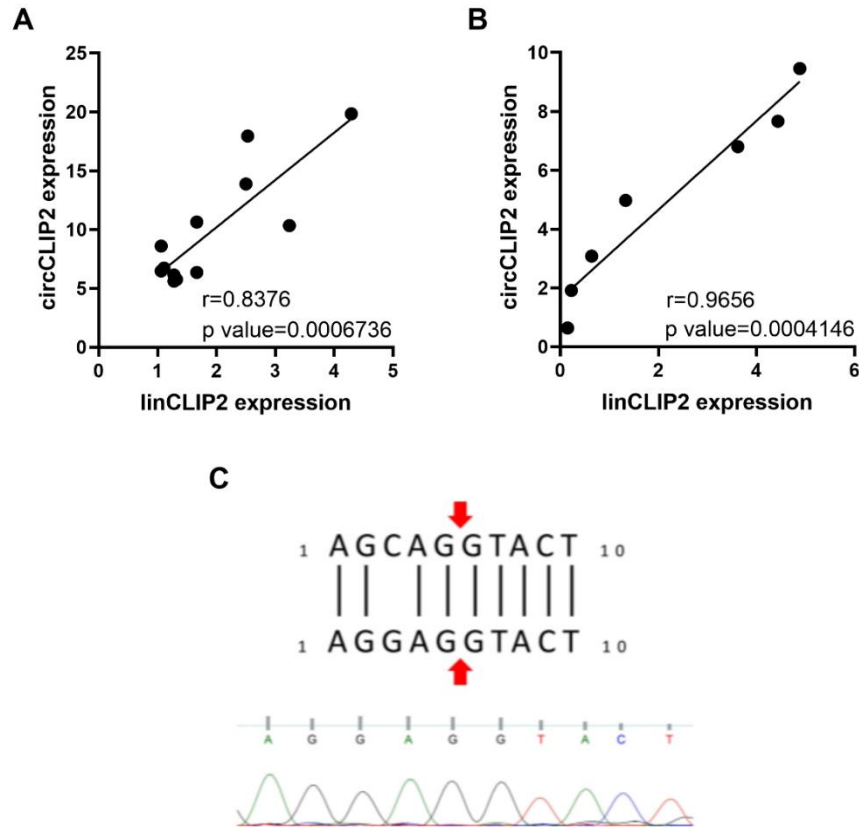


**Figure 5. Expression level correlation of CLIP2 gene transcripts in primary and recurrent GBM. A, B.** Pearson correlation of circCLIP2 and its linear counterpart expression level in primary (A) and recurrent (B) GBM tissue. **C.** Sanger sequencing result of the circCLIP2 PCR product showing the backsplice junction sequence. The backsplice junction of circCLIP2 is indicated by the red arrows.

To establish the cellular localization of circCLIP2 cellular fractionation analysis was performed. Once the cellular and nuclear fraction was separated, the expression level of the cellular fractionation marker - GAPDH was established. To differentiate between cytoplasmic and nuclear fractions, the primers were designed to amplify the exon-exon sequence of GAPDH transcript for cytoplasmic detection only, as they are specific for the mature GAPDH mRNA which underwent splicing. On the contrary, the intron sequence of the GAPDH transcript has been evaluated to detect transcripts specific to the nuclear fraction (Fig. 6A). Cellular fractionation showed that circCLIP2 is predominantly localized in the cytoplasm of GBM cells, which allowed to conduct the functional analyses with the loss-of-function approach utilizing siRNA. (Fig. 6B). The circCLIP2 was more abundant in the cytoplasmic fraction, reaching 1,99-fold in U251-MG and 1,84-fold in U138-MG cell lines, compared to the total fraction. In the nucleus, the circCLIP2 fraction reached 0,31-fold and 0,14-fold in the abovementioned cell

lines, respectively. However, the result established for the U251-MG cell line was not statistically significant.

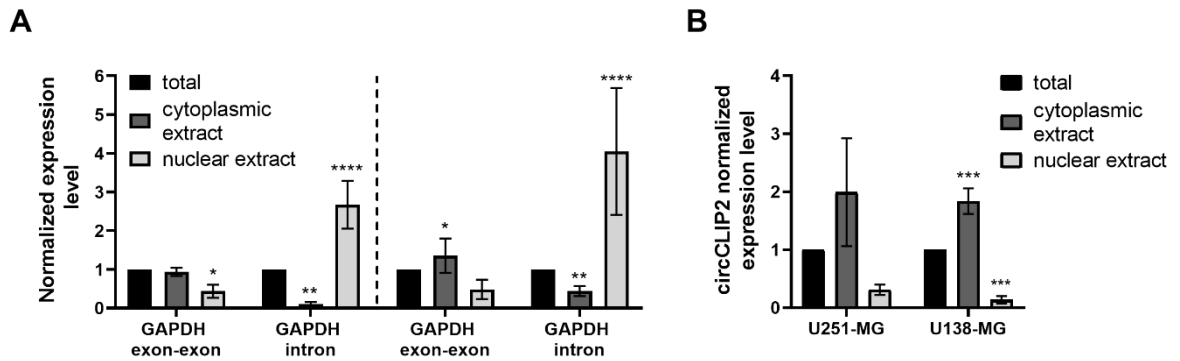


**Figure 6. Cellular location of circCLIP2 established by subcellular fractionation.** A. The circCLIP2 cellular localization establishment revealed circCLIP2 abundance in the cytoplasmic fraction of the U251-MG and U138-MG cells. Total: whole-cell RNA, cytoplasmic extract: cytoplasmic fraction, nuclear extract: nuclear fraction. B. Data are shown as the mean  $\pm$  SD values and results were statistically evaluated using one-way ANOVA followed by post hoc Bonferroni test. Statistically significant results were denoted by the following symbols: \* for  $p < 0.05$ ; \*\* for  $p < 0.01$ ; \*\*\* for  $p < 0.001$ ; \*\*\*\* for  $p < 0.0001$  and no statistical significance for  $p > 0.05$ .

#### 4.1.2. Knock-down of CLIP2 gene transcripts

To identify the proper model for future functional research, the expression level of the CLIP2 gene isoforms in two GBM cell lines - U251-MG and U138-MG was assessed. The circCLIP2 expression level is significantly elevated in both cell lines, with a fold change of 3.67-fold and 2.6-fold, respectively. Moreover, the linear isoform's expression level decreased in both GBM cell lines compared to the healthy brain reference, reaching only 0.06-fold and 0.09-fold, respectively (Fig.7).

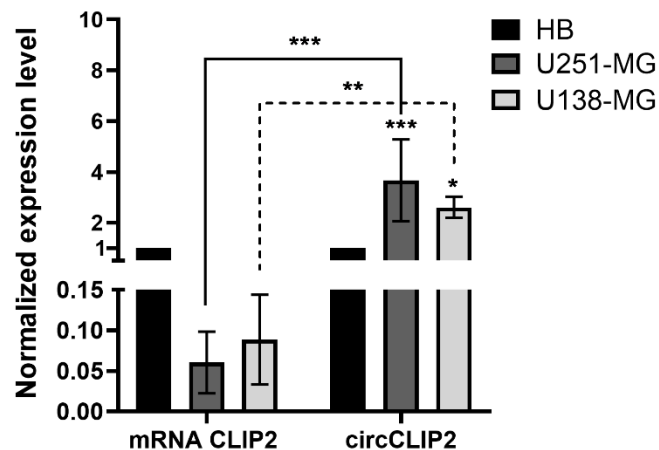


**Figure 7. Estimation of the expression level of *CLIP2* gene linear and circular transcripts in U251-MG and U138-MG GBM cell lines.** The expression level of *CLIP2* gene transcripts in GBM cell lines was compared to the healthy brain reference (HB). Data are shown as the mean  $\pm$  SD values and results were statistically evaluated using one-way ANOVA followed by post hoc Bonferroni test. Statistically significant results were denoted by the following symbols: \* for  $p < 0.05$ ; \*\* for  $p < 0.01$ ; \*\*\* for  $p < 0.001$ ; \*\*\*\* for  $p < 0.0001$  and no statistical significance for  $p > 0.05$ .

Subsequently, based on the corresponding circ*CLIP2* expression pattern in GBM cell lines compared to the GBM tissues, the *CLIP2* gene isoforms loss of function experiments were performed. For the *CLIP2* gene isoforms knockdown, both the abovementioned GBM cell lines (Fig. 9 A, B) and 3D models - U251-MG- and U138-MG-derived spheroids (Fig. 9 C, D) were subjected.

To explore the potential role of circ*CLIP2*, the synthetic oligoribonucleotides (siRNAs) were designed to implement a loss-of-function method. siRNAs were designed to bind the covalent bond area in circRNAs, which is commonly referred to as the head-to-tail junction or back splice junction site. Simultaneously, the level and functional potential of the linear counterpart were also analyzed during the experiments involving knockdown and functional analyses of circular transcripts to confirm or reject its potential involvement in the analyzed process. The siRNA silencing of the circ*CLIP2* counterpart was designed to target the exclusive mRNA sequence, which is not included in the circ*CLIP2* structure. The principle of siRNA design for circular and linear transcripts is presented in Figure 8.

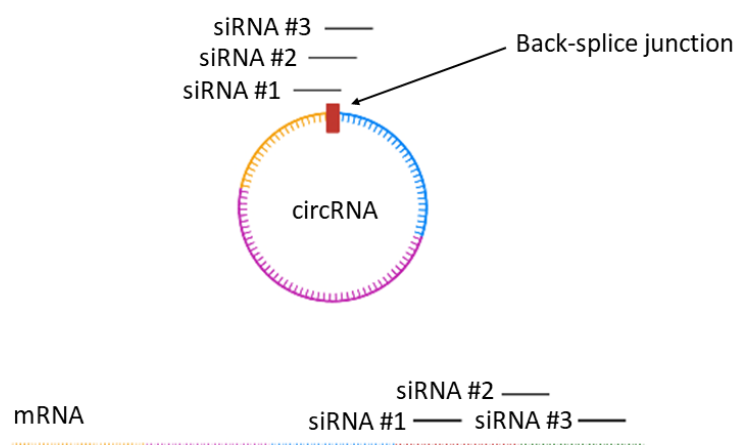


**Figure 8. Schematic localization of the siRNAs targeting separately circRNAs back-splice junction site and the corresponding mRNA.** The siRNAs are designed to target the back-splice junction site only in circRNAs and the exclusive sequence of its corresponding mRNA to avoid the simultaneous knock-down of both isoforms.

U251-MG and U138-MG cells and spheroids were transfected with 100 nM of siRNA specific to either linear CLIP2 transcript (si-mRNA CLIP2) or circCLIP2 (si-circCLIP2). SiRNA without a specific target in human cells (C) was applied as a control. In the case of adherent cell lines, the knockdown of circCLIP2 determined by RT-qPCR was more efficient in U138-MG (~84%) than in U-251-MG (~52%). The linear CLIP2 silencing efficiency was ~85% in both cell lines (Fig. 9 A, B), with a ~20% decrease in the expression of circCLIP2 after si-mRNA transfection in U138-MG (Fig. 9B). The knockdown of linear isoform in cell line-derived spheres amounted to nearly 96% and 79% drop after the knockdown carried out in U251-MG- and U138-MG-derived spheroids, respectively (Fig. 9 C, D). A striking drop in expression level was also noticed upon circCLIP2 knock-down reaching 74% and 64% for U251-MG- and U138-MG-derived spheroids, respectively, with no statistically significant deregulation of the counterpart isoform. Considering the substantial and specific silencing of either linear or circular CLIP2, both cell lines were used in downstream experiments.

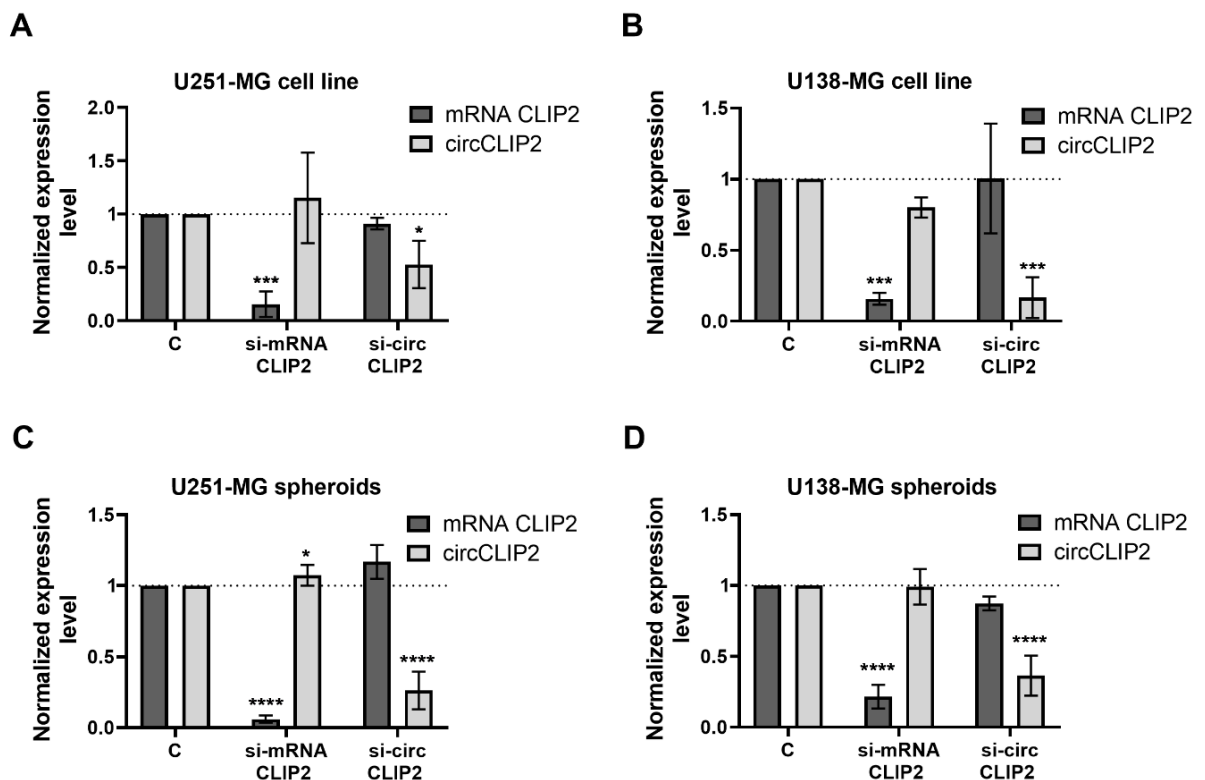


**Figure 9. Loss-of-function approach to downregulate the expression level of *CLIP2* gene linear and circular transcripts.** **A, B.** Knock-down of the linear and circular transcript of the *CLIP2* gene in U251-MG (A) and U138-MG (B) cell lines. **C, D.** Knock-down of the circular and linear transcript of the *CLIP2* gene in U251-MG (C) and U138-MG (D) spheroids. The efficiency of the downregulation was established by RT-qPCR analysis and scrambled siRNA (C) served as a control. Data are shown as the mean  $\pm$  SD values and results were statistically

evaluated using one-way ANOVA followed by post hoc Bonferroni test. Statistically significant results were denoted by the following symbols: \* for  $p < 0.05$ ; \*\* for  $p < 0.01$ ; \*\*\* for  $p < 0.001$ ; \*\*\*\* for  $p < 0.0001$  and no statistical significance for  $p > 0.05$ .

#### 4.1.3. Functional assays upon CLIP2 gene transcripts knock-down

The establishment of putative circCLIP2 function in GBM, and the functional assays after the CLIP2 gene isoforms knockdown were performed, which allowed to assess the impact of circCLIP2 on key processes leading to the GBM onset and tumor progression.

As the excessive proliferation of tumor cells facilitated by sustained proliferative signaling is one of the hallmarks of cancer that ultimately leads to tumor growth and invasion, I sought to determine how the knock-down of circCLIP2 and its corresponding mRNA influences the oncogenic properties of GBM cell lines. For both analyzed cell lines, the downregulation of circCLIP2 expression level led to a substantial drop in cell proliferative potential reaching 68% for U251-MG (Fig. 10 A) and 70% for U138-MG (Fig. 10 B). Interestingly, no statistically significant changes in GBM cell proliferation were observed after linear CLIP2 silencing, which was confirmed in both studied cell lines.

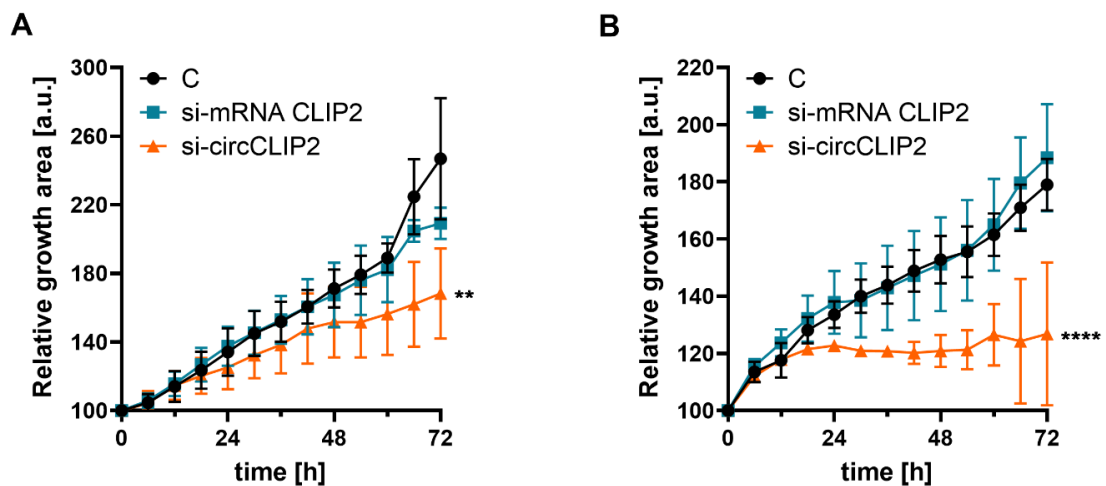


**Figure 10. circCLIP2 is involved in GBM cell proliferation. A, B.** Proliferation rates of U251-MG (A) and U138-MG (B) after *CLIP2* gene linear and circular transcripts knock-down. Data are shown as the mean  $\pm$  SD values and results were statistically evaluated using one-way ANOVA followed by post hoc Bonferroni test. Statistically significant results were denoted by the following symbols: \* for  $p < 0.05$ ; \*\* for  $p < 0.01$ ; \*\*\* for  $p < 0.001$ ; \*\*\*\* for  $p < 0.0001$  and no statistical significance for  $p > 0.05$ .

Cancer cells are known to evade anti-growth signals to continue proliferating. This ability to avoid signals that hinder cell growth is a major characteristic of cancer cells. The

capacity of the tumor mass to grow is coupled not only with excessive tumor cell proliferation but also with cell migration to invade the surrounding tissues. Therefore, the migratory potential of the GBM cells after *CLIP2* gene isoforms knockdown was studied by wound healing assay. The analysis is based on the creation of the scratch on a cell monolayer to detect the rate of cells migrating into empty dish spaces to close the wound. The assay was finished when the control wound (C) was completely healed (after 48 hours in the U251-MG cell line and 72 hours in the U138-MG cell line). The largest unhealed area for samples with circCLIP2 knock-down accounted for 40.02% and 53.04% of the original wound area in U251-MG and U138-MG after 48 and 72 hours, respectively (Fig. 11 A-D). Analyzing the same time points in control cells, the unhealed area reached 1.95% and 6.8%, respectively. Consistently with proliferation results, no statistically significant effect on wound healing after linear CLIP2 silencing was observed (Fig. 11 A-D).

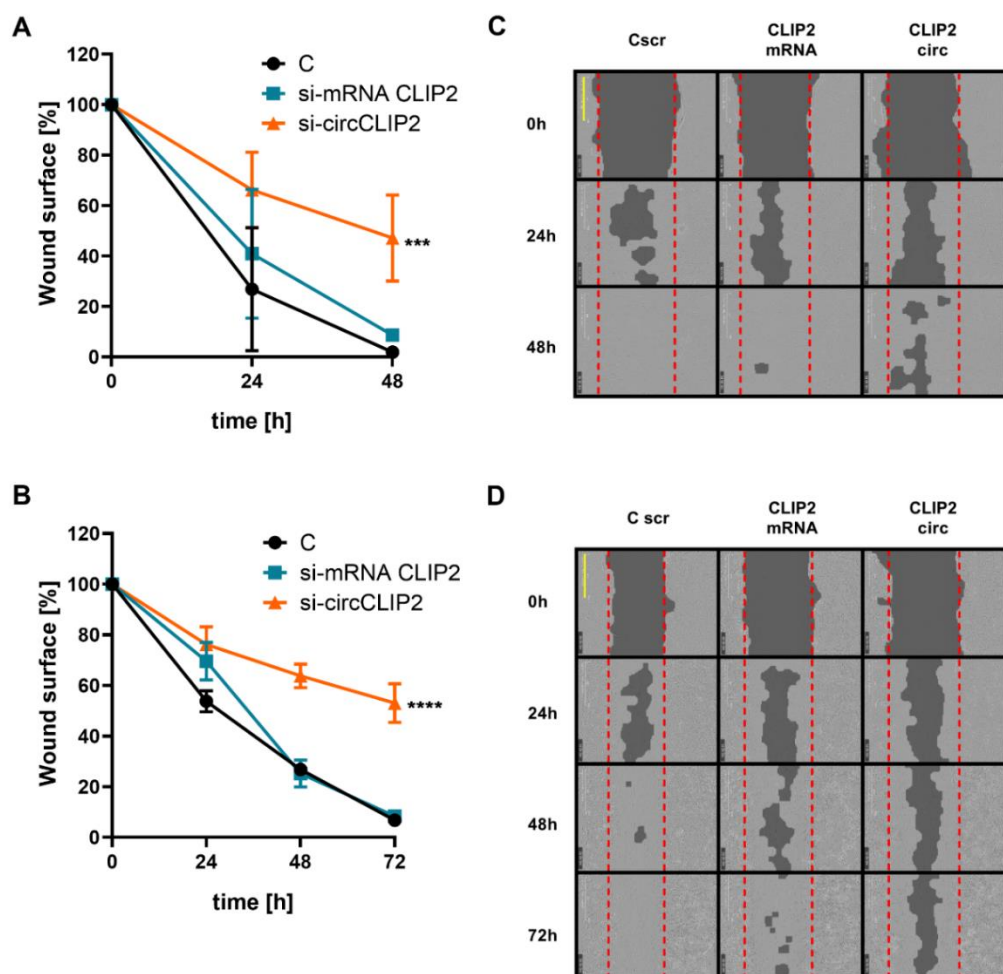


**Figure 11. circCLIP2 is involved in GBM cell motility.** A, B. Migration rate assessed by wound healing assay performed utilizing U251-MG (A) and U138-MG (B) after *CLIP2* gene linear and circular transcripts knock-down.

**C, D.** Representative panel of micrographs presenting the migration rate of U251-MG (C) and U138-MG (D) after *CLIP2* gene linear and circular transcripts knock-down. Micrographs were captured every 24 hours until the wound formed on cells transfected with unspecified siRNA (C) was closed. Data are shown as the mean  $\pm$  SD values and results were statistically evaluated using one-way ANOVA followed by post hoc Bonferroni test. Statistically significant results were denoted by the following symbols: \* for  $p < 0.05$ ; \*\* for  $p < 0.01$ ; \*\*\* for  $p < 0.001$ ; \*\*\*\* for  $p < 0.0001$  and no statistical significance for  $p > 0.05$ .

As one of the principles of tumor metastasis is tumor invasion, tightly linked with the two abovementioned processes, which are tumor cell proliferation and migration, the invasive potential of GBM cells after *CLIP2* gene transcripts knock-down was evaluated. The invasion assay was conducted using spheroids derived from U251-MG and U138-MG cell lines, taking into consideration the complex 3-dimensional structure of GBM, which could mimic the tumor's spatial form better than the adherent cell lines. Spheroids were subjected to the *CLIP2* gene transcripts knock-down. After 96 hours significant drop of invasive properties for both cell lines spheroids was observed – 0.62-fold and 0.75-fold for U251-MG- and U138-MG-derived spheroids, respectively (Fig. 12 A-D). Knock-down of the *CLIP2* mRNA counterpart does not significantly impact spheres invasion in both of the cell lines reaching 1.05-fold and 1.17-fold for U251-MG- and U138-MG-derived spheroids, respectively (Fig. 12 A-D). These results highlight the significant role of circ*CLIP2* in the regulation of oncogenic potential not only in adherent cells but also in the cells forming more complex 3D structures.

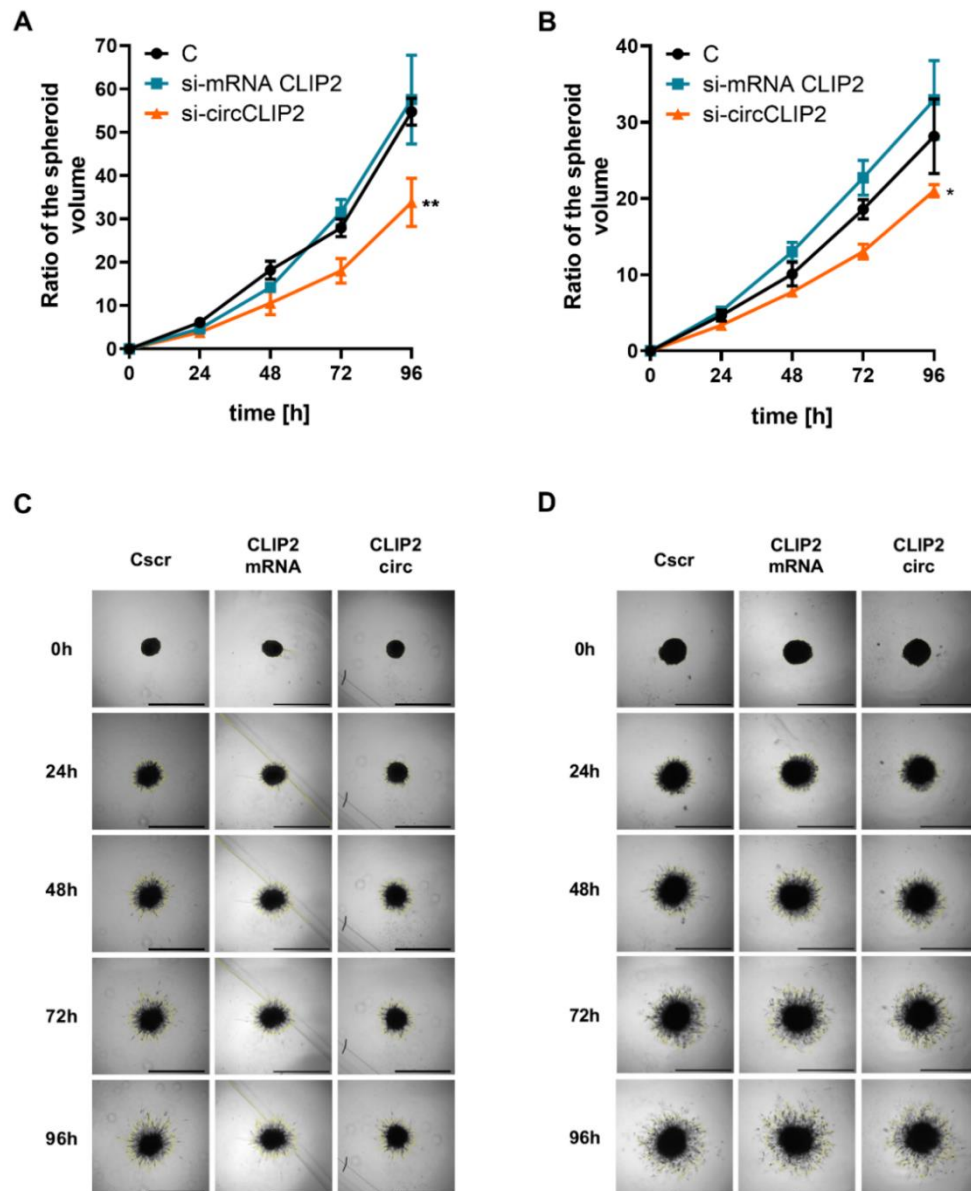


**Figure 12. circCLIP2 knock-down hinders the invasiveness of GBM spheroids.** **A, B.** Ratio of the U251-MG (A) and U138-MG (B) spheroid volume after *CLIP2* gene linear and circular transcripts knock-down. **C, D.** Representative panel of the U251-MG (C) and U138-MG (D) spheroid volume changes over 96 hours. The results were compared to the non-specific scrambled siRNA control – C. Data are shown as the mean  $\pm$  SD values and results were statistically evaluated using one-way ANOVA followed by post hoc Bonferroni test. Statistically significant results were denoted by the following symbols: \* for  $p < 0.05$ ; \*\* for  $p < 0.01$ ; \*\*\* for  $p < 0.001$ ; \*\*\*\* for  $p < 0.0001$  and no statistical significance for  $p > 0.05$ .

#### 4.1.4. Induction of epithelial-to-mesenchymal transition

In the course of the research, the potential connection between the observed phenotypic changes resulting from circCLIP2 knock-down and the process of epithelial-to-mesenchymal transition has been explored, as EMT is strongly associated with increased tumor migration,

invasion, and metastasis. First, the EMT biomarkers expression level after the knock-down of both CLIP2 gene isoforms in U251-MG and U138-MG cell lines was studied. The expression level of all the analyzed EMT biomarkers significantly decreased in both cell lines after the knock-down of circCLIP2 (Fig. 13 A, B). The most significant drop was observed for SNAI1 and VIM in U251-MG, reaching 0.49-fold and 0.63-fold, respectively. Silencing of linear CLIP2 affects only N-cadherin in U251-MG and VIM in U138-MG.

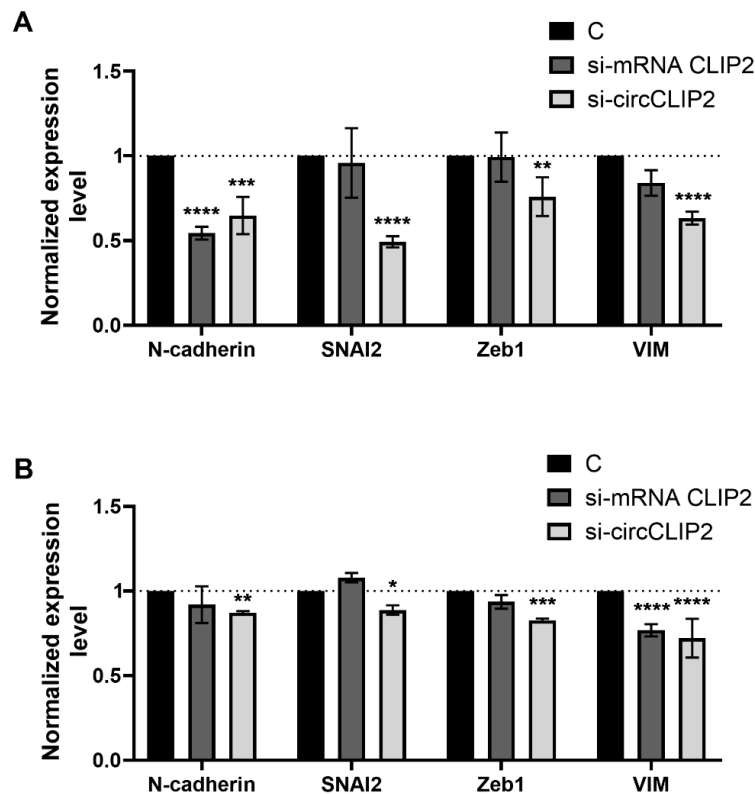


**Figure 13. circCLIP2 is involved in GBM epithelial-to-mesenchymal transition.** A, B. RT-qPCR analysis of the expression level of EMT biomarkers after *CLIP2* gene linear and circular transcripts knock-down in U251-MG (A) and U138-MG (B) cell lines. Data are shown as the mean  $\pm$  SD values, and results were statistically evaluated using one-way ANOVA followed by post hoc Bonferroni test. Statistically significant results were denoted by the following symbols: \* for  $p < 0.05$ ; \*\* for  $p < 0.01$ ; \*\*\* for  $p < 0.001$ ; \*\*\*\* for  $p < 0.0001$  and no statistical significance for  $p > 0.05$ .

Based on the analysis of EMT biomarkers upon CLIP2 gene isoforms knock-down, the U251-MG cell line was chosen for further induction of EMT by TGF $\beta$  stimulation, as it showed deeper downregulation and the effect was observed both after circCLIP2 and CLIP2 mRNA knockdown. The cells were subjected to TGF $\beta$  treatment for 24 and 48 hours. After this time, a significantly higher expression level of EMT biomarkers was observed. The highest expression

level of EMT biomarkers was observed after 48 hours of TGF $\beta$  treatment, and the most deregulated biomarker was SNAI2 amounting to 8.06-fold and 7.22-fold for 2 ng and 5 ng of TGF $\beta$  stimulation, respectively (Fig.14 A, B).

The elevated circCLIP2 expression level was observed in both time points after the application of 5 ng of TGF $\beta$ , reaching 1.26-fold and 1.70-fold after 24 and 48 hours, respectively. In 2 ng of TGF $\beta$  dosage, the statistically significant upregulation of circCLIP2 was obtained after 48 hours only, amounting to 1.73-fold (Fig. 14 C, D). Interestingly, in all investigated time points and concentrations of TGF $\beta$ , the CLIP2 mRNA exhibited decreased expression level, however, the results were not statistically significant in all cases.

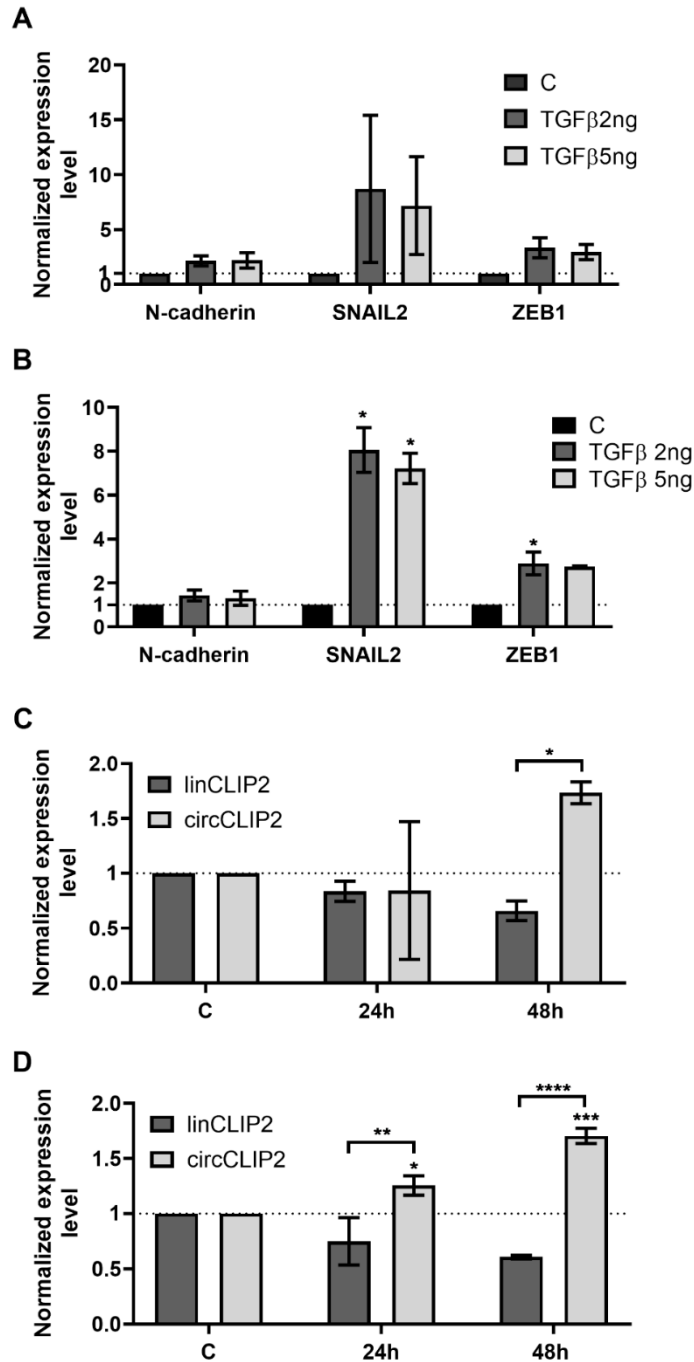


**Figure 14. circCLIP2 is involved in GBM epithelial-to-mesenchymal transition. A, B.** The expression level of EMT biomarkers after the EMT induction in U251-MG adherent cells by after 24h (A) and 48h (B) of TGFβ treatment C, D. Analysis of the expression level of CLIP2 gene transcripts in EMT-induced U251-MG adherent cell line by 2 ng (C) and 5 ng (D). The results were compared to untreated adherent U251-MG cells and spheroids, respectively - C. Data are shown as the mean ± SD values, and results were statistically evaluated using one-way ANOVA followed by post hoc Bonferroni test. Statistically significant results were denoted by the following symbols: \* for p<0.05; \*\* for p<0.01; \*\*\* for p<0.001; \*\*\*\* for p<0.0001 and no statistical significance for p>0.05.

#### 4.1.5. Expression level of CLIP2 gene transcripts in glioma stem cells

The EMT process and the presence of cancer stem cells subpopulation are two critical factors in tumor growth, resistance to therapy, tumor metastasis, and relapse. It is known that CSCs are closely related to EMT but also are key drivers of tumor invasiveness and aggressiveness. Hence, the study was focused on GSCs analysis in U251-MG and U138-MG spheroids. Initially, the study focused on the effects of hypoxia conditions in the GBM cell line-derived spheroids. Hypoxia, a condition when cells are deprived of sufficient oxygen amount, is the most detrimental factor for the survival of GBM patients, as it promotes drug resistance and invasion and inhibition of immune responses. More importantly, hypoxia promotes the emergence of glioma stem cell by inducing stem cell marker genes, including OCT4, NANOG, SOX2, Kruppel-like factor 4 (KLF4), and cMYC, which was also revealed to state a critical factor for radioresistance induction. Taking the abovementioned into consideration, the study of GSCs started with the circCLIP2 evaluation in normoxia and hypoxia conditions.

U251-MG and U138-MG spheroids were cultured in oxygen deficiency conditions for 5 days and in due time, the expression level of hypoxia biomarkers was analyzed. After 5 days of oxygen deficiency, striking upregulation of hypoxia biomarkers was observed, especially for U251-MG-derived spheroids (7.5-fold, 8.62-fold, and 6.27-fold for GLUT1, ANG, and PDK1, respectively), and slightly lower one for U138-MG-derived spheroids (3.55-fold, 2.43-fold and 2.52-fold for GLUT1, ANG, and PDK1, respectively), confirming the accuracy of the assay (Fig. 15 A). Furthermore, the expression level of CLIP2 gene isoforms in both lines of spheroids cultured in hypoxia conditions was investigated. The expression level of circCLIP2 was found to be significantly higher in both types of spheroids, showing a 3.38-fold and 1.58-fold increase in U251-MG and U138-MG spheroids, respectively. Similarly, the mRNA expression level of the *CLIP2* gene was also elevated by approximately 2.07-fold and 1.89-fold in U251-MG and U138-MG spheroids, respectively, which is presented in Figure 15 B.

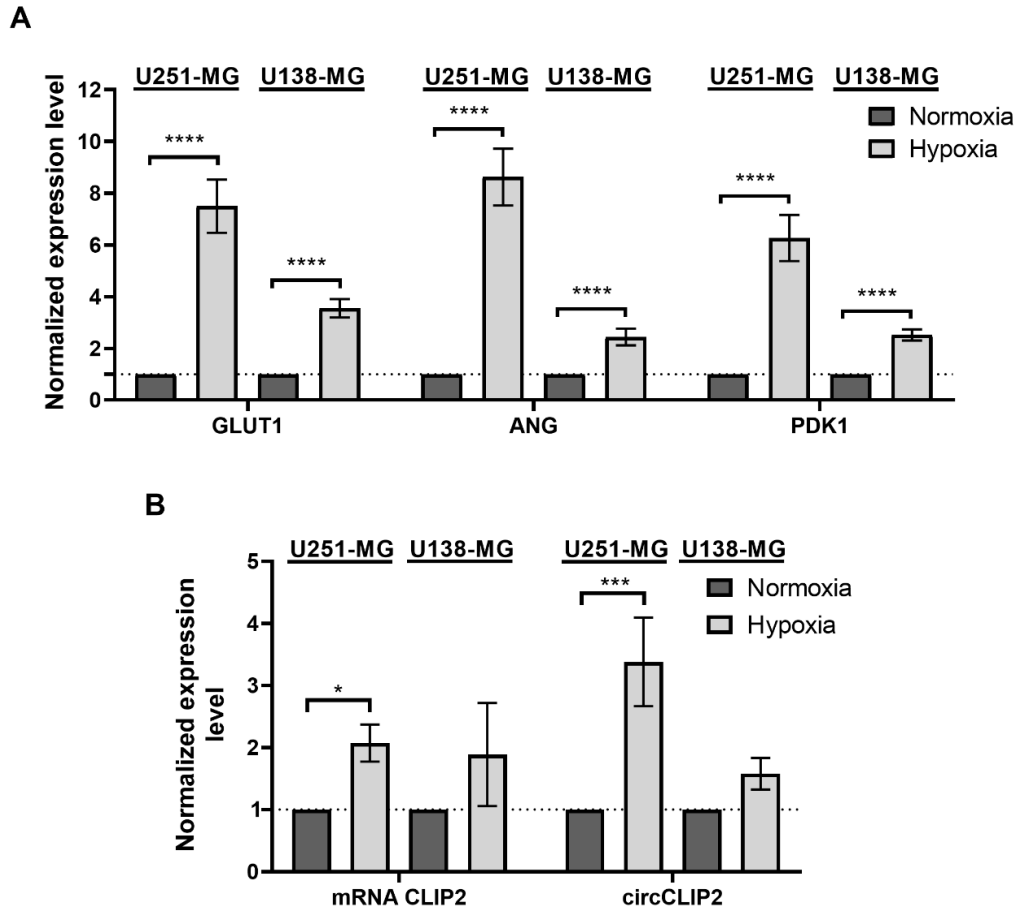


**Figure 15. Expression level of *CLIP2* gene transcripts in GBM cells in hypoxia conditions. A.** Expression level of hypoxia markers in GBM cells in hypoxia and normoxia conditions. **B.** Expression level of *CLIP2* gene transcripts in GBM cells in hypoxia conditions. Normoxia conditions were used as a control (C). Data are shown as the mean  $\pm$  SD values and results were statistically evaluated using one-way ANOVA followed by post hoc Bonferroni test. Statistically significant results were denoted by the following symbols: \* for  $p < 0.05$ ; \*\* for  $p < 0.01$ ; \*\*\* for  $p < 0.001$ ; \*\*\*\* for  $p < 0.0001$  and no statistical significance for  $p > 0.05$ .

Moreover, utilizing U251-MG and U138-MG spheroids, the fraction of GSCs (marked as CD133+) was separated from the remaining types of cells (FT, flow through) based on CD133 expression. The expression level of GSC biomarkers in both fractions was analyzed to confirm proper separation (Fig. 16A, B). A higher expression level of analyzed markers in the CD133+ fraction was observed. However, the results are statistically significant for the Nanog biomarker in U251-MG-derived spheroids only (Fig. 16A). Subsequently, the expression level of circular and linear CLIP2 isoforms in both spheroid lines was established. The upregulated expression level of both isoforms in GSCs in U251-MG-derived spheroids reached 4.43-fold for circular and 2.84-fold for linear isoforms (Fig. 16C). However, in U138-MG-derived

spheres GSCs only linear CLIP2 was upregulated (1.32-fold), whereas circCLIP2 expression levels were similar in both fractions (Fig. 16C).

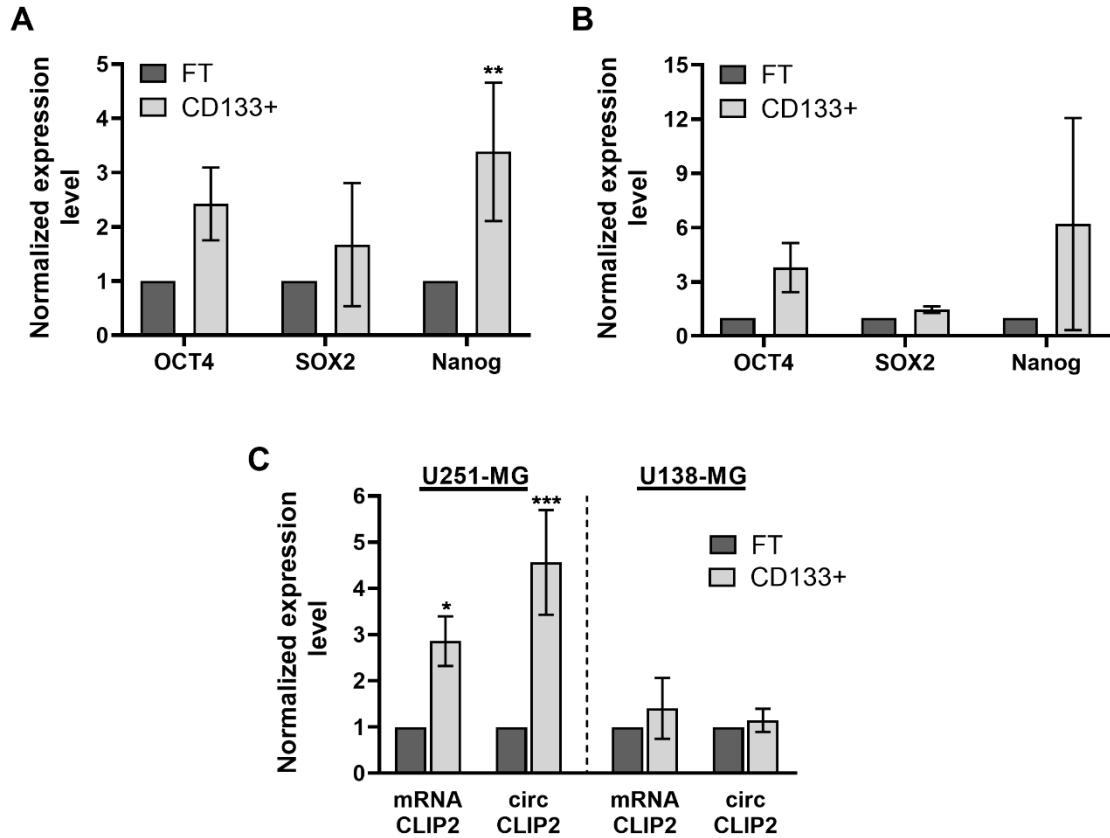


**Figure 16. circCLIP2 knock-down leads to decreased glioma stem cell biomarkers.** A, B. Expression level of GSCs markers in the U251-MG (A) and U138-MG (B) spheroids, CD133+ fraction obtained from individual spheroids and flow through fraction (FT) containing no CD133 positive cells. C. Expression level of *CLIP2* gene transcripts in CD133 positive (CD133+) and negative (FT) fractions of U251-MG and U138-MG spheroids. Data are shown as the mean  $\pm$  SD values and results were statistically evaluated using one-way ANOVA followed by post hoc Bonferroni test. Statistically significant results were denoted by the following symbols: \* for  $p < 0.05$ ; \*\* for  $p < 0.01$ ; \*\*\* for  $p < 0.001$ ; \*\*\*\* for  $p < 0.0001$  and no statistical significance for  $p > 0.05$ .

Furthermore, to validate whether circCLIP2 might promote glioma stemness, the analysis of the expression level of CLIP2 gene isoforms was evaluated utilizing the U-251-MG and U138-MG spheroids subjected to the CLIP2 gene isoforms knock-down (Fig. 17 A, B). The study revealed that circCLIP2 knock-down mediates the downregulation of stemness markers, such as SOX2, Nanog, and OCT4. In the case of the U251-MG spheroids, a 0.74-fold and 0.78-fold decrease of Sox 2 and Nanog was observed, respectively, and no statistical significance for Oct 4 (Fig. 17A). In the U138-MG cell line, a stronger effect and higher drop of GSCs

biomarkers reaching 0.8-fold, 0.5-fold, and 0.6-fold for Oct 4, Sox 2, and Nanog was observed, respectively (Fig. 17B). After linear transcript knock-down in U138-MG, we also observed statistically significant disruption of GSCs biomarkers, which was most effective in both types of spheroids regarding Sox and Nanog biomarkers, reaching 0.74-fold and 0.78-fold in U251-MG spheroids and 0.49-fold and 0.61-fold in U138-MG spheroids.

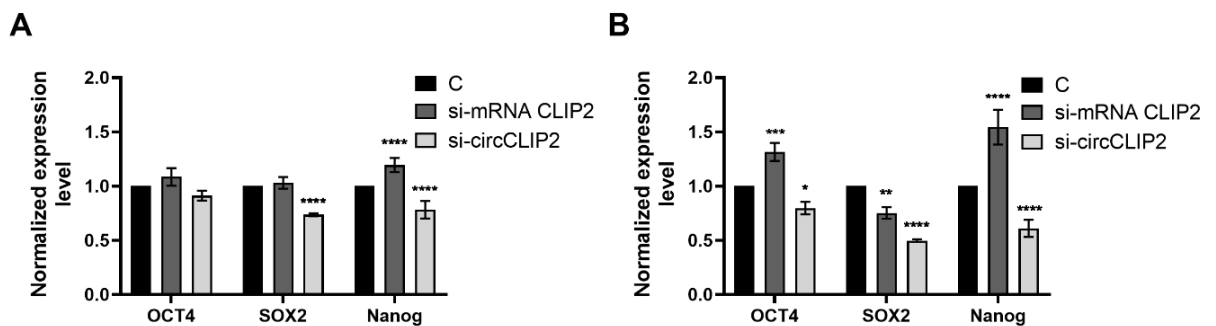


**Figure 17. circCLIP2 knock-down leads to decreased glioma stem cell biomarkers. A, B.** Expression level of GSCs biomarkers in U251-MG (A) and U138-MG (B) cell lines after *CLIP2* gene linear and circular transcripts knock-down. Data are shown as the mean  $\pm$  SD values, and results were statistically evaluated using one-way ANOVA followed by post hoc Bonferroni test. Statistically significant results were denoted by the following symbols: \* for  $p < 0.05$ ; \*\* for  $p < 0.01$ ; \*\*\* for  $p < 0.001$ ; \*\*\*\* for  $p < 0.0001$  and no statistical significance for  $p > 0.05$ .

## 4.2. Global analysis of circRNAs landscape in glioblastoma

To identify the circRNAs landscape in primary and recurrent GBM, RNA sequencing has been performed utilizing GBM patients' tissues. This approach aimed to characterize the global circRNAs expression pattern in GBM, as well as their utility as GBM molecular biomarkers.

### 4.2.1. Identification of circRNAs in primary and recurrent glioblastoma with RNA sequencing

CircCLIP2 was identified by Song et al. (209) as one out of eight upregulated circRNAs in GBM patient samples compared to control brain tissue. In point of fact, the literature data and the abovementioned experiments suggest its potential role in GBM progression, having an impact, especially on GBM cells proliferation and motility. Therefore, we put special attention on the identification of the wide range of circRNAs in primary and recurrent GBM tissues, which also might be involved in the process of gliomagenesis and GBM progression. We

collected 23 primary and 3 recurrent GBM patients tissues in collaboration with the Department and Clinic of Neurosurgery and Neurotraumatology at the University of Medical Sciences in Poznań and the Department of Neurosurgery at the Multidisciplinary City Hospital in Poznań. Prior to the surgery, the approval of the Bioethics Council of the Poznan University of Medical Science Council (consent number 534/18) and the donors' consent had been obtained. Even though we subjected to the RNA-seq three recurrent GBM samples only, as patients suffering from recurrent GBM occurs rarely, the analysis provides new insight into circRNAs landscape in recurrent GBM.

The RNA sequencing has been performed to establish circRNAs expression profiles in primary and recurrent GBM (primary GBM n=23 and recurrent GBM n=3, Table 11) compared to the healthy brain reference (n=41 HB samples, Table 11). A total of 29141 circRNAs were identified in all samples, and 10790 of them were co-expressed in both types of GBM and HB samples (Fig. 18A). Interestingly, 4306 and 1273 circRNAs were unique for primary GBM and recurrent GBM tissues, respectively, in comparison to HB samples (Fig. 18 B, C). The differential gene expression analysis between primary GBM and healthy brain reference revealed 1211 circRNAs differentially expressed between GBM and HB tissues with a log<sub>2</sub> fold change in the range between 8.9 and -5.6 (p-value <0.05). The vast majority of 1056 (87%) circRNAs were downregulated in GBM samples, while only 155 were upregulated. Moreover, the differential gene expression analysis between recurrent GBM and primary GBM samples revealed 3 circRNAs upregulated in recurrent GBM.

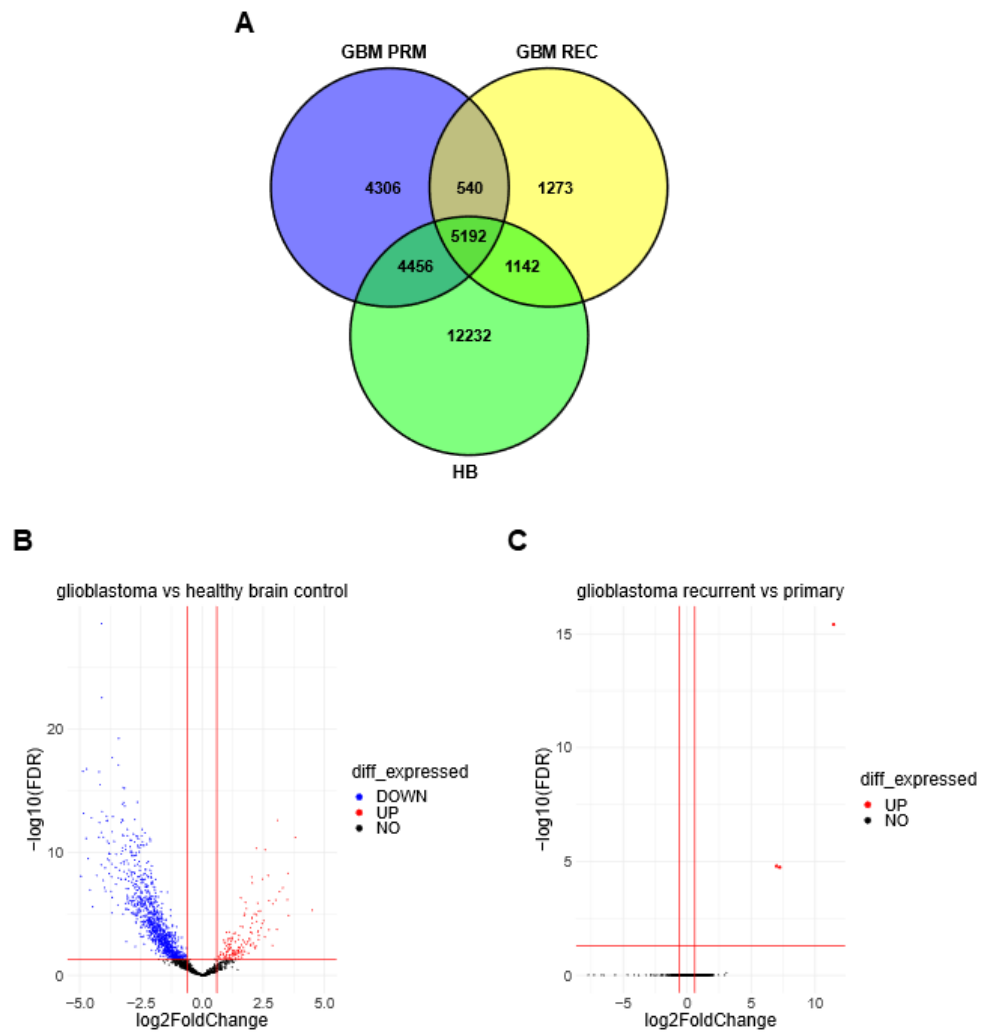


**Figure 18. Identification of circRNAs in primary and recurrent GBM tissues.** **A.** Venn diagram presents an overlap between circRNAs expressed in analyzed primary and recurrent GBM tissues and healthy brain reference. **B, C.** Volcano plot illustrating differentially expressed circRNAs in primary GBM compared to healthy brain reference (**B**) and recurrent GBM compared to primary GBM (**C**). The blue and red dots in Volcano plots indicate downregulated and upregulated circRNAs, respectively.

#### 4.2.2. Selection of proper circRNAs for further research in primary GBM

CircRNAs for further experimental validation were selected, taking into account the expression level and the described function of their linear counterparts. The selected circRNAs were as follows: most downregulated circRNAs detected in primary GBM - CADPS2, EPB41L5, UNC13C, USP45, and most upregulated circRNAs in primary GBM - ARID1A, GUSBP1, PLOD2, VCAN, compared to the HB control with the p-value cutoff <0.05 (Fig. 19).

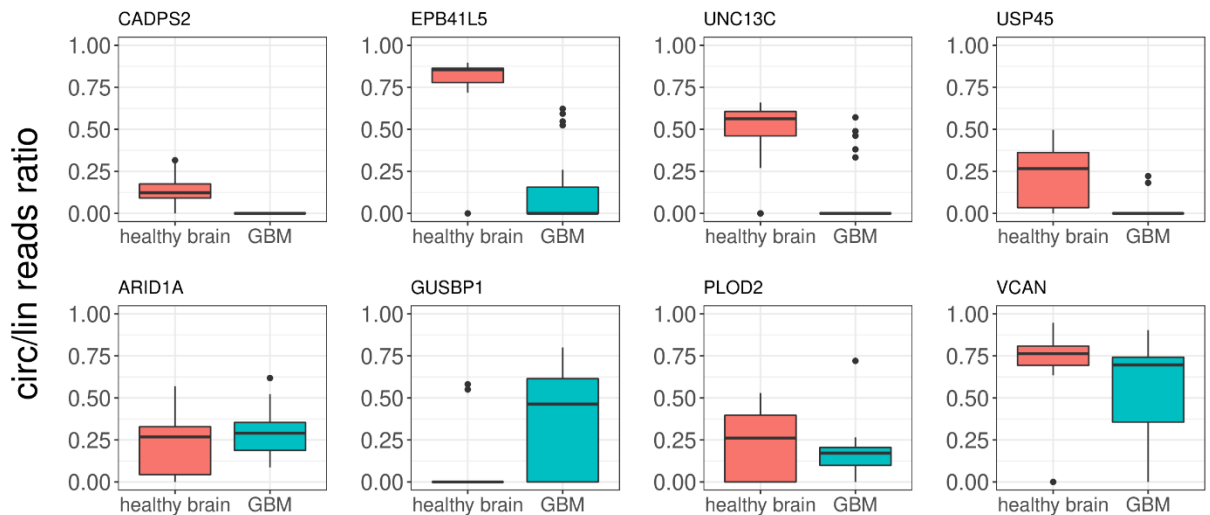


**Figure 19. Expression level of selected deregulated circRNAs revealed by RNA-seq.** Boxplots illustrating the ratio of circular to linear RNA expression levels in RNA-seq analysis of selected transcripts in primary GBM compared to the healthy brain reference.

Selected circRNAs were verified by RT-qPCR analysis, utilizing RNA from all sequenced primary GBM tissues that were available (n=8). The primer sequences are presented in Table 25. The RT-qPCR analysis revealed a higher expression level of linear counterparts of selected circRNAs, which was observed in all cases, with an exceptionally marked increase of VCAN gene transcripts (circular 4.54-fold change and linear 4.44-fold change) (Fig. 20A). Regarding downregulated circRNAs, simultaneous downregulation of their linear transcripts was observed, with one exception – circEPB41L5, characterized by the upregulated expression level of its linear counterpart (circular 0.04-fold change and linear 4,85-fold change) (Fig. 19B). Comparison of selected circRNAs expression levels between RNA-seq and RT-qPCR results showed the same trend of expression pattern estimated in both analyses (Fig. 20C). Interestingly, a significant Pearson correlation of circular and linear transcript expression level for UNC13C ( $r=0.997$ ,  $p<0,001$ ) and VCAN ( $r=0.6957$ ,  $p=0.05533$ ) was observed (Fig. 20D).

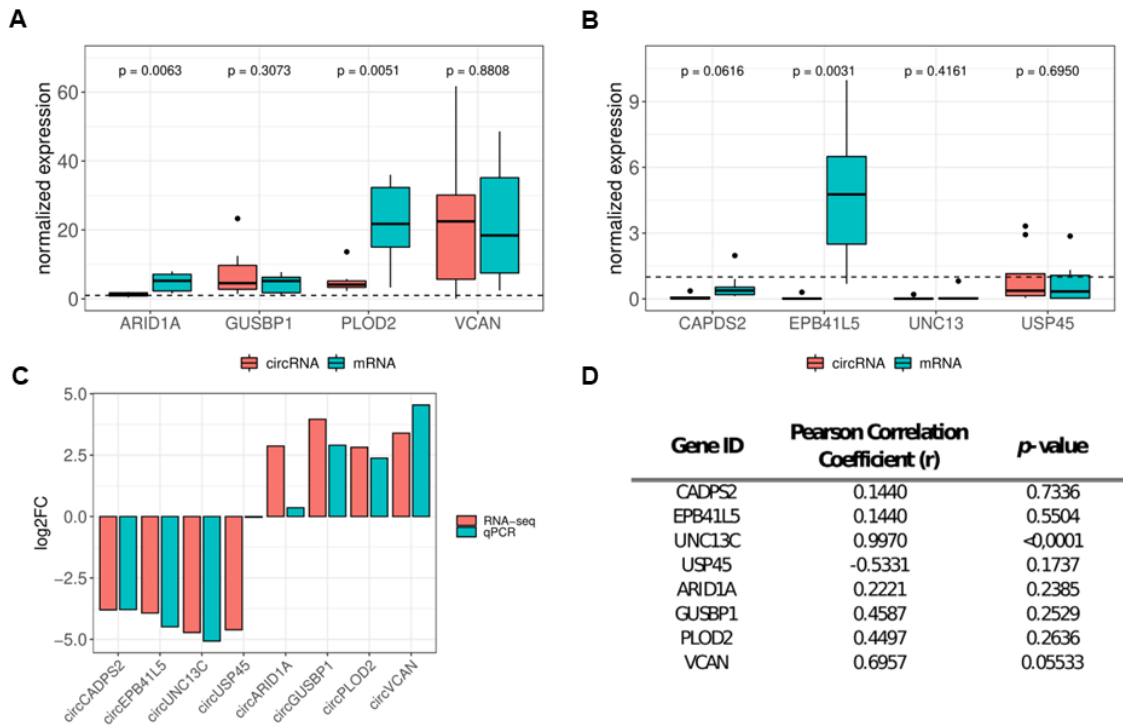


**Figure 20. RT-qPCR validation of the expression pattern of selected circRNAs and their linear counterparts identified as deregulated in primary GBM.** A. RT-qPCR results of circular and linear RNA expression levels of selected upregulated gene candidates in GBM-PRM normalized to HB control. B. RT-qPCR results of the circular and linear expression level of selected downregulated gene candidates in GBM-PRM normalized to HB control. Dashed horizontal lines on A and B panels indicate expression level in HB samples. C. Log2 fold change comparison of selected circRNAs based on RT-qPCR and RNA-seq analysis. D. Pearson correlation of validated circRNAs and their linear counterparts.

#### 4.2.3. Selection of proper circRNAs for further research in recurrent GBM

The differential gene expression analysis between recurrent GBM and primary GBM revealed 3 circRNAs exhibiting the upregulated expression pattern were as follows: EGFR, HLA-B, and a new, not previously annotated intergenic circRNA from chromosome 6 region 29913011-29976954 (Fig. 21).

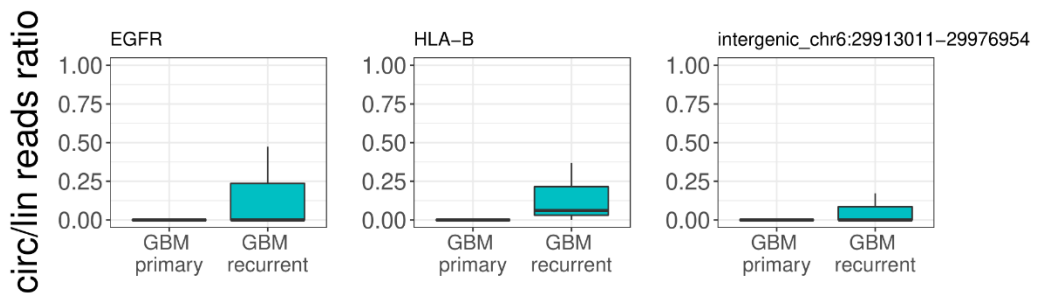


**Figure 21. Expression level of selected deregulated circRNAs revealed by RNA-seq.** Boxplots illustrating the ratio of circular to linear RNA expression levels in RNA-seq analysis of selected transcripts in recurrent GBM compared to the primary GBM.

The circRNA expression pattern was confirmed by RT-qPCR analysis using RNA from all recurrent GBM samples used in the RNA-seq and four more samples collected afterward. Among the analyzed candidates, we observed upregulation of circRNAs compared to their linear counterparts, with substantial overexpression of circEGFR reaching ~12000-fold change (Fig. 22 A). High overexpression of circEGFR was observed in both RNA-seq and RT-qPCR (11.4- and 12.84-fold change, respectively) (Fig. 22 A, B). The Pearson correlation between circular and linear isoforms of EGFR and HLA-B was highly positive, with *r* values of 0.9175 and 0.8896, respectively (Fig. 22C).

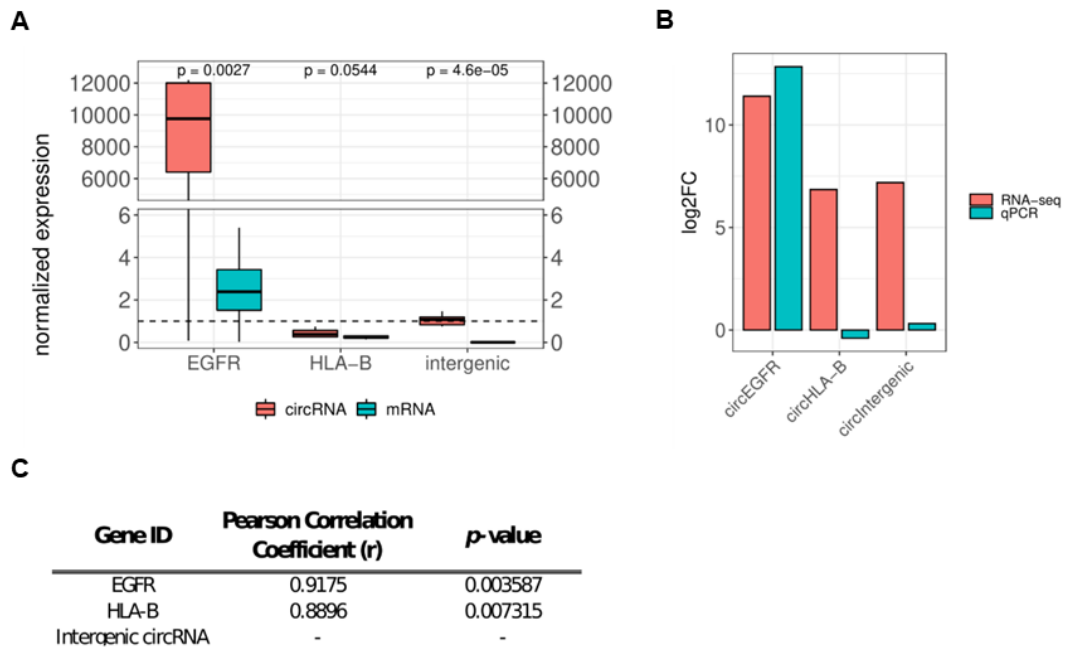


**Figure 22. RT-qPCR validation of the expression pattern of selected circRNAs and their linear counterparts identified as deregulated in recurrent GBM.** **A.** RT-qPCR results of the circular and linear expression level of selected upregulated gene candidates in GBM-REC normalized to GBM-PRM. The dashed horizontal line indicates the expression level in GBM-PRM. **B.** Log<sub>2</sub> fold change comparison of selected circRNAs based on RT-qPCR and RNA-seq analysis. All data are shown as the mean ± SD values. **C.** Pearson correlation of circular and linear counterparts of selected candidates in GBM-REC (GBM-REC vs GBM-PRM).

#### 4.2.4. Clustering of glioblastoma tissues into molecular subtypes and the identification of subtype-specific circRNAs

Using a list of 840 genes gathered from the TCGA GBM dataset and literature (409), followed by other genes that have been reported to be significant for GBM molecular subtyping including SLC12A5, SYT1, GABRA1, NEFL, CDKN1A, NF1, MET, PDGFRA, BOP1, ILR4, the samples used in the study were clustered into molecular subtypes (Fig. 23 A, B). Among 23 GBM samples, all of the reported four distinct molecular subgroups were distinguished: classical (5 samples), mesenchymal (8 samples), neural (5 samples), and proneural (5 samples) (Fig. 23A). To examine whether different GBM subtypes could be associated with distinct circRNA expression signatures, the circMeta R package was applied.

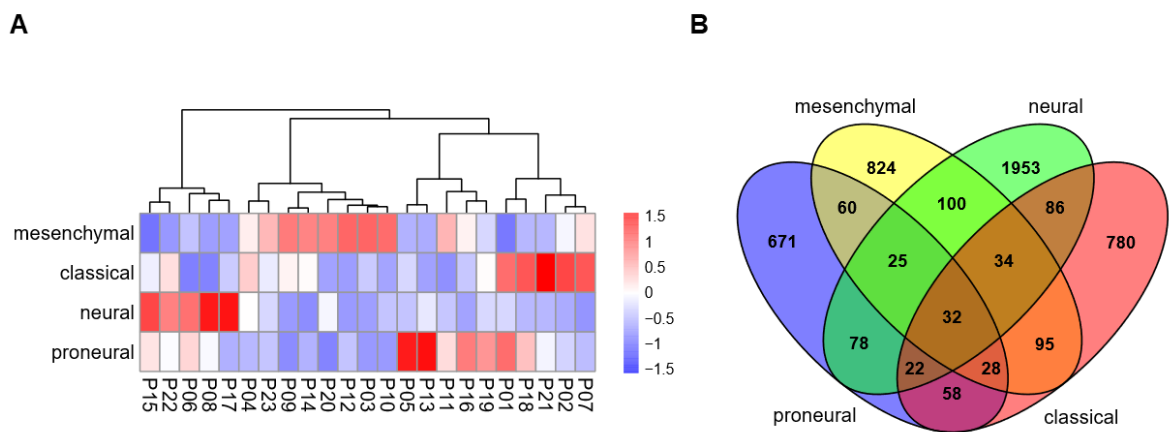


**Figure 23. Representation of subtype-specific circRNA in GBM tissues subjected to RNA sequencing.** A. Venn diagram shows the number of the identified circRNAs in detected GBM subtypes. B. Heatmap presenting subtype classification of the GBM samples used in the study and the subtype-specific circRNAs identified in presented GBM subtypes.

Interestingly, several circRNAs allowing for GBM subtype differentiation were discovered. The neural GBM subtype is characterized by 54 upregulated and no downregulated circRNAs in comparison to other subtypes. The two most upregulated circRNA are novel circRNA derived from AC011995.3 lncRNA (5,69-fold) and circNALCN (5,69-fold). Mesenchymal samples showed 6 upregulated circRNAs, with the most upregulated circCOL4A1 (8.01-fold) and circCOL4A2 (7.84-fold) and 2 downregulated circRNAs - circRBM39 (-4.57-fold) and circRIMS2 (-5.92-fold), in comparison to other samples. The characteristics of circRNAs identified as differentially expressed in neural and mesenchymal GBM subtypes are displayed in Tables 28 and 29 in the Attachments section. However, no

significantly up- or downregulated circRNAs specific to classical and proneural GBM samples were found.

#### **4.3. Generation of assembloids as a complex model for glioblastoma invasion study**

Brain tumor cells create an appropriate microenvironment for migration and invasion by modifying and degrading the extracellular matrix (ECM) and enhancing the ability of GBM cells to invade surrounding tissues, which leads to a desperate need for new and innovative GBM invasion models (588). Currently, available models are mostly based on the co-culture of either glioblastoma stem cells alone or as patient-derived neurospheres and GBM organoids fused with human cerebral organoids. Despite the lack of advanced structural and functional characteristics, generated systems encounter substantial limitations, which are distinctive of *in vitro* cancer model formation, such as an inability to simulate the interactions between tumor cells and the healthy microenvironment, followed by the absence of blood vessels and immune cell, among others (538).

Therefore, as a part of my doctoral research, I aimed to generate and characterize novel models for GBM research, with a strong emphasis put on the invasion processes of GBM cells into the healthy surrounding tissue. In light of the aforementioned obstacles, I conducted the study, which aimed at the delivery and characterization of a complex and innovative GBM invasion model comprised of human cerebral organoids with patient-derived GBM organoids co-cultured into so-called assembloids. The project has been conducted as a part of the FEBS Short-Term Fellowship that I was awarded by the FEBS Committee. The study was carried out at the Organoid Platform, Max Delbrück Center for Molecular Medicine, with the scientific guidance of the Head of the Organoid Platform – Dr. Agnieszka Rybak-Wolf.

In more detail, the aims of the project were:

**1. Creation of a complex *in vitro* model for tumor invasion by combining human cerebral organoids and glioblastoma organoids into assembloids.** The proposed structures provided a physiologically relevant model for monitoring the early and late tumor invasion stages based on the interaction of GBM with healthy cells.

**2. Characterization of the assembloids, GBM organoids, and cerebral organoids.** Despite the in-depth characterization, the analyses were conducted to assess transcriptional and proteomic changes, with special regard to the circRNAs and ECM study, as one of the potential key factors of GBM invasion.

Generation of the assembloids was conducted in the Organoid Platform at Max Delbrück Center for Molecular Medicine (MDC) in Berlin, which supported the study by the delivery of cerebral organoids. Glioblastoma organoids were cultured by the author of this work.

#### **4.3.1. Generation of glioblastoma organoids**

The tumor tissue extracted during the tumor resection has been utilized to obtain a new, three-dimensional model for *in vivo* glioblastoma research – glioblastoma organoids (GBO). The tumor tissues were extracted at the Department and Clinic of Neurosurgery and Neurotraumatology of the Medical University of Karol Marcinkowski in Poznan and the Department of Neurosurgery at the Multidisciplinary City Hospital in Poznan. Prior to the surgery, the approval of the Bioethics Council of the Poznan University of Medical Science Council (consent number 534/18) and the donors' consent had been obtained.

The obtained tissues were cleaned, and the areas abundant in necrotic spots and blood vessels were removed, as presented in Figure 24. Furthermore, the tissue was cut into 1 mm diameter pieces and placed in a culture medium according to the procedure proposed by Jacob and colleagues (580). The applied protocol allows maintenance of the cytoarchitecture and cell-cell interactions of original tumors and limits the usage of specific cell populations in culture, as the glioblastoma organoids are generated without the step of dissociation of the resected tumor tissue into single cells. Within 1-2 weeks, the cut tumor structures develop round-in-shape organoids of a size within the range of 200 - 500  $\mu\text{m}$ . To prevent hypoxia gradients that cause necrotic cell death in the inner core area, larger GBOs are cut into 0.5 – 1 mm diameter pieces during propagation. The presented protocol was chosen to generate the GBOs as it greatly reflects the tumor tissue structure. Obtained organoids are reported to maintain parental tumor heterogeneity, gene expression pattern, and mutation profile (580).

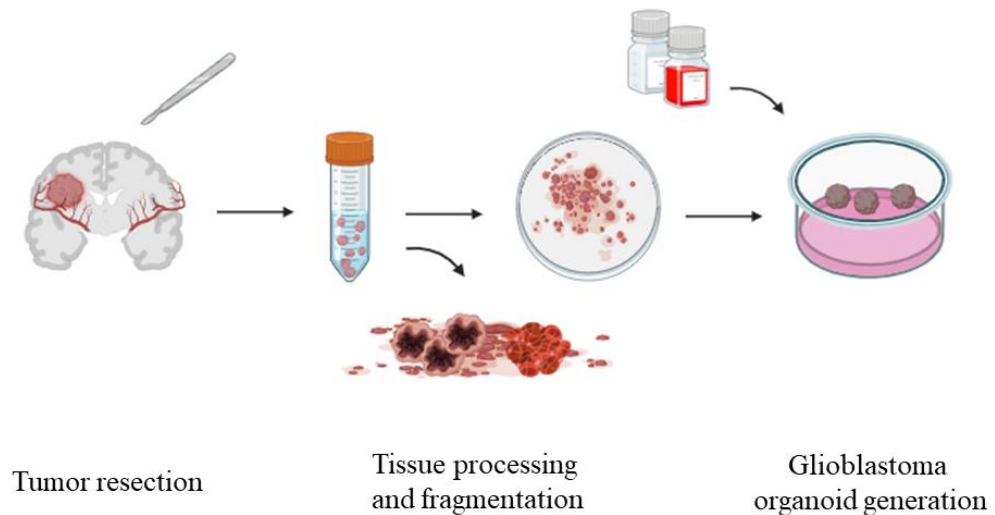


**Figure 24. Generation of the glioblastoma organoid from the GBM patients' tissue.** Glioblastoma organoids were obtained based on Jacob and colleagues' protocol utilizing the fresh GBM patients' tissue immediately after the surgical tumor resection (580). The tissue was deprived of the blood clots and necrotic spots and further was dissected into 0.5 to 1 mm diameter pieces using fine dissection scissors. The minced tissue was cultured in the presence of proper media and supplements (Table 17) for 2-3 weeks to form the glioblastoma organoids.

For the purpose of GBM invasion model generation, three primary cell lines were cultivated to form the glioblastoma organoids. The obtained lines were named P061, P064, and 141222 GBO and were maintained in continuous culture in the Department of Molecular Neurooncology IBCH PAS.

#### 4.3.2. Generation of assembloids

The obtained glioblastoma organoid allowed to generate of a complex model of GBM invasion into surrounding healthy brain structures. The novel model was obtained by the co-culture of the cerebral organoid and glioblastoma organoid into a so-called assembloid, as depicted in Figure 25. In the course of the study, we obtained the following assembloid lines: ABO T106\_P061, ABO T106\_P064, and ABO T106\_GBO 141222. The characteristics of both types of organoids on the day of assembloid generation are depicted in Table 18. Both types of organoids were co-cultured for 21 days to study the early events of GBM cell invasion.

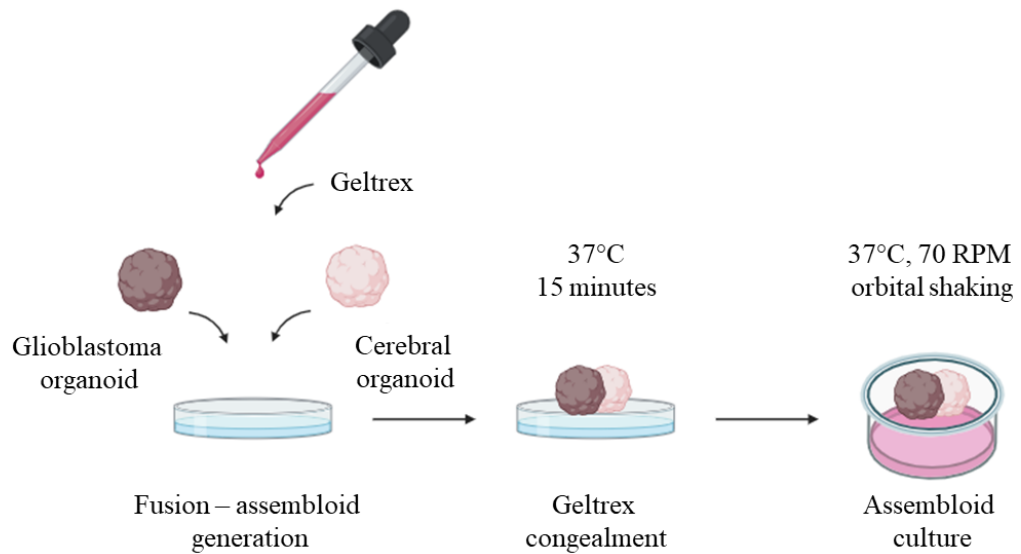


**Figure 25. Generation of the assembloid by the fusion of glioblastoma organoid (GBO) derived from GBM patient tissue and cerebral organoid (HBO) generated from iPSCs.** The organoids were fused with the application of Geltrex to facilitate the fusion and further invasion of the GBM organoid cells. Assembloids were cultured for 21 days in standard culture conditions on the orbital shaking platform.

#### 4.3.3. Characterization of assembloids by immunofluorescence

The generated three-dimensional cultures were fixed and subjected to immunofluorescent imaging to evaluate their structure and composition. The panel of antibodies listed in Table 20 was applied in the study. Although efforts were made, no antibodies were found useful in effectively distinguishing between a healthy organoid and a glioblastoma organoid. For the immunofluorescent imaging purpose, only the P064 and 141222 GBO were subjected, followed by the cerebral organoid derived from T106 iPSCs (induced pluripotent stem cells) and generated assembloids - the ABO T106\_P064 and ABO T106\_GBO 141222.

The imaging showed significant differences in the structure and cellular composition of the studied models. A culture derived from glioblastoma cells shows no intrinsic structurization characteristic of cerebral organoids. GBO 141222 was stained for TNC, which is the extracellular matrix protein upregulated in GBM and for homeodomain-only protein homeobox, HOPX, a transcriptional regulator and marker for outer radial glia in normal human development, which is presented in Figure 26 (589,590) As the micrography depicts, both TNC and HOPX are evenly distributed in the GBM organoid, which is in line with what was stated by the authors of the GBO generation protocol GBOs are densely packed with cells and show no structural organization, however, this might also vary among GBM patients as a consequence of high tumor heterogeneity (580). Even though there is no biomarker exclusively expressed by

GBM cells, TNC, due to its significant overexpression in GBM could serve as a GBM biomarker over the course of the research. As a future perspective, GBM cells transduced with the viral vector containing e.g. green fluorescent protein (GFP) or red fluorescent protein RFP could be applied to distinguish both types of cells.

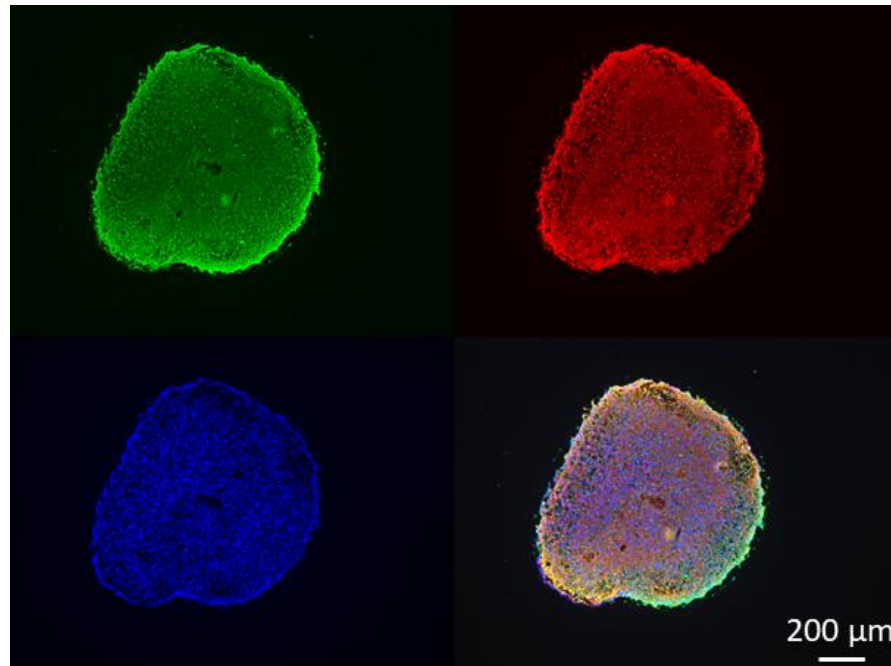


**Figure 26. Fluorescent imaging of GBO 141222.** The micrograph presents the glioblastoma organoid expressing TNC (in green), the extracellular matrix protein and HOPX (in red), a transcriptional regulator and marker for outer radial glia in normal human neurodevelopment. Nuclei have been stained with DAPI (in blue).

ABO T106\_GBO 141222 assembloids also were stained for TNC and HOPX. For the invasion study purpose, is important to note that HOPX has also been described as a marker of a recently described subpopulation of glioma stem cells, which were reported to drive GBM progression. Figure 27 presents the assembly of GBM and cerebral organoids, with the border, present in the common contact area and marked with the white arrows. Near the contact area, the GBM invasive front is present. It is characterized by the abundance of cells expressing TNC, which are infiltrating the cerebral organoid area. The even distribution of TNC across the entire GBO is particularly interesting, as in GBO only, TNC was shown to be present predominantly in the GBO core, which might suggest its involvement in the formation of the invasive front and cancer cells spreading.

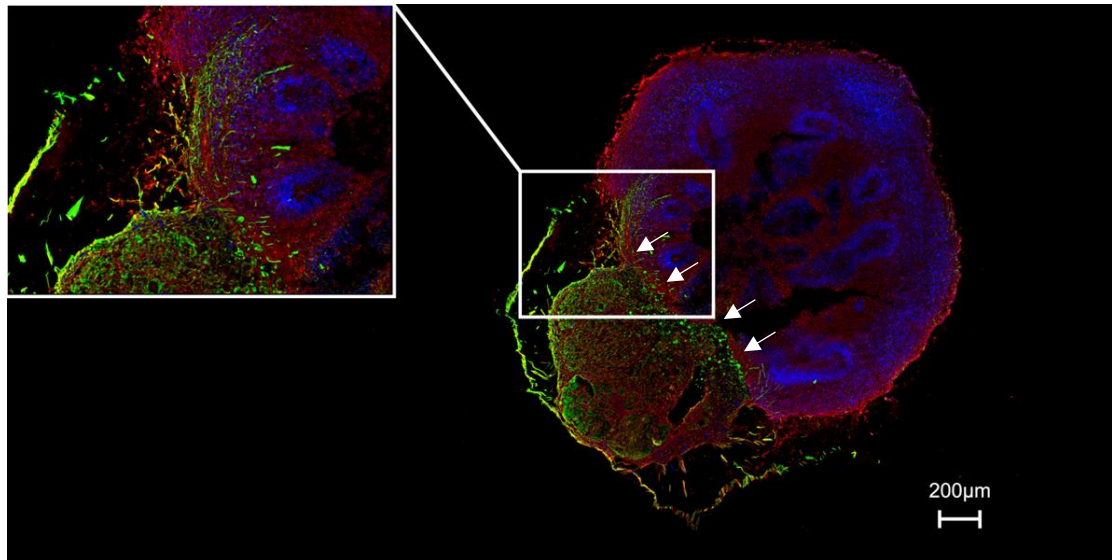


**Figure 27. Fluorescent imaging of ABO T106\_GBO 141222 assembloid.** The micrograph presents the assembloid expressing TNC (in green), the extracellular matrix protein and HOPX (in red) a transcriptional regulator and marker for outer radial glia in normal human neurodevelopment. Nuclei has been stained with DAPI (in blue). White arrows indicate the contact area of both organoids. Left bottom – GBO, right upper – HBO.

GBO P064 were stained for GFAP, which is a member of the cytoskeletal protein family, widely expressed in astroglial cells in neural stem cells and for TUJ1, a protein detected in immature neurons (Fig. 28) (591,592). As stated in terms of GBO 141222, GFAP- and TUJ-expressing cells are also evenly distributed in the GBO P064, however, the concentration of GFAP-expressing cells is more noticeable also in the GBO core.

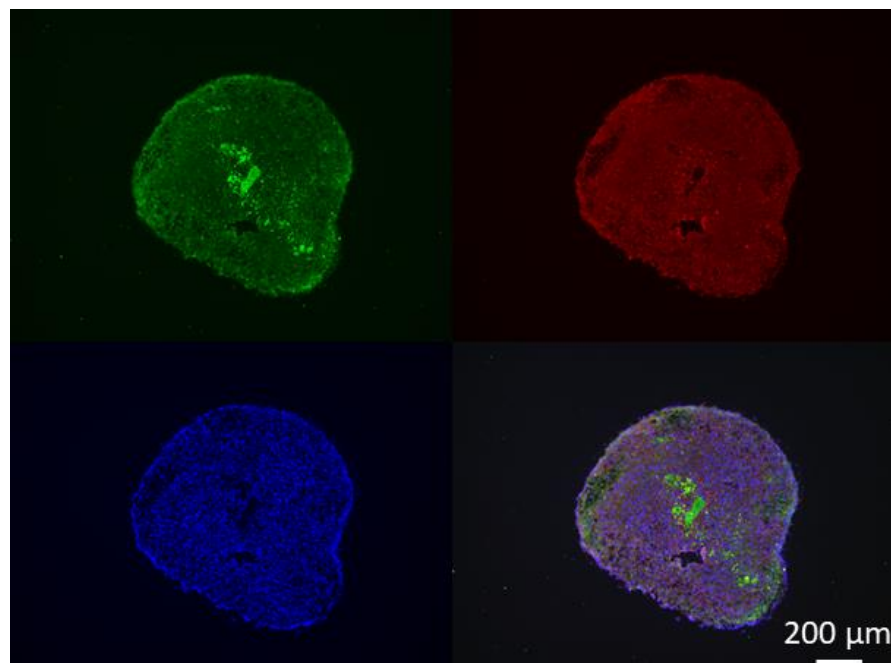


**Figure 28. Fluorescent imaging of GBO P064.** The micrography presents the assembloid expressing GFAP (in green), a member of the cytoskeletal protein family, which is widely expressed in astroglial cells and in neural stem cells and TUJ1 (in red), a protein detected in immature neurons. Nuclei have been stained with DAPI (in blue).

ABO T106\_P064 assembloids also were stained for GFAP and TUJ1. GFAP-expressing cells are present predominantly in the GBO part of the assembloid (left) and invade the cerebral organoid in an interesting manner. As presented in Figure 29 with the white arrows, they migrate around the densely-packed cortical loops of the cerebral organoids instead of infiltrating through the cortical loop mass. This might suggest certain strategy of the cells in terms of selecting the infiltration route with the preclusion of the difficult-to-pass structures of healthy tissue.

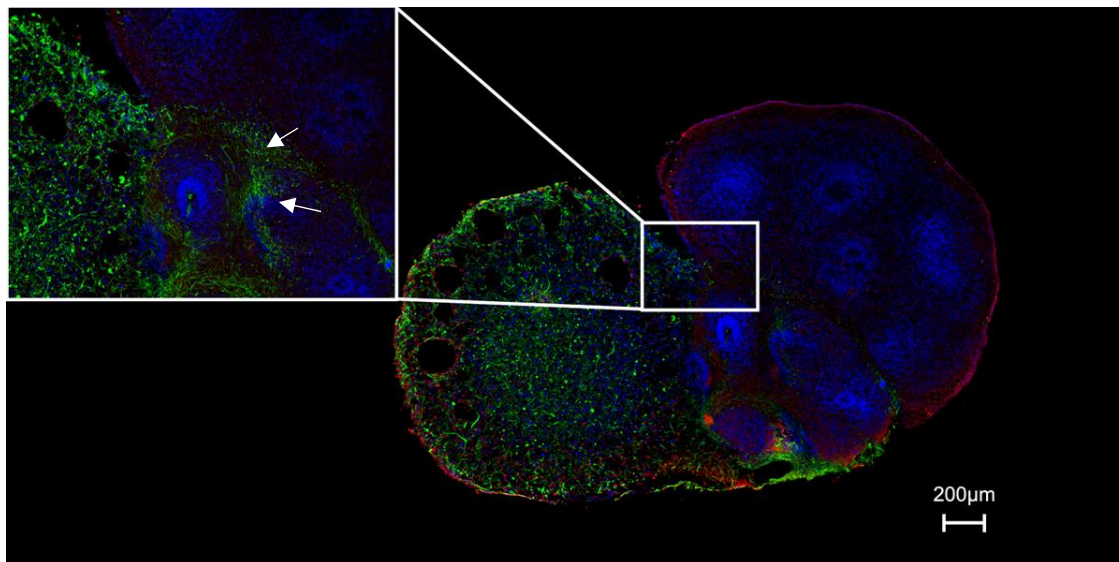


**Figure 29. Fluorescent imaging of ABO T106\_P064 assembloid.** The micrography presents the assembloid expressing GFAP (in green), a member of the cytoskeletal protein family, which is widely expressed in astroglial cells and in neural stem cells, and TUJ1 (in red), a protein detected in immature neurons. Nuclei has been stained with DAPI (in blue). Left – GBO, right – HBO.

#### 4.3.4. Characterization of circRNAs landscape assembloids

RNA sequencing analysis was performed to identify the changes on the transcriptomic level following the tumor invasion into the surrounding healthy environment. The assembloids named ABO T106\_P061, ABO T106\_P064, and ABO T106\_GBO 141222 were subjected to the analysis, along with their structural components serving as a control - glioblastoma organoids, and human cerebral organoids. RNA sequencing was performed to describe the landscape of circRNA population upon undergoing glioblastoma invasion. The most significant

differences in circRNAs expression profiles have been noticed when comparing assembloids to GBM organoids. The differential gene expression showed the deregulation of 14 circRNA among these subsets, revealing two novel circRNA, presented in Table 27. One of the novel circRNAs (ENSG00000224078) derives from SNHG14, a small nucleolar RNA host gene 14, while the other one, the most upregulated circular transcript, presumably does not possess the linear counterpart. Furthermore, chromosome X-related circRNAs were identified, namely BRWD3, which has been reported to promote tumorigenesis of breast cancer (593).

Gene ID	Chromosome	Start	End	LFC	p-value	ENSEMBL best transcript
	chr6	61652255	61697253	5,66	3,87E-05	
<b>RAPGEF2</b>	chr4	159186642	159243791	5,31	0,000172	ENSG00000109756
<b>PGAP1</b>	chr2	196912882	196920150	5,17	0,000202	ENSG00000197121
<b>EPB41L5</b>	chr2	120127688	120175004	5,14	5,29E-05	ENSG00000115109
<b>SHANK2</b>	chr11	70659828	70661678	5,00	0,000271	ENSG00000162105
-	chr15	25266431	25278884	4,99	0,000265	ENSG00000224078
<b>SLC4A7</b>	chr3	27379249	27424152	4,31	8,03E-05	ENSG00000033867
<b>BRWD3</b>	chrX	80733456	80736088	4,28	0,000753	ENSG00000165288
<b>ZNF730</b>	chr19	23134080	23136043	3,97	8,93E-05	ENSG00000183850
<b>ARPP21</b>	chr3	35679787	35691005	3,73	0,000199	ENSG00000172995
<b>SLC4A7</b>	chr3	27383153	27424152	3,17	0,000648	ENSG00000033867
<b>MGAT5</b>	chr2	134317529	134318739	3,09	0,000516	ENSG00000152127
<b>MAML2</b>	chr11	96091892	96093517	-3,33	0,001092	ENSG00000184384
<b>CNIH3</b>	chr1	224730462	224734706	-3,88	0,000647	ENSG00000143786

**Table 27. The differentially expressed circRNAs detected in assembloids compared to the GBM organoids.**

## **5. Discussion**

Brain tumors constitute an exceptional group of malignancies due to their location, significantly confining the application of conventional methods of diagnosis and treatment (594,595). One of the most frequently occurring and extremely aggressive brain tumor types is GBM, characterized by a high ability to infiltrate into the surrounding tissues (596,597). Nowadays, much effort has been made to extend the life of patients and improve their quality. Nevertheless, methods of fast and accurate diagnosis and treatment, allowing for patient-tailored therapy are still in high demand, as commonly used approaches do not bring the expected results (598,599). The newly discovered functions of circRNAs, allowed for the extension of the pool of molecules with diagnostic potential (179,600,601). Despite comprehensive studies on the identification of circRNAs involved in tumorigenesis, followed by the determination of their exact function and relevance as potential biomarkers or therapeutic targets, still much remains to be discovered. To determine the overall potential of circular transcripts as diagnostic or therapeutic molecules, both the expression of circular and linear forms of the corresponding genes should be evaluated(119)

### **5.1. The role of circCLIP2 in GBM**

CircCLIP2 has been previously suggested to act as an oncogenic molecule in GBM, (209) as well as a promising biomarker of high-grade serous ovarian cancer (HGSOC) (602). In addition, a few reports show its high upregulation in primary brain tumors (209,281,282). This work demonstrated a significant interplay between key processes affecting the development and progression of GBM. To begin with, it confirmed elevated expression levels of circCLIP2 in primary and recurrent GBM, as well as GBM cell lines. Nevertheless, the major aim was to investigate the potential role of circCLIP2 utilizing functional analyses.

#### **5.1.1. The impact of circCLIP2 on cell proliferation and motility**

First, the proliferation assay upon circCLIP2 knock-down was performed revealing the dropped proliferative potential of the GBM cells. Impaired proliferation has been already reported upon circCLIP2 knock-down acting via miR-195-5p/HMGB3 axis by activation Wnt/ $\beta$ -catenin signaling (281). However, the known factors contributing to GBM's poor prognosis and treatment resistance are migration and invasion (603). The presented study demonstrates, that the knock-down of circCLIP2 leads to diminished GBM cell motility and invasive potential. Importantly, the specific downregulation of the circCLIP2 expression only

was obtained, with no significant alteration in the expression level of linear CLIP2 transcript at the same time.

This finding suggests distinct properties of both circular and linear isoforms of CLIP2. All aforementioned processes have been recognized as the main drivers of EMT in GBM(604,605). EMT is a biological process that allows immobile epithelial cells to undergo biochemical changes and induces a mesenchymal cell phenotype (604,605). As EMT increases the migratory, invasive, and metastatic potential, the expression level of circCLIP2 in EMT-induced cells was investigated. The obtained data indicated elevated expression levels of circCLIP2, which might be evidence of a phenotypic shift of the transition from epithelial to mesenchymal state. It is widely demonstrated that glioma cells undergoing EMT acquire the potential to initiate invasion and metastasis, which is also confirmed by our invasion assay data. EMT is known to be affected by the tumor microenvironment, particularly the hypoxic niche (606). Moreover, hypoxia enhances migration and invasion in GBM by promoting a HIF1 $\alpha$ -ZEB1 axis-mediated mesenchymal shift (606). The presented study shows that both CLIP2 gene isoforms are upregulated in oxygen deficiency conditions, with a strong prevalence of circCLIP2.

Interestingly, there are other circRNAs described as significant for GBM cell proliferation and motility. The majority of these operate as the ceRNA via the interaction with miRNAs, leading to miRNA sponging and the disruption of its target mRNA expression level. For example, EIF4A3 upon binding to MMP9 mRNA induces circ-MMP9 cyclization and promotes circ-MMP9 expression in GBM. MMP9, which is involved in the degradation of the extracellular matrix, facilitates the proliferative capacity of GBM cells by acting as a sponge for miR-124, indirectly regulating the expression of CDK4 and AURKA (265) Furthermore, circRNAs can regulate cell proliferation by binding with multiple miRNAs to control the expression of downstream genes. For instance, circ-FOXO3 can bind with both miR-138-5p and miR-432-5p to regulate nuclear factor of activated T-cells 5 (NFAT5) expression, promoting cell proliferation (272). Multiple examples of circRNA-driven regulation might be presented in relation to the GBM cells' migratory and invasive potential, contributing to tumor metastasis. In the process of metastasis, cancer cells employ an intricate mechanism called cytoskeletal remodeling to form protrusions, which in turn exert mechanical forces to detach the cell from the surrounding extracellular matrix. Several circRNAs play a key role in the invasion and metastasis of GBM, such as the abovementioned circ-MMP9 (607) and circ-FOXO3 (272), but also circ-SMARCA5 (608), circ-EPB41L5 (609), circRPPH1\_025 (610),

circ-ENTPD7 (269), circCD44 (213) circ-PARP4 (268), circPTK2 (611), circCDC45 (612), circ-PITX1 (613), and many more.

An interesting hypothesis states the ‘Go or Grow’ mechanism describing the migration/proliferation dichotomy. A specific relationship has been observed between the migratory and proliferative behavior of GBM cells in cell culture characterized by separation of cell motion and proliferation since highly motile glioma cells tend to have lower proliferation rates, and conversely, highly proliferating cells are characterized by low motility. It has been described that the process of cell movement and proliferation share common signaling pathways, suggesting a specific type of mechanism regulating both processes (614). One of the pathways has been proposed by Hatzikirou and colleagues indicating that the oxygen shortage might be responsible for the transition from a highly proliferative to an invasive phenotype in a growing tumor (615). The authors also propose that the “Go or Grow” mechanism and hypoxia conditions in a developing tumor are sufficient to trigger the switch from a proliferative to an invasive phenotype in some cells, which might be a consequence of phenotypic plasticity and microenvironmental factors (615). CircCLIP2 states an interesting case as its knockdown leads to the drop of both proliferative and migratory potential, which is not in line with the “Go or Grow” hypothesis. Moreover, circCLIP2 shows a disrupted expression pattern in oxygen deficiency conditions, which in this work is also linked with the enhancement of GBM migration and invasion by promoting the mesenchymal shift of the neoplastic cells.

### **5.1.2. Determination of potential circCLIP2 mode of action**

On the other hand, both the EMT process and hypoxia conditions are significantly linked with the GSCs subpopulation, as these processes mostly overlap with the acquirement of stem cell properties in differentiated tumor cells. Indeed, the study shows the overexpression of circCLIP2 isoform only in the GSCs fraction extracted from GBM spheroids. Interestingly, the knockdown of SOX2 – one of the GSCs markers caused a decreased expression of CLIP2 mRNA in NGS data. Moreover, a high dependency of invasion changes upon the knock-down of circCLIP2 on the presence of GSCs in both sphere lines was revealed, as U251-MG-derived spheres seem to be more abundant in GSCs and show higher invasion potential than U138-MG-derived ones. As the GSCs subpopulation plays an important role in GBM chemotherapy resistance and sustaining the GBM heterogeneity, it is necessary to establish its potential association with linear and circular CLIP2 transcripts. Since the results present that the expression of circCLIP2 highly correlates to CD133 fraction, it might suggest the conclusion about the importance of this molecule for the invasion and potential tumor progression.

Moreover, hypoxia is related not only to EMT and the resulting migration and invasion but also to the aforementioned proliferation changes. Interestingly, hypoxia in cancer can result from the fast proliferation of the cells, as this leads to some tumor cells being located far from oxygen-supplying blood vessels, causing limited oxygen diffusion (616).

## **5.2. CircRNAs landscape in primary and recurrent GBM**

Glioblastoma, which is classified as IV-grade glioma, is the most lethal, aggressive, and malignant among brain tumors in adults with a median survival of 14.6 months when treatment is administered (337). Considering the lack of effective therapy and high inter- and intra-tumoral heterogeneity, an urgent need has arisen to seek new molecular GBM signatures. These could serve as potential diagnostic and prognostic markers as well as therapeutic targets. The most common molecular classification parameter of GBM is the presence of mutations in isocitrate dehydrogenase *IDH1* and *IDH2* genes predicting response to treatment and survival rate (617). An additional gene expression-based molecular classification has been proposed by Verhaak et al. classifying GBM into 4 molecular subtypes: proneural, classical, mesenchymal, and neural(409) Each of the presented groups is distinguished by specific gene expression patterns associated with different tumor aggressiveness and prognosis for treatment response. This classification has become a basis for an intensive search of molecular clustering based on ncRNA expression. Changes in their expression patterns are known to affect tumorigenesis and cancer progression by disrupting complex networks and specific molecular events in other types of cancers. For instance, a GBM molecular classification based on microRNA expression pattern in GSCs has been proposed (618).

Recent advances in the field of ncRNAs have been particularly focused on circRNAs which can be distinguished from other classes of RNAs due to their covalently closed structure. They are single-stranded RNA molecules lacking free ends, generated in the process of alternative splicing referred to as “back-splicing”. Due to their intrinsic resistance to exonuclease cleavage, circRNAs have a longer half-life in comparison to their linear counterparts, making them potentially prominent biomarkers. So far, the involvement of circRNAs in gene expression has been found in the regulation of parental gene transcription and translation. Moreover, they are known to act as miRNA and protein sponges, which might affect molecular balance in transcriptome regulation. Eventually, some of the circRNAs can be translated into proteins.

Altogether, considering the wide spectrum of action and the possible impact of circular RNAs on many cellular pathways, circRNAs could have a significant impact on GBM

progression and development, response to treatment and survival rate (101,619,620). Interestingly, it has been discovered that the healthy brain is enriched with highly tissue- and cell-specific circRNAs. Regarding circRNA formation and possible factors accountable for their disruption, reports are revealing an important role in interactions between RBPs and circRNAs during their biogenesis and maintenance (222,621). So far, the expression pattern and molecular mechanism of action of only a few circRNAs have been characterized in GBM, and the global landscape of circRNA expression and interactome is still missing. Based on NGS data from 26 tumor tissue samples of GBM patients, a global expression pattern of circRNAs in comparison to healthy brain tissues as well as primary and recurrent tumors was characterized and presented in this work. In addition, circRNA distribution in each molecular subtype was investigated to establish their putative role in GBM differentiation and utility as a prognostic, therapeutic, and diagnostic biomarker.

### **5.2.1. Characterization of circRNA landscape in GBM**

The second part of the research presents the circRNA landscape investigated in 23 primary and 3 recurrent GBM patient-derived samples. The study revealed almost 30 thousand circRNAs among the healthy brain reference, primary, and recurrent GBM altogether.

#### **5.2.1.1. Primary GBM**

Moreover, it allowed to distinguish 1270 differentially expressed circRNAs in GBM-PRM samples in comparison to healthy brain reference with almost 90% being downregulated. These findings are in accordance with previously published molecular profiles of circRNAs in different cancer types, including circRNA profiling from 5 GBM patients, in which downregulation of circRNA expression levels compared to HB controls is also observed (258,261,622–624). Further, common downregulation of circRNAs observed in cancer cells can be caused by their extensive proliferation. As previously suggested, this could dilute the concentration of stable circRNAs (258,625). It is also supported by the opposite phenomena, namely the accumulation of circRNA in the non-proliferating aging mouse brain, mainly composed of post-mitotic cells (626). On the contrary, in T-cell acute lymphoblastic leukemia (T-ALL) the majority of deregulated circRNAs showed increased expression in comparison to normal thymocytes (627,628). Tumor cells display a high rate of transcription, especially in aggressive cancers like GBM (628), while the increased incidence of back-splicing happens rather when co-transcriptional processing activities are inhibited or slowed down (629). This is in agreement with presented results, where circRNA downregulation is in most cases

independent of changes in their linear counterparts which suggest no impairment in the transcription process but rather the back-splicing involvement.

Previous studies have shown that dysregulation of circRNAs might exert oncogenic functions in GBM, both downregulated in high-grade glioma circBRAF and upregulated in GBM circPITX1 are associated with poor patients' prognosis (261,273). In our study, among downregulated circRNAs, circEBP41L5 was detected as the most decreased one in GBM and displays the biggest discrepancy between the expression of linear and circular transcripts. In the literature, circEBP41L5 is described as a GBM suppressor that acts through miR-19a sponging (609), thus it could serve as a prognostic or therapeutic molecule for novel clinical approaches. Remaining downregulated circRNAs might potentially act as suppressors and require further studies to better understand the mechanism underlying GBM.

In the remaining upregulated circRNA in GBM, the most upregulated appeared to be circVCAN which high expression is observed also in gastric cancer and radioresistant glioma tissues and its knockdown resulted in the inhibition of cell proliferation, migration, and invasion, and accelerated apoptosis by regulating miR-587 or miR-1183 (630,631). Another verified differentially expressed circRNA with elevated expression levels in our GBM tissues – circPLOC2 was also found upregulated in GBM in a previous study (209). This finding indicates a great potential of circPLOC2 as a biomarker of GBM. CircPLOC2 has also been described as a promoter of tumorigenesis and recurrence biomarker in colon cancer (632,633). It is also frequently upregulated under hypoxia conditions in HeLa and MCF-7 cancer cell lines which mimic oxygen-deprived core of tumor mass (634). There are no literature reports on selected circARID1A and circGUSPB1 which are overexpressed in GBM. The mRNA of the ARID1A gene emerged as a cancer suppressor in different cancers. The absence of ARID1A in cancer can lead to widespread dysregulation of gene expression in cancer initiation, promotion, and progression (635,636).

#### **5.2.1.1. Recurrent GBM**

Interestingly, the RNA-seq analysis revealed only three circRNAs exhibiting deregulated expression patterns in recurrent GBM compared to the healthy brain control. This could support the hypothesis of increased expression level of circRNAs in aggressive tumors, however differentially expressed circRNAs in recurrent samples, namely circEGFR, circHLA-B and intergenic circRNA, exhibit no change of expression pattern in primary GBM. Due to the limited number of samples, circRNAs identified as deregulated in recurrent GBM are considered as promising but preliminary results. The most overexpressed circRNA in recurrent

GBM tissues is circEGFR. CircEGFR is encoded by the EGFR gene which is a well-established oncogene in various cancers (637,638). In contrast, circEFGR was also found as an inhibitor of the malignant progression of glioma by regulating the levels of miR-183-5p and TUSC2 (639). Since there are different circEGFR isoforms originating from different genomic locations, the isoform defined in the mentioned report (hsa\_circ\_0080223) shows downregulation in tumor tissues, however, circEGFR identified in the presented work (hsa\_circ\_0080229) is upregulated. Another study, consistent with abovementioned findings, indicates that hsa\_circ\_0080229 upregulates the expression of murine double minute-2 (MDM2) and promotes glioma tumorigenesis and invasion via the miR-1827 sponging mechanism (640). This proposes that the expression of circEGFR is increasing with tumor progression. CircEGFR analysis presented in the abovementioned study, although to a limited number of samples, supported this hypothesis and it could be significant to further examine additional glioma tissues of different histopathological grades in the future. An interesting explanation of such a significant upregulation of circEGFR in RT-qPCR validation might state the rolling circle amplification. In this process, a primer is amplified to form a long single-stranded nucleic acid using a circular template, leading to the concatemer formation, that is significantly larger than any copies of the single-stranded RNA (641).

For a set of the abovementioned down- and up-regulated circRNAs along with their linear counterparts, transcriptomic results were validated by RT-qPCR. The results obtained from RT-qPCR are highly consistent with RNA-seq results. Quantitative differences for some circRNA can be explained by the high intratumoral heterogeneity of GBM tumors since different fragments of the same tissue were used for our RNA-seq and RT-qPCR validations.

### **5.2.2. Molecular subtyping of GBM tissues**

GBM is a heterogeneous disease that can be classified into four known molecular subtypes according to mutation landscape and gene expression pattern (409). The investigated 23 primary GBM samples represent all of the known subtypes, namely: classical (5 samples), mesenchymal (8 samples), neural (5 samples), and proneural (5 samples). It has been found that the neural subtype is the most similar to the HB samples, according to the circRNA expression pattern. In the neural subtype compared to other subtypes 54 differentially overexpressed circRNAs were identified. These finding confirms the literature reports that the neural subtype might be non-enhancing tumor margins contamination and is the most similar to samples derived from normal brain tissue (642–644). The two most upregulated circRNA are novel circRNA derived from AC011995.3 lncRNA and circNALCN.

Interestingly, circNALCN has already been shown to act as a miR-493-3p sponge in GBM. By binding the miR-493-3p, circNALCN regulates PTEN expression and inhibits glioma progression. Moreover, due to the observed circNALCN downregulation both in GBM tissues and analyzed GBM cell lines and the abovementioned GBM progression inhibition, it has been proposed to state a promising diagnostic biomarker and therapeutic target for glioma patients (645). Mesenchymal samples showed 6 upregulated circRNAs, with the most upregulated circCOL4A1 and most downregulated circRBM39, in comparison to other samples. So far none of the most deregulated circRNA appeared as significant in GBM, however, the circRBM39 is linked with Parkinson's disease (646). Even though circCOL4A1 and the second upregulated circRNA - circCOL1A2 are not linked with GBM development, the transcriptomic profiling of U87MG brain-invasive derivatives revealed that strongly upregulated transcripts are linked with ECM components encompassing multiple collagen members, including both subunits of collagen I and collagen V, and COL8A1, as well as multiple collagen-interacting proteins and collagen-processing enzymes (647).

### **5.3. Assembloids as complex GBM model for the tumor invasion study**

The study of circRNAs which might be involved in high GBM aggressiveness and invasiveness required a complex model of GBM cells infiltrating healthy tissue, with sustained cell-to-cell, cell-to-microenvironment interactions. As 2D and less complex 3D models lack the natural GBM tissue architecture, we developed a novel and innovative organoid-based model for GBM invasion study.

Organoids derived from GBM tissue have become an intriguing cancer research model in recent years. This complex GBM model utilizes tumor tissue derived from a patient after the surgical tumor resection, thus it greatly resembles the natural tumor microenvironment and complexity. The GBM organoid generation procedure was adopted from the protocol published by Jacob et al. in 2020 (580), which assumes the application of the GBM patient's tissue to generate the GBM organoids instead of the tumor mass dissociated into a single cell suspension. This type of culture allows the cancer cells to grow in the natural environment and sustains the cell-to-cell contact, which facilitates the generation of the organoid structure and promotes further intercellular interactions (648). Organoids generated in this manner exhibit a high cell density, indicating strong connections between cancer cells (580). One of the biggest obstacles facing organoid models is their long formation time and demanding growth conditions. In order to use this model in research which assumes high throughput assays such as testing new low-

molecular drugs anti-cancer drugs, the automation adjustments and protocols need to be applied.

In the last decades, researchers made impressive progress in the field of reconstructing organ-like tissues, which have the potential to serve as an advanced system, especially in cancer research (538,649). Currently available models are mostly based on the co-culture of either GSC or dissociated GBM tissue alone, or patient-derived neurospheres with human cerebral organoids. Along with the generation of GBM organoids, significant effort has been made to create a co-culture system comprised of human cerebral organoids and glioblastoma organoids, however, the aforementioned model has not been fully characterized yet (580). Despite the lack of advanced structural and functional characterization, generated systems encounter substantial limitations, which are characteristic of *in vitro* cancer model formation, such as an inability to simulate the interactions between tumor cells and the healthy microenvironment, low throughput capabilities resulting from limited patients tissue amount, followed by the absence of blood vessels and immune cell, among others.

GBM organoids can be used to study the invasion of single glioblastoma cell into a structure resembling the human brain. In the presented study cerebral organoids delivered by Dr. Agnieszka Rybak-Wolf from Organoid Platform, Max Delbrück Center for Molecular Medicine served as a model of the healthy brain. Interactions between cancer cells and healthy cells are highly important in the process of glioblastoma development and invasion. Undoubtedly, the biggest advantage of the presented assembloid model is the high level of GBOs resemblance to the patient's tissue, as no other model cannot reflect the patient's characteristics to this extent. Moreover, this makes a closely physiologically relevant environment for tumor-healthy tissue interaction giving a more complex model for GBM invasion study. The GBM infiltration in a healthy brain must be driven by a highly complex GBM ecosystem (650). Therefore, In the context of TME, assembloids constitute a great model for the investigation of ECM structure, cell-cell, and cell-matrix interactions in order to define complex ECM changes during tumorigenesis. The part of the dissertation devoted to the assembloid generation exhibited also some limitations and required further research to adjust the model for high-throughput studies. The obstacles, that need to be addressed and analyzed in order to implement a high-throughput scale are as follows:

- a high heterogeneity among the GBM patients, which a high amount of tissue samples and generated assembloids to obtain the statistically significant outcome,

- the necessity of GBO culture's scale enhancement, which is strictly connected to and restricted by the amount of patient tissue obtained during the surgical resection of the tumor,
- a need for further optimization of the GBO and HBO fusion, especially the factors such as the time of culture and optimal timepoints application, potential generation of the assembloids without the usage of Geltrex and any other external chemicals, which might impact or modulate cell behavior,
- the optimization of the GBO and HBO size and age selection, facilitating the repeatability of the assembloids generation and assembloid-based assay results,
- lack of immune system components and vascularization both in GBO and assembloid models, which are known to be significant for GBM growth and spread.

## 6. Conclusions

Collectively, it has been found that circCLIP2 is highly overexpressed in primary and recurrent GBM. Presented data might suggest that circCLIP2 could be, directly or indirectly, implicated in the regulation of GBM proliferation, migration, and invasion processes, and, consequently, the onset and progression of GBM. The role of circCLIP2 in these processes might be potentially connected to the hypoxia-dependent EMT process including the significance of GSCs, however, the detailed pathway has not been established. Obtained results present the potential implication of circCLIP2 in GBM aggressiveness and tumor metastasis, however, to confirm that and unravel the most probable mechanism of circCLIP2 action further analyses are required.

Moreover, in this study, the circRNA expression profile in GBM was determined revealing hundreds of deregulated circRNAs, many known to regulate processes important for cancerogenesis. Very often circRNA expression changes are associated with mRNA expression changes. Results presented in this study can set a background for several hypotheses about molecular mechanisms and the clinical relevance of circRNA-related mechanisms in GBM. Additionally, the overview of GBM subtype-specific circRNAs has been delivered in this work. GBM subtype-specific circRNAs might state promising molecules when applied as prognostic, diagnostic, or therapeutic targets. The subtype-specific circRNA approach might state the window for a slightly more personalized treatment approach, which is in high demand regarding GBM.

The last part of this dissertation states the generation and characterization of the assembloid model, developed to provide comprehensive knowledge about the GBM invasion process. It allows to investigate the GBM cellular composition, spatial transcriptomic architecture during the invasion process as well as the proteomic, metabolomic, and secretome profile to deeply characterize the GBM invasion based on the microenvironmental signals, cell-to-cell and cell-to-TME communications events. This model allows for the observation of early and late events of GBM invasion into the surrounding environment and following the events that lead to the fully invasive phenotype development. The invasion-related changes could then be associated with the interactions between the tumor cells and brain parenchyma and might include: the changes in the transcriptomic profiles of the interacting cells, the content of the cell during the time of invasion, the changes between the cells as well the cells and interacting environment, thus as the consequence, the changes in the functional status of the tumor such as enhanced motility, adhesion or cells rigidity.

Concerning the contribution of circRNAs to the GBM investigation, this work evidence:

- 1. CircCLIP2 plays a significant role in GBM progression.** CircCLIP2 knockdown directly or indirectly reduces the proliferation, migration, and invasion of GBM cells, which might suggest the potential role of circCLIP2 in GBM progression. Proposed mechanisms of circCLIP2 action might include the processes related to the EMT process and/or GSCs fraction.
- 2. CircRNAs are abundant and show disrupted expression pattern in GBM.** Almost 30,000 identified circRNAs were identified in the group of primary and recurrent GBM and healthy brain reference by RNA-seq of the GBM patients tissue and the control, where 4663 were deregulated exclusively in primary and 1255 in recurrent GBM. Among these, 978 circRNAs were identified as downregulated and 129 upregulated in primary GBM. Only 3 circRNAs were identified as disrupted in recurrent GBM compared to healthy brain reference.
- 3. CircRNAs are differentially expressed among GBM subtypes.** CircRNAs identified in GBM tissues subjected to RNA-seq exhibit specific expression pattern in four GBM subtypes, which after wide investigation could be considered as promising prognostic and therapeutic targets as well as GBM biomarker for molecular diagnostics purposes.
- 4. I have identified GBM circRNAs specifically expressed in GBM tissues, which can be further considered as the potential new therapeutic targets.** Moreover, the differential analysis of the GBM primary and recurrent tumors reveals exclusively expressed circRNA that possibly could serve as the GBM progression markers. It is worth to mention, that two of identified in GBM-REC circRNA are new molecules, not previously reported.
- 5. GBM research greatly benefits from 3D structure deployment as they better recapitulate the tumor microenvironment than 2D cultures.** Assembloids as a co-culture of GBM organoids and cerebral organoids state a promising model for early and late events of GBM invasion and can be still improved by supporting the assembloid vasculature and immune cells enrichment. Nonetheless, based on this novel and highly sophisticated model, I have identified two circRNAs that could be considered as the new GBM invasion markers, being undetectable in the others GBM models.
- 6. GBM assembloids could be a promising model in the area of modern GBM therapy that uses the assembloids for *in vitro* drug screening.** The personalized GBM assembloids could also serve as a platform for pharmacological screening to select patient-specific treatment, as a step forward in personalized GBM therapy.

## 7. Attachments

Gene ID	ENSEMBL	Chromosome	Start	End	LFC	p-value	FDR
COL4A1	ENSG00000187498	chr13	110827687	110829071	8,01	1,333E-06	0,000651962
COL1A2	ENSG00000164692	chr7	94047043	94049596	7,84	1,676E-06	0,000651962
CPSF6	ENSG00000111605	chr12	69644909	69656342	3,24	0,0005645	0,049634316
SSH2	ENSG00000141298	chr17	28011581	28030080	2,14	0,000638	0,049634316
FNDC3B	ENSG00000075420	chr3	171965323	171969331	1,32	0,0002543	0,039569779
FCHO2	ENSG00000157107	chr5	72370569	72373320	1,30	0,0004036	0,044854413
TASOR	ENSG00000163946	chr3	56694759	56707753	-2,48	0,0006365	0,049634316
TBCEL	ENSG00000154114	chr11	120916383	120930794	-2,62	5,23E-05	0,013069658
RBM39	ENSG00000131051	chr20	34309662	34313077	-4,57	0,000377	0,044854413
RIMS2	ENSG00000176406	chr8	105080740	105161076	-5,92	6,72E-05	0,013069658

**Table 28. CircRNAs identified as exclusively expressed in the mesenchymal subtype of analyzed GBM tissues.** Analysis performed by our collaborator – Dr. Marcin Sajek.

Gene ID	ENSEMBL	Chromosome	Start	End	LFC	p-value	FDR
-	ENSG00000237720	chr2	2840691	2842060	5,6894	1,636E-06	8,49899E-05
NALCN	ENSG00000102452	chr13	101997617	102051516	5,6874	6,836E-09	2,76113E-06
ERC1	ENSG00000082805	chr12	1399018	1519619	5,4212	1,639E-06	8,49899E-05
MLIP	ENSG00000146147	chr6	54013854	54095715	5,3212	3,045E-06	0,000131632
-	-	chr9	26424107	26569673	5,2897	2,24E-05	0,000645589
MLIP	ENSG00000146147	chr6	54013854	54067031	5,1664	3,261E-07	2,81882E-05
-	-	chr6	62362160	62407158	4,9282	1,991E-07	1,936E-05
SGMS1	ENSG00000198964	chr10	52193236	52350007	4,8173	2,07E-05	0,000619259
SLC4A7	ENSG00000033867	chr3	27420740	27465643	4,7097	3,893E-08	5,04834E-06
EPB41L5	ENSG00000115109	chr2	120885264	120932580	4,6171	2,95E-08	5,04834E-06
KLHL24	ENSG00000114796	chr3	183368084	183390272	4,6056	1,065E-08	2,76113E-06
LPXN	ENSG00000110031	chr11	58317259	58318705	4,6022	8,821E-07	5,71873E-05
-	-	chr13	84376512	84389879	4,2922	5,15E-05	0,001214178
RAPGEF5	ENSG00000136237	chr7	22330794	22357656	4,2516	9,819E-06	0,000381951
SLC8A1	ENSG00000183023	chr2	40366541	40405633	4,1873	0,00034	0,005751134
MAP7	ENSG00000135525	chr6	136704809	136710655	4,1777	0,0004087	0,006624414
AGTPBP1	ENSG00000135049	chr9	88190230	88248289	4,0639	8,136E-07	5,71873E-05
ZFYVE16	ENSG00000039319	chr5	79745410	79770649	4,0324	1,342E-05	0,000474525
PSMB1	ENSG00000008018	chr6	170846322	170858201	3,9555	9,737E-09	2,76113E-06
SATB1	ENSG00000182568	chr3	18419662	18462483	3,9517	0,000175	0,003321201
RAPGEF5	ENSG00000136237	chr7	22347958	22357656	3,9114	3,208E-05	0,000860736
FMN1	ENSG00000248905	chr15	33149216	33194241	3,9058	3,2E-05	0,000860736
UNC13C	ENSG00000137766	chr15	54304845	54308083	3,8912	0,0005386	0,008552107
KLHL24	ENSG00000114796	chr3	183361268	183390272	3,8332	3,624E-08	5,04834E-06
RAPGEF5	ENSG00000136237	chr7	22306583	22357656	3,8241	0,0001444	0,002807806

<b>PCLO</b>	ENSG00000186472	chr7	82763566	82764972	3,7468	2,559E-06	0,000117119
<b>KCNN2</b>	ENSG00000080709	chr5	113740135	113740553	3,6815	1,309E-06	7,83495E-05
<b>RIMS2</b>	ENSG00000176406	chr8	105080740	105161076	3,5979	4,238E-05	0,001046778
<b>SFRP4</b>	ENSG00000106483	chr7	38050523	38053183	3,5751	0,0017181	0,021464066
<b>TMEFF1</b>	ENSG00000241697	chr9	103261047	103312442	3,4808	0,0003092	0,005372671
<b>ERC1</b>	ENSG00000082805	chr12	1399018	1481143	3,4319	3,847E-07	2,99307E-05
<b>PPP1R13B</b>	ENSG00000088808	chr14	104245082	104263855	3,4187	0,0007505	0,010957512
<b>ATRNL1</b>	ENSG00000107518	chr10	116879949	117001514	3,3502	0,0033568	0,03305813
<b>MAP7</b>	ENSG00000135525	chr6	136709531	136710655	3,3037	1,752E-05	0,000567904
<b>RIMS1</b>	ENSG00000079841	chr6	73016961	73043538	3,2585	3,992E-05	0,0010353
<b>ZDBF2</b>	ENSG00000204186	chr2	207144264	207162097	3,2082	0,0016783	0,021464066
<b>ATRNL1</b>	ENSG00000107518	chr10	116879949	116931050	3,1481	2,047E-06	9,95524E-05
<b>PSMB1</b>	ENSG0000008018	chr6	170852689	170858201	3,12	0,0003577	0,005920912
<b>SLC45A4</b>	ENSG00000022567	chr8	142264088	142264728	3,0635	1,643E-07	1,82591E-05
<b>MTCL1</b>	ENSG00000168502	chr18	8718422	8720494	3,0028	5,941E-05	0,001359541
<b>BTBD7</b>	ENSG00000011114	chr14	93760204	93762503	2,9758	0,0002488	0,004501288
<b>ARHGAP32</b>	ENSG00000134909	chr11	128993341	129034322	2,9752	0,0030848	0,031419117
<b>ANKS1B</b>	ENSG00000185046	chr12	100166700	100175875	2,9408	0,0012832	0,017212233
<b>CHD9</b>	ENSG00000177200	chr16	53288350	53308214	2,9253	0,0023718	0,027541547
<b>-</b>	<b>-</b>	chr7	86223627	86226365	2,916	0,002484	0,02821497
<b>KLHL24</b>	ENSG00000114796	chr3	183361268	183369064	2,8542	8,395E-06	0,000343742
<b>SMAD2</b>	ENSG00000175387	chr18	45391430	45423180	2,7906	0,0042306	0,038598644
<b>PTK2</b>	ENSG00000169398	chr8	141745350	141762415	2,7544	0,0055264	0,047772734
<b>RNF138</b>	ENSG00000134758	chr18	29691717	29704808	2,7173	0,0042212	0,038598644
<b>AKT3</b>	ENSG00000117020	chr1	243708812	243859018	2,6876	2,047E-05	0,000619259
<b>DGKB</b>	ENSG00000136267	chr7	14613837	14712652	2,6367	0,0009166	0,012966407
<b>PAK3</b>	ENSG00000077264	chrX	110385324	110416309	2,6004	0,001783	0,021464066
<b>PTK2</b>	ENSG00000169398	chr8	141749117	141762415	2,5754	0,0005694	0,008641482
<b>ATRNL1</b>	ENSG00000107518	chr10	116879949	116975638	2,5043	0,0043202	0,038633631
<b>WDR7</b>	ENSG00000091157	chr18	54426096	54448887	2,4944	0,0035696	0,034285692
<b>MINDY3</b>	ENSG00000148481	chr10	15875629	15889942	2,4205	0,0001065	0,002180128
<b>FUT8</b>	ENSG00000033170	chr14	66028055	66028484	2,4126	0,0017898	0,021464066
<b>ZCCHC7</b>	ENSG00000147905	chr9	37126309	37127260	2,3914	0,0017479	0,021464066
<b>AAGAB</b>	ENSG00000103591	chr15	67524152	67529158	2,3414	1,703E-05	0,000567904
<b>VRK1</b>	ENSG00000100749	chr14	97299804	97327072	2,311	0,0012131	0,016558098
<b>AKT3</b>	ENSG00000117020	chr1	243776973	243859018	2,2616	0,0026601	0,029565199
<b>SLC25A26</b>	ENSG00000144741	chr3	66286968	66313803	2,2542	0,0032033	0,031950878
<b>DCUN1D4</b>	ENSG00000109184	chr4	52729603	52758017	2,2374	0,0005683	0,008641482
<b>LINC00632</b>	ENSG00000203930	chrX	139865340	139866824	2,2288	0,0003108	0,005372671
<b>MARCHF6</b>	ENSG00000145495	chr5	10415600	10417516	2,1158	4,306E-05	0,001046778
<b>SOBP</b>	ENSG00000112320	chr6	107824861	107827631	2,0793	8,759E-05	0,001841726
<b>SENPP6</b>	ENSG00000112701	chr6	76344423	76388643	2,0572	0,0054072	0,047267582
<b>PTP4A2</b>	ENSG00000184007	chr1	32381496	32385259	2,0238	1,198E-05	0,000443942
<b>TMCC1</b>	ENSG00000172765	chr3	129546646	129551669	1,9703	0,0036652	0,034758765
<b>MIB1</b>	ENSG00000101752	chr18	19345733	19359646	1,9507	7,078E-05	0,001573294

<b>SHOC2</b>	ENSG00000108061	chr10	112723883	112745523	1,9157	0,0028903	0,0303872
<b>TMEFF1</b>	ENSG00000241697	chr9	103261047	103279053	1,8738	0,0007605	0,010957512
<b>CCSER2</b>	ENSG00000107771	chr10	86198268	86237420	1,87	0,001919	0,022620906
<b>TTC28</b>	ENSG00000100154	chr22	28692186	28693840	1,8592	0,0029525	0,030627666
<b>EXOC6B</b>	ENSG00000144036	chr2	72958136	72960247	1,8274	0,0037082	0,034758765
<b>RERE</b>	ENSG00000142599	chr1	8601273	8617582	1,8063	0,0005776	0,008641482
<b>ARHGAP5</b>	ENSG00000100852	chr14	32559708	32563592	1,7885	0,0028091	0,0303872
<b>PHF21A</b>	ENSG00000135365	chr11	46098305	46113774	1,7769	7,613E-05	0,001645193
<b>LRP6</b>	ENSG00000070018	chr12	12397196	12397589	1,7364	0,0025024	0,02821497
<b>SLAIN1</b>	ENSG00000139737	chr13	78293667	78327493	1,734	0,0035397	0,034285692
<b>ASPH</b>	ENSG00000198363	chr8	62593527	62596747	1,6865	0,0042667	0,038598644
<b>SETD3</b>	ENSG00000183576	chr14	99924616	99932150	1,6841	0,0001148	0,002290111
<b>ARHGAP5</b>	ENSG00000100852	chr14	32559708	32586493	1,6804	0,0001813	0,003358681
<b>RSRC1</b>	ENSG00000174891	chr3	157839892	157841780	1,6744	0,0028783	0,0303872
<b>R3HDM1</b>	ENSG00000048991	chr2	136432902	136437894	1,6218	0,0028132	0,0303872
<b>HERC1</b>	ENSG00000103657	chr15	63988323	64008672	1,5609	0,0031096	0,031419117
<b>STK39</b>	ENSG00000198648	chr2	168920010	168986268	1,555	0,0014485	0,01910096
<b>TULP4</b>	ENSG00000130338	chr6	158703295	158735300	1,4732	0,0017933	0,021464066
<b>EXOC6B</b>	ENSG00000144036	chr2	72945232	72960247	1,4385	0,0011483	0,01595258
<b>NIPBL</b>	ENSG00000164190	chr5	36953720	36976504	1,4316	0,0053183	0,047018814

**Table 29. CircRNAs identified as exclusively expressed in a neural subtype of analyzed GBM tissues.**

Analysis performed by our collaborator – Dr. Marcin Sajek.

## 8. References

1. Sun W, Zhou H, Han X, Hou L, Xue X. Circular RNA: A novel type of biomarker for glioma (Review). *Mol Med Rep*. 2021 Jun 24;24(2):602.
2. Sun J, Li B, Shu C, Ma Q, Wang J. Functions and clinical significance of circular RNAs in glioma. *Mol Cancer*. 2020 Dec 15;19(1):34.
3. Sanger HL, Klotz G, Riesner D, Gross HJ, Kleinschmidt AK. Viroids are single-stranded covalently closed circular RNA molecules existing as highly base-paired rod-like structures. *Proc Natl Acad Sci U S A*. 1976 Nov;73(11):3852–6.
4. Hsu MT, Coca-Prados M. Electron microscopic evidence for the circular form of RNA in the cytoplasm of eukaryotic cells. *Nature*. 1979 Jul 26;280(5720):339–40.
5. Shen T, Han M, Wei G, Ni T. An intriguing RNA species--perspectives of circularized RNA. *Protein Cell*. 2015 Dec;6(12):871–80.
6. Goel A, Ward DG, Gordon NS, Abbotts B, Zeegers MP, Cheng KK, et al. Back-Splicing Transcript Isoforms (Circular RNAs) Affect Biologically Relevant Pathways and Offer an Additional Layer of Information to Stratify NMIBC Patients. *Front Oncol*. 2020;10:812.
7. Wang J, Zhu M, Pan J, Chen C, Xia S, Song Y. Circular RNAs: a rising star in respiratory diseases. *Respir Res*. 2019 Jan 5;20(1):3.
8. Guo JU, Agarwal V, Guo H, Bartel DP. Expanded identification and characterization of mammalian circular RNAs. *Genome Biol*. 2014 Jul 29;15(7):409.
9. Rybak-Wolf A, Stottmeister C, Glažar P, Jens M, Pino N, Giusti S, et al. Circular RNAs in the Mammalian Brain Are Highly Abundant, Conserved, and Dynamically Expressed. *Mol Cell*. 2015 Jun 4;58(5):870–85.
10. Rybak-Wolf A, Stottmeister C, Glažar P, Jens M, Pino N, Giusti S, et al. Circular RNAs in the Mammalian Brain Are Highly Abundant, Conserved, and Dynamically Expressed. *Mol Cell*. 2015 Jun 4;58(5):870–85.
11. Salzman J, Chen RE, Olsen MN, Wang PL, Brown PO. Cell-type specific features of circular RNA expression. *PLoS Genet*. 2013;9(9):e1003777.
12. Santer L, Bär C, Thum T. Circular RNAs: A Novel Class of Functional RNA Molecules with a Therapeutic Perspective. *Mol Ther*. 2019 Aug 7;27(8):1350–63.
13. Gao X, Ma XK, Li X, Li GW, Liu CX, Zhang J, et al. Knockout of circRNAs by base editing back-splice sites of circularized exons. *Genome Biol*. 2022 Jan 10;23(1):16.
14. Hentze MW, Preiss T. Circular RNAs: splicing's enigma variations. *EMBO J*. 2013 Apr 3;32(7):923–5.
15. Ebbesen KK, Kjems J, Hansen TB. Circular RNAs: Identification, biogenesis and function. *Biochim Biophys Acta*. 2016 Jan;1859(1):163–8.
16. Kartha R V, Subramanian S. Competing endogenous RNAs (ceRNAs): new entrants to the intricacies of gene regulation. *Front Genet*. 2014;5:8.
17. Ashwal-Fluss R, Meyer M, Pamudurti NR, Ivanov A, Bartok O, Hanan M, et al. circRNA biogenesis competes with pre-mRNA splicing. *Mol Cell*. 2014 Oct 2;56(1):55–66.

18. Patop IL, Wüst S, Kadener S. Past, present, and future of circRNAs. *EMBO J*. 2019 Aug 15;38(16):e100836.
19. Li J, Sun D, Pu W, Wang J, Peng Y. Circular RNAs in Cancer: Biogenesis, Function, and Clinical Significance. *Trends Cancer*. 2020 Apr;6(4):319–36.
20. Li J, Sun D, Pu W, Wang J, Peng Y. Circular RNAs in Cancer: Biogenesis, Function, and Clinical Significance. *Trends Cancer*. 2020 Apr;6(4):319–36.
21. Nisar S, Bhat AA, Singh M, Karedath T, Rizwan A, Hashem S, et al. Insights Into the Role of CircRNAs: Biogenesis, Characterization, Functional, and Clinical Impact in Human Malignancies. *Front Cell Dev Biol*. 2021;9:617281.
22. Watts ME, Oksanen M, Lejerkrans S, Mastropasqua F, Gorospe M, Tammimies K. Circular RNAs arising from synaptic host genes during human neuronal differentiation are modulated by SFPQ RNA-binding protein. *BMC Biol*. 2023 May 26;21(1):127.
23. Panda AC. Circular RNAs Act as miRNA Sponges. *Adv Exp Med Biol*. 2018;1087:67–79.
24. Das A, Sinha T, Shyamal S, Panda AC. Emerging Role of Circular RNA-Protein Interactions. *Noncoding RNA*. 2021 Aug 4;7(3).
25. Okholm TLH, Sathe S, Park SS, Kamstrup AB, Rasmussen AM, Shankar A, et al. Transcriptome-wide profiles of circular RNA and RNA-binding protein interactions reveal effects on circular RNA biogenesis and cancer pathway expression. *Genome Med*. 2020 Dec 7;12(1):112.
26. Zhao H, Zhou Q, Li X. Protein Bait Hypothesis: circRNA-Encoded Proteins Competitively Inhibit Cognate Functional Isoforms. *Trends Genet*. 2021 Jul;37(7):616–24.
27. Chen R, Yang T, Jin B, Xu W, Yan Y, Wood N, et al. CircTmeff1 Promotes Muscle Atrophy by Interacting with TDP-43 and Encoding A Novel TMEFF1-339aa Protein. *Adv Sci (Weinh)*. 2023 Jun;10(17):e2206732.
28. Wawrzyniak O, Zarębska Ż, Kuczyński K, Gotz-Więckowska A, Rolle K. Protein-Related Circular RNAs in Human Pathologies. *Cells*. 2020 Aug 6;9(8).
29. Meganck RM, Liu J, Hale AE, Simon KE, Fanous MM, Vincent HA, et al. Engineering highly efficient backsplicing and translation of synthetic circRNAs. *Mol Ther Nucleic Acids*. 2021 Mar 5;23:821–34.
30. Qi Y, Han W, Chen D, Zhao J, Bai L, Huang F, et al. Engineering circular RNA regulators to specifically promote circular RNA production. *Theranostics*. 2021;11(15):7322–36.
31. Chen R, Wang SK, Belk JA, Amaya L, Li Z, Cardenas A, et al. Engineering circular RNA for enhanced protein production. *Nat Biotechnol*. 2023 Feb;41(2):262–72.
32. Nicot C. circRNAs shed light on cancer diagnosis and treatment. *Mol Cancer*. 2022 Apr 29;21(1):107.
33. Rahmani-Kukia N, Abbasi A. New insights on circular RNAs and their potential applications as biomarkers, therapeutic agents, and preventive vaccines in viral infections: with a glance at SARS-CoV-2. *Mol Ther Nucleic Acids*. 2022 Sep 13;29:705–17.
34. Verduci L, Tarcitano E, Strano S, Yarden Y, Blandino G. CircRNAs: role in human diseases and potential use as biomarkers. *Cell Death Dis*. 2021 May 11;12(5):468.

35. He L, Qiu L, Chen F, Chen T, Peng F, Li Z, et al. Dysregulation of global circular RNA abundance regulated by spliceosomes predicts prognosis in hepatocellular carcinoma. *Hepatol Commun*. 2022 Dec;6(12):3578–91.
36. Huang Y, Zhang C, Xiong J, Ren H. Emerging important roles of circRNAs in human cancer and other diseases. *Genes Dis*. 2021 Jul;8(4):412–23.
37. Sun M, Yang Y. Biological functions and applications of circRNA-next generation of RNA-based therapy. *J Mol Cell Biol*. 2023 May 5;
38. He AT, Liu J, Li F, Yang BB. Targeting circular RNAs as a therapeutic approach: current strategies and challenges. *Signal Transduct Target Ther*. 2021 May 21;6(1):185.
39. Wu J, Qi X, Liu L, Hu X, Liu J, Yang J, et al. Emerging Epigenetic Regulation of Circular RNAs in Human Cancer. *Mol Ther Nucleic Acids*. 2019 Jun 7;16:589–96.
40. Zhang Z, Yang T, Xiao J. Circular RNAs: Promising Biomarkers for Human Diseases. *EBioMedicine*. 2018 Aug;34:267–74.
41. Liu J, Liu T, Wang X, He A. Circles reshaping the RNA world: from waste to treasure. *Mol Cancer*. 2017 Mar 9;16(1):58.
42. Geng X, Jia Y, Zhang Y, Shi L, Li Q, Zang A, et al. Circular RNA: biogenesis, degradation, functions and potential roles in mediating resistance to anticarcinogens. *Epigenomics*. 2020 Feb;12(3):267–83.
43. Gao X, Ma XK, Li X, Li GW, Liu CX, Zhang J, et al. Knockout of circRNAs by base editing back-splice sites of circularized exons. *Genome Biol*. 2022 Jan 10;23(1):16.
44. Li X, Yang L, Chen LL. The Biogenesis, Functions, and Challenges of Circular RNAs. *Mol Cell*. 2018 Aug 2;71(3):428–42.
45. Ding C, Zhou Y. Insights into circular RNAs: Biogenesis, function and their regulatory roles in cardiovascular disease. *J Cell Mol Med*. 2023 May;27(10):1299–314.
46. Liu J, Liu T, Wang X, He A. Circles reshaping the RNA world: from waste to treasure. *Mol Cancer*. 2017 Mar 9;16(1):58.
47. Wu J, Qi X, Liu L, Hu X, Liu J, Yang J, et al. Emerging Epigenetic Regulation of Circular RNAs in Human Cancer. *Mol Ther Nucleic Acids*. 2019 Jun 7;16:589–96.
48. Verduci L, Strano S, Yarden Y, Blandino G. The circRNA-microRNA code: emerging implications for cancer diagnosis and treatment. *Mol Oncol*. 2019 Apr;13(4):669–80.
49. Starke S, Jost I, Rossbach O, Schneider T, Schreiner S, Hung LH, et al. Exon circularization requires canonical splice signals. *Cell Rep*. 2015 Jan 6;10(1):103–11.
50. Chen LL, Yang L. Regulation of circRNA biogenesis. *RNA Biol*. 2015;12(4):381–8.
51. Zhang Z, Yang T, Xiao J. Circular RNAs: Promising Biomarkers for Human Diseases. *EBioMedicine*. 2018 Aug;34:267–74.
52. Liu J, Liu T, Wang X, He A. Circles reshaping the RNA world: from waste to treasure. *Mol Cancer*. 2017 Mar 9;16(1):58.
53. Barrett SP, Wang PL, Salzman J. Circular RNA biogenesis can proceed through an exon-containing lariat precursor. *Elife*. 2015 Jun 9;4:e07540.

54. Rahmani-Kukia N, Abbasi A. New insights on circular RNAs and their potential applications as biomarkers, therapeutic agents, and preventive vaccines in viral infections: with a glance at SARS-CoV-2. *Mol Ther Nucleic Acids*. 2022 Sep 13;29:705–17.
55. Hwang T, Kim S, Chowdhury T, Yu HJ, Kim KM, Kang H, et al. Genome-wide perturbations of Alu expression and Alu-associated post-transcriptional regulations distinguish oligodendroglioma from other gliomas. *Commun Biol*. 2022 Jan 18;5(1):62.
56. Gruhl F, Janich P, Kaessmann H, Gatfield D. Circular RNA repertoires are associated with evolutionarily young transposable elements. *Elife*. 2021 Sep 20;10.
57. Wilusz JE. Repetitive elements regulate circular RNA biogenesis. *Mob Genet Elements*. 2015;5(3):1–7.
58. Yu CY, Kuo HC. The emerging roles and functions of circular RNAs and their generation. *J Biomed Sci*. 2019 Apr 25;26(1):29.
59. Koh W, Pan W, Gawad C, Fan HC, Kerchner GA, Wyss-Coray T, et al. Noninvasive in vivo monitoring of tissue-specific global gene expression in humans. *Proc Natl Acad Sci U S A*. 2014 May 20;111(20):7361–6.
60. Zhang Z, Yang T, Xiao J. Circular RNAs: Promising Biomarkers for Human Diseases. *EBioMedicine*. 2018 Aug;34:267–74.
61. Liu J, Liu T, Wang X, He A. Circles reshaping the RNA world: from waste to treasure. *Mol Cancer*. 2017 Mar 9;16(1):58.
62. Czubak K, Sedehizadeh S, Kozłowski P, Wojciechowska M. An Overview of Circular RNAs and Their Implications in Myotonic Dystrophy. *Int J Mol Sci*. 2019 Sep 6;20(18).
63. Das A, Sinha T, Shyamal S, Panda AC. Emerging Role of Circular RNA-Protein Interactions. *Noncoding RNA*. 2021 Aug 4;7(3).
64. Conn SJ, Pillman KA, Toubia J, Conn VM, Salmanidis M, Phillips CA, et al. The RNA binding protein quaking regulates formation of circRNAs. *Cell*. 2015 Mar 12;160(6):1125–34.
65. Quan G, Li J. Circular RNAs: biogenesis, expression and their potential roles in reproduction. *J Ovarian Res*. 2018 Jan 17;11(1):9.
66. Ashwal-Fluss R, Meyer M, Pamudurti NR, Ivanov A, Bartok O, Hanan M, et al. circRNA biogenesis competes with pre-mRNA splicing. *Mol Cell*. 2014 Oct 2;56(1):55–66.
67. Conn SJ, Pillman KA, Toubia J, Conn VM, Salmanidis M, Phillips CA, et al. The RNA binding protein quaking regulates formation of circRNAs. *Cell*. 2015 Mar 12;160(6):1125–34.
68. Holdt LM, Kohlmaier A, Teupser D. Molecular roles and function of circular RNAs in eukaryotic cells. *Cell Mol Life Sci*. 2018 Mar;75(6):1071–98.
69. Errichelli L, Dini Modigliani S, Laneve P, Colantoni A, Legnini I, Caputo D, et al. FUS affects circular RNA expression in murine embryonic stem cell-derived motor neurons. *Nat Commun*. 2017 Mar 30;8:14741.
70. Li D, Yang Y, Li ZQ, Li LC, Zhu XH. Circular RNAs: from biogenesis and function to diseases. *Chin Med J (Engl)*. 2019 Oct 20;132(20):2457–64.
71. Li GW, Xie XS. Central dogma at the single-molecule level in living cells. *Nature*. 2011 Jul 20;475(7356):308–15.

72. Rodriguez MS, Dargemont C, Stutz F. Nuclear export of RNA. *Biol Cell*. 2004 Oct;96(8):639–55.
73. Köhler A, Hurt E. Exporting RNA from the nucleus to the cytoplasm. *Nat Rev Mol Cell Biol*. 2007 Oct;8(10):761–73.
74. Ron M, Ulitsky I. Context-specific effects of sequence elements on subcellular localization of linear and circular RNAs. *Nat Commun*. 2022 May 5;13(1):2481.
75. Bach DH, Lee SK, Sood AK. Circular RNAs in Cancer. *Mol Ther Nucleic Acids*. 2019 Jun 7;16:118–29.
76. Shang Q, Yang Z, Jia R, Ge S. The novel roles of circRNAs in human cancer. *Mol Cancer*. 2019 Jan 9;18(1):6.
77. Nisar S, Bhat AA, Singh M, Karedath T, Rizwan A, Hashem S, et al. Insights Into the Role of CircRNAs: Biogenesis, Characterization, Functional, and Clinical Impact in Human Malignancies. *Front Cell Dev Biol*. 2021;9:617281.
78. He AT, Liu J, Li F, Yang BB. Targeting circular RNAs as a therapeutic approach: current strategies and challenges. *Signal Transduct Target Ther*. 2021 May 21;6(1):185.
79. Zhou WY, Cai ZR, Liu J, Wang DS, Ju HQ, Xu RH. Circular RNA: metabolism, functions and interactions with proteins. *Mol Cancer*. 2020 Dec 14;19(1):172.
80. Stagsted LV, Nielsen KM, Daugaard I, Hansen TB. Noncoding AUG circRNAs constitute an abundant and conserved subclass of circles. *Life Sci Alliance*. 2019 Jun;2(3).
81. Huang A, Zheng H, Wu Z, Chen M, Huang Y. Circular RNA-protein interactions: functions, mechanisms, and identification. *Theranostics*. 2020;10(8):3503–17.
82. Li Z, Kearse MG, Huang C. The nuclear export of circular RNAs is primarily defined by their length. *RNA Biol*. 2019 Jan;16(1):1–4.
83. Li Z, Kearse MG, Huang C. The nuclear export of circular RNAs is primarily defined by their length. *RNA Biol*. 2019 Jan;16(1):1–4.
84. Zhang J, Zhang X, Li C, Yue L, Ding N, Riordan T, et al. Circular RNA profiling provides insights into their subcellular distribution and molecular characteristics in HepG2 cells. *RNA Biol*. 2019 Feb;16(2):220–32.
85. Zhao Q, Liu J, Deng H, Ma R, Liao JY, Liang H, et al. Targeting Mitochondria-Located circRNA SCAR Alleviates NASH via Reducing mROS Output. *Cell*. 2020 Oct 1;183(1):76–93.e22.
86. Zhang J, Zhang X, Li C, Yue L, Ding N, Riordan T, et al. Circular RNA profiling provides insights into their subcellular distribution and molecular characteristics in HepG2 cells. *RNA Biol*. 2019 Feb;16(2):220–32.
87. Ron M, Ulitsky I. Context-specific effects of sequence elements on subcellular localization of linear and circular RNAs. *Nat Commun*. 2022 May 5;13(1):2481.
88. Li Z, Cheng Y, Wu F, Wu L, Cao H, Wang Q, et al. The emerging landscape of circular RNAs in immunity: breakthroughs and challenges. *Biomark Res*. 2020;8:25.
89. Huang Y, Zhang C, Xiong J, Ren H. Emerging important roles of circRNAs in human cancer and other diseases. *Genes Dis*. 2021 Jul;8(4):412–23.

90. Arnaiz E, Sole C, Manterola L, Iparraguirre L, Otaegui D, Lawrie CH. CircRNAs and cancer: Biomarkers and master regulators. *Semin Cancer Biol.* 2019 Oct;58:90–9.
91. Fischer JW, Leung AKL. CircRNAs: a regulator of cellular stress. *Crit Rev Biochem Mol Biol.* 2017 Apr;52(2):220–33.
92. Tao M, Zheng M, Xu Y, Ma S, Zhang W, Ju S. CircRNAs and their regulatory roles in cancers. *Mol Med.* 2021 Aug 26;27(1):94.
93. Wang P, Zhang Y, Deng L, Qu Z, Guo P, Liu L, et al. The function and regulation network mechanism of circRNA in liver diseases. *Cancer Cell Int.* 2022 Mar 31;22(1):141.
94. Sakshi S, Jayasuriya R, Ganesan K, Xu B, Ramkumar KM. Role of circRNA-miRNA-mRNA interaction network in diabetes and its associated complications. *Mol Ther Nucleic Acids.* 2021 Dec 3;26:1291–302.
95. Piwecka M, Glažar P, Hernandez-Miranda LR, Memczak S, Wolf SA, Rybak-Wolf A, et al. Loss of a mammalian circular RNA locus causes miRNA deregulation and affects brain function. *Science.* 2017 Sep 22;357(6357).
96. Chen YM, Zheng YL, Su X, Wang XQ. Crosstalk Between MicroRNAs and Circular RNAs in Human Diseases: A Bibliographic Study. *Front Cell Dev Biol.* 2021;9:754880.
97. Mitra A, Pfeifer K, Park KS. Circular RNAs and competing endogenous RNA (ceRNA) networks. *Transl Cancer Res.* 2018 Jun;7(Suppl 5):S624–8.
98. O’Brien J, Hayder H, Zayed Y, Peng C. Overview of MicroRNA Biogenesis, Mechanisms of Actions, and Circulation. *Front Endocrinol (Lausanne).* 2018;9:402.
99. Verduci L, Strano S, Yarden Y, Blandino G. The circRNA-microRNA code: emerging implications for cancer diagnosis and treatment. *Mol Oncol.* 2019 Apr;13(4):669–80.
100. Piwecka M, Glažar P, Hernandez-Miranda LR, Memczak S, Wolf SA, Rybak-Wolf A, et al. Loss of a mammalian circular RNA locus causes miRNA deregulation and affects brain function. *Science.* 2017 Sep 22;357(6357).
101. Yu CY, Kuo HC. The emerging roles and functions of circular RNAs and their generation. *J Biomed Sci.* 2019 Apr 25;26(1):29.
102. Condrat CE, Thompson DC, Barbu MG, Bugnar OL, Boboc A, Cretoiu D, et al. miRNAs as Biomarkers in Disease: Latest Findings Regarding Their Role in Diagnosis and Prognosis. *Cells.* 2020 Jan 23;9(2).
103. Chen X, Zhou M, Yant L, Huang C. Circular RNA in disease: Basic properties and biomedical relevance. *Wiley Interdiscip Rev RNA.* 2022 Nov;13(6):e1723.
104. Kouhsar M, Kashaninia E, Mardani B, Rabiee HR. CircWalk: a novel approach to predict CircRNA-disease association based on heterogeneous network representation learning. *BMC Bioinformatics.* 2022 Aug 11;23(1):331.
105. Jiang MP, Xu WX, Hou JC, Xu Q, Wang DD, Tang JH. The Emerging Role of the Interactions between Circular RNAs and RNA-binding Proteins in Common Human Cancers. *J Cancer.* 2021;12(17):5206–19.
106. Du WW, Zhang C, Yang W, Yong T, Awan FM, Yang BB. Identifying and Characterizing circRNA-Protein Interaction. *Theranostics.* 2017;7(17):4183–91.

107. Zang J, Lu D, Xu A. The interaction of circRNAs and RNA binding proteins: An important part of circRNA maintenance and function. *J Neurosci Res.* 2020 Jan;98(1):87–97.
108. Yang Y, Hou Z, Ma Z, Li X, Wong KC. iCircRBP-DHN: identification of circRNA-RBP interaction sites using deep hierarchical network. *Brief Bioinform.* 2021 Jul 20;22(4).
109. Zhang K, Pan X, Yang Y, Shen HB. CRIP: predicting circRNA-RBP-binding sites using a codon-based encoding and hybrid deep neural networks. *RNA.* 2019 Dec;25(12):1604–15.
110. Dudekula DB, Panda AC, Grammatikakis I, De S, Abdelmohsen K, Gorospe M. CircInteractome: A web tool for exploring circular RNAs and their interacting proteins and microRNAs. *RNA Biol.* 2016;13(1):34–42.
111. Zhao H, Zhu M, Limbo O, Russell P. RNase H eliminates R-loops that disrupt DNA replication but is nonessential for efficient DSB repair. *EMBO Rep.* 2018 May;19(5).
112. Schaeffer D, Tsanova B, Barbas A, Reis FP, Dastidar EG, Sanchez-Rotunno M, et al. The exosome contains domains with specific endoribonuclease, exoribonuclease and cytoplasmic mRNA decay activities. *Nat Struct Mol Biol.* 2009 Jan;16(1):56–62.
113. Huang A, Zheng H, Wu Z, Chen M, Huang Y. Circular RNA-protein interactions: functions, mechanisms, and identification. *Theranostics.* 2020;10(8):3503–17.
114. Jia R, Xiao MS, Li Z, Shan G, Huang C. Defining an evolutionarily conserved role of GW182 in circular RNA degradation. *Cell Discov.* 2019;5:45.
115. Yang Q, Du WW, Wu N, Yang W, Awan FM, Fang L, et al. A circular RNA promotes tumorigenesis by inducing c-myc nuclear translocation. *Cell Death Differ.* 2017 Sep;24(9):1609–20.
116. Pamudurti NR, Patop IL, Krishnamoorthy A, Bartok O, Maya R, Lerner N, et al. circMbl functions in cis and in trans to regulate gene expression and physiology in a tissue-specific fashion. *Cell Rep.* 2022 Apr 26;39(4):110740.
117. Bose R, Ain R. Regulation of Transcription by Circular RNAs. *Adv Exp Med Biol.* 2018;1087:81–94.
118. Yang L, Fu J, Zhou Y. Circular RNAs and Their Emerging Roles in Immune Regulation. *Front Immunol.* 2018;9:2977.
119. Ashwal-Fluss R, Meyer M, Pamudurti NR, Ivanov A, Bartok O, Hanan M, et al. circRNA biogenesis competes with pre-mRNA splicing. *Mol Cell.* 2014 Oct 2;56(1):55–66.
120. Pamudurti NR, Patop IL, Krishnamoorthy A, Bartok O, Maya R, Lerner N, et al. circMbl functions in cis and in trans to regulate gene expression and physiology in a tissue-specific fashion. *Cell Rep.* 2022 Apr 26;39(4):110740.
121. Wei J, Li M, Xue C, Chen S, Zheng L, Deng H, et al. Understanding the roles and regulation patterns of circRNA on its host gene in tumorigenesis and tumor progression. *J Exp Clin Cancer Res.* 2023 Apr 15;42(1):86.
122. Li Z, Huang C, Bao C, Chen L, Lin M, Wang X, et al. Exon-intron circular RNAs regulate transcription in the nucleus. *Nat Struct Mol Biol.* 2015 Mar;22(3):256–64.
123. Wang H, Gao X, Yu S, Wang W, Liu G, Jiang X, et al. Circular RNAs regulate parental gene expression: A new direction for molecular oncology research. *Front Oncol.* 2022;12:947775.

124. Shao T, Pan YH, Xiong XD. Circular RNA: an important player with multiple facets to regulate its parental gene expression. *Mol Ther Nucleic Acids*. 2021 Mar 5;23:369–76.
125. Feng Y, Yang Y, Zhao X, Fan Y, Zhou L, Rong J, et al. Circular RNA circ0005276 promotes the proliferation and migration of prostate cancer cells by interacting with FUS to transcriptionally activate XIAP. *Cell Death Dis*. 2019 Oct 17;10(11):792.
126. Yang F, Hu A, Li D, Wang J, Guo Y, Liu Y, et al. Circ-HuR suppresses HuR expression and gastric cancer progression by inhibiting CNBP transactivation. *Mol Cancer*. 2019 Nov 13;18(1):158.
127. Shao T, Pan YH, Xiong XD. Circular RNA: an important player with multiple facets to regulate its parental gene expression. *Mol Ther Nucleic Acids*. 2021 Mar 5;23:369–76.
128. Du WW, Fang L, Yang W, Wu N, Awan FM, Yang Z, et al. Induction of tumor apoptosis through a circular RNA enhancing Foxo3 activity. *Cell Death Differ*. 2017 Feb;24(2):357–70.
129. Crossley MP, Bocek M, Cimprich KA. R-Loops as Cellular Regulators and Genomic Threats. *Mol Cell*. 2019 Feb 7;73(3):398–411.
130. Bhatia V, Herrera-Moyano E, Aguilera A, Gómez-González B. The Role of Replication-Associated Repair Factors on R-Loops. *Genes (Basel)*. 2017 Jun 27;8(7).
131. Uruci S, Lo CSY, Wheeler D, Taneja N. R-Loops and Its Chro-Mates: The Strange Case of Dr. Jekyll and Mr. Hyde. *Int J Mol Sci*. 2021 Aug 17;22(16).
132. Xu X, Zhang J, Tian Y, Gao Y, Dong X, Chen W, et al. CircRNA inhibits DNA damage repair by interacting with host gene. *Mol Cancer*. 2020 Aug 24;19(1):128.
133. Chen CK, Cheng R, Demeter J, Chen J, Weingarten-Gabbay S, Jiang L, et al. Structured elements drive extensive circular RNA translation. *Mol Cell*. 2021 Oct 21;81(20):4300-4318.e13.
134. Yang Y, Wang Z. IRES-mediated cap-independent translation, a path leading to hidden proteome. *J Mol Cell Biol*. 2019 Oct 25;11(10):911–9.
135. Kaiser C, Dobrikova EY, Bradrick SS, Shveygert M, Herbert JT, Gromeier M. Activation of cap-independent translation by variant eukaryotic initiation factor 4G in vivo. *RNA*. 2008 Oct;14(10):2170–82.
136. Godet AC, David F, Hantelys F, Tatin F, Lacazette E, Garmy-Susini B, et al. IRES Trans-Acting Factors, Key Actors of the Stress Response. *Int J Mol Sci*. 2019 Feb 20;20(4).
137. Chen CK, Cheng R, Demeter J, Chen J, Weingarten-Gabbay S, Jiang L, et al. Structured elements drive extensive circular RNA translation. *Mol Cell*. 2021 Oct 21;81(20):4300-4318.e13.
138. Huang X, Guo H, Wang L, Yang L, Shao Z, Zhang W. Recent advances in crosstalk between N6-methyladenosine (m6A) modification and circular RNAs in cancer. *Mol Ther Nucleic Acids*. 2022 Mar 8;27:947–55.
139. Yang Y, Fan X, Mao M, Song X, Wu P, Zhang Y, et al. Extensive translation of circular RNAs driven by N6-methyladenosine. *Cell Res*. 2017 May;27(5):626–41.
140. Meng E, Deng J, Jiang R, Wu H. CircRNA-Encoded Peptides or Proteins as New Players in Digestive System Neoplasms. *Front Oncol*. 2022;12:944159.

141. Fan X, Yang Y, Chen C, Wang Z. Pervasive translation of circular RNAs driven by short IRES-like elements. *Nat Commun.* 2022 Jun 29;13(1):3751.
142. Wang J, Zhu S, Meng N, He Y, Lu R, Yan GR. ncRNA-Encoded Peptides or Proteins and Cancer. *Mol Ther.* 2019 Oct 2;27(10):1718–25.
143. Zhang M, Zhao K, Xu X, Yang Y, Yan S, Wei P, et al. A peptide encoded by circular form of LINC-PINT suppresses oncogenic transcriptional elongation in glioblastoma. *Nat Commun.* 2018 Oct 26;9(1):4475.
144. Wang J, Zhu S, Meng N, He Y, Lu R, Yan GR. ncRNA-Encoded Peptides or Proteins and Cancer. *Mol Ther.* 2019 Oct 2;27(10):1718–25.
145. Wu P, Mo Y, Peng M, Tang T, Zhong Y, Deng X, et al. Emerging role of tumor-related functional peptides encoded by lncRNA and circRNA. *Mol Cancer.* 2020 Feb 4;19(1):22.
146. Memczak S, Jens M, Elefsinioti A, Torti F, Krueger J, Rybak A, et al. Circular RNAs are a large class of animal RNAs with regulatory potency. *Nature.* 2013 Mar 21;495(7441):333–8.
147. Chen JB, Dong SS, Yao S, Duan YY, Hu WX, Chen H, et al. Modeling circRNA expression pattern with integrated sequence and epigenetic features demonstrates the potential involvement of H3K79me2 in circRNA expression. *Bioinformatics.* 2020 Sep 15;36(18):4739–48.
148. Rybak-Wolf A, Stottmeister C, Glažar P, Jens M, Pino N, Giusti S, et al. Circular RNAs in the Mammalian Brain Are Highly Abundant, Conserved, and Dynamically Expressed. *Mol Cell.* 2015 Jun 4;58(5):870–85.
149. Salzman J, Chen RE, Olsen MN, Wang PL, Brown PO. Cell-type specific features of circular RNA expression. *PLoS Genet.* 2013;9(9):e1003777.
150. Xia S, Feng J, Lei L, Hu J, Xia L, Wang J, et al. Comprehensive characterization of tissue-specific circular RNAs in the human and mouse genomes. *Brief Bioinform.* 2017 Nov 1;18(6):984–92.
151. Venø MT, Hansen TB, Venø ST, Clausen BH, Grebing M, Finsen B, et al. Spatio-temporal regulation of circular RNA expression during porcine embryonic brain development. *Genome Biol.* 2015 Nov 5;16:245.
152. You X, Vlatkovic I, Babic A, Will T, Epstein I, Tushev G, et al. Neural circular RNAs are derived from synaptic genes and regulated by development and plasticity. *Nat Neurosci.* 2015 Apr;18(4):603–10.
153. Westholm JO, Miura P, Olson S, Shenker S, Joseph B, Sanfilippo P, et al. Genome-wide analysis of drosophila circular RNAs reveals their structural and sequence properties and age-dependent neural accumulation. *Cell Rep.* 2014 Dec 11;9(5):1966–80.
154. Guo JU, Agarwal V, Guo H, Bartel DP. Expanded identification and characterization of mammalian circular RNAs. *Genome Biol.* 2014 Jul 29;15(7):409.
155. Cortés-López M, Gruner MR, Cooper DA, Gruner HN, Voda AI, van der Linden AM, et al. Global accumulation of circRNAs during aging in *Caenorhabditis elegans*. *BMC Genomics.* 2018 Jan 3;19(1):8.
156. Wu W, Zhang J, Cao X, Cai Z, Zhao F. Exploring the cellular landscape of circular RNAs using full-length single-cell RNA sequencing. *Nat Commun.* 2022 Jun 10;13(1):3242.

157. Curry-Hyde A, Gray LG, Chen BJ, Ueberham U, Arendt T, Janitz M. Cell type-specific circular RNA expression in human glial cells. *Genomics*. 2020 Nov;112(6):5265–74.
158. Qin T, Li J, Zhang KQ. Structure, Regulation, and Function of Linear and Circular Long Non-Coding RNAs. *Front Genet*. 2020;11:150.
159. Enuka Y, Lauriola M, Feldman ME, Sas-Chen A, Ulitsky I, Yarden Y. Circular RNAs are long-lived and display only minimal early alterations in response to a growth factor. *Nucleic Acids Res*. 2016 Feb 18;44(3):1370–83.
160. Jeck WR, Sorrentino JA, Wang K, Slevin MK, Burd CE, Liu J, et al. Circular RNAs are abundant, conserved, and associated with ALU repeats. *RNA*. 2013 Feb;19(2):141–57.
161. Jiang C, Zeng X, Shan R, Wen W, Li J, Tan J, et al. The Emerging Picture of the Roles of CircRNA-CDR1as in Cancer. *Front Cell Dev Biol*. 2020;8:590478.
162. Ren L, Jiang Q, Mo L, Tan L, Dong Q, Meng L, et al. Mechanisms of circular RNA degradation. *Commun Biol*. 2022 Dec 9;5(1):1355.
163. Wang M, Yu F, Li P, Wang K. Emerging Function and Clinical Significance of Exosomal circRNAs in Cancer. *Mol Ther Nucleic Acids*. 2020 Sep 4;21:367–83.
164. Wang Y, Liu J, Ma J, Sun T, Zhou Q, Wang W, et al. Exosomal circRNAs: biogenesis, effect and application in human diseases. *Mol Cancer*. 2019 Jul 5;18(1):116.
165. Ye D, Gong M, Deng Y, Fang S, Cao Y, Xiang Y, et al. Roles and clinical application of exosomal circRNAs in the diagnosis and treatment of malignant tumors. *J Transl Med*. 2022 Apr 5;20(1):161.
166. Hon KW, Ab-Mutalib NS, Abdullah NMA, Jamal R, Abu N. Extracellular Vesicle-derived circular RNAs confers chemoresistance in Colorectal cancer. *Sci Rep*. 2019 Nov 11;9(1):16497.
167. Stella M, Falzone L, Caponnetto A, Gattuso G, Barbagallo C, Battaglia R, et al. Serum Extracellular Vesicle-Derived circHIPK3 and circSMARCA5 Are Two Novel Diagnostic Biomarkers for Glioblastoma Multiforme. *Pharmaceuticals (Basel)*. 2021 Jun 27;14(7).
168. Li X, Zhang JL, Lei YN, Liu XQ, Xue W, Zhang Y, et al. Linking circular intronic RNA degradation and function in transcription by RNase H1. *Sci China Life Sci*. 2021 Nov;64(11):1795–809.
169. Zheng ZM. Circular RNAs and RNase L in PKR activation and virus infection. *Cell Biosci*. 2019;9:43.
170. Hansen TB, Wiklund ED, Bramsen JB, Villadsen SB, Statham AL, Clark SJ, et al. miRNA-dependent gene silencing involving Ago2-mediated cleavage of a circular antisense RNA. *EMBO J*. 2011 Sep 30;30(21):4414–22.
171. Pan Z, Li GF, Sun ML, Xie L, Liu D, Zhang Q, et al. MicroRNA-1224 Splicing CircularRNA-Filip11 in an Ago2-Dependent Manner Regulates Chronic Inflammatory Pain via Targeting Ubr5. *J Neurosci*. 2019 Mar 13;39(11):2125–43.
172. Zhang L, Hou C, Chen C, Guo Y, Yuan W, Yin D, et al. The role of N6-methyladenosine (m6A) modification in the regulation of circRNAs. *Mol Cancer*. 2020 Jun 10;19(1):105.
173. Park OH, Ha H, Lee Y, Boo SH, Kwon DH, Song HK, et al. Endoribonucleolytic Cleavage of m6A-Containing RNAs by RNase P/MRP Complex. *Mol Cell*. 2019 May 2;74(3):494–507.e8.

174. Guo Y, Guo Y, Chen C, Fan D, Wu X, Zhao L, et al. Circ3823 contributes to growth, metastasis and angiogenesis of colorectal cancer: involvement of miR-30c-5p/TCF7 axis. *Mol Cancer*. 2021 Jun 25;20(1):93.
175. Fischer JW, Busa VF, Shao Y, Leung AKL. Structure-Mediated RNA Decay by UPF1 and G3BP1. *Mol Cell*. 2020 Apr 2;78(1):70-84.e6.
176. Guo Y, Zhu X, Zeng M, Qi L, Tang X, Wang D, et al. A diet high in sugar and fat influences neurotransmitter metabolism and then affects brain function by altering the gut microbiota. *Transl Psychiatry*. 2021 May 27;11(1):328.
177. Lasda E, Parker R. Circular RNAs Co-Precipitate with Extracellular Vesicles: A Possible Mechanism for circRNA Clearance. *PLoS One*. 2016;11(2):e0148407.
178. Chen L, Shan G. CircRNA in cancer: Fundamental mechanism and clinical potential. *Cancer Lett*. 2021 May 1;505:49–57.
179. Sharma AR, Bhattacharya M, Bhakta S, Saha A, Lee SS, Chakraborty C. Recent research progress on circular RNAs: Biogenesis, properties, functions, and therapeutic potential. *Mol Ther Nucleic Acids*. 2021 Sep 3;25:355–71.
180. Zhang Y, Jia DD, Zhang YF, Cheng MD, Zhu WX, Li PF, et al. The emerging function and clinical significance of circRNAs in Thyroid Cancer and Autoimmune Thyroid Diseases. *Int J Biol Sci*. 2021;17(7):1731–41.
181. Haque S, Harries LW. Circular RNAs (circRNAs) in Health and Disease. *Genes (Basel)*. 2017 Nov 28;8(12).
182. Verduci L, Tarcitano E, Strano S, Yarden Y, Blandino G. CircRNAs: role in human diseases and potential use as biomarkers. *Cell Death Dis*. 2021 May 11;12(5):468.
183. Cheng F, Zheng B, Si S, Wang J, Zhao G, Yao Z, et al. The Roles of CircRNAs in Bladder Cancer: Biomarkers, Tumorigenesis Drivers, and Therapeutic Targets. *Front Cell Dev Biol*. 2021;9:666863.
184. Fontemaggi G, Turco C, Esposito G, Di Agostino S. New Molecular Mechanisms and Clinical Impact of circRNAs in Human Cancer. *Cancers (Basel)*. 2021 Jun 24;13(13).
185. Liu J, Zhang X, Yan M, Li H. Emerging Role of Circular RNAs in Cancer. *Front Oncol*. 2020;10:663.
186. Zhang MX, Wang JL, Mo CQ, Mao XP, Feng ZH, Li JY, et al. CircME1 promotes aerobic glycolysis and sunitinib resistance of clear cell renal cell carcinoma through cis-regulation of ME1. *Oncogene*. 2022 Aug;41(33):3979–90.
187. Lu H, Han X, Ren J, Ren K, Li Z, Sun Z. Circular RNA HIPK3 induces cell proliferation and inhibits apoptosis in non-small cell lung cancer through sponging miR-149. *Cancer Biol Ther*. 2020;21(2):113–21.
188. Yang Y, Wang D, Tao K, Wang G. Circular RNA circLRCH3 Inhibits Proliferation, Migration, and Invasion of Colorectal Cancer Cells Through miRNA-223/LPP Axis. *Onco Targets Ther*. 2022;15:541–54.
189. Mo Y, Wang Y, Zhang S, Xiong F, Yan Q, Jiang X, et al. Circular RNA circRNF13 inhibits proliferation and metastasis of nasopharyngeal carcinoma via SUMO2. *Mol Cancer*. 2021 Aug 31;20(1):112.

190. Zhong Z, Lv M, Chen J. Screening differential circular RNA expression profiles reveals the regulatory role of circTCF25-miR-103a-3p/miR-107-CDK6 pathway in bladder carcinoma. *Sci Rep.* 2016 Aug 3;6:30919.
191. Zhang Z, Zhao H, Zhou G, Han R, Sun Z, Zhong M, et al. Circ\_0002623 promotes bladder cancer progression by regulating the miR-1276/SMAD2 axis. *Cancer Sci.* 2022 Apr;113(4):1250–63.
192. Ma X, Ying Y, Sun J, Xie H, Li J, He L, et al. circKDM4C enhances bladder cancer invasion and metastasis through miR-200bc-3p/ZEB1 axis. *Cell Death Discov.* 2021 Nov 23;7(1):365.
193. Wu S, Xu H, Zhang R, Wang X, Yang J, Li X, et al. Circular RNA circLAMA3 inhibits the proliferation of bladder cancer by directly binding an mRNA. *Mol Ther Oncolytics.* 2022 Mar 17;24:742–54.
194. Liang HF, Zhang XZ, Liu BG, Jia GT, Li WL. Circular RNA circ-ABCB10 promotes breast cancer proliferation and progression through sponging miR-1271. *Am J Cancer Res.* 2017;7(7):1566–76.
195. Chen B, Wei W, Huang X, Xie X, Kong Y, Dai D, et al. circEPSTI1 as a Prognostic Marker and Mediator of Triple-Negative Breast Cancer Progression. *Theranostics.* 2018;8(14):4003–15.
196. Li X, Ma N, Zhang Y, Wei H, Zhang H, Pang X, et al. Circular RNA circNRIP1 promotes migration and invasion in cervical cancer by sponging miR-629-3p and regulating the PTP4A1/ERK1/2 pathway. *Cell Death Dis.* 2020 May 26;11(5):399.
197. Wang W, Luo H, Chang J, Yang X, Zhang X, Zhang Q, et al. Circular RNA circ0001955 promotes cervical cancer tumorigenesis and metastasis via the miR-188-3p/NCAPG2 axis. *J Transl Med.* 2023 May 29;21(1):356.
198. Zhang C, Liu P, Huang J, Liao Y, Pan C, Liu J, et al. Circular RNA hsa\_circ\_0043280 inhibits cervical cancer tumor growth and metastasis via miR-203a-3p/PAQR3 axis. *Cell Death Dis.* 2021 Sep 29;12(10):888.
199. Wang R, Wang J, Chen Y, Chen Y, Xi Q, Sun L, et al. Circular RNA circLDLR facilitates cancer progression by altering the miR-30a-3p/SOAT1 axis in colorectal cancer. *Cell Death Discov.* 2022 Jul 11;8(1):314.
200. Pan F, Zhang D, Li N, Liu M. Circular RNA circFAT1(e2) Promotes Colorectal Cancer Tumorigenesis via the miR-30e-5p/ITGA6 Axis. *Comput Math Methods Med.* 2021;2021:9980459.
201. Huang G, Zhu H, Shi Y, Wu W, Cai H, Chen X. cir-ITCH plays an inhibitory role in colorectal cancer by regulating the Wnt/ $\beta$ -catenin pathway. *PLoS One.* 2015;10(6):e0131225.
202. Huang G, Liang M, Liu H, Huang J, Li P, Wang C, et al. CircRNA hsa\_circRNA\_104348 promotes hepatocellular carcinoma progression through modulating miR-187-3p/RTKN2 axis and activating Wnt/ $\beta$ -catenin pathway. *Cell Death Dis.* 2020 Dec 14;11(12):1065.
203. Gao P, Yang Y, Li X, Zhao Q, Liu Y, Dong C, et al. Circular RNA hsa\_circ\_0098181 inhibits metastasis in hepatocellular carcinoma by activating the Hippo signaling pathway via interaction with eEF2. *Ann Hepatol.* 2023;28(5):101124.
204. He T, Tao W, Zhang LL, Wang BY, Li K, Lu HM, et al. CircSCAF8 promotes growth and metastasis of prostate cancer through the circSCAF8-miR-140-3p/miR-335-LIF pathway. *Cell Death Dis.* 2022 Jun 2;13(6):517.

205. Li H, Zhi Y, Ma C, Shen Q, Sun F, Cai C. Circ\_0062020 Knockdown Strengthens the Radiosensitivity of Prostate Cancer Cells. *Cancer Manag Res.* 2020;12:11701–12.
206. Zhang Y, Liu F, Feng Y, Xu X, Wang Y, Zhu S, et al. CircRNA circ\_0006156 inhibits the metastasis of prostate cancer by blocking the ubiquitination of S100A9. *Cancer Gene Ther.* 2022 Nov;29(11):1731–41.
207. Wu X, Zhou J, Zhao L, Yang Z, Yang C, Chen Y, et al. CircCYP24A1 hampered malignant phenotype of renal cancer carcinoma through modulating CMTM-4 expression via sponging miR-421. *Cell Death Dis.* 2022 Feb 26;13(2):190.
208. Pan X, Huang B, Ma Q, Ren J, Liu Y, Wang C, et al. Circular RNA circ-TNPO3 inhibits clear cell renal cell carcinoma metastasis by binding to IGF2BP2 and destabilizing SERPINH1 mRNA. *Clin Transl Med.* 2022 Jul;12(7):e994.
209. Song X, Zhang N, Han P, Moon BS, Lai RK, Wang K, et al. Circular RNA profile in gliomas revealed by identification tool UROBORUS. *Nucleic Acids Res.* 2016 May 19;44(9):e87.
210. Wang R, Zhang S, Chen X, Li N, Li J, Jia R, et al. EIF4A3-induced circular RNA MMP9 (circMMP9) acts as a sponge of miR-124 and promotes glioblastoma multiforme cell tumorigenesis. *Mol Cancer.* 2018 Nov 23;17(1):166.
211. Hardee ME, Zagzag D. Mechanisms of glioma-associated neovascularization. *Am J Pathol.* 2012 Oct;181(4):1126–41.
212. Long N, Xu X, Lin H, Lv Y, Zou S, Cao H, et al. Circular RNA circPOSTN promotes neovascularization by regulating miR-219a-2-3p/STC1 axis and stimulating the secretion of VEGFA in glioblastoma. *Cell Death Discov.* 2022 Aug 4;8(1):349.
213. Feng J, Ren X, Fu H, Li D, Chen X, Zu X, et al. LRRC4 mediates the formation of circular RNA CD44 to inhibit GBM cell proliferation. *Mol Ther Nucleic Acids.* 2021 Dec 3;26:473–87.
214. Liu Y, Li Z, Zhang M, Zhou H, Wu X, Zhong J, et al. Rolling-translated EGFR variants sustain EGFR signaling and promote glioblastoma tumorigenicity. *Neuro Oncol.* 2021 May 5;23(5):743–56.
215. Guo G, Gong K, Beckley N, Zhang Y, Yang X, Chkheidze R, et al. EGFR ligand shifts the role of EGFR from oncogene to tumour suppressor in EGFR-amplified glioblastoma by suppressing invasion through BIN3 upregulation. *Nat Cell Biol.* 2022 Aug;24(8):1291–305.
216. Gao X, Xia X, Li F, Zhang M, Zhou H, Wu X, et al. Circular RNA-encoded oncogenic E-cadherin variant promotes glioblastoma tumorigenicity through activation of EGFR-STAT3 signalling. *Nat Cell Biol.* 2021 Mar;23(3):278–91.
217. Xia X, Li X, Li F, Wu X, Zhang M, Zhou H, et al. A novel tumor suppressor protein encoded by circular AKT3 RNA inhibits glioblastoma tumorigenicity by competing with active phosphoinositide-dependent Kinase-1. *Mol Cancer.* 2019 Aug 30;18(1):131.
218. Yang Y, Gao X, Zhang M, Yan S, Sun C, Xiao F, et al. Novel Role of FBXW7 Circular RNA in Repressing Glioma Tumorigenesis. *J Natl Cancer Inst.* 2018 Mar 1;110(3):304–15.
219. Li X, Gao X, Zhang N. Perspective on novel proteins encoded by circular RNAs in glioblastoma. *Cancer Biol Med.* 2022 Feb 14;19(3):278–83.
220. McCormack V, Aggarwal A. Early cancer diagnosis: reaching targets across whole populations amidst setbacks. *Br J Cancer.* 2021 Mar;124(7):1181–2.

221. Zhou Q, Ju LL, Ji X, Cao YL, Shao JG, Chen L. Plasma circRNAs as Biomarkers in Cancer. *Cancer Manag Res.* 2021;13:7325–37.
222. Meng S, Zhou H, Feng Z, Xu Z, Tang Y, Li P, et al. CircRNA: functions and properties of a novel potential biomarker for cancer. *Mol Cancer.* 2017 May 23;16(1):94.
223. Ding X, Yang L, Geng X, Zou Y, Wang Z, Li Y, et al. CircRNAs as potential biomarkers for the clinicopathology and prognosis of glioma patients: a meta-analysis. *BMC Cancer.* 2020 Oct 15;20(1):1005.
224. Pan Z, Zhao R, Li B, Qi Y, Qiu W, Guo Q, et al. EWSR1-induced circNEIL3 promotes glioma progression and exosome-mediated macrophage immunosuppressive polarization via stabilizing IGF2BP3. *Mol Cancer.* 2022 Jan 14;21(1):16.
225. Xia D, Gu X. Plasmatic exosome-derived circRNAs panel act as fingerprint for glioblastoma. *Aging.* 2021 Aug 12;13(15):19575–86.
226. Lai H, Li Y, Zhang H, Hu J, Liao J, Su Y, et al. exoRBase 2.0: an atlas of mRNA, lncRNA and circRNA in extracellular vesicles from human biofluids. *Nucleic Acids Res.* 2022 Jan 7;50(D1):D118–28.
227. Zhao S, Li S, Liu W, Wang Y, Li X, Zhu S, et al. Circular RNA Signature in Lung Adenocarcinoma: A MiOncoCirc Database-Based Study and Literature Review. *Front Oncol.* 2020;10:523342.
228. Li F, Yang Q, He AT, Yang BB. Circular RNAs in cancer: Limitations in functional studies and diagnostic potential. *Semin Cancer Biol.* 2021 Oct;75:49–61.
229. Holdt LM, Kohlmaier A, Teupser D. Circular RNAs as Therapeutic Agents and Targets. *Front Physiol.* 2018;9:1262.
230. Li X, Liu CX, Xue W, Zhang Y, Jiang S, Yin QF, et al. Coordinated circRNA Biogenesis and Function with NF90/NF110 in Viral Infection. *Mol Cell.* 2017 Jul 20;67(2):214–227.e7.
231. Wang Z, Ma K, Pitts S, Cheng Y, Liu X, Ke X, et al. Novel circular RNA circNF1 acts as a molecular sponge, promoting gastric cancer by absorbing miR-16. *Endocr Relat Cancer.* 2019 Mar;26(3):265–77.
232. Min X, Liu DL, Xiong XD. Circular RNAs as Competing Endogenous RNAs in Cardiovascular and Cerebrovascular Diseases: Molecular Mechanisms and Clinical Implications. *Front Cardiovasc Med.* 2021;8:682357.
233. Liang D, Wilusz JE. Short intronic repeat sequences facilitate circular RNA production. *Genes Dev.* 2014 Oct 15;28(20):2233–47.
234. Meganck RM, Borchardt EK, Castellanos Rivera RM, Scalabrino ML, Wilusz JE, Marzluff WF, et al. Tissue-Dependent Expression and Translation of Circular RNAs with Recombinant AAV Vectors In Vivo. *Mol Ther Nucleic Acids.* 2018 Dec 7;13:89–98.
235. Lavenniah A, Luu TDA, Li YP, Lim TB, Jiang J, Ackers-Johnson M, et al. Engineered Circular RNA Sponges Act as miRNA Inhibitors to Attenuate Pressure Overload-Induced Cardiac Hypertrophy. *Mol Ther.* 2020 Jun 3;28(6):1506–17.
236. Zhang XO, Wang HB, Zhang Y, Lu X, Chen LL, Yang L. Complementary sequence-mediated exon circularization. *Cell.* 2014 Sep 25;159(1):134–47.

237. Ivanov A, Memczak S, Wyler E, Torti F, Porath HT, Orejuela MR, et al. Analysis of intron sequences reveals hallmarks of circular RNA biogenesis in animals. *Cell Rep.* 2015 Jan 13;10(2):170–7.
238. Løvendorf MB, Holm A, Petri A, Thue CA, Uchida S, Venø MT, et al. Knockdown of Circular RNAs Using LNA-Modified Antisense Oligonucleotides. *Nucleic Acid Ther.* 2023 Jan;33(1):45–57.
239. Pamudurti NR, Patop IL, Krishnamoorthy A, Ashwal-Fluss R, Bartok O, Kadener S. An in vivo strategy for knockdown of circular RNAs. *Cell Discov.* 2020;6:52.
240. Zhang Y, Nguyen TM, Zhang XO, Wang L, Phan T, Clohessy JG, et al. Optimized RNA-targeting CRISPR/Cas13d technology outperforms shRNA in identifying functional circRNAs. *Genome Biol.* 2021 Jan 21;22(1):41.
241. Guarnerio J, Bezzi M, Jeong JC, Paffenholz S V, Berry K, Naldini MM, et al. Oncogenic Role of Fusion-circRNAs Derived from Cancer-Associated Chromosomal Translocations. *Cell.* 2016 Apr 7;165(2):289–302.
242. Scharner J, Ma WK, Zhang Q, Lin KT, Rigo F, Bennett CF, et al. Hybridization-mediated off-target effects of splice-switching antisense oligonucleotides. *Nucleic Acids Res.* 2020 Jan 24;48(2):802–16.
243. Yasuhara H, Yoshida T, Sasaki K, Obika S, Inoue T. Reduction of Off-Target Effects of Gapmer Antisense Oligonucleotides by Oligonucleotide Extension. *Mol Diagn Ther.* 2022 Jan;26(1):117–27.
244. Liu X, Zhang Y, Zhou S, Dain L, Mei L, Zhu G. Circular RNA: An emerging frontier in RNA therapeutic targets, RNA therapeutics, and mRNA vaccines. *J Control Release.* 2022 Aug;348:84–94.
245. Traber GM, Yu AM. RNAi-Based Therapeutics and Novel RNA Bioengineering Technologies. *J Pharmacol Exp Ther.* 2023 Jan;384(1):133–54.
246. Song Z, Jia R, Tang M, Xia F, Xu H, Li Z, et al. Antisense oligonucleotide technology can be used to investigate a circular but not linear RNA-mediated function for its encoded gene locus. *Sci China Life Sci.* 2021 May;64(5):784–94.
247. Apostolidi M, Stamatopoulou V. Aberrant splicing in human cancer: An RNA structural code point of view. *Front Pharmacol.* 2023;14:1137154.
248. Ren S, Huang M, Bai R, Chen L, Yang J, Zhang J, et al. Efficient Modulation of Exon Skipping via Antisense Circular RNAs. *Research (Wash D C).* 2023;6:0045.
249. Migault M, Donnou-Fournet E, Galibert MD, Gilot D. Definition and identification of small RNA sponges: Focus on miRNA sequestration. *Methods.* 2017 Mar 15;117:35–47.
250. Gong L, Zhou X, Sun J. Circular RNAs Interaction with MiRNAs: Emerging Roles in Breast Cancer. *Int J Med Sci.* 2021;18(14):3182–96.
251. Breuer J, Rossbach O. Production and Purification of Artificial Circular RNA Sponges for Application in Molecular Biology and Medicine. *Methods Protoc.* 2020 May 26;3(2).
252. Kameda S, Ohno H, Saito H. Synthetic circular RNA switches and circuits that control protein expression in mammalian cells. *Nucleic Acids Res.* 2023 Feb 28;51(4):e24.

253. Zhan W, Yan T, Gao J, Song M, Wang T, Lin F, et al. [Role of circular RNAs in immune-related diseases]. *Nan Fang Yi Ke Da Xue Xue Bao*. 2022 Feb 20;42(2):163–70.
254. Breuer J, Barth P, Noe Y, Shalamova L, Goesmann A, Weber F, et al. What goes around comes around: Artificial circular RNAs bypass cellular antiviral responses. *Mol Ther Nucleic Acids*. 2022 Jun 14;28:623–35.
255. Bai Y, Liu D, He Q, Liu J, Mao Q, Liang Z. Research progress on circular RNA vaccines. *Front Immunol*. 2022;13:1091797.
256. Amaya L, Grigoryan L, Li Z, Lee A, Wender PA, Pulendran B, et al. Circular RNA vaccine induces potent T cell responses. *Proc Natl Acad Sci U S A*. 2023 May 16;120(20):e2302191120.
257. Pfaffenrot C, Preußner C. Establishing essential quality criteria for the validation of circular RNAs as biomarkers. *Biomol Detect Quantif*. 2019 Mar;17:100085.
258. Vo JN, Cieslik M, Zhang Y, Shukla S, Xiao L, Zhang Y, et al. The Landscape of Circular RNA in Cancer. *Cell*. 2019 Feb 7;176(4):869-881.e13.
259. Guo L, Jia L, Luo L, Xu X, Xiang Y, Ren Y, et al. Critical Roles of Circular RNA in Tumor Metastasis via Acting as a Sponge of miRNA/isomiR. *Int J Mol Sci*. 2022 Jun 24;23(13).
260. Zhang Q, Wang W, Zhou Q, Chen C, Yuan W, Liu J, et al. Roles of circRNAs in the tumour microenvironment. *Mol Cancer*. 2020 Jan 23;19(1):14.
261. Zhu J, Ye J, Zhang L, Xia L, Hu H, Jiang H, et al. Differential Expression of Circular RNAs in Glioblastoma Multiforme and Its Correlation with Prognosis. *Transl Oncol*. 2017 Apr;10(2):271–9.
262. Xu H, Zhang Y, Qi L, Ding L, Jiang H, Yu H. NFIX Circular RNA Promotes Glioma Progression by Regulating miR-34a-5p via Notch Signaling Pathway. *Front Mol Neurosci*. 2018;11:225.
263. Salami R, Salami M, Mafi A, Vakili O, Asemi Z. Circular RNAs and glioblastoma multiforme: focus on molecular mechanisms. *Cell Commun Signal*. 2022 Jan 28;20(1):13.
264. Ahmed SP, Castresana JS, Shahi MH. Role of Circular RNA in Brain Tumor Development. *Cells*. 2022 Jul 6;11(14).
265. Guo X, Piao H. Research Progress of circRNAs in Glioblastoma. *Front Cell Dev Biol*. 2021;9:791892.
266. Mousavi SM, Derakhshan M, Baharlooi F, Dashti F, Mirazimi SMA, Mahjoubin-Tehran M, et al. Non-coding RNAs and glioblastoma: Insight into their roles in metastasis. *Mol Ther Oncolytics*. 2022 Mar 17;24:262–87.
267. Wang J, Li T, Wang B. Circ-UBAP2 functions as sponges of miR-1205 and miR-382 to promote glioma progression by modulating STC1 expression. *Cancer Med*. 2021 Mar;10(5):1815–28.
268. Zhou J, Wang H, Hong F, Hu S, Su X, Chen J, et al. CircularRNA circPARP4 promotes glioblastoma progression through sponging miR-125a-5p and regulating FUT4. *Am J Cancer Res*. 2021;11(1):138–56.
269. Zhu F, Cheng C, Qin H, Wang H, Yu H. A novel circular RNA circENTPD7 contributes to glioblastoma progression by targeting ROS1. *Cancer Cell Int*. 2020;20:118.

270. Sun Y, Ma G, Xiang H, Wang X, Wang H, Zhang Y, et al. circFLNA promotes glioblastoma proliferation and invasion by negatively regulating miR-199-3p expression. *Mol Med Rep*. 2021 Nov;24(5).
271. Chen B, Wang M, Huang R, Liao K, Wang T, Yang R, et al. Circular RNA circLGMN facilitates glioblastoma progression by targeting miR-127-3p/LGMN axis. *Cancer Lett*. 2021 Dec 1;522:225–37.
272. Zhang S, Liao K, Miao Z, Wang Q, Miao Y, Guo Z, et al. CircFOXO3 promotes glioblastoma progression by acting as a competing endogenous RNA for NFAT5. *Neuro Oncol*. 2019 Oct 9;21(10):1284–96.
273. Qian L, Guan J, Wu Y, Wang Q. Upregulated circular RNA circ\_0074027 promotes glioblastoma cell growth and invasion by regulating miR-518a-5p/IL17RD signaling pathway. *Biochem Biophys Res Commun*. 2019 Mar 19;510(4):515–9.
274. Zhou M, Li H, Chen K, Ding W, Yang C, Wang X. CircSKA3 Downregulates miR-1 Through Methylation in Glioblastoma to Promote Cancer Cell Proliferation. *Cancer Manag Res*. 2021;13:509–14.
275. Liu L, Jia L, Shao J, Liu H, Wu Q, Wu X. Circular RNA circNF1 siRNA Silencing Inhibits Glioblastoma Cell Proliferation by Promoting the Maturation of miR-340. *Front Neurol*. 2021;12:658076.
276. Tian XL, Kadaba R, You SA, Liu M, Timur AA, Yang L, et al. Identification of an angiogenic factor that when mutated causes susceptibility to Klippel-Trenaunay syndrome. *Nature*. 2004 Feb 12;427(6975):640–5.
277. He Z, Ruan X, Liu X, Zheng J, Liu Y, Liu L, et al. FUS/circ\_002136/miR-138-5p/SOX13 feedback loop regulates angiogenesis in Glioma. *J Exp Clin Cancer Res*. 2019 Feb 8;38(1):65.
278. Zhang Y, Zhang XO, Chen T, Xiang JF, Yin QF, Xing YH, et al. Circular intronic long noncoding RNAs. *Mol Cell*. 2013 Sep 26;51(6):792–806.
279. Conn VM, Hugouvieux V, Nayak A, Conos SA, Capovilla G, Cildir G, et al. A circRNA from SEPALLATA3 regulates splicing of its cognate mRNA through R-loop formation. *Nat Plants*. 2017 Apr 18;3:17053.
280. Glažar P, Papavasileiou P, Rajewsky N. circBase: a database for circular RNAs. *RNA*. 2014 Nov;20(11):1666–70.
281. Xiao B, Lv SG, Wu MJ, Shen XL, Tu W, Ye MH, et al. Circ\_CLIP2 promotes glioma progression through targeting the miR-195-5p/HMGB3 axis. *J Neurooncol*. 2021 Sep;154(2):131–44.
282. Li H, Xia T, Guan Y, Yu Y. Sevoflurane Regulates Glioma Progression by Circ\_0002755/miR-628-5p/MAGT1 Axis. *Cancer Manag Res*. 2020;12:5085–98.
283. Bray F, Laversanne M, Weiderpass E, Soerjomataram I. The ever-increasing importance of cancer as a leading cause of premature death worldwide. *Cancer*. 2021 Aug 15;127(16):3029–30.
284. Siegel RL, Miller KD, Wagle NS, Jemal A. Cancer statistics, 2023. *CA Cancer J Clin*. 2023 Jan;73(1):17–48.

285. Radke J, Ishaque N, Koll R, Gu Z, Schumann E, Sieverling L, et al. The genomic and transcriptional landscape of primary central nervous system lymphoma. *Nat Commun.* 2022 May 10;13(1):2558.
286. Lapointe S, Perry A, Butowski NA. Primary brain tumours in adults. *Lancet.* 2018 Aug 4;392(10145):432–46.
287. Salari N, Ghasemi H, Fatahian R, Mansouri K, Dokaneheifard S, Shiri MH, et al. The global prevalence of primary central nervous system tumors: a systematic review and meta-analysis. *Eur J Med Res.* 2023 Jan 20;28(1):39.
288. Sorribes IC, Moore MNJ, Byrne HM, Jain H V. A Biomechanical Model of Tumor-Induced Intracranial Pressure and Edema in Brain Tissue. *Biophys J.* 2019 Apr 23;116(8):1560–74.
289. Buckner JC, Brown PD, O’Neill BP, Meyer FB, Wetmore CJ, Uhm JH. Central nervous system tumors. *Mayo Clin Proc.* 2007 Oct;82(10):1271–86.
290. Arora RS, Alston RD, Eden TOB, Estlin EJ, Moran A, Birch JM. Age-incidence patterns of primary CNS tumors in children, adolescents, and adults in England. *Neuro Oncol.* 2009 Aug;11(4):403–13.
291. Hanif F, Muzaffar K, Perveen K, Malhi SM, Simjee SU. Glioblastoma Multiforme: A Review of its Epidemiology and Pathogenesis through Clinical Presentation and Treatment. *Asian Pac J Cancer Prev.* 2017 Jan 1;18(1):3–9.
292. Pandit S, Adhikari A. Syndromes Associated with Brain Tumors. In: Evidence based practice in Neuro-oncology. Singapore: Springer Singapore; 2021. p. 413–8.
293. Walid MS. Prognostic factors for long-term survival after glioblastoma. *Perm J.* 2008;12(4):45–8.
294. Ostrom QT, Price M, Neff C, Cioffi G, Waite KA, Kruchko C, et al. CBTRUS Statistical Report: Primary Brain and Other Central Nervous System Tumors Diagnosed in the United States in 2015–2019. *Neuro Oncol.* 2022 Oct 5;24(Supplement\_5):v1–95.
295. Louis DN, Perry A, Wesseling P, Brat DJ, Cree IA, Figarella-Branger D, et al. The 2021 WHO Classification of Tumors of the Central Nervous System: a summary. *Neuro Oncol.* 2021 Aug 2;23(8):1231–51.
296. Chojak R, Koźba-Gosztyła M, Słychan K, Gajos D, Kotas M, Tyliczszak M, et al. Impact of surgical resection of butterfly glioblastoma on survival: a meta-analysis based on comparative studies. *Sci Rep.* 2021 Jul 6;11(1):13934.
297. Adeberg S, König L, Bostel T, Harrabi S, Welzel T, Debus J, et al. Glioblastoma recurrence patterns after radiation therapy with regard to the subventricular zone. *Int J Radiat Oncol Biol Phys.* 2014 Nov 15;90(4):886–93.
298. Kanderi T, Gupta V. Glioblastoma Multiforme. 2023.
299. Grochans S, Cybulska AM, Simińska D, Korbecki J, Kojder K, Chlubek D, et al. Epidemiology of Glioblastoma Multiforme-Literature Review. *Cancers (Basel).* 2022 May 13;14(10).
300. Ostrom QT, Bauchet L, Davis FG, Deltour I, Fisher JL, Langer CE, et al. The epidemiology of glioma in adults: a “state of the science” review. *Neuro Oncol.* 2014 Jul;16(7):896–913.

301. Sturm D, Bender S, Jones DTW, Lichter P, Grill J, Becher O, et al. Paediatric and adult glioblastoma: multiform (epi)genomic culprits emerge. *Nat Rev Cancer*. 2014 Feb;14(2):92–107.
302. Torp SH, Solheim O, Skjulsvik AJ. The WHO 2021 Classification of Central Nervous System tumours: a practical update on what neurosurgeons need to know-a minireview. *Acta Neurochir (Wien)*. 2022 Sep;164(9):2453–64.
303. Boele FW, Rooney AG, Grant R, Klein M. Psychiatric symptoms in glioma patients: from diagnosis to management. *Neuropsychiatr Dis Treat*. 2015;11:1413–20.
304. IJzerman-Korevaar M, Snijders TJ, de Graeff A, Teunissen SCCM, de Vos FYF. Prevalence of symptoms in glioma patients throughout the disease trajectory: a systematic review. *J Neurooncol*. 2018 Dec;140(3):485–96.
305. Stec NE, Walbert T. Neuro-oncology and supportive care: the role of the neurologist. *Neurol Sci*. 2022 Feb;43(2):939–50.
306. Leo RJ, Frodey JN, Ruggieri ML. Subtle neuropsychiatric symptoms of glioblastoma multiforme misdiagnosed as depression. *BMJ Case Rep*. 2020 Mar 17;13(3).
307. Javadi SAHS, Rezaei B. Brain tumors and indications for brain imaging in patients with psychiatric manifestations: a case report. *Middle East Current Psychiatry*. 2021 Dec 1;28(1):56.
308. Huang RY, Neagu MR, Reardon DA, Wen PY. Pitfalls in the neuroimaging of glioblastoma in the era of antiangiogenic and immuno/targeted therapy - detecting illusive disease, defining response. *Front Neurol*. 2015;6:33.
309. D'Alessio A, Proietti G, Sica G, Scicchitano BM. Pathological and Molecular Features of Glioblastoma and Its Peritumoral Tissue. *Cancers (Basel)*. 2019 Apr 3;11(4).
310. Jia Q, Wang A, Yuan Y, Zhu B, Long H. Heterogeneity of the tumor immune microenvironment and its clinical relevance. *Exp Hematol Oncol*. 2022 Apr 23;11(1):24.
311. Parker NR, Khong P, Parkinson JF, Howell VM, Wheeler HR. Molecular heterogeneity in glioblastoma: potential clinical implications. *Front Oncol*. 2015;5:55.
312. Pope WB, Brandal G. Conventional and advanced magnetic resonance imaging in patients with high-grade glioma. *The quarterly journal of nuclear medicine and molecular imaging : official publication of the Italian Association of Nuclear Medicine (AIMN) [and] the International Association of Radiopharmacology (IAR), [and] Section of the Society of*. 2018 Sep;62(3):239–53.
313. Bernstock JD, Gary SE, Klinger N, Valdes PA, Ibn Essayed W, Olsen HE, et al. Standard clinical approaches and emerging modalities for glioblastoma imaging. *Neurooncol Adv*. 2022;4(1):vdac080.
314. Kim SJ, Lim HK, Lee HY, Choi CG, Lee DH, Suh DC, et al. Dual-energy CT in the evaluation of intracerebral hemorrhage of unknown origin: differentiation between tumor bleeding and pure hemorrhage. *AJNR Am J Neuroradiol*. 2012 May;33(5):865–72.
315. Roozpeykar S, Azizian M, Zamani Z, Farzan MR, Veshnavei HA, Tavoosi N, et al. Contrast-enhanced weighted-T1 and FLAIR sequences in MRI of meningeal lesions. *Am J Nucl Med Mol Imaging*. 2022;12(2):63–70.

316. Varuna Shree N, Kumar TNR. Identification and classification of brain tumor MRI images with feature extraction using DWT and probabilistic neural network. *Brain Inform.* 2018 Mar;5(1):23–30.
317. Lohrke J, Frenzel T, Endrikat J, Alves FC, Grist TM, Law M, et al. 25 Years of Contrast-Enhanced MRI: Developments, Current Challenges and Future Perspectives. *Adv Ther.* 2016 Jan;33(1):1–28.
318. Drake LR, Hillmer AT, Cai Z. Approaches to PET Imaging of Glioblastoma. *Molecules.* 2020 Jan 28;25(3).
319. Mikkelsen VE, Solheim O, Salvesen Ø, Torp SH. The histological representativeness of glioblastoma tissue samples. *Acta Neurochir (Wien).* 2021 Jul;163(7):1911–20.
320. Comba A, Faisal SM, Varela ML, Hollon T, Al-Holou WN, Umemura Y, et al. Uncovering Spatiotemporal Heterogeneity of High-Grade Gliomas: From Disease Biology to Therapeutic Implications. *Front Oncol.* 2021;11:703764.
321. Dahuja G, Gupta A, Jindal A, Jain G, Sharma S, Kumar A. Clinicopathological Correlation of Glioma Patients with respect to Immunohistochemistry Markers: A Prospective Study of 115 Patients in a Tertiary Care Hospital in North India. *Asian J Neurosurg.* 2021;16(4):732–7.
322. Lee KS, Choe G, Nam KH, Seo AN, Yun S, Kim KJ, et al. Immunohistochemical classification of primary and secondary glioblastomas. *Korean J Pathol.* 2013 Dec;47(6):541–8.
323. Ali SMA, Shamim MS, Enam SA, Ahmad Z, Adnan Y, Farooqui HA. Immunohistochemical Detection and Prognostic Significance of p53, Epidermal Growth Factor Receptor, Murine Double Minute 2, and Isocitrate Dehydrogenase 1 in Glioblastoma Multiforme Patients of Pakistan. *Clin Med Insights Oncol.* 2022;16:11795549221119108.
324. Marton E, Giordan E, Siddi F, Curzi C, Canova G, Scarpa B, et al. Over ten years overall survival in glioblastoma: A different disease? *J Neurol Sci.* 2020 Jan 15;408:116518.
325. Xiong Z, Yang Q, Li X. Effect of intra- and inter-tumoral heterogeneity on molecular characteristics of primary IDH-wild type glioblastoma revealed by single-cell analysis. *CNS Neurosci Ther.* 2020 Sep;26(9):981–9.
326. DeCordova S, Shastri A, Tsolaki AG, Yasmin H, Klein L, Singh SK, et al. Molecular Heterogeneity and Immunosuppressive Microenvironment in Glioblastoma. *Front Immunol.* 2020;11:1402.
327. Shergalis A, Bankhead A, Luesakul U, Muangsinn N, Neamati N. Current Challenges and Opportunities in Treating Glioblastoma. *Pharmacol Rev.* 2018 Jul;70(3):412–45.
328. Seker-Polat F, Pinarbasi Degirmenci N, Solaroglu I, Bagci-Onder T. Tumor Cell Infiltration into the Brain in Glioblastoma: From Mechanisms to Clinical Perspectives. *Cancers (Basel).* 2022 Jan 17;14(2).
329. Giambra M, Di Cristofori A, Valtorta S, Manfrellotti R, Bigioger V, Basso G, et al. The peritumoral brain zone in glioblastoma: where we are and where we are going. *J Neurosci Res.* 2023 Feb;101(2):199–216.
330. Sacko O, Benouaich-Amiel A, Brandicourt P, Niaré M, Charni S, Cavandoli C, et al. The Impact of Surgery on the Survival of Patients with Recurrent Glioblastoma. *Asian J Neurosurg.* 2021;16(1):1–7.

331. Park JK, Hodges T, Arko L, Shen M, Dello Iacono D, McNabb A, et al. Scale to predict survival after surgery for recurrent glioblastoma multiforme. *J Clin Oncol*. 2010 Aug 20;28(24):3838–43.
332. Wang L, Liang B, Li YI, Liu X, Huang J, Li YM. What is the advance of extent of resection in glioblastoma surgical treatment-a systematic review. *Chin Neurosurg J*. 2019;5:2.
333. Molinaro AM, Hervey-Jumper S, Morshed RA, Young J, Han SJ, Chunduru P, et al. Association of Maximal Extent of Resection of Contrast-Enhanced and Non-Contrast-Enhanced Tumor With Survival Within Molecular Subgroups of Patients With Newly Diagnosed Glioblastoma. *JAMA Oncol*. 2020 Apr 1;6(4):495–503.
334. Mitusova K, Peltek OO, Karpov TE, Muslimov AR, Zyuzin M V, Timin AS. Overcoming the blood-brain barrier for the therapy of malignant brain tumor: current status and prospects of drug delivery approaches. *J Nanobiotechnology*. 2022 Sep 15;20(1):412.
335. Wu D, Chen Q, Chen X, Han F, Chen Z, Wang Y. The blood-brain barrier: structure, regulation, and drug delivery. *Signal Transduct Target Ther*. 2023 May 25;8(1):217.
336. Tamimi AF, Juweid M. Epidemiology and Outcome of Glioblastoma. 2017.
337. Stupp R, Mason WP, van den Bent MJ, Weller M, Fisher B, Taphoorn MJB, et al. Radiotherapy plus concomitant and adjuvant temozolomide for glioblastoma. *N Engl J Med*. 2005 Mar 10;352(10):987–96.
338. Lakomy R, Kazda T, Selingerova I, Poprach A, Pospisil P, Belanova R, et al. Real-World Evidence in Glioblastoma: Stupp’s Regimen After a Decade. *Front Oncol*. 2020;10:840.
339. Internò V, Messina R, Bertero L, Ricci AA, Rosito L, Bonaparte I, et al. Silibinin plus Stupp protocol as conversion therapy for unresectable glioblastoma with pSTAT3 expression, an oasis in the desert? A case report description. *Current Problems in Cancer: Case Reports*. 2023 Mar;9:100222.
340. Jackson C, Westphal M, Quiñones-Hinojosa A. Complications of glioma surgery. *Handb Clin Neurol*. 2016;134:201–18.
341. Rončević A, Koruga N, Soldo Koruga A, Rončević R, Rotim T, Šimundić T, et al. Personalized Treatment of Glioblastoma: Current State and Future Perspective. *Biomedicines*. 2023 May 30;11(6).
342. Bonosi L, Marrone S, Benigno UE, Buscemi F, Musso S, Porzio M, et al. Maximal Safe Resection in Glioblastoma Surgery: A Systematic Review of Advanced Intraoperative Image-Guided Techniques. *Brain Sci*. 2023 Jan 28;13(2).
343. Didolkar MS, Covell DG, Jackson AJ, Walker AP, Kalidindi SR. Pharmacokinetics of 5-fluorouracil following different routes of intrahepatic administration in the canine model. *Cancer Res*. 1984 Nov;44(11):5105–9.
344. Barz M, Gerhardt J, Bette S, Aftahy AK, Huber T, Combs SE, et al. Prognostic value of tumour volume in patients with a poor Karnofsky performance status scale - a bicentric retrospective study. *BMC Neurol*. 2021 Nov 15;21(1):446.
345. Yamada S, Muragaki Y, Maruyama T, Komori T, Okada Y. Role of neurochemical navigation with 5-aminolevulinic acid during intraoperative MRI-guided resection of intracranial malignant gliomas. *Clin Neurol Neurosurg*. 2015 Mar;130:134–9.

346. Rodríguez-Camacho A, Flores-Vázquez JG, Moscardini-Martelli J, Torres-Ríos JA, Olmos-Guzmán A, Ortiz-Arce CS, et al. Glioblastoma Treatment: State-of-the-Art and Future Perspectives. *Int J Mol Sci.* 2022 Jun 29;23(13).
347. Motomura K, Ohka F, Aoki K, Saito R. Supratotal Resection of Gliomas With Awake Brain Mapping: Maximal Tumor Resection Preserving Motor, Language, and Neurocognitive Functions. *Front Neurol.* 2022;13:874826.
348. Pirro V, Alfaro CM, Jarmusch AK, Hattab EM, Cohen-Gadol AA, Cooks RG. Intraoperative assessment of tumor margins during glioma resection by desorption electrospray ionization-mass spectrometry. *Proc Natl Acad Sci U S A.* 2017 Jun 27;114(26):6700–5.
349. Chen R, Brown HM, Cooks RG. Metabolic profiles of human brain parenchyma and glioma for rapid tissue diagnosis by targeted desorption electrospray ionization mass spectrometry. *Anal Bioanal Chem.* 2021 Oct;413(25):6213–24.
350. Calligaris D, Caragacianu D, Liu X, Norton I, Thompson CJ, Richardson AL, et al. Application of desorption electrospray ionization mass spectrometry imaging in breast cancer margin analysis. *Proc Natl Acad Sci U S A.* 2014 Oct 21;111(42):15184–9.
351. Devillers C, Chanconie M. [Effect of 2,4-dinitrophenol on the segmentation of the trout (*Salmo irideus* Gib.) egg]. *Acta Embryol Exp (Palermo).* 1972;3:279–88.
352. Henderson F, Jones E, Denbigh J, Christie L, Chapman R, Hoyes E, et al. 3D DESI-MS lipid imaging in a xenograft model of glioblastoma: a proof of principle. *Sci Rep.* 2020 Oct 5;10(1):16512.
353. Garza KY, Feider CL, Klein DR, Rosenberg JA, Brodbelt JS, Eberlin LS. Desorption Electrospray Ionization Mass Spectrometry Imaging of Proteins Directly from Biological Tissue Sections. *Anal Chem.* 2018 Jul 3;90(13):7785–9.
354. Margulis K, Chiou AS, Aasi SZ, Tibshirani RJ, Tang JY, Zare RN. Distinguishing malignant from benign microscopic skin lesions using desorption electrospray ionization mass spectrometry imaging. *Proc Natl Acad Sci U S A.* 2018 Jun 19;115(25):6347–52.
355. Mann J, Ramakrishna R, Magge R, Wernicke AG. Advances in Radiotherapy for Glioblastoma. *Front Neurol.* 2017;8:748.
356. Taylor A, Powell MEB. Intensity-modulated radiotherapy--what is it? *Cancer Imaging.* 2004 Mar 26;4(2):68–73.
357. Barnett GC, West CML, Dunning AM, Elliott RM, Coles CE, Pharoah PDP, et al. Normal tissue reactions to radiotherapy: towards tailoring treatment dose by genotype. *Nat Rev Cancer.* 2009 Feb;9(2):134–42.
358. Olcina MM, Giaccia AJ. Reducing radiation-induced gastrointestinal toxicity - the role of the PHD/HIF axis. *J Clin Invest.* 2016 Oct 3;126(10):3708–15.
359. Barazzuol L, Coppes RP, van Luijk P. Prevention and treatment of radiotherapy-induced side effects. *Mol Oncol.* 2020 Jul;14(7):1538–54.
360. Pasquier D, Le Tinier F, Bennadji R, Jouin A, Horn S, Escande A, et al. Intensity-modulated radiation therapy with simultaneous integrated boost for locally advanced breast cancer: a prospective study on toxicity and quality of life. *Sci Rep.* 2019 Feb 26;9(1):2759.

361. Lorentini S, Amelio D, Giri MG, Fellin F, Meliado G, Rizzotti A, et al. IMRT or 3D-CRT in glioblastoma? A dosimetric criterion for patient selection. *Technol Cancer Res Treat*. 2013 Oct;12(5):411–20.
362. Huh SJ, Park W, Choi DH. Recent trends in intensity-modulated radiation therapy use in Korea. *Radiat Oncol J*. 2019 Dec;37(4):249–53.
363. König L, Jäkel C, von Knebel Doeberitz N, Kieser M, Eberle F, Münter M, et al. Glioblastoma radiotherapy using Intensity modulated Radiotherapy (IMRT) or proton Radiotherapy-GRIPS Trial (Glioblastoma Radiotherapy via IMRT or Proton BeamS): a study protocol for a multicenter, prospective, open-label, randomized, two-arm, phase III study. *Radiat Oncol*. 2021 Dec 20;16(1):240.
364. Saeed AM, Khairmar R, Sharma AM, Larson GL, Tsai HK, Wang CJ, et al. Clinical Outcomes in Patients with Recurrent Glioblastoma Treated with Proton Beam Therapy Reirradiation: Analysis of the Multi-Institutional Proton Collaborative Group Registry. *Adv Radiat Oncol*. 2020;5(5):978–83.
365. Awada H, Paris F, Pecqueur C. Exploiting radiation immunostimulatory effects to improve glioblastoma outcome. *Neuro Oncol*. 2023 Mar 14;25(3):433–46.
366. Chau B, LaGuardia J, Hui C, Ye L, Xing Y, Massarelli E, et al. Narrative review of immunotherapy and radiation therapy in elderly patients. *Transl Cancer Res*. 2021 May;10(5):2620–31.
367. Wesolowski JR, Rajdev P, Mukherji SK. Temozolomide (Temodar). *AJNR Am J Neuroradiol*. 2010 Sep;31(8):1383–4.
368. Newlands ES, Stevens MF, Wedge SR, Wheelhouse RT, Brock C. Temozolomide: a review of its discovery, chemical properties, pre-clinical development and clinical trials. *Cancer Treat Rev*. 1997 Jan;23(1):35–61.
369. Singh N, Miner A, Hennis L, Mittal S. Mechanisms of temozolomide resistance in glioblastoma - a comprehensive review. *Cancer Drug Resist*. 2021;4(1):17–43.
370. Ortiz R, Perazzoli G, Cabeza L, Jiménez-Luna C, Luque R, Prados J, et al. Temozolomide: An Updated Overview of Resistance Mechanisms, Nanotechnology Advances and Clinical Applications. *Curr Neuropharmacol*. 2021;19(4):513–37.
371. Dresemann G. Temozolomide in malignant glioma. *Onco Targets Ther*. 2010 Sep 7;3:139–46.
372. Lee SY. Temozolomide resistance in glioblastoma multiforme. *Genes Dis*. 2016 Sep;3(3):198–210.
373. Delello Di Filippo L, Hofstätter Azambuja J, Paes Dutra JA, Tavares Luiz M, Lobato Duarte J, Nicoleti LR, et al. Improving temozolomide biopharmaceutical properties in glioblastoma multiforme (GBM) treatment using GBM-targeting nanocarriers. *Eur J Pharm Biopharm*. 2021 Nov;168:76–89.
374. Ishiguro K, Shyam K, Penketh PG, Baumann RP, Sartorelli AC, Rutherford TJ, et al. Expression of O6-Methylguanine-DNA Methyltransferase Examined by Alkyl-Transfer Assays, Methylation-Specific PCR and Western Blots in Tumors and Matched Normal Tissue. *J Cancer Ther*. 2013 Jun;4(4):919–31.
375. Yu W, Zhang L, Wei Q, Shao A. O6-Methylguanine-DNA Methyltransferase (MGMT): Challenges and New Opportunities in Glioma Chemotherapy. *Front Oncol*. 2019;9:1547.

376. Kitange GJ, Carlson BL, Schroeder MA, Grogan PT, Lamont JD, Decker PA, et al. Induction of MGMT expression is associated with temozolomide resistance in glioblastoma xenografts. *Neuro Oncol.* 2009 Jun;11(3):281–91.
377. Tsai CK, Huang LC, Wu YP, Kan IY, Hueng DY. SNAP reverses temozolomide resistance in human glioblastoma multiforme cells through down-regulation of MGMT. *FASEB J.* 2019 Dec;33(12):14171–84.
378. Wang N, Huang R, Yang K, He Y, Gao Y, Dong D. Interfering with mitochondrial dynamics sensitizes glioblastoma multiforme to temozolomide chemotherapy. *J Cell Mol Med.* 2022 Feb;26(3):893–912.
379. Ozawa T, Rodriguez M, Zhao G, Yao TW, Fischer WN, Jandeleit B, et al. A Novel Blood-Brain Barrier-Permeable Chemotherapeutic Agent for the Treatment of Glioblastoma. *Cureus.* 2021 Aug;13(8):e17595.
380. Xiao ZZ, Wang ZF, Lan T, Huang WH, Zhao YH, Ma C, et al. Carmustine as a Supplementary Therapeutic Option for Glioblastoma: A Systematic Review and Meta-Analysis. *Front Neurol.* 2020;11:1036.
381. Pająk B. Looking for the Holy Grail-Drug Candidates for Glioblastoma Multiforme Chemotherapy. *Biomedicines.* 2022 Apr 26;10(5).
382. Lin SH, Kleinberg LR. Carmustine wafers: localized delivery of chemotherapeutic agents in CNS malignancies. *Expert Rev Anticancer Ther.* 2008 Mar;8(3):343–59.
383. National Institute of Diabetes and Digestive and Kidney Diseases. LiverTox: Clinical and Research Information on Drug-Induced Liver Injury. . 2012.
384. Rominiyi O, Vanderlinden A, Clenton SJ, Bridgewater C, Al-Tamimi Y, Collis SJ. Tumour treating fields therapy for glioblastoma: current advances and future directions. *Br J Cancer.* 2021 Feb;124(4):697–709.
385. Arvind R, Chandana SR, Borad MJ, Pennington D, Mody K, Babiker H. Tumor-Treating Fields: A fourth modality in cancer treatment, new practice updates. *Crit Rev Oncol Hematol.* 2021 Dec;168:103535.
386. Guberina N, Pöttgen C, Kebir S, Lazaridis L, Scharmberg C, Lübcke W, et al. Combined radiotherapy and concurrent tumor treating fields (TTFields) for glioblastoma: Dosimetric consequences on non-coplanar IMRT as initial results from a phase I trial. *Radiat Oncol.* 2020 Apr 19;15(1):83.
387. Tanzhu G, Chen L, Xiao G, Shi W, Peng H, Chen D, et al. The schemes, mechanisms and molecular pathway changes of Tumor Treating Fields (TTFields) alone or in combination with radiotherapy and chemotherapy. *Cell Death Discov.* 2022 Oct 11;8(1):416.
388. Wang M, Zhang C, Wang X, Yu H, Zhang H, Xu J, et al. Tumor-treating fields (TTFields)-based cocktail therapy: a novel blueprint for glioblastoma treatment. *Am J Cancer Res.* 2021;11(4):1069–86.
389. Tawbi HA, Forsyth PA, Hodi FS, Algazi AP, Hamid O, Lao CD, et al. Long-term outcomes of patients with active melanoma brain metastases treated with combination nivolumab plus ipilimumab (CheckMate 204): final results of an open-label, multicentre, phase 2 study. *Lancet Oncol.* 2021 Dec;22(12):1692–704.

390. Serra-Bellver P, Versluis JM, Oberoi HK, Zhou C, Slattery TD, Khan Y, et al. Real-world outcomes with ipilimumab and nivolumab in advanced melanoma: a multicentre retrospective study. *Eur J Cancer*. 2022 Nov;176:121–32.
391. Ventola CL. *Cancer Immunotherapy, Part 1: Current Strategies and Agents*. P T. 2017 Jun;42(6):375–83.
392. Sahu M, Suryawanshi H. Immunotherapy: The future of cancer treatment. *J Oral Maxillofac Pathol*. 2021;25(2):371.
393. Rocha Pinheiro SL, Lemos FFB, Marques HS, Silva Luz M, de Oliveira Silva LG, Faria Souza Mendes Dos Santos C, et al. Immunotherapy in glioblastoma treatment: Current state and future prospects. *World J Clin Oncol*. 2023 Apr 24;14(4):138–59.
394. Bausart M, Pr at V, Malfanti A. Immunotherapy for glioblastoma: the promise of combination strategies. *J Exp Clin Cancer Res*. 2022 Jan 25;41(1):35.
395. Bianconi A, Palmieri G, Aruta G, Monticelli M, Zeppa P, Tartara F, et al. Updates in Glioblastoma Immunotherapy: An Overview of the Current Clinical and Translational Scenario. *Biomedicines*. 2023 May 24;11(6).
396. Kitada T, DiAndreth B, Teague B, Weiss R. Programming gene and engineered-cell therapies with synthetic biology. *Science*. 2018 Feb 9;359(6376).
397. Banerjee K, N n ez FJ, Haase S, McClellan BL, Faisal SM, Carney S V, et al. Current Approaches for Glioma Gene Therapy and Virotherapy. *Front Mol Neurosci*. 2021;14:621831.
398. Karlsson J, Luly KM, Tzeng SY, Green JJ. Nanoparticle designs for delivery of nucleic acid therapeutics as brain cancer therapies. *Adv Drug Deliv Rev*. 2021 Dec;179:113999.
399. Leong TW, Pal A, Cai Q, Gao Z, Li X, Bleris L, et al. Clinical gene therapy development for the central nervous system: Candidates and challenges for AAVs. *J Control Release*. 2023 May;357:511–30.
400. Puhl DL, D'Amato AR, Gilbert RJ. Challenges of gene delivery to the central nervous system and the growing use of biomaterial vectors. *Brain Res Bull*. 2019 Aug;150:216–30.
401. Chouhan RS, Horvat M, Ahmed J, Alhokbany N, Alshehri SM, Gandhi S. Magnetic Nanoparticles-A Multifunctional Potential Agent for Diagnosis and Therapy. *Cancers (Basel)*. 2021 May 5;13(9).
402. Caspani S, Magalh es R, Ara jo JP, Sousa CT. Magnetic Nanomaterials as Contrast Agents for MRI. *Materials (Basel)*. 2020 Jun 5;13(11).
403. Tang L, Feng Y, Gao S, Mu Q, Liu C. Nanotherapeutics Overcoming the Blood-Brain Barrier for Glioblastoma Treatment. *Front Pharmacol*. 2021;12:786700.
404. Hersh AM, Alomari S, Tyler BM. Crossing the Blood-Brain Barrier: Advances in Nanoparticle Technology for Drug Delivery in Neuro-Oncology. *Int J Mol Sci*. 2022 Apr 9;23(8).
405. Asija S, Chatterjee A, Goda JS, Yadav S, Chekuri G, Purwar R. Oncolytic immunovirotherapy for high-grade gliomas: A novel and an evolving therapeutic option. *Front Immunol*. 2023;14:1118246.
406. Yoon AR, Rivera-Cruz C, Gimble JM, Yun CO, Figueiredo ML. Immunotherapy by mesenchymal stromal cell delivery of oncolytic viruses for treating metastatic tumors. *Mol Ther Oncolytics*. 2022 Jun 16;25:78–97.

407. Torrisi F, Alberghina C, D'Aprile S, Pavone AM, Longhitano L, Giallongo S, et al. The Hallmarks of Glioblastoma: Heterogeneity, Intercellular Crosstalk and Molecular Signature of Invasiveness and Progression. *Biomedicines*. 2022 Mar 30;10(4).
408. Hoadley KA, Yau C, Hinoue T, Wolf DM, Lazar AJ, Drill E, et al. Cell-of-Origin Patterns Dominate the Molecular Classification of 10,000 Tumors from 33 Types of Cancer. *Cell*. 2018 Apr 5;173(2):291-304.e6.
409. Verhaak RGW, Hoadley KA, Purdom E, Wang V, Qi Y, Wilkerson MD, et al. Integrated genomic analysis identifies clinically relevant subtypes of glioblastoma characterized by abnormalities in PDGFRA, IDH1, EGFR, and NF1. *Cancer Cell*. 2010 Jan 19;17(1):98–110.
410. Chen R, Smith-Cohn M, Cohen AL, Colman H. Glioma Subclassifications and Their Clinical Significance. *Neurotherapeutics*. 2017 Apr;14(2):284–97.
411. Hanahan D. Hallmarks of Cancer: New Dimensions. *Cancer Discov*. 2022 Jan;12(1):31–46.
412. van Zijl F, Krupitza G, Mikulits W. Initial steps of metastasis: cell invasion and endothelial transmigration. *Mutat Res*. 2011;728(1–2):23–34.
413. Gupta GP, Massagué J. Cancer metastasis: building a framework. *Cell*. 2006 Nov 17;127(4):679–95.
414. Fares J, Fares MY, Khachfe HH, Salhab HA, Fares Y. Molecular principles of metastasis: a hallmark of cancer revisited. *Signal Transduct Target Ther*. 2020 Mar 12;5(1):28.
415. Garcia-Montano LA, Licon-Munoz Y, Martinez FJ, Keddari YR, Ziemke MK, Chohan MO, et al. Dissecting intra-tumor heterogeneity in the glioblastoma microenvironment using fluorescence-guided multiple sampling. *Mol Cancer Res*. 2023 May 9;
416. Skaga E, Kuleskiy E, Fayzullin A, Sandberg CJ, Potdar S, Kytälä A, et al. Intertumoral heterogeneity in patient-specific drug sensitivities in treatment-naïve glioblastoma. *BMC Cancer*. 2019 Jun 25;19(1):628.
417. Ramón Y Cajal S, Sesé M, Capdevila C, Aasen T, De Mattos-Arruda L, Diaz-Cano SJ, et al. Clinical implications of intratumor heterogeneity: challenges and opportunities. *J Mol Med (Berl)*. 2020 Feb;98(2):161–77.
418. Bergmann N, Delbridge C, Gempt J, Feuchtinger A, Walch A, Schirmer L, et al. The Intratumoral Heterogeneity Reflects the Intertumoral Subtypes of Glioblastoma Multiforme: A Regional Immunohistochemistry Analysis. *Front Oncol*. 2020;10:494.
419. Bastiancich C, Da Silva A, Estève MA. Photothermal Therapy for the Treatment of Glioblastoma: Potential and Preclinical Challenges. *Front Oncol*. 2020;10:610356.
420. Lauko A, Lo A, Ahluwalia MS, Lathia JD. Cancer cell heterogeneity & plasticity in glioblastoma and brain tumors. *Semin Cancer Biol*. 2022 Jul;82:162–75.
421. Burger PC, Green SB. Patient age, histologic features, and length of survival in patients with glioblastoma multiforme. *Cancer*. 1987 May 1;59(9):1617–25.
422. Nobusawa S, Lachuer J, Wierinckx A, Kim YH, Huang J, Legras C, et al. Intratumoral patterns of genomic imbalance in glioblastomas. *Brain Pathol*. 2010 Sep;20(5):936–44.
423. Vilar JB, Christmann M, Tomicic MT. Alterations in Molecular Profiles Affecting Glioblastoma Resistance to Radiochemotherapy: Where Does the Good Go? *Cancers (Basel)*. 2022 May 13;14(10).

424. Sottoriva A, Spiteri I, Piccirillo SGM, Touloumis A, Collins VP, Marioni JC, et al. Intratumor heterogeneity in human glioblastoma reflects cancer evolutionary dynamics. *Proc Natl Acad Sci U S A*. 2013 Mar 5;110(10):4009–14.
425. Szyłberg M, Sokal P, Śledzińska P, Bebyn M, Krajewski S, Szyłberg Ł, et al. MGMT Promoter Methylation as a Prognostic Factor in Primary Glioblastoma: A Single-Institution Observational Study. *Biomedicines*. 2022 Aug 20;10(8).
426. Kim DC, Kim KU, Kim YZ. Prognostic Role of Methylation Status of the MGMT Promoter Determined Quantitatively by Pyrosequencing in Glioblastoma Patients. *J Korean Neurosurg Soc*. 2016 Jan;59(1):26–36.
427. Cabrini G, Fabbri E, Lo Nigro C, Dechecchi MC, Gambari R. Regulation of expression of O6-methylguanine-DNA methyltransferase and the treatment of glioblastoma (Review). *Int J Oncol*. 2015 Aug;47(2):417–28.
428. Xie Q, Wu TP, Gimple RC, Li Z, Prager BC, Wu Q, et al. N6-methyladenine DNA Modification in Glioblastoma. *Cell*. 2018 Nov 15;175(5):1228-1243.e20.
429. Osuka S, Van Meir EG. Overcoming therapeutic resistance in glioblastoma: the way forward. *J Clin Invest*. 2017 Feb 1;127(2):415–26.
430. Wu H, Guo C, Wang C, Xu J, Zheng S, Duan J, et al. Single-cell RNA sequencing reveals tumor heterogeneity, microenvironment, and drug-resistance mechanisms of recurrent glioblastoma. *Cancer Sci*. 2023 Jun;114(6):2609–21.
431. Brassart-Pasco S, Brézillon S, Brassart B, Ramont L, Oudart JB, Monboisse JC. Tumor Microenvironment: Extracellular Matrix Alterations Influence Tumor Progression. *Front Oncol*. 2020;10:397.
432. Baghban R, Roshangar L, Jahanban-Esfahlan R, Seidi K, Ebrahimi-Kalan A, Jaymand M, et al. Tumor microenvironment complexity and therapeutic implications at a glance. *Cell Commun Signal*. 2020 Apr 7;18(1):59.
433. Xing F, Saidou J, Watabe K. Cancer associated fibroblasts (CAFs) in tumor microenvironment. *Front Biosci (Landmark Ed)*. 2010 Jan 1;15(1):166–79.
434. Sahai E, Astsaturov I, Cukierman E, DeNardo DG, Egeblad M, Evans RM, et al. A framework for advancing our understanding of cancer-associated fibroblasts. *Nat Rev Cancer*. 2020 Mar;20(3):174–86.
435. Grum-Schwensen B, Klingelhofer J, Berg CH, El-Naaman C, Grigorian M, Lukanidin E, et al. Suppression of tumor development and metastasis formation in mice lacking the S100A4(mts1) gene. *Cancer Res*. 2005 May 1;65(9):3772–80.
436. Rodemann HP, Müller GA. Characterization of human renal fibroblasts in health and disease: II. In vitro growth, differentiation, and collagen synthesis of fibroblasts from kidneys with interstitial fibrosis. *Am J Kidney Dis*. 1991 Jun;17(6):684–6.
437. Baginska J, Viry E, Paggetti J, Medves S, Berchem G, Moussay E, et al. The critical role of the tumor microenvironment in shaping natural killer cell-mediated anti-tumor immunity. *Front Immunol*. 2013 Dec 25;4:490.
438. Whiteside TL. The tumor microenvironment and its role in promoting tumor growth. *Oncogene*. 2008 Oct 6;27(45):5904–12.

439. Anderson NM, Simon MC. The tumor microenvironment. *Curr Biol.* 2020 Aug 17;30(16):R921–5.
440. Luo P, Wang P, Xu J, Hou W, Xu P, Xu K, et al. Immunomodulatory role of T helper cells in rheumatoid arthritis : a comprehensive research review. *Bone Joint Res.* 2022 Jul;11(7):426–38.
441. Luckheeram RV, Zhou R, Verma AD, Xia B. CD4<sup>+</sup>T cells: differentiation and functions. *Clin Dev Immunol.* 2012;2012:925135.
442. Maurer S, Ferrari de Andrade L. NK Cell Interaction With Platelets and Myeloid Cells in the Tumor Milieu. *Front Immunol.* 2020;11:608849.
443. Yu Y. The Function of NK Cells in Tumor Metastasis and NK Cell-Based Immunotherapy. *Cancers (Basel).* 2023 Apr 16;15(8).
444. Lo Nigro C, Macagno M, Sangiolo D, Bertolaccini L, Aglietta M, Merlano MC. NK-mediated antibody-dependent cell-mediated cytotoxicity in solid tumors: biological evidence and clinical perspectives. *Ann Transl Med.* 2019 Mar;7(5):105.
445. Mattiola I. Immune Circuits to Shape Natural Killer Cells in Cancer. *Cancers (Basel).* 2021 Jun 28;13(13).
446. Anderson KG, Stromnes IM, Greenberg PD. Obstacles Posed by the Tumor Microenvironment to T cell Activity: A Case for Synergistic Therapies. *Cancer Cell.* 2017 Mar 13;31(3):311–25.
447. Balta E, Wabnitz GH, Samstag Y. Hijacked Immune Cells in the Tumor Microenvironment: Molecular Mechanisms of Immunosuppression and Cues to Improve T Cell-Based Immunotherapy of Solid Tumors. *Int J Mol Sci.* 2021 May 27;22(11).
448. Saman H, Raza SS, Uddin S, Rasul K. Inducing Angiogenesis, a Key Step in Cancer Vascularization, and Treatment Approaches. *Cancers (Basel).* 2020 May 6;12(5).
449. Lugano R, Ramachandran M, Dimberg A. Tumor angiogenesis: causes, consequences, challenges and opportunities. *Cell Mol Life Sci.* 2020 May;77(9):1745–70.
450. Ghosh M, Lenkiewicz AM, Kaminska B. The Interplay of Tumor Vessels and Immune Cells Affects Immunotherapy of Glioblastoma. *Biomedicines.* 2022 Sep 15;10(9):2292.
451. Lamplugh Z, Fan Y. Vascular Microenvironment, Tumor Immunity and Immunotherapy. *Front Immunol.* 2021;12:811485.
452. Ferrara N, Gerber HP. The Role of Vascular Endothelial Growth Factor in Angiogenesis. *Acta Haematol.* 2001;106(4):148–56.
453. Johnson KE, Wilgus TA. Vascular Endothelial Growth Factor and Angiogenesis in the Regulation of Cutaneous Wound Repair. *Adv Wound Care (New Rochelle).* 2014 Oct 1;3(10):647–61.
454. Bernardo-Castro S, Sousa JA, Brás A, Cecília C, Rodrigues B, Almendra L, et al. Pathophysiology of Blood–Brain Barrier Permeability Throughout the Different Stages of Ischemic Stroke and Its Implication on Hemorrhagic Transformation and Recovery. *Front Neurol.* 2020 Dec 9;11.
455. Geindreau M, Bruchard M, Vegran F. Role of Cytokines and Chemokines in Angiogenesis in a Tumor Context. *Cancers (Basel).* 2022 May 16;14(10).

456. Hambardzumyan D, Bergers G. Glioblastoma: Defining Tumor Niches. *Trends Cancer*. 2015 Dec;1(4):252–65.
457. Uribe D, Niechi I, Rackov G, Erices JI, San Martín R, Quezada C. Adapt to Persist: Glioblastoma Microenvironment and Epigenetic Regulation on Cell Plasticity. *Biology (Basel)*. 2022 Feb 16;11(2).
458. Chen Z, Han F, Du Y, Shi H, Zhou W. Hypoxic microenvironment in cancer: molecular mechanisms and therapeutic interventions. *Signal Transduct Target Ther*. 2023 Feb 17;8(1):70.
459. Emami Nejad A, Najafgholian S, Rostami A, Sistani A, Shojaeifar S, Esparvarinha M, et al. The role of hypoxia in the tumor microenvironment and development of cancer stem cell: a novel approach to developing treatment. *Cancer Cell Int*. 2021 Jan 20;21(1):62.
460. Kabakov AE, Yakimova AO. Hypoxia-Induced Cancer Cell Responses Driving Radioresistance of Hypoxic Tumors: Approaches to Targeting and Radiosensitizing. *Cancers (Basel)*. 2021 Mar 4;13(5).
461. Luo Z, Tian M, Yang G, Tan Q, Chen Y, Li G, et al. Hypoxia signaling in human health and diseases: implications and prospects for therapeutics. *Signal Transduct Target Ther*. 2022 Jul 7;7(1):218.
462. Boyd NH, Tran AN, Bernstock JD, Etminan T, Jones AB, Gillespie GY, et al. Glioma stem cells and their roles within the hypoxic tumor microenvironment. *Theranostics*. 2021;11(2):665–83.
463. Shi T, Zhu J, Zhang X, Mao X. The Role of Hypoxia and Cancer Stem Cells in Development of Glioblastoma. *Cancers (Basel)*. 2023 May 4;15(9):2613.
464. Sonbol HS. Extracellular Matrix Remodeling in Human Disease. *J Microsc Ultrastruct*. 2018;6(3):123–8.
465. Huang J, Zhang L, Wan D, Zhou L, Zheng S, Lin S, et al. Extracellular matrix and its therapeutic potential for cancer treatment. *Signal Transduct Target Ther*. 2021 Apr 23;6(1):153.
466. Northey JJ, Przybyla L, Weaver VM. Tissue Force Programs Cell Fate and Tumor Aggression. *Cancer Discov*. 2017 Nov 1;7(11):1224–37.
467. Faisal SM, Comba A, Varela ML, Argento AE, Brumley E, Abel C, et al. The complex interactions between the cellular and non-cellular components of the brain tumor microenvironmental landscape and their therapeutic implications. *Front Oncol*. 2022;12:1005069.
468. Gordon-Weeks A, Yuzhalin AE. Cancer Extracellular Matrix Proteins Regulate Tumour Immunity. *Cancers (Basel)*. 2020 Nov 11;12(11).
469. Grabowska M, Kuczyński K, Piwecka M, Rabiasz A, Zemła J, Głodowicz P, et al. miR-218 affects the ECM composition and cell biomechanical properties of glioblastoma cells. *J Cell Mol Med*. 2022 Jul;26(14):3913–30.
470. Koh I, Cha J, Park J, Choi J, Kang SG, Kim P. The mode and dynamics of glioblastoma cell invasion into a decellularized tissue-derived extracellular matrix-based three-dimensional tumor model. *Sci Rep*. 2018 Mar 15;8(1):4608.

471. Eid RA, Alaa Edeen M, Shedid EM, Kamal ASS, Warda MM, Mamdouh F, et al. Targeting Cancer Stem Cells as the Key Driver of Carcinogenesis and Therapeutic Resistance. *Int J Mol Sci.* 2023 Jan 16;24(2).
472. Molczyk C, Singh RK. CXCR1: A Cancer Stem Cell Marker and Therapeutic Target in Solid Tumors. *Biomedicines.* 2023 Feb 16;11(2).
473. Nallasamy P, Nimmakayala RK, Parte S, Are AC, Batra SK, Ponnusamy MP. Tumor microenvironment enriches the stemness features: the architectural event of therapy resistance and metastasis. *Mol Cancer.* 2022 Dec 22;21(1):225.
474. Qin S, Jiang J, Lu Y, Nice EC, Huang C, Zhang J, et al. Emerging role of tumor cell plasticity in modifying therapeutic response. *Signal Transduct Target Ther.* 2020 Oct 7;5(1):228.
475. Aponte PM, Caicedo A. Stemness in Cancer: Stem Cells, Cancer Stem Cells, and Their Microenvironment. *Stem Cells Int.* 2017;2017:5619472.
476. Najafi M, Farhood B, Mortezaee K. Cancer stem cells (CSCs) in cancer progression and therapy. *J Cell Physiol.* 2019 Jun;234(6):8381–95.
477. Tang X, Zuo C, Fang P, Liu G, Qiu Y, Huang Y, et al. Targeting Glioblastoma Stem Cells: A Review on Biomarkers, Signal Pathways and Targeted Therapy. *Front Oncol.* 2021;11:701291.
478. Razi S, Haghparast A, Chodari Khameneh S, Ebrahimi Sadrabadi A, Aziziyan F, Bakhtiyari M, et al. The role of tumor microenvironment on cancer stem cell fate in solid tumors. *Cell Commun Signal.* 2023 Jun 16;21(1):143.
479. Alves AL V, Gomes INF, Carloni AC, Rosa MN, da Silva LS, Evangelista AF, et al. Role of glioblastoma stem cells in cancer therapeutic resistance: a perspective on antineoplastic agents from natural sources and chemical derivatives. *Stem Cell Res Ther.* 2021 Mar 24;12(1):206.
480. Mattei V, Santilli F, Martellucci S, Delle Monache S, Fabrizi J, Colapietro A, et al. The Importance of Tumor Stem Cells in Glioblastoma Resistance to Therapy. *Int J Mol Sci.* 2021 Apr 8;22(8).
481. Singh SK, Hawkins C, Clarke ID, Squire JA, Bayani J, Hide T, et al. Identification of human brain tumour initiating cells. *Nature.* 2004 Nov 18;432(7015):396–401.
482. Karbanová J, Missol-Kolka E, Fonseca AV, Lorra C, Janich P, Hollerová H, et al. The stem cell marker CD133 (Prominin-1) is expressed in various human glandular epithelia. *J Histochem Cytochem.* 2008 Nov;56(11):977–93.
483. Yao J, Zhang T, Ren J, Yu M, Wu G. Effect of CD133/prominin-1 antisense oligodeoxynucleotide on in vitro growth characteristics of Huh-7 human hepatocarcinoma cells and U251 human glioma cells. *Oncol Rep.* 2009 Oct;22(4):781–7.
484. Dahlrot RH, Bangsø JA, Petersen JK, Rosager AM, Sørensen MD, Reifenberger G, et al. Prognostic role of Ki-67 in glioblastomas excluding contribution from non-neoplastic cells. *Sci Rep.* 2021 Sep 9;11(1):17918.
485. Lee CC, Lai JH, Hueng DY, Ma HI, Chung YC, Sun YY, et al. Disrupting the CXCL12/CXCR4 axis disturbs the characteristics of glioblastoma stem-like cells of rat RG2 glioblastoma. *Cancer Cell Int.* 2013 Aug 21;13(1):85.
486. Flüh C, Hattermann K, Mehdorn HM, Synowitz M, Held-Feindt J. Differential expression of CXCR4 and CXCR7 with various stem cell markers in paired human primary and recurrent glioblastomas. *Int J Oncol.* 2016 Apr;48(4):1408–16.

487. Singh D, Arora R, Kaur P, Singh B, Mannan R, Arora S. Overexpression of hypoxia-inducible factor and metabolic pathways: possible targets of cancer. *Cell Biosci.* 2017;7:62.
488. Rajabi A, Kayedi M, Rahimi S, Dashti F, Mirazimi SMA, Homayoonfal M, et al. Non-coding RNAs and glioma: Focus on cancer stem cells. *Mol Ther Oncolytics.* 2022 Dec 15;27:100–23.
489. Auffinger B, Spencer D, Pytel P, Ahmed AU, Lesniak MS. The role of glioma stem cells in chemotherapy resistance and glioblastoma multiforme recurrence. *Expert Rev Neurother.* 2015;15(7):741–52.
490. Huang Y, Hong W, Wei X. The molecular mechanisms and therapeutic strategies of EMT in tumor progression and metastasis. *J Hematol Oncol.* 2022 Sep 8;15(1):129.
491. Kim DH, Xing T, Yang Z, Dudek R, Lu Q, Chen YH. Epithelial Mesenchymal Transition in Embryonic Development, Tissue Repair and Cancer: A Comprehensive Overview. *J Clin Med.* 2017 Dec 22;7(1).
492. Kalluri R, Weinberg RA. The basics of epithelial-mesenchymal transition. *J Clin Invest.* 2009 Jun;119(6):1420–8.
493. Seyfried TN, Huysentruyt LC. On the origin of cancer metastasis. *Crit Rev Oncog.* 2013;18(1–2):43–73.
494. Ribatti D, Tamma R, Annese T. Epithelial-Mesenchymal Transition in Cancer: A Historical Overview. *Transl Oncol.* 2020 Jun;13(6):100773.
495. Son H, Moon A. Epithelial-mesenchymal Transition and Cell Invasion. *Toxicol Res.* 2010 Dec;26(4):245–52.
496. Garcia MA, Nelson WJ, Chavez N. Cell-Cell Junctions Organize Structural and Signaling Networks. *Cold Spring Harb Perspect Biol.* 2018 Apr 2;10(4).
497. Serrano-Gomez SJ, Maziveyi M, Alahari SK. 26905733. *Mol Cancer.* 2016 Feb 24;15:18.
498. Dongre A, Weinberg RA. New insights into the mechanisms of epithelial-mesenchymal transition and implications for cancer. *Nat Rev Mol Cell Biol.* 2019 Feb;20(2):69–84.
499. Yang J, Antin P, Berx G, Blanpain C, Brabletz T, Bronner M, et al. Guidelines and definitions for research on epithelial-mesenchymal transition. *Nat Rev Mol Cell Biol.* 2020 Jun;21(6):341–52.
500. Ray I, Michael A, Meira LB, Ellis PE. The Role of Cytokines in Epithelial-Mesenchymal Transition in Gynaecological Cancers: A Systematic Review. *Cells.* 2023 Jan 26;12(3).
501. Narang V, Wong SY, Leong SR, Harish B, Abastado JP, Gouaillard A. Selection of Mesenchymal-Like Metastatic Cells in Primary Tumors - An in silico Investigation. *Front Immunol.* 2012;3:88.
502. Majc B, Sever T, Zarić M, Breznik B, Turk B, Lah TT. Epithelial-to-mesenchymal transition as the driver of changing carcinoma and glioblastoma microenvironment. *Biochim Biophys Acta Mol Cell Res.* 2020 Oct;1867(10):118782.
503. Creighton CJ, Li X, Landis M, Dixon JM, Neumeister VM, Sjolund A, et al. Residual breast cancers after conventional therapy display mesenchymal as well as tumor-initiating features. *Proc Natl Acad Sci U S A.* 2009 Aug 18;106(33):13820–5.

504. Bajetto A, Thellung S, Dellacasagrande I, Pagano A, Barbieri F, Florio T. Cross talk between mesenchymal and glioblastoma stem cells: Communication beyond controversies. *Stem Cells Transl Med.* 2020 Nov;9(11):1310–30.
505. Li GC, Zhang HW, Zhao QC, Sun LI, Yang JJ, Hong L, et al. Mesenchymal stem cells promote tumor angiogenesis via the action of transforming growth factor  $\beta$ 1. *Oncol Lett.* 2016 Feb;11(2):1089–94.
506. Velásquez C, Mansouri S, Mora C, Nassiri F, Suppiah S, Martino J, et al. Molecular and Clinical Insights into the Invasive Capacity of Glioblastoma Cells. *J Oncol.* 2019;2019:1740763.
507. Slack FJ, Chinnaiyan AM. The Role of Non-coding RNAs in Oncology. *Cell.* 2019 Nov 14;179(5):1033–55.
508. Yan H, Bu P. Non-coding RNA in cancer. *Essays Biochem.* 2021 Oct 27;65(4):625–39.
509. Zhang Y, Yang M, Yang S, Hong F. Role of noncoding RNAs and untranslated regions in cancer: A review. *Medicine.* 2022 Aug 19;101(33):e30045.
510. Zhang P, Wu W, Chen Q, Chen M. Non-Coding RNAs and their Integrated Networks. *J Integr Bioinform.* 2019 Jul 13;16(3).
511. Statello L, Guo CJ, Chen LL, Huarte M. Gene regulation by long non-coding RNAs and its biological functions. *Nat Rev Mol Cell Biol.* 2021 Feb;22(2):96–118.
512. Latowska J, Grabowska A, Zarębska Ż, Kuczyński K, Kuczyńska B, Rolle K. Non-coding RNAs in Brain Tumors, the Contribution of lncRNAs, circRNAs, and snoRNAs to Cancer Development-Their Diagnostic and Therapeutic Potential. *Int J Mol Sci.* 2020 Sep 23;21(19).
513. Mafi A, Rahmati A, Babaei Aghdam Z, Salami R, Salami M, Vakili O, et al. Recent insights into the microRNA-dependent modulation of gliomas from pathogenesis to diagnosis and treatment. *Cell Mol Biol Lett.* 2022 Aug 3;27(1):65.
514. Shea A, Harish V, Afzal Z, Chijioke J, Kedir H, Dusmatova S, et al. MicroRNAs in glioblastoma multiforme pathogenesis and therapeutics. *Cancer Med.* 2016 Aug;5(8):1917–46.
515. Lang MF, Yang S, Zhao C, Sun G, Murai K, Wu X, et al. Genome-wide profiling identified a set of miRNAs that are differentially expressed in glioblastoma stem cells and normal neural stem cells. *PLoS One.* 2012;7(4):e36248.
516. Agrawal R, Pandey P, Jha P, Dwivedi V, Sarkar C, Kulshreshtha R. Hypoxic signature of microRNAs in glioblastoma: insights from small RNA deep sequencing. *BMC Genomics.* 2014 Aug 17;15(1):686.
517. Piwecka M, Rolle K, Belter A, Barciszewska AM, Żywicki M, Michalak M, et al. Comprehensive analysis of microRNA expression profile in malignant glioma tissues. *Mol Oncol.* 2015 Aug;9(7):1324–40.
518. Gvaldin DY, Pushkin AA, Timoshkina NN, Rostorguev EE, Nalgiev AM, Kit OI. Integrative analysis of mRNA and miRNA sequencing data for gliomas of various grades. *Egyptian Journal of Medical Human Genetics.* 2020 Dec 10;21(1):73.
519. Kim TM, Huang W, Park R, Park PJ, Johnson MD. A developmental taxonomy of glioblastoma defined and maintained by MicroRNAs. *Cancer Res.* 2011 May 1;71(9):3387–99.

520. Sanchez Calle A, Kawamura Y, Yamamoto Y, Takeshita F, Ochiya T. Emerging roles of long non-coding RNA in cancer. *Cancer Sci.* 2018 Jul;109(7):2093–100.
521. Wang D, Fu CW, Fan DQ. Participation of tumor suppressors long non-coding RNA MEG3, microRNA-377 and PTEN in glioma cell invasion and migration. *Pathol Res Pract.* 2019 Oct;215(10):152558.
522. El Fatimy R, Subramanian S, Uhlmann EJ, Krichevsky AM. Genome Editing Reveals Glioblastoma Addiction to MicroRNA-10b. *Mol Ther.* 2017 Feb 1;25(2):368–78.
523. Kondo Y, Katsushima K, Ohka F, Natsume A, Shinjo K. Epigenetic dysregulation in glioma. *Cancer Sci.* 2014 Apr;105(4):363–9.
524. Yang X, Liu M, Li M, Zhang S, Hiju H, Sun J, et al. Epigenetic modulations of noncoding RNA: a novel dimension of Cancer biology. *Mol Cancer.* 2020 Mar 24;19(1):64.
525. Lenda B, Żebrowska-Nawrocka M, Turek G, Balcerczak E. Zinc Finger E-Box Binding Homeobox Family: Non-Coding RNA and Epigenetic Regulation in Gliomas. *Biomedicines.* 2023 May 5;11(5).
526. Mekala JR, Adusumilli K, Chamarthy S, Angirekula HSR. Novel sights on therapeutic, prognostic, and diagnostics aspects of non-coding RNAs in glioblastoma multiforme. *Metab Brain Dis.* 2023 Aug;38(6):1801–29.
527. Lu C, Wei Y, Wang X, Zhang Z, Yin J, Li W, et al. DNA-methylation-mediated activating of lncRNA SNHG12 promotes temozolomide resistance in glioblastoma. *Mol Cancer.* 2020 Feb 10;19(1):28.
528. Winkle M, El-Daly SM, Fabbri M, Calin GA. Noncoding RNA therapeutics - challenges and potential solutions. *Nat Rev Drug Discov.* 2021 Aug;20(8):629–51.
529. Dai L, Liang W, Shi Z, Li X, Zhou S, Hu W, et al. Systematic characterization and biological functions of non-coding RNAs in glioblastoma. *Cell Prolif.* 2023 Mar;56(3):e13375.
530. He X, Qi Y, Zhang X, Liu X, Li X, Li S, et al. Current landscape of tumor-derived exosomal ncRNAs in glioma progression, detection, and drug resistance. *Cell Death Dis.* 2021 Dec 9;12(12):1145.
531. Zanganeh S, Abbasgholinejad E, Doroudian M, Esmaelizad N, Farjadian F, Benhabbour SR. The Current Landscape of Glioblastoma Biomarkers in Body Fluids. *Cancers (Basel).* 2023 Jul 26;15(15).
532. Wang H, Peng R, Wang J, Qin Z, Xue L. Circulating microRNAs as potential cancer biomarkers: the advantage and disadvantage. *Clin Epigenetics.* 2018;10:59.
533. Winkler J, Abisoye-Ogunniyan A, Metcalf KJ, Werb Z. Concepts of extracellular matrix remodelling in tumour progression and metastasis. *Nat Commun.* 2020 Oct 9;11(1):5120.
534. Rybin MJ, Ivan ME, Ayad NG, Zeier Z. Organoid Models of Glioblastoma and Their Role in Drug Discovery. *Front Cell Neurosci.* 2021;15:605255.
535. Jubelin C, Muñoz-Garcia J, Griscom L, Cochonneau D, Ollivier E, Heymann MF, et al. Three-dimensional in vitro culture models in oncology research. *Cell Biosci.* 2022 Sep 11;12(1):155.
536. Yang R, Guo J, Lin Z, Song H, Feng Z, Ou Y, et al. The combination of two-dimensional and three-dimensional analysis methods contributes to the understanding of glioblastoma spatial heterogeneity. *J Biophotonics.* 2020 Feb;13(2):e201900196.

537. Linkous A, Balamatsias D, Snuderl M, Edwards L, Miyaguchi K, Milner T, et al. Modeling Patient-Derived Glioblastoma with Cerebral Organoids. *Cell Rep.* 2019 Mar 19;26(12):3203-3211.e5.
538. Gomez GA, Oksdath M, Brown MP, Ebert LM. New approaches to model glioblastoma in vitro using brain organoids: implications for precision oncology. *Transl Cancer Res.* 2019 Dec;8(Suppl 6):S606–11.
539. Gómez-Oliva R, Domínguez-García S, Carrascal L, Abalos-Martínez J, Pardillo-Díaz R, Verástegui C, et al. Evolution of Experimental Models in the Study of Glioblastoma: Toward Finding Efficient Treatments. *Front Oncol.* 2020;10:614295.
540. Kodack DP, Farago AF, Dastur A, Held MA, Dardaei L, Friboulet L, et al. Primary Patient-Derived Cancer Cells and Their Potential for Personalized Cancer Patient Care. *Cell Rep.* 2017 Dec 12;21(11):3298–309.
541. Leite DM, Zvar Baskovic B, Civita P, Neto C, Gumbleton M, Pilkington GJ. A human co-culture cell model incorporating microglia supports glioblastoma growth and migration, and confers resistance to cytotoxics. *FASEB J.* 2020 Jan;34(1):1710–27.
542. Azzarelli R, Ori M, Philpott A, Simons BD. Three-dimensional model of glioblastoma by co-culturing tumor stem cells with human brain organoids. *Biol Open.* 2021 Feb 22;10(2).
543. Temple J, Velliou E, Shehata M, Lévy R. Current strategies with implementation of three-dimensional cell culture: the challenge of quantification. *Interface Focus.* 2022 Oct 6;12(5):20220019.
544. Foster NC, Hall NM, Haj AJ El. Two-Dimensional and Three-Dimensional Cartilage Model Platforms for Drug Evaluation and High-Throughput Screening Assays. *Tissue Eng Part B Rev.* 2022 Apr;28(2):421–36.
545. Andreatta F, Beccaceci G, Fortuna N, Celotti M, De Felice D, Lorenzoni M, et al. The Organoid Era Permits the Development of New Applications to Study Glioblastoma. *Cancers (Basel).* 2020 Nov 9;12(11).
546. Geraghty RJ, Capes-Davis A, Davis JM, Downward J, Freshney RI, Knezevic I, et al. Guidelines for the use of cell lines in biomedical research. *Br J Cancer.* 2014 Sep 9;111(6):1021–46.
547. Paolillo M, Comincini S, Schinelli S. In Vitro Glioblastoma Models: A Journey into the Third Dimension. *Cancers (Basel).* 2021 May 18;13(10).
548. Wei R, Liu S, Zhang S, Min L, Zhu S. Cellular and Extracellular Components in Tumor Microenvironment and Their Application in Early Diagnosis of Cancers. *Anal Cell Pathol (Amst).* 2020;2020:6283796.
549. Phon BWS, Kamarudin MNA, Bhuvanendran S, Radhakrishnan AK. Transitioning pre-clinical glioblastoma models to clinical settings with biomarkers identified in 3D cell-based models: A systematic scoping review. *Biomed Pharmacother.* 2022 Jan;145:112396.
550. Gutschner T, Diederichs S. The hallmarks of cancer: a long non-coding RNA point of view. *RNA Biol.* 2012 Jun;9(6):703–19.
551. Gomez-Roman N, Chong MY, Chahal SK, Caragher SP, Jackson MR, Stevenson KH, et al. Radiation Responses of 2D and 3D Glioblastoma Cells: A Novel, 3D-specific Radioprotective Role of VEGF/Akt Signaling through Functional Activation of NHEJ. *Mol Cancer Ther.* 2020 Feb;19(2):575–89.

552. Loewa A, Feng JJ, Hedtrich S. Human disease models in drug development. *Nature reviews bioengineering*. 2023 May 11;1–15.
553. He Q, Chen J, Yan J, Cai S, Xiong H, Liu Y, et al. Tumor microenvironment responsive drug delivery systems. *Asian J Pharm Sci*. 2020 Jul;15(4):416–48.
554. Zhou H, Wang M, Zhang Y, Su Q, Xie Z, Chen X, et al. Functions and clinical significance of mechanical tumor microenvironment: cancer cell sensing, mechanobiology and metastasis. *Cancer Commun (Lond)*. 2022 May;42(5):374–400.
555. Soubéran A, Tchoghandjian A. Practical Review on Preclinical Human 3D Glioblastoma Models: Advances and Challenges for Clinical Translation. *Cancers (Basel)*. 2020 Aug 19;12(9).
556. Li W, Zhou Z, Zhou X, Khoo BL, Gunawan R, Chin YR, et al. 3D Biomimetic Models to Reconstitute Tumor Microenvironment In Vitro: Spheroids, Organoids, and Tumor-on-a-Chip. *Adv Healthc Mater*. 2023 Jul;12(18):e2202609.
557. Rao SS, Lannutti JJ, Viapiano MS, Sarkar A, Winter JO. Toward 3D biomimetic models to understand the behavior of glioblastoma multiforme cells. *Tissue Eng Part B Rev*. 2014 Aug;20(4):314–27.
558. Abedin MJ, Michelhaugh SK, Mittal S, Berdichevsky Y. 3D models of glioblastoma interaction with cortical cells. *Front Bioeng Biotechnol*. 2023;11:1150772.
559. Oliver L, Álvarez-Arenas A, Salaud C, Jiménez-Sánchez J, Calvo GF, Belmonte-Beitia J, et al. A Simple 3D Cell Culture Method for Studying the Interactions between Human Mesenchymal Stromal/Stem Cells and Patients Derived Glioblastoma. *Cancers (Basel)*. 2023 Feb 18;15(4).
560. Azzarelli R. Organoid Models of Glioblastoma to Study Brain Tumor Stem Cells. *Front Cell Dev Biol*. 2020;8:220.
561. Sanchez-Rubio A, Jayawarna V, Maxwell E, Dalby MJ, Salmeron-Sanchez M. Keeping It Organized: Multicompartment Constructs to Mimic Tissue Heterogeneity. *Adv Healthc Mater*. 2023 Jul;12(17):e2202110.
562. Shin DS, Anseth KS. Recent advances in 3D models of tumor invasion. *Curr Opin Biomed Eng*. 2021 Sep;19.
563. Pinto B, Henriques AC, Silva PMA, Bousbaa H. Three-Dimensional Spheroids as In Vitro Preclinical Models for Cancer Research. *Pharmaceutics*. 2020 Dec 6;12(12).
564. Roy SM, Garg V, Barman S, Ghosh C, Maity AR, Ghosh SK. Kinetics of Nanomedicine in Tumor Spheroid as an In Vitro Model System for Efficient Tumor-Targeted Drug Delivery With Insights From Mathematical Models. *Front Bioeng Biotechnol*. 2021;9:785937.
565. Stanković T, Ranđelović T, Dragoj M, Stojković Burić S, Fernández L, Ochoa I, et al. In vitro biomimetic models for glioblastoma—a promising tool for drug response studies. *Drug Resist Updat*. 2021 Mar;55:100753.
566. Han SJ, Kwon S, Kim KS. Challenges of applying multicellular tumor spheroids in preclinical phase. *Cancer Cell Int*. 2021 Mar 4;21(1):152.
567. Fitzgerald AA, Li E, Weiner LM. 3D Culture Systems for Exploring Cancer Immunology. *Cancers (Basel)*. 2020 Dec 28;13(1).

568. Li Q, Lin H, Rauch J, Deleyrolle LP, Reynolds BA, Viljoen HJ, et al. Scalable Culturing of Primary Human Glioblastoma Tumor-Initiating Cells with a Cell-Friendly Culture System. *Sci Rep.* 2018 Feb 23;8(1):3531.
569. Barbosa MAG, Xavier CPR, Pereira RF, Petrikaitė V, Vasconcelos MH. 3D Cell Culture Models as Recapitulators of the Tumor Microenvironment for the Screening of Anti-Cancer Drugs. *Cancers (Basel).* 2021 Dec 31;14(1).
570. Domínguez-Oliva A, Hernández-Ávalos I, Martínez-Burnes J, Olmos-Hernández A, Verduzco-Mendoza A, Mota-Rojas D. The Importance of Animal Models in Biomedical Research: Current Insights and Applications. *Animals (Basel).* 2023 Mar 31;13(7).
571. Lenin S, Ponthier E, Scheer KG, Yeo ECF, Tea MN, Ebert LM, et al. A Drug Screening Pipeline Using 2D and 3D Patient-Derived In Vitro Models for Pre-Clinical Analysis of Therapy Response in Glioblastoma. *Int J Mol Sci.* 2021 Apr 21;22(9).
572. Parra-Cantu C, Li W, Quiñones-Hinojosa A, Zhang YS. 3D bioprinting of glioblastoma models. *J 3D Print Med.* 2020 Jun;4(2):113–25.
573. Mazrouei R, Velasco V, Esfandyarpour R. 3D-bioprinted all-inclusive bioanalytical platforms for cell studies. *Sci Rep.* 2020 Sep 4;10(1):14669.
574. Yin H, Marshall D. Microfluidics for single cell analysis. *Curr Opin Biotechnol.* 2012 Feb;23(1):110–9.
575. Ngo H, Amartumur S, Tran VTA, Tran M, Diep YN, Cho H, et al. In Vitro Tumor Models on Chip and Integrated Microphysiological Analysis Platform (MAP) for Life Sciences and High-Throughput Drug Screening. *Biosensors (Basel).* 2023 Feb 6;13(2).
576. Truong D, Fiorelli R, Barrientos ES, Melendez EL, Sanai N, Mehta S, et al. A three-dimensional (3D) organotypic microfluidic model for glioma stem cells - Vascular interactions. *Biomaterials.* 2019 Apr;198:63–77.
577. Hasin Y, Seldin M, Lusic A. Multi-omics approaches to disease. *Genome Biol.* 2017 May 5;18(1):83.
578. Migliozi S, Oh YT, Hasanain M, Garofano L, D'Angelo F, Najac RD, et al. Integrative multi-omics networks identify PKC $\delta$  and DNA-PK as master kinases of glioblastoma subtypes and guide targeted cancer therapy. *Nat Cancer.* 2023 Feb;4(2):181–202.
579. Vinci M, Gowan S, Boxall F, Patterson L, Zimmermann M, Court W, et al. Advances in establishment and analysis of three-dimensional tumor spheroid-based functional assays for target validation and drug evaluation. *BMC Biol.* 2012 Mar 22;10:29.
580. Jacob F, Salinas RD, Zhang DY, Nguyen PTT, Schnoll JG, Wong SZH, et al. A Patient-Derived Glioblastoma Organoid Model and Biobank Recapitulates Inter- and Intra-tumoral Heterogeneity. *Cell.* 2020 Jan 9;180(1):188-204.e22.
581. Bolger AM, Lohse M, Usadel B. Trimmomatic: a flexible trimmer for Illumina sequence data. *Bioinformatics.* 2014 Aug 1;30(15):2114–20.
582. Li H. Toward better understanding of artifacts in variant calling from high-coverage samples. *Bioinformatics.* 2014 Oct 15;30(20):2843–51.
583. Chen L, Wang F, Bruggeman EC, Li C, Yao B. circMeta: a unified computational framework for genomic feature annotation and differential expression analysis of circular RNAs. *Bioinformatics.* 2020 Jan 15;36(2):539–45.

584. Robinson MD, McCarthy DJ, Smyth GK. `edgeR`: a Bioconductor package for differential expression analysis of digital gene expression data. *Bioinformatics*. 2010 Jan 1;26(1):139–40.
585. Wickham H. *Data Analysis*. In 2016. p. 189–201.
586. Wickham H. *ggplot2*. Cham: Springer International Publishing; 2016.
587. Sonesson C, Love MI, Robinson MD. Differential analyses for RNA-seq: transcript-level estimates improve gene-level inferences. *F1000Res*. 2015 Dec 30;4:1521.
588. So JS, Kim H, Han KS. Mechanisms of Invasion in Glioblastoma: Extracellular Matrix, Ca<sup>2+</sup> Signaling, and Glutamate. *Front Cell Neurosci*. 2021;15:663092.
589. Kundu P, Santosh V, Kondaiah P. Mechanisms of cell competition in glioblastoma: A narrative review. *Glioma*. 2020;3(4):154.
590. Li Y, Zhang LN, Chong L, Liu Y, Xi FY, Zhang H, et al. Prenatal ethanol exposure impairs the formation of radial glial fibers and promotes the transformation of GFAP $\delta$ -positive radial glial cells into astrocytes. *Mol Med Rep*. 2021 Feb 9;23(4):274.
591. Jung CS, Foerch C, Schänzer A, Heck A, Plate KH, Seifert V, et al. Serum GFAP is a diagnostic marker for glioblastoma multiforme. *Brain*. 2007 Dec;130(Pt 12):3336–41.
592. Zhang J, Jiao J. Molecular Biomarkers for Embryonic and Adult Neural Stem Cell and Neurogenesis. *Biomed Res Int*. 2015;2015:727542.
593. Meng X, Li W, Meng Z, Li Y. EIF4A3-induced circBRWD3 promotes tumorigenesis of breast cancer through miR-142-3p\_miR-142-5p/RAC1/PAK1 signaling. *BMC Cancer*. 2022 Nov 28;22(1):1225.
594. Aldape K, Brindle KM, Chesler L, Chopra R, Gajjar A, Gilbert MR, et al. Challenges to curing primary brain tumours. *Nat Rev Clin Oncol*. 2019 Aug 7;16(8):509–20.
595. Zaccagna F, Grist JT, Quartuccio N, Riemer F, Fraioli F, Caracò C, et al. Imaging and treatment of brain tumors through molecular targeting: Recent clinical advances. *Eur J Radiol*. 2021 Sep;142:109842.
596. Davis M. Glioblastoma: Overview of Disease and Treatment. *Clin J Oncol Nurs*. 2016 Oct 1;20(5):S2–8.
597. Diao W, Tong X, Yang C, Zhang F, Bao C, Chen H, et al. Behaviors of Glioblastoma Cells in in Vitro Microenvironments. *Sci Rep*. 2019 Jan 14;9(1):85.
598. Hassn Mesrati M, Behrooz AB, Y. Abuhamad A, Syahir A. Understanding Glioblastoma Biomarkers: Knocking a Mountain with a Hammer. *Cells*. 2020 May 16;9(5):1236.
599. Lane R, Simon T, Vintu M, Solkin B, Koch B, Stewart N, et al. Cell-derived extracellular vesicles can be used as a biomarker reservoir for glioblastoma tumor subtyping. *Commun Biol*. 2019 Aug 19;2(1):315.
600. Booth TC, Grzeda M, Chelliah A, Roman A, Al Busaidi A, Dragos C, et al. Imaging Biomarkers of Glioblastoma Treatment Response: A Systematic Review and Meta-Analysis of Recent Machine Learning Studies. *Front Oncol*. 2022 Jan 31;12.
601. Duhamel M, Drelich L, Wisztorski M, Aboulouard S, Gimeno JP, Ogrinc N, et al. Spatial analysis of the glioblastoma proteome reveals specific molecular signatures and markers of survival. *Nat Commun*. 2022 Nov 4;13(1):6665.

602. Gao Y, Zhang C, Liu Y, Wang M. Circular RNA profiling reveals circRNA1656 as a novel biomarker in high grade serous ovarian cancer. *Biosci Trends*. 2019 Apr 30;13(2):204–11.
603. Guo X, Jiao H, Cao L, Meng F. Biological implications and clinical potential of invasion and migration related miRNAs in glioma. *Front Integr Neurosci*. 2022 Nov 21;16.
604. Liu X, Chen JY, Chien Y, Yang YP, Chen MT, Lin LT. Overview of the molecular mechanisms of migration and invasion in glioblastoma multiforme. *Journal of the Chinese Medical Association*. 2021 Jul 1;84(7):669–77.
605. IWADATE Y. Epithelial-mesenchymal transition in glioblastoma progression. *Oncol Lett*. 2016 Mar;11(3):1615–20.
606. Joseph J V., Conroy S, Pavlov K, Sontakke P, Tomar T, Eggens-Meijer E, et al. Hypoxia enhances migration and invasion in glioblastoma by promoting a mesenchymal shift mediated by the HIF1 $\alpha$ -ZEB1 axis. *Cancer Lett*. 2015 Apr;359(1):107–16.
607. Wang R, Zhang S, Chen X, Li N, Li J, Jia R, et al. EIF4A3-induced circular RNA MMP9 (circMMP9) acts as a sponge of miR-124 and promotes glioblastoma multiforme cell tumorigenesis. *Mol Cancer*. 2018 Nov 23;17(1):166.
608. Barbagallo D, Caponnetto A, Barbagallo C, Battaglia R, Mirabella F, Brex D, et al. The GAUGAA Motif Is Responsible for the Binding between circSMARCA5 and SRSF1 and Related Downstream Effects on Glioblastoma Multiforme Cell Migration and Angiogenic Potential. *Int J Mol Sci*. 2021 Feb 7;22(4).
609. Lv T, Miao Y, Xu T, Sun W, Sang Y, Jia F, et al. Circ-EPB41L5 regulates the host gene EPB41L5 via sponging miR-19a to repress glioblastoma tumorigenesis. *Aging*. 2020 Jan 6;12(1):318–39.
610. Soongsathitanon J, Jamjuntra P, Sumransub N, Yangngam S, De la Fuente M, Landskron G, et al. Crosstalk between Tumor-Infiltrating Immune Cells and Cancer-Associated Fibroblasts in Tumor Growth and Immunosuppression of Breast Cancer. *J Immunol Res*. 2021;2021:8840066.
611. Chen W, Wang N, Lian M. CircRNA circPTK2 Might Suppress Cancer Cell Invasion and Migration of Glioblastoma by Inhibiting miR-23a Maturation. *Neuropsychiatr Dis Treat*. 2021;17:2767–74.
612. Liu R, Dai W, Wu A, Li Y. CircCDC45 promotes the malignant progression of glioblastoma by modulating the miR-485-5p/CSF-1 axis. *BMC Cancer*. 2021 Oct 9;21(1):1090.
613. Lv X, Wang M, Qiang J, Guo S. Circular RNA circ-PITX1 promotes the progression of glioblastoma by acting as a competing endogenous RNA to regulate miR-379-5p/MAP3K2 axis. *Eur J Pharmacol*. 2019 Nov 15;863:172643.
614. Giese A, Bjerkvig R, Berens ME, Westphal M. Cost of Migration: Invasion of Malignant Gliomas and Implications for Treatment. *Journal of Clinical Oncology*. 2003 Apr 15;21(8):1624–36.
615. Hatzikirou H, Basanta D, Simon M, Schaller K, Deutsch A. “Go or grow”: the key to the emergence of invasion in tumour progression? *Math Med Biol*. 2012 Mar;29(1):49–65.
616. Park JH, Lee HK. Current Understanding of Hypoxia in Glioblastoma Multiforme and Its Response to Immunotherapy. *Cancers (Basel)*. 2022 Feb 24;14(5):1176.

617. Yan H, Parsons DW, Jin G, McLendon R, Rasheed BA, Yuan W, et al. IDH1 and IDH2 mutations in gliomas. *N Engl J Med*. 2009 Feb 19;360(8):765–73.
618. Godlewski J, Ferrer-Luna R, Rooj AK, Mineo M, Ricklefs F, Takeda YS, et al. MicroRNA Signatures and Molecular Subtypes of Glioblastoma: The Role of Extracellular Transfer. *Stem Cell Reports*. 2017 Jun;8(6):1497–505.
619. Wilusz JE. A 360° view of circular RNAs: From biogenesis to functions. *WIREs RNA*. 2018 Jul 14;9(4).
620. Ebbesen KK, Hansen TB, Kjems J. Insights into circular RNA biology. *RNA Biol*. 2017 Aug 3;14(8):1035–45.
621. Okholm TLH, Sathe S, Park SS, Kamstrup AB, Rasmussen AM, Shankar A, et al. Transcriptome-wide profiles of circular RNA and RNA-binding protein interactions reveal effects on circular RNA biogenesis and cancer pathway expression. *Genome Med*. 2020 Dec 7;12(1):112.
622. Wu JS, Jarvis SM, Young JD. The human erythrocyte nucleoside and glucose transporters are both band 4.5 membrane polypeptides. *Biochem J*. 1983 Sep 15;214(3):995–7.
623. Xuan L, Qu L, Zhou H, Wang P, Yu H, Wu T, et al. Circular RNA: a novel biomarker for progressive laryngeal cancer. *Am J Transl Res*. 2016;8(2):932–9.
624. Zheng Q, Bao C, Guo W, Li S, Chen J, Chen B, et al. Circular RNA profiling reveals an abundant circHIPK3 that regulates cell growth by sponging multiple miRNAs. *Nat Commun*. 2016 Apr 6;7(1):11215.
625. Bachmayr-Heyda A, Reiner AT, Auer K, Sukhbaatar N, Aust S, Bachleitner-Hofmann T, et al. Correlation of circular RNA abundance with proliferation – exemplified with colorectal and ovarian cancer, idiopathic lung fibrosis and normal human tissues. *Sci Rep*. 2015 Jan 27;5(1):8057.
626. Gruner H, Cortés-López M, Cooper DA, Bauer M, Miura P. CircRNA accumulation in the aging mouse brain. *Sci Rep*. 2016 Dec 13;6(1):38907.
627. Buratin A, Paganin M, Gaffo E, Dal Molin A, Roels J, Germano G, et al. Large-scale circular RNA deregulation in T-ALL: unlocking unique ectopic expression of molecular subtypes. *Blood Adv*. 2020 Dec 8;4(23):5902–14.
628. Zatzman M, Fuligni F, Ripsman R, Suwal T, Comitani F, Edward LM, et al. Widespread hypertranscription in aggressive human cancers. *Sci Adv*. 2022 Nov 25;8(47).
629. Liang D, Tatomer DC, Luo Z, Wu H, Yang L, Chen LL, et al. The Output of Protein-Coding Genes Shifts to Circular RNAs When the Pre-mRNA Processing Machinery Is Limiting. *Mol Cell*. 2017 Dec;68(5):940-954.e3.
630. Zhu C, Mao X, Zhao H. The circ\_VCAN with radioresistance contributes to the carcinogenesis of glioma by regulating microRNA-1183. *Medicine*. 2020 Feb;99(8):e19171.
631. Yang L, Zhou Y ning, Zeng M miao, Zhou N, Wang B sheng, Li B, et al. Circular RNA Circ-0002570 Accelerates Cancer Progression by Regulating VCAN via MiR-587 in Gastric Cancer. *Front Oncol*. 2021 Oct 6;11.
632. Li Y, Ma H. circRNA PLOD2 promotes tumorigenesis and Warburg effect in colon cancer by the miR-513a-5p/SIX1/LDHA axis. *Cell Cycle*. 2022 Dec 2;21(23):2484–98.

633. Brown JR, Chinnaiyan AM. The Potential of Circular RNAs as Cancer Biomarkers. *Cancer Epidemiology, Biomarkers & Prevention*. 2020 Dec 1;29(12):2541–55.
634. Di Liddo A, de Oliveira Freitas Machado C, Fischer S, Ebersberger S, Heumüller AW, Weigand JE, et al. A combined computational pipeline to detect circular RNAs in human cancer cells under hypoxic stress. *J Mol Cell Biol*. 2019 Oct 25;11(10):829–44.
635. Zhang X, Zhang Y, Zhao J, Wu Y, Zhang N, Shen W. ARID1A mutations in cancer development: mechanism and therapy. *Carcinogenesis*. 2023 May 27;44(3):197–208.
636. Xu S, Tang C. The Role of ARID1A in Tumors: Tumor Initiation or Tumor Suppression? *Front Oncol*. 2021 Oct 4;11.
637. Ma J, Chen C, Fan Z, Zhang Y, Ji J, Wei D, et al. CircEGFR reduces the sensitivity of pirarubicin and regulates the malignant progression of triple-negative breast cancer via the miR-1299/EGFR axis. *Int J Biol Macromol*. 2023 Jul;244:125295.
638. Fu P, Lin L, Zhou H, Zhao S, Jie Z. Circular RNA circEGFR regulates tumor progression via the miR-106a-5p/DDX5 axis in colorectal cancer. *Brazilian Journal of Medical and Biological Research*. 2021;54(8).
639. Guo Q, Guo J, Liu W, Hu S, Hu X, Wang Q, et al. Circ-EGFR Functions as an Inhibitory Factor in the Malignant Progression of Glioma by Regulating the miR-183-5p/TUSC2 Axis. *Cell Mol Neurobiol*. 2022 Oct 15;42(7):2245–56.
640. Zhou Z, Zheng X, Mei X, Li W, Qi S, Deng Y, et al. Hsa\_circ\_0080229 upregulates the expression of murine double minute-2 (MDM2) and promotes glioma tumorigenesis and invasion via the miR-1827 sponging mechanism. *Ann Transl Med*. 2021 May;9(9):762–762.
641. Boss M, Arenz C. A Fast and Easy Method for Specific Detection of Circular RNA by Rolling-Circle Amplification. *Chembiochem*. 2020 Mar 16;21(6):793–6.
642. Gill BJ, Pisapia DJ, Malone HR, Goldstein H, Lei L, Sonabend A, et al. MRI-localized biopsies reveal subtype-specific differences in molecular and cellular composition at the margins of glioblastoma. *Proceedings of the National Academy of Sciences*. 2014 Aug 26;111(34):12550–5.
643. Wang Q, Hu B, Hu X, Kim H, Squatrito M, Scarpace L, et al. Tumor Evolution of Glioma-Intrinsic Gene Expression Subtypes Associates with Immunological Changes in the Microenvironment. *Cancer Cell*. 2017 Jul;32(1):42-56.e6.
644. Mao X gang, Xue X yan, Wang L, Lin W, Zhang X. Deep learning identified glioblastoma subtypes based on internal genomic expression ranks. *BMC Cancer*. 2022 Dec 20;22(1):86.
645. Liu Y, Chen S, Peng G, Liao Y, Fan X, Zhang Z, et al. CircRNA NALCN acts as an miR-493-3p sponge to regulate PTEN expression and inhibit glioma progression. *Cancer Cell Int*. 2021 Jun 10;21(1):307.
646. Doxakis E. Insights into the multifaceted role of circular RNAs: implications for Parkinson's disease pathogenesis and diagnosis. *NPJ Parkinsons Dis*. 2022 Jan 10;8(1):7.
647. Pencheva N, de Gooijer MC, Vis DJ, Wessels LFA, Würdinger T, van Tellingen O, et al. Identification of a Druggable Pathway Controlling Glioblastoma Invasiveness. *Cell Rep*. 2017 Jul 5;20(1):48–60.
648. Klein E, Hau AC, Oudin A, Golebiewska A, Niclou SP. Glioblastoma Organoids: Pre-Clinical Applications and Challenges in the Context of Immunotherapy. *Front Oncol*. 2020;10:604121.

649. Silvia N, Dai G. CEREBRAL ORGANOID AS A MODEL FOR GLIOBLASTOMA MULTIFORME. *Curr Opin Biomed Eng.* 2020 Mar;13:152–9.
650. Vollmann-Zwerenz A, Leidgens V, Feliciello G, Klein CA, Hau P. Tumor Cell Invasion in Glioblastoma. *Int J Mol Sci.* 2020 Mar 12;21(6).